Stony Brook University

Particle-Reactive Radionuclides (^{234}Th, ^{7}Be and ^{210}Pb) as Tracers of Sediment Dynamics in an Urban Coastal Lagoon (Jamaica Bay, NY)

A Dissertation Presented by

Alisha Anne Renfro

to

The Graduate School

in Partial fulfillment of the

Requirements

For the degree of

Doctor of Philosophy

in

Marine and Atmospheric Sciences

Stony Brook University

December 2010

The Graduate School

Alisha Anne Renfro

We, the dissertation committee for the above candidate for the

Doctor of Philosophy degree,

hereby recommend acceptance of this dissertation.

J. Kirk Cochran
Dissertation Advisor
Professor, School of Marine and Atmospheric Science, Stony Brook University

Robert C. Aller
Chair of Defense
Distinguished Professor, School of Marine and Atmospheric Science, Stony Brook University

Robert E. Wilson
Associate Professor, School of Marine and Atmospheric Science, Stony Brook University

Steven L. Goodbred Jr.
Associate Professor, Vanderbilt University

Mead A. Allison
Associate Director, Institute for Geophysics,
University of Texas at Austin

This dissertation is accepted by the Graduate School

Lawrence Martin
Dean of the Graduate School

Abstract of the Dissertation

Particle-Reactive Radionuclides (^{234}Th, ^{7}Be and ^{210}Pb) as Tracers of Sediment Dynamics in an Urban Coastal Lagoon (Jamaica Bay, NY)

by

Alisha Anne Renfro

Doctor of Philosophy

in

Marine and Atmospheric Science

Stony Brook University

2010

This study has been motivated by the issue of marsh loss in Jamaica Bay, New York. A deficit in sediment supply has been implicated as a factor in the dramatic marsh loss, and we have used particle-reactive natural radionuclides as tracers for the transport and deposition of particles in the bay. The short-lived radionuclides ^{7}Be (half-life = 53.3 days) and ^{234}Th (half-life = 24.1 days) serve as tracers of particle dynamics on short-term (seasonal) time scales, while the longer lived ^{210}Pb (half-life = 22.3 y) traces the fate of particles on decadal time scales. In Jamaica Bay, the well-characterized supply of ^{7}Be and ^{210}Pb from the atmosphere comprised 77-92% and 23-48% of the supply of these radionuclides, respectively and is augmented by inputs of these radionuclides from CSO events that add storm water to the bay. Mean $^{234}Th_{xs}$ inventories in the subtidal sediments in 2004 – 2006 ranged from 3.4 to 5.6 dpm cm^{-2}. The supply of ^{234}Th from decay of dissolved ^{238}U in situ is ~ 0.9 dpm cm^{-2} and is augmented by particles with

excess ^{234}Th transported into the bay from the New York Bight. Inventories of excess ^{234}Th in bay sediments show significant temporal variation, as evidenced in four sampling campaigns of the bay carried out in 2004-2006. The upper 5 cm of subtidal sediments were sampled to insure that the entire $^{234}Th_{xs}$ inventory was obtained and could be counted quickly, but additional samples in fine-particle dominated sediments indicated that 79 – 100% of the $^{234}Th_{xs}$ inventory was confined to a highly active veneer of sediment. Results indicate that ^{234}Th is deposited in sediments of the western bay during times of low wave height outside the bay and winds out of the south. However, particles and associated ^{234}Th in the highly active surficial sediments are transported to the northeastern portion of the bay (e.g. Grassy Bay) following storms and winds out of the southwest. We have used a mass balance of ^{234}Th in the bay to estimate an annual input of sediment of 4.3 to 35.8 x 10^{10} g y^{-1} from the New York Bight into the bay. A mass balance of ^{210}Pb for Jamaica Bay indicated that a sediment import of 4.2 to 15.8 × 10^{10} g y^{-1} would be needed to balance the bay's ^{210}Pb budget. Both these radionuclide-based sediment import estimates are upper limits. We have also used down-core distributions of excess ^{210}Pb activity to estimate average long-term rates of sediment deposition in the muddy sediments of the bay to be 0.47 ± 0.27 g cm^{-2} y^{-1} (7.6 ± 1.4 × 10^{10} g y^{-1}). A sediment import of 5.8 – 8.8 × 10^{10} g y^{-1} would be required to balance the sediment budget of the bay. This annual import estimate is higher than a previous estimate made from the attempt at a sediment budget for the bay (1.5 – 2.9 × 10^{10} g y^{-1}). However, estimates from the mass balances of the radionuclides and the sediment budgets all indicate that there is an import of sediment from into Jamaica Bay. Measurements of ^{7}Be and ^{234}Th in marsh peat complement the distribution of these radionuclides in subtidal

sediments. While ^{7}Be was observed at all sites sampled (ranging from 0.7 to 3.2 dpm cm^{-2}), as a consequence of its direct supply to the marsh from the atmosphere. In contrast, the input of ^{234}Th depends on the supply of particles from the subtidal to the marsh surface. Inventories of $^{234}Th_{xs}$ on the marshes ranged from 0 – 9.8 dpm cm^{-2} with higher mean inventories observed on the marshes in the western bay in both September-2004 and May-2005 (6.0 ± 1.3 and 3.4 ± 1.3 dpm cm^{-2}, respectively) than in the eastern bay (4.1 ± 1.2 and 1.8 ± 1.7 dpm cm^{-2}, respectively). Elevated inventories of ^{234}Th are typically observed near marsh edges, although the pattern is complicated by the proximity of interior sites to tidal creeks that serve as conduits for sediment supply to the marsh. Sediment accumulation on the marshes was estimated using the $^{234}Th_{xs}$ inventories measured on the marsh islands and the activity of $^{234}Th_{xs}$ in the upper 5 mm of the fine-fraction sediments near the marsh islands. Sediment accumulation rates derived from this method ranged from 0 to 2.5 g cm^{-2} y^{-1}, while mass accumulation rates on the marshes, derived from ^{210}Pb geochronologies in a previous study ranged from 0.05 – 0.1 g cm^{-2} y^{-1}. The difference in these two methods may reflect sampling bias to the marsh edges during this study, where deposition is likely higher, and the short-term patterns of deposition, reflected with the $^{234}Th_{xs}$ inventories.

TABLE OF CONTENTS

List of Tables

List of Figures

ACKNOWLEDGEMENTS

I would like to express my heartfelt thanks to my advisor Kirk Cochran for his support and encouragement throughout the years. He has given me the opportunity to produce a scientific work of which I am proud. He has also given me ample opportunity to conduct other types of research and present my work in a variety of locations.

I would also like to thanks my committee members: Steve Goodbred, Robert Aller, Robert Wilson and Mead Allison. Steve Goodbred gave me the chance to come to Stony Brook and work on a really great project and for that I am grateful. Robert Aller has always been supportive, provoked a lively discussion about my science, and always has suggestions about how to address a problem. Bob Wilson has been an important resource in helping me understand the hydrodynamics of the bay. Mead Allison has been able to look at the work presented in this document with "new" eyes and given helpful suggestions for framing the data presented here.

The funding for this research was provided by the National Park Service. The Park Service has been a great organization to work with. They have given us help out in the field, given us places to dock our boats, when needed, and have been great supporters of the research. In particular I would like to thank Charles Roman and Patricia Rafferty.

I would also like to thank the people at SOMAS who have helped me over years. David Hirschberg who has provided me with much needed help both in the field and in the lab. In addition I've had a large cast of people who have volunteered their time and energy to helping me with field work over the years, including: Aaron Beck, Alex Kolker, Kimberly Rogers, Beth Weinman and Juliet Kinney.

Finally, I would like to thank my friends and family for the support over the years. They might understand what I do or why I do it, but they have always been there for me.

CHAPTER 1

Introduction

Jamaica Bay is a back barrier coastal lagoon located on the southern coast of western Long Island and is surrounded by the New York City boroughs of Brooklyn and Queens and connected to the ocean by Rockaway Inlet (Fig. 1-1). Naturally occurring changes and man-made modifications to Jamaica Bay in the 20th century have had lasting effects on its geomorphology and hydrodynamics. The most significant naturally occurring change was a 1.4 km westward migration of Rockaway Inlet between the mid-1800s to the 1930s when the Breezy Point Jetty was built (Black, 1981; Swanson and Wilson, 2008). In the early 1900s the federal government and the city of New York undertook a project to dredge the inlet and the northeast channel for shipping purposes. Further efforts were planned to dredge much of the bay, eliminating the marsh islands, transforming Jamaica Bay into a major shipping port. These plans were eventually abandoned, but other modification were made to the bay such as filling of marsh islands along the periphery of the bay, extensive bulkheading and further dredging of the Rockaway Inlet and the northeastern channel in the 1930s (Black, 1981). In the 1940s Grassy Bay in the northeastern part of the bay was dredged to obtain material for an expansion of Idlewild Airport (now known as John F. Kennedy Airport; Black, 1981; Swanson and Wilson, 2008).

Channel dredging in Jamaica Bay has increased the volume of the bay while marsh filling and bulkheading along the bay periphery has decreased the total area of the bay (Black, 1981). In 1899, prior to when the first major modifications were made to the bay, the tidal range was relatively uniform throughout the bay (Swanson and Wilson,

2008). Dredging of the Rockaway Inlet channel, North Channel, Broad Channel, and excavation of Grassy Bay deepened the mean depth of the bay from 1 to 5 meters (Fig. 1-1). Historic tide stations in Jamaica Bay indicate that a deviation in tidal range became prominent in the 1940s with a higher tidal range in the Bay's interior than at the inlet. This change in tidal range coincides with many of the man-made modification to the bay. Historical evidence indicates that before the 1900s the bay was weakly ebb dominated while in present day there is flood dominance (Swanson and Wilson, 2008).

Today, Jamaica Bay is a shallow, weakly stratified and tidally active environment with estuarine circulation (Gordon et al., 2005; R.E. Wilson, pers. comm.). In the summer, winds move landward out of the southeast and in the winter, winds are out of the northwest. The tidal range (M_2) of Jamaica Bay is amplified from the western end to the far northeastern side of the basin (Grassy Bay) by a factor 1.2. The resulting barotropic tidal flow is flood dominant throughout the bay and contributes to maintain significant tidal flow through the bay's main channels (North Channel, Beach Channel and Broad Channel; Fig. 1-1). The barotropic tidal flow coupled with baroclinic estuarine circulation likely results in an increase of the flood-dominant shear stress along the bottom, enhancing the import of fine-grained material into the bay (R.E. Wilson, pers. comm.).

In addition to altering the bay's hydrodynamics, modification have altered the basic physiography of the bay. In the present day, Jamaica Bay is divided into two sections (west and east) by Broad Channel Island. In the western bay, deep channels are located along the northern border (North Channel; depth ~ 7.5 m) and along the southern border (Beach Channel; depth ~ 5.5 m; Fig. 1-2). In the eastern bay the Beach Channel

continues along the southern edge (depth ~ 11.5 m) while the North Channel, narrows and connects to Grassy Bay (Fig. 1-2). Grassy Bay, located in the northeastern part of Jamaica Bay, is deep (~ 11.5 m) and is to some extent isolated from much of the rest of the bay with exchange limited to the North Channel and through Broad Channel (depth ~ 6.5 m; Fig. 1-2). Stratification in Grassy Bay is more pronounced than in other regions in the bay, particularly during the summer (Rubenstone, 2005). Grassy Bay is suspected to be a significant sediment sink within the bay. The changes to the bay's physiography and hydrodynamics have likely altered the major pathways and sinks for sediment in the subtidal bay.

Much like the bay itself, the drainage basin of Jamaica Bay has also undergone significant changes since the first Europeans settled in the area in the mid-1600s. Prior to 1865, the upland area around the bay was mostly used for small-scale farming, while fishing in the bay was limited to recreation and as a supplement of the food supply. In the late 1800s manufacturing, construction, fish oil and fertilizer factories were present and there was general population increase around the bay. Also during the 1800s oyster and clam harvesting became an important fishery. The end of the shellfishing industry in Jamaica Bay was not due to a disappearance of oysters and clams, but rather was mandated by health officials in 1921 due to the contamination from the sewage discharge into the bay (Black, 1981).

Today most of the fresh water entering Jamaica Bay is discharged from one of four waste water treatment plants – Coney Island, Jamaica, Rockaway, and the 26th Ward (Fig. 1-1; Beck et al., 2007). These plants service over 2 million people and have a drainage area of 200 km^2. Municipal and storm water runoff are combined (CSO system)

and the four wastewater treatment plants deliver an average of 261 million gallons per day to the bay (Benotti and Brownawell, 2007). However, during moderate to heavy rainfall events the water entering the system can overload the capacity of the wastewater treatment plant causing the plant to be bypassed and untreated water and sewage to enter the bay via outfalls (Fig. 1-3). CSO events can deliver pollutants and waters high in nitrogen (nitrate, nitrite, ammonia, and organic nitrogen) to the waters of Jamaica Bay (Benotti et al., 2007; Benotti and Brownawell, 2007).

In 1972, Jamaica Bay became a Gateway National Recreation Area under management of the National Park Service. In spite of this protection of the bay, wetland loss from 1975-1999 was extensive (Hartig et al., 2002). Speculation as to the causes affecting wetland losses in Jamaica Bay are: failure of the marshes to keep pace with sea level rise (Hartig et al., 2002), possibly due to a lack of sediment supply (Gordon and Houghton, 2004; Hartig et al., 2002), pollution impacts (Kolker, 2005), and physical alterations (Swanson and Wilson, 2008). The primary purpose of this thesis is to use a suite of naturally occurring radionuclides to examine sedimentary and material exchange processes that potentially impact the marshes of Jamaica Bay.

Naturally occurring particle reactive radionuclides (e.g. ^{234}Th, ^{7}Be, ^{210}Pb) are useful tracers in coastal systems (Feng et al., 1999a; Giffin and Corbett, 2003). Their well-characterized sources permit construction of mass balances and their strong association with particles permits them to be used to evaluate fluxes of sediment transport and redistribution. The short-lived radionuclides, ^{234}Th (half-life = 24.1 days) and ^{7}Be (half-life = 53.3 days) are particularly useful in studying processes that operate over seasonal time scales. ^{210}Pb (half-life = 22.3 years), in contrast, is useful for studying

processes on longer time-scales (<100 years; Sharma et al., 1987). In addition, the sources of these radionuclides differ: ^{234}Th has an oceanic source, while ^{7}Be and ^{210}Pb have an atmospheric source (Baskaran and Swarzenski, 2006; Feng et al., 1999b; Vogler et al., 1996).

^{234}Th is produced through the decay of its parent isotope ^{238}U, a primordial radionuclide that is released from rocks to solution during chemical weathering. Under oxic conditions, ^{238}U is present in the 6+ valence state and forms a soluble uranyl carbonate complexes, $UO_2(CO_3)_2^{-2}$ and $UO_2(CO_3)_3^{-4}$ (Chabaux, et al., 2008; Ku et al., 1977). Under special conditions, such as high phosphate concentrations and organic-rich water, additional U-complexes may be present (Chabaux et al., 2003; McKee, 2008). Under anoxic conditions, ^{238}U can be reduced to the 4+ valence state and can then be scavenged onto particle surfaces. Due to its long half-life and low particle reactivity under oxic conditions, ^{238}U is well-mixed in the oceans making it, in general, conservative with salinity (Baskaran and Swarzenski, 2006; Feng et al., 1999b). Conservative behavior of ^{238}U can be evaluated by comparing its activity with respect to salinity (Boyle et al., 1974), and this behavior has been observed in estuaries in the U.S. (Feng et al., 1999a), India (Ray et al., 1995) and the U.K. (Toole et al., 1987). The general relationship between ^{238}U and salinity in the open ocean is: ^{238}U (dpm L^{-1}) = 0.0704 × Salinity (Rutgers van der Loeff et al., 2006). In the Hudson estuary the relationship between salinity and ^{238}U is similar to that for the open ocean is: ^{238}U (dpm L^{-1}) = 0.0707 × salinity + 0.0276 (Feng et al., 1999a). However, it is worth noting that non-conservative behavior of ^{238}U has been demonstrated in some estuaries including the Forth estuary (Toole et al., 1987), the Amazon River (Mckee et al., 1987) and the

Ogeechee and Savannah Rivers (Maeda and Windom, 1982). The non-conservative behavior of uranium observed in the Amazon River may have resulted from the desorption of uranium in high-alkalinity pore waters due to suboxic diagenesis following sediment deposition or the release of uranium of ferric hydroxide coatings on sediments (McKee et al., 1987).

Thorium-234, unlike its parent isotope, is present as the Th 4+ ion (or as a $Th(OH)_x$ complex), as such it is particle-reactive under most conditions and is readily scavenged on to available particle surfaces ($K_d = 1 - 50 \times 10^5$), and may be removed from the water column (Baskaran and Santschi, 1993; Feng et al., 1999a). This creates disequilibrium between ^{234}Th and ^{238}U, leaving the water column depleted in ^{234}Th. Since production of ^{234}Th is dependent on dissolved ^{238}U, and dissolved ^{238}U activity varies as a function of salinity, ^{234}Th production in the water column is lower in fresher reaches of an estuary and increases with increasing salinity. The residence time of ^{234}Th in the water column within estuarine waters was first quantified using $^{234}Th/^{238}U$ by Aller and Cochran (1976). They found that the residence time of ^{234}Th was short (~1.4 days) as the ^{234}Th was rapidly scavenged on to particles that then settled to the bottom sediments. Similar residence times of ^{234}Th in the water column were found in Narragansett Bay (1-20 d; Santschi et al., 1979), the Yangtze River estuary, China (< 1 d; McKee et al., 1984), the Amazon estuarine system (4-5 de; McKee et al., 1986), and Hudson River estuary (2-12 d; Feng et al., 1999a). However, depending on the system, ^{234}Th that is scavenged onto particles, ^{234}Th may remain suspended in the water column until it decays or may be advected and deposited (Fig. 1-4; Aller and Cochran, 1976; Feng et al., 1999a; Feng et al., 1999b).

^{234}Th has also been used to quantify sediment deposition, mixing and transport in estuaries. In addition to estimating residence time of ^{234}Th in the water column in Long Island Sound, Aller and Cochran (1976) found excess ^{234}Th ($^{234}Th_{xs}$) in sediments down to 4 cm which indicated rapid mixing by deposit-feed organisms. In work conducted by Aller et al. (1980) the mean $^{234}Th_{xs}$ inventory in the subtidal sediments of Long Island Sound was approximately in balance with the expected for the average water depth, but surpluses and deficits were observed, depending on location. Aller et al. (1980) ascribed this observation to lateral redistribution of particles in the Sound. Work done by DeMaster et al (1985) and McKee et al. (1983) used the distribution of ^{234}Th in the sediments to estimate sediment deposition in the estuarine zone of the Yangtze River and found that deposition varied seasonally with high deposition near the river mouth that was subsequently redistributed down the estuarine system as a result of winter storms.

Feng et al. used ^{234}Th, ^{7}Be and ^{210}Pb as tracers to study short- and long-term variation in the transport of sediment and associated contaminants in the Hudson River Estuary (Feng et al., 1999b). They found that ^{234}Th and ^{7}Be activities on particles ranged from 0 to 71 dpm g^{-1} and 0 to 57 dpm g^{-1}, respectively. The highest particle activities were consistently measured at the highest salinity stations sampled (Feng et al., 1999a). The results from this study suggests that during low-flow river conditions there is a transport of particles labeled with ^{234}Th and ^{7}Be from higher salinity areas to lower salinities due to estuarine circulation (Feng et al., 1999b).

In contrast to ^{234}Th, ^{7}Be is produced in the lower stratosphere and upper troposphere of the atmosphere through cosmic-ray spallation reactions involving nitrogen and oxygen (Feng et al., 1999a; Ioannidou and Papastefanou, 2006; Kaste et al., 2002).

^{7}Be production in the atmosphere varies by latitude, altitude, and solar activity, with production increasing poleward. As well, highest production occurs between 12 and 20 km altitude and varies with the 11-year solar cycle. Mixing between the stratosphere and troposphere can occur, generally during the spring, but possibly also during intense thunderstorms. This mixing may increase the ^{7}Be concentration in the upper troposphere and its flux to the Earth's surface because ^{7}Be in the troposphere adsorbs electrostatically to aerosols that can be delivered through wet and dry precipitation to the Earth's surface (Baskaran and Santchi, 1993; Feng, et al., 1999a; Giffen and Corbett, 2003; Kaste et al., 2002).

Despite the variations in production within the troposphere and stratosphere, a major control on the ^{7}Be flux appears to be delivery through wet precipitation (Canuel et al., 1990, Dibb, 1989; Olsen et al., 1985; Turekian et al., 1983; Zhu and Olsen, 2008). ^{7}Be delivered through wet precipitation is in the 2+ valence state (Kaste et al., 2002) and can be scavenged onto particles in terrestrial soils or aquatic (freshwater or marine) environments. ^{7}Be has an affinity for fine-grained particles and in estuarine systems has a K_d of 1-10x10^4 (Kaste et al., 2002), somewhat less than that of ^{234}Th. Olsen et al. (1986) observed that ^{7}Be activities on suspended particles were highest in high-energy environments where particle residence times in the water column were long and lowest in low-energy environments where sedimentation rates were high.

As with ^{234}Th, scavenged ^{7}Be can be transport with particles through an estuarine system (Fig. 1-4). Indeed, ^{7}Be has been used in a variety of ways to study estuarine systems. For example Olsen et al. (1989) used the ratio of ^{7}Be to ^{210}Pb to quantify sediment resuspension in the Savannah Estuary. Feng et al. (1999a) used ^{7}Be and ^{234}Th

as coupled tracers in the water column of the Hudson River Estuary and to characterize transport through the system. ^{7}Be was used as tracer of sediment accumulation in sediments not affected by bioturbation. ^{7}Be can be used to determine sediment accumulation rates. Accumulation rates derived from ^{7}Be were found to be comparable to longer-term accumulation rates derived using ^{210}Pb by both Canuel et al. (1990) and Dibb and Rice (1989). ^{7}Be can be used to tracer recent pulse of river borne sediment. For example, Canuel et al. (1990) used ^{7}Be to quantify the impacts of storm events by identifying "new" pulses of sediment and Sommerfield et al. (1999) used it as a tracer of fine-grained sediment delivered to the northern California continental margin from the Eel River. Sommerfield et al. (1999) found that after periods of extremely high river discharge, terrestrial derived ^{7}Be was present in shelf and slope deposits.

^{210}Pb, like ^{234}Th, is a member of the ^{238}U decay series. ^{238}U decays through a series of radionuclides to ^{226}Ra (half-life = 1600 years). The decay product of ^{226}Ra is ^{222}Rn (half-life = 3.83 days), a noble gas, that can escape from soils and rocks into the atmosphere. However, not all ^{222}Rn escapes and some remains in the solid phase and decays (Matisoff et al., 2005). The ^{222}Rn that escapes to the atmosphere then decays eventually into ^{210}Pb. ^{210}Pb in the atmosphere becomes associated with aerosols and removed from the atmosphere through wet and dry deposition. As a result, the downward supply of ^{210}Pb to nearby coastal systems is via direct atmospheric deposition, the production of ^{210}Pb from dissolved ^{226}Ra being small (Fig. 1-4; Appleby and Oldfield, 1992; Le Cloarec et al., 2007; Matisoff et al., 2005).

Appleby and Oldfield (1992) observed that the atmospheric flux of ^{210}Pb varies with the amount of precipitation over short-term scales, similar to ^{7}Be. However, over

longer time scales (several years), ^{210}Pb flux at a given location does appear to be somewhat steady (±10%), although its input from the atmosphere is regionally variable (Baskaran, 1995; Graustein and Turekian, 1996; Turekian et al., 1977). Atmospherically deposited ^{210}Pb is scavenged on to particle surfaces ($K_d = 10^3–10^6$) and ^{210}Pb has been used extensively to derive sediment accumulation rates in marsh and estuarine systems (Appleby and Oldfield, 1992; Church et al., 2006; Cochran et al., 1998a; Cochran et al., 1998b; Corbett et al., 2006; Corbett et al., 2007).

This dissertation focuses on using these naturally occurring radionuclides ^{234}Th, ^{7}Be and ^{210}Pb to better understand particle dynamics in an urban coastal lagoon (Jamaica Bay, NY). To this end, it is necessary to characterize the mass balances of these radionuclides and their distributions in the subtidal sediments of Jamaica Bay, NY. Thus, the main objectives are:

1) To quantify the inventories of short-lived radionuclides, ^{7}Be, ^{234}Th and ^{210}Pb in the subtidal sediment in Jamaica Bay over spatial and temporal scales.

2) To measure longer-term accumulation rates (~100 years) throughout Jamaica Bay using ^{210}Pb, and compare these long-term rates to the short-term trends seen in ^{234}Th and ^{7}Be.

3) To determine spatial and temporal patterns of ^{7}Be and ^{234}Th inventories in surface sediments on select healthy and degrading marsh islands within Jamaica Bay and compare these patterns with those the subtidal sediments.

The chapters of this dissertation are presented in the form of manuscripts. Each chapter focuses on a specific topic and addresses specific problems dealing with sediment dynamics within the Bay. Chapter 2 focuses on the distribution of $^{234}Th_{xs}$ inventories in Jamaica Bay sediments over four spatially detailed cruises conducted in 2004-2006 and characterizes the mass balance of $^{234}Th_{xs}$ in the bay. Chapter 3 focuses on the mass balance of ^{210}Pb in the Bay and the long-term sediment accumulation rates compared with the short-term mass accumulation rates estimated from the ^{234}Th balance. Chapter 4 focuses on the spatial and temporal distribution of ^{7}Be inventories throughout the bay during the four sampling cruises. The atmospheric flux of ^{7}Be to the area is characterized through an atmospheric collector deployed from April-2008 to December-2009 to examine the relationship between precipitation and the atmospheric flux of ^{7}Be. Finally Chapter 5 focuses on the distribution of $^{234}Th_{xs}$ and ^{7}Be on the marsh islands of Jamaica Bay and relates these radionuclides to short-term storage and long-term deposition of sediment on the marsh islands, as well as in the subtidal bay.

References

Aller, R.C., Benninger, L.K. and J.K. Cochran (1980) Tracking particle-associated processes in nearshore environments by use of Th-234 and U-238 disequilibrium. *Earth Planet. Sci. Lett.* 47: 161-175.

Aller, R.C. and J.K. Cochran (1976) ^{234}Th/^{238}U disequilibrium in near-shore sediment: Particle reworking and diagenetic time scales. *Earth Planet. Sci. Let., 29: 37-50.*

Appleby, P.G. and F. Oldfield (1992) Applications of Lead-210 to sedimentation studies. M. Ivanovich and R.S. Harmon (eds), Uranium-Series Disequilibrium: Applications to Environmental Problems, Clarendon Press, Oxford, pp. 731-778

Baskaran, M. (1995) A search for the seasonal variability of the depositional fluxes of ^{7}Be and ^{210}Pb. *Journal of Geophysical Research* 100: 2833-2840.

Baskaran, M. and P.H. Santchi (1993) The role of particles and colloids in the transport of radionuclides in the coastal environments of Texas. *Marine Chemistry* 43: 95-114.

Baskaran, M. and P.W. Swarzenski (2006) Seasonal variations on the residence times and partitioning of short-lived radionuclides (^{234}Th, ^{7}Be and ^{210}Pb) and depositional fluxes of ^{7}Be and ^{210}Pb in Tampa Bay, Florida. *Marine Chemistry* 104: 27-42.

Beck, A.J., J.P. Rapaglia, J.K. Cochran and H.J. Bokuniewicz (2007) Radium mass-balance in Jamaica Bay, NY: Evidence for a substantial flux of submarine groundwater. *Marine Chemistry* 106: 419-441.

Benotti, M.J. and B.J. Brownawell (2007) Distriubtion of pharmaceuticals in an urban estuary during both dry- and wet-weather conditions. *Environmental Science and Technology* 41: 5795-5802.

Benotti, M. J., M. Abbene and S. A Terracciano (2007) Nitrogen Loading in Jamaica Bay, Long Island, New York: Predevelopment to 2005. USGS Open File Report SIR 2007-5051, 17 pp.

Black, F.R. (1981) *Jamaica Bay: A History*. Gateway National Recreation Area New York, New Jersey.

Boyle, E.A.R., A.T. Collier, J.M. Dengler, A.C. Ng and R.F. Stallard (1974) On the chemical mass balance in estuaries. *Geochimica et Cosmochimica Acta*, 38: 1719-1728

Canuel,, E.A., C.S. Martens, and L.K. Benninger (1990) Seasonal variations in ^{7}Be activity in the sediments of Cape Lookout Bight, North Carolina. *Geochimica et Cosmochimica Acta* 54: 237-245.

Chabaux, F., B. Bourdon and J. Riotte (2008) U-Series geochemistry in weathering profiles, river waters and lakes. S. Krishnaswami and J.K. Cochran (eds). U-Th Series Nuclides in Aquatic Systems, pp. 49-91.

Church, T.M., C.K. Sommerfield, D.J. Velinsky, D. Point, C. Benoit, D. Amouroux, D. Plaa and O.F.X. Donard (2006) *Marine Chemistry* 102: 72-95.

Cochran, J.K., D.J. Hirschberg, J. Wang and C. Dere (1998) Atmospheric deposition of metals to coastal waters (Long Island Sound, New York U.S.A.): Evidence from saltmarsh deposits. *Estuarine, Coastal and Shelf Science* 46; 503-522.

Cochran, J.K., M. Frignani, M. Salamanca, L.G. Bellucci and S. Guerzoni (1998) Lead-210 as a tracer of atmospheric input of heavy metals in the northern Venice Lagoon. *Marine Chemistry* 62: 15-29.

Corbett, D.R., B. McKee and M. Allison (2006) Nature of decadal-scale sediment accumulation on the western shelf of the Mississippi River delta. *Continental Shelf Research* 26, 2125-2140.

Corbett, D.R., D. Vance, E. Letrick, D. Mallinson and S. Culver (2007) Decadal-scale sediment dynamics and environmental change in the Albemarle Estuarine System, North Carolina. *Estuarine, Coastal and Shelf Science* 71: 717-729.

Dibb, J. E. (1989) Atmospheric deposition of beryllium-7 in the Chesapeake Bay region. *Journal of Geophysical Research* 94: 2261-2265.

Dibb, J.E. and D.L. Rice (1989) Temporal and spatial distribution of beryllium-7 in the sediments of Chesapeake Bay. *Estuarine, Coastal and Shelf Science* 28: 395-406.

DeMaster, D.J., B.A. McKee, C.A. Nittrouer, J.C. Quian and G.D. Cheng (1985) Rates of sediment accumulation and particle reworking based on radiochemical measurements from continental-shelf deposits in the East China Sea. *Continental Shelf Research* 4: 143-158.

Feng, H., J.K. Cochran and D.J. Hirschberg (1999a) ^{234}Th and ^{7}Be as tracers for the transport and dynamics of suspended particles in partially mixed estuary. *Geochimica et Cosmochimica Acta*, 63: 2487-2505.

Feng, H., J.K. Cochran and D.J. Hirschberg (1999b) ^{234}Th and ^{7}Be as tracers for transport and sources of particle-associated contaminants in the Hudson River Estuary. *The Science of the Total Environment* 237/238: 401-418.

Giffin, D. and D. R. Corbett (2003) Evaluation of sediment dynamics in coastal systems via short-lived radioisotopes. *Journal of Marine Systems* 42: 83-96.

Gordon, A., B. Huber and R. Houghton (2005) Temperature, salinity and currents in Jamaica Bay. Integrated Reconnaissance of the Physical and Biogeochemical Characteristics of Jamaica Bay: Initial Activity Phase. A Coordinated Program f the Gateway National Recreation Area and the Coumbia Earth Institute, pp. 46-50.

Gordon, A.L. and R.W. Houghton (2004) The water of Jamaica Bay: impact on sediment budget. In: *Proceeding, Jamaica Bay's Disappearing Salt Marshes.* New York: Jamaica Bay Institute, Gateway National Recreational Area, National Park Service.

Graustein, W.C. and K.K. Turekian (1996) Be-7 and Pb-210 indicate an upper troposphere source for elevated ozone in the summertime subtropical free troposphere of the eastern North Atlantic. *Geophysical Research Letters* 23: 539-542.

Hartig, E.K., V. Gornitz, A. Kolker, F. Mushacke, and D. Fallon (2002) Anthropogenic and climate-change impacts on salt marshes of Jamaica Bay, New York City. *Wetlands* 22: 71-89.

Houghton, R., A. Gordon and B. Huber (2005) Dye Tracer Experiments in Jamaica Bay. Integrated Reconnaissance of the Physical and Biogeochemical Characteristics of Jamaica Bay: Initial Activity Phase. A Coordinated Program f the Gateway National Recreation Area and the Coumbia Earth Institute, pp. 51-53.

Ioannidou, A. and C. Papastefanou (2006) Precipitation scavenging of ^{7}Be and ^{137}Cs radionuclides in air. *Journal of Environmental Radioactivity* 85: 121-136.

Kaste, J.M., S.A. Norton, C.T. Hess (2002) Enviromental chemistry of beryllium-7. P.H. Ribbe and J.J. Rosso (eds). Beryllium: Mineralogy, petrology, and geochemistry, Reviews in Mineralogy and Geochemistry, vol. 50, pp. 291-312.

Kolker, A. (2005) The Impacts of Climate Variability and Anthropogenic Activities on Salt Marsh Accretion and Loss on Long Island. Stony Brook, New York: Stony Brook University Ph.D. thesis, 278p.

Ku, T.-L., K.G. Knauss and G.G. Mathieu (1977) Uranium in the open ocean: concentration and isotopic composition. *Deep Sea Research*: 24: 1005-1017.

Le Cloarec, M-F., P. Bonté, I. Lefèvre, J-M Mouchel and S. Colbert (2007) Distribution of ^{7}Be, ^{210}Pb and ^{137}Cs in watersheds of different scales in the Seine River basin: Inventories and residence times. *Science of the Total Environment* 375: 125-139.

Matisoff, G., C.W. Wilson and P.J. Whiting (2005) The ^{7}Be/^{210}Pb ratio as an indicator of suspended sediment age or fraction of new sediment in suspension. *Earth Surface Processes and landforms* 30: 1191-1201.

Maeda, M. and H.L. Windom (1982) Behavior of uranium in two estuaries of the southeastern United States. *Marine Chemistry* 11: 427-436.

McKee, B.A. (2008) U- and Th-series nuclides in estuarine environments. Krishnaswami and J.K. Cochran (eds). U-Th Series Nuclides in Aquatic Systems, pp. 193-218.

McKee, B.A., D.J. DeMaster and C.A. Nittrouer (1984) The use of Th-234/U-238 disequilibrium to examine the fate of particle-reactive species on the Yangtze River. *Geology* 11: 631-633.

McKee, B.A., D.J. DeMaster and C.A. Nittrouer (1986) Temporal variability in the partitioning of thorium between dissolved and particulate phases on the Amazon shelf: Implication for the scavenging of particle-reactive species. *Continental Shelf Research* 6: 87-106.

McKee, B.A., D.J. DeMaster and C.A. Nittrouger (1987) Uranium geochemistry on the Amazon shelf: evidence for uranium release from bottom sediments. *Geochimica et Cosmochimica Acta* 51: 2779-2786.

McKee, B.A., C.A. Nittrouer and D.J. DeMaster (1983) Concepts of sediment deposition and accumulation applied to the continental shelf near the mouth of the Yangtze River. *Geology* 11: 631-633.

Olsen, C.R., I.L. Larsen, P.D. Lowry, and N.H. Cutshall, J.F. Todd, G.T.F. Wong and W.H. Casey (1985) Atmospheric fluxes and marsh-soil inventories of ^{7}Be and ^{210}Pb. *Journal of Geophysical Research* 90: 10487-10495.

Olsen, C.R., I.L. Larsen, P.D. Lowry, and N.H. Cutshall (1986) Geochemistry and deposition of ^{7}Be in river-estuarine and coastal waters. *Journal of Geophysical Research* 91: 896-908.

Olsen, C.R., M. Thein, I.L. Larsen, P.D. Lowry, P.J. Mulhooland, N.H. Cutshall, J.T. Byrd and H.L. Windom (1989) Plutonium, lead-210, and carbon isotopes in the Savannah Estuary: Riverborne versus marine sources. *Environmental Science and Technology* 23: 1475-1481.

Ray, S.B., M. Mohanti and B.L.K. Somayajulu (1995) Uranium isotopes in the Mahanadi River-Estuarine system, India. *Estuarine, Coastal and Shelf Science* 40: 635-645.

Rubbenstone, J. (2005) Stable isotope evidence for water mass mixing in Jamaica Bay. Integrated Reconnaissance of the Physical and Biogeochemical Characteristics of Jamaica Bay: Initial Activity Phase. A Coordinated Program f the Gateway National Recreation Area and the Columbia Earth Institute, pp. 54-59.

Rutgers van der Loeff, M. R., M. M. Sarin, M. Baskaran, C. Benitez-Nelson, K. O. Buesseler, M. Charette, M. Dai, O. Gustafsson, P. Masqué, P. J. Morris, K. Orlandini, A. Rodriguez y Baena, N. Savoye, S. Schmidt, R. Turnewitsch, I. Vöge and J. T. Waples (2006) A review of present techniques and methodological advances in analyzing ^{234}Th in aquatic systems. *Marine Chemistry* 100: 190-212.

Santschi, P.H., Y.H. Li and J. Bell (1979) Natural radionuclides in the water of Narragansett Bay. *Earth and Planet. Sci. Lett.* 45: 201-213.

Sharma, P., L.R. Gardner, W.S. Moore and M.S. Bollinger (1987) Sedimentation and bioturbation in a salt marsh as revealed by ^{210}Pb, ^{137}Cs and ^{7}Be studies. *Limnology and Oceanography* 32: 313-326.

Sommerfield, C.K., C.A. Nittrouer and C.R. Alexander (1999) ^{7}Be as a tracer of flood sedimentation on the northern California continental margin. *Continental Shelf Research* 19: 335-361.

Swanson, L.R. and R. E. Wilson (2008) Increased tidal ranges coinciding with Jamaica Bay development contribute to marsh flooding. *Jounral of Coastal Research* 24: 1565-1569.

Toole, J., M.S. Baxter and J. Thomson (1987) The behavior of uranium isotopes with salinity changes in three UK estuaries. *Estuarine, Coastal and Shelf Science* 25: 283-297.

Turekian, K.K., Y. Nozaki, and L. Benninger (1977) Geochemistry of atmospheric radon and radon products. *Annual Review of Earth and Planetary Science* 5: 227-255.

Turekian, K. K., L. K. Benninger and E. P. Dion (1983) ^{7}Be and ^{210}Pb total depositional fluxes at New Haven, Connecticut, and Bermuda. *Journal of Geophysical Research* 88: 5411-5415.

Vogler, S, M. Jung and A. Mangini (1996) Scavenging of ^{234}Th and ^{7}Be in Lake Constance. *Limnology and Oceanography* 41: 1384-1393.

Zhu, J. and C.R. Olsen (2009) Beryllium-7 atmospheric deposition and sediment inventories in the Neponset River estuary, Massachusetts, USA. *Journal of Environmental Radioactivity* 100: 192-197.

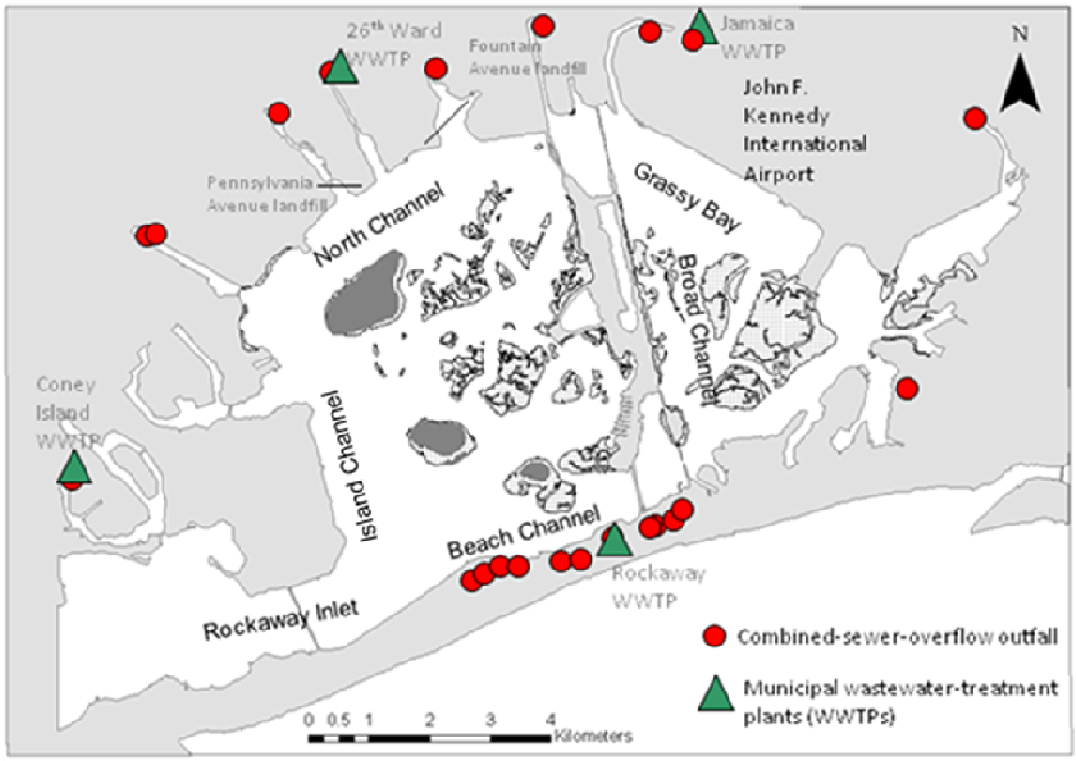

Figure 1-1. Location map of wastewater treatment plants and combined-sewage overflow outfall (adapted from Benotti et al., 2007) Dark areas in the marshes indicate the location of dredge spoil.

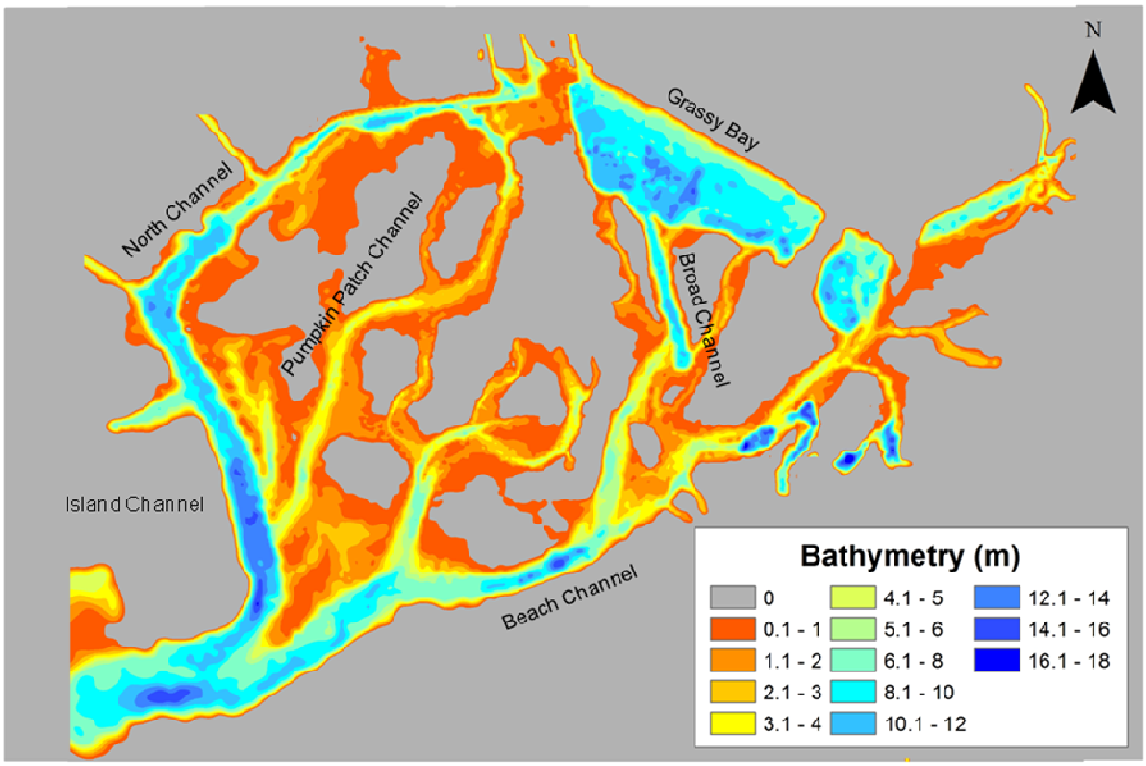

Figure 1-2 Bathymetry of Jamaica Bay (data provided by R.E. Wilson).

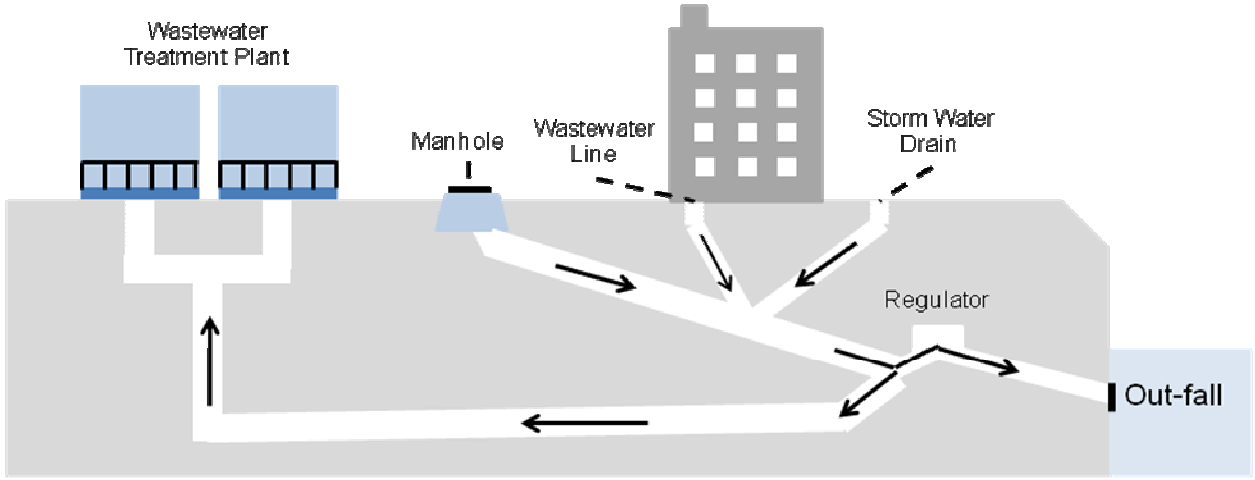

Figure 1-3. Schematic of a combined-sewer system where wastewater from homes and business combines with runoff from the streets during rainfall events. During certain rainfall events the amount of wastewater exceeds the capacity of the treatment plant and the regulator allows the overflow to directly enter the waterways (adapted from Ascher, 2005 and Duhigg, 2009).

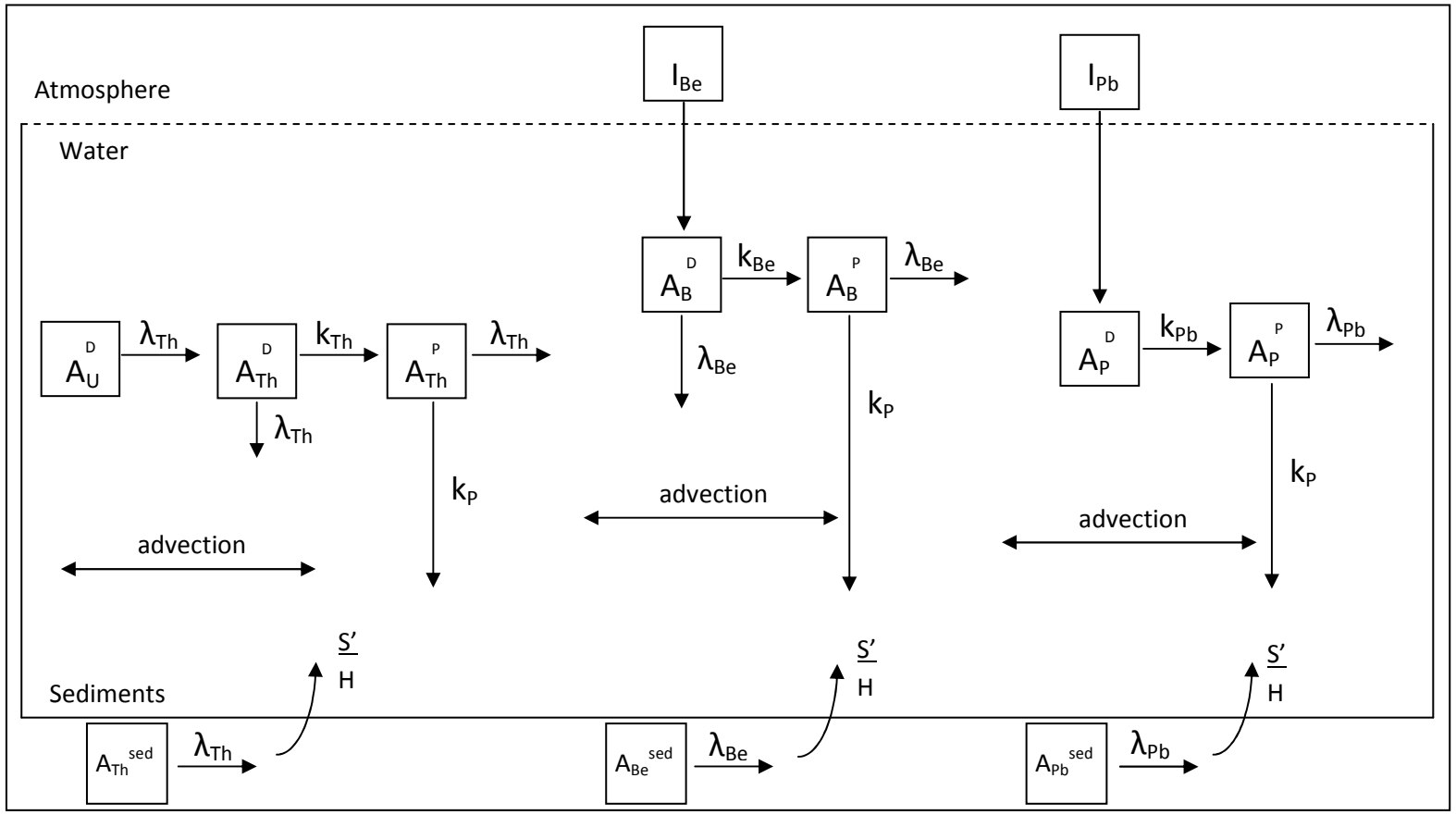

Fig. 1-4. Conceptual model of inputs and cycling of ^{234}Th, ^{7}Be, and ^{210}Pb within an estuarine system. A_U^D represents activity (dpm cm^{-3}) of dissolved ^{238}U, A_{Th}^D, A_{Be}^D, A_{Pb}^D is dissolved ^{234}Th, ^{7}Be, and ^{210}Pb activity (dpm cm-3), A_{Th}^P, A_{Be}^P, A_{Pb}^P represents the particle-associated ^{234}Th, ^{7}Be, and ^{210}Pb activity (dpm cm-3), I_{Be} and I_{Pb} is the flux of ^{7}Be and ^{210}Pb into the estuary from the atmosphere (dpm cm^{-2} day^{-1}), respectively, λ_{Th}, λ_{Be}, and λ_{Pb} represents the decay constants (per day)of the radionuclides, k_{Th}, k_{Be}, and k_{Pb} represents the particle scavenging rate constant (per day) for each radionuclide, k_P is the particle removal rate constant (per day), S' represents the particle resuspension rate (g cm^{-2} day^{-1}), h is the water depth (cm), A_{Th}^{sed}, A_{Be}^{sed}, A_{Pb}^{sed} is the activity in the surficial bottom sediments (figure adapted from Feng et al., 1999).

CHAPTER 2

Excess ^{234}Th Inventories in the Subtidal Sediments of an Urban Coastal Lagoon (Jamaica Bay, NY): A Tracer of Sediment Input and Redistribution

1. Abstract

^{234}Th (half-life = 24.1 days) is a naturally occurring, particle reactive radionuclide produced in seawater through the decay of its parent isotope ^{238}U, which is generally conservative with salinity. The inventory of $^{234}Th_{xs}$ was measured in the surficial bottom sediments in Jamaica Bay, NY during four cruises in September-2004, May-2005, November-2005 and July-2006. Although the $^{234}Th_{xs}$ inventories in the sediments varied spatially throughout the bay, the mean inventory for the four cruises ranged from 3.4 to 5.6 dpm cm^{-2}. $^{234}Th_{xs}$ inventories in the upper 5 cm of the sediments were 2-5 times in surplus relative to the ^{234}Th production in the water column suggesting an import of ^{234}Th from the ocean either in the dissolved form or associated with particles. Specific activities of ^{234}Th on inorganic particles in the water column ranged from ~ (0.1 - 0.5 dpm L^{-1} or 5.2 – 40.7 dpm g^{-1}) with the highest activities found at the inlet and just within the bay. Total ^{234}Th activity in the water column ranged from 0.1 to 0.7 dpm L^{-1} with the highest total ^{234}Th activity measured at the inlet. "Dissolved" ^{234}Th activity (Total ^{234}Th – ^{234}Th activity on particles) was 0.2 dpm L^{-1} at the inlet site. The presence of dissolved ^{234}Th and the high specific activity on particles at the inlet suggests that the surplus of ^{234}Th measured within the sediments is supplied by an import of both dissolved ^{234}Th and $^{234}Th_{xs}$ particulates imported from the ocean. Using a mass balance of ^{234}Th in the sediments in surplus to that produced within the bay, import of sediment into the bay was

estimated to be 4.3 to 35.8 x 10^{10} g y^{-1}. A previous attempt at a sediment budget based on sediment deposition in the subtidal bay and on the marshes using ^{210}Pb geochronologies suggested that 1.5 to 2.9 x 10^{10} g y^{-1} of sediment needed to be imported into Jamaica Bay to keep the sediment budget in balance. The differences in the import estimate between this and previous studies may be a result of limited sampling at the inlet during this study and the occurrence of events such as storms that could temporarily enhance sediment import.

2. Introduction

Previous studies have used ^{234}Th in a range of environments in order to understand mixing in the water column, sediment transport, deposition, and resuspension (Aller and Cochran, 1976; Aller et al., 1980; DeMaster et al., 1985; DeMaster et al., 1986; Feng et al., 1999a; Feng et al., 1999b; Giffen and Corbett, 2003; McKee et al., 1983). Naturally occurring radionuclides, such as ^{234}Th (half-life = 24.1 days) have been useful in studies within coastal areas due to high particle reactivity, a well-established decay rate, and a well-constrained sourced (Feng, et al., 1999a). Short-lived radionuclides are particularly useful in studying processes that operate on seasonal time scales.

^{234}Th is produced in an estuary through the decay of its parent isotope ^{238}U, a primordial radionuclide that is typically conservative with salinity. Under oxic condtions ^{238}U is part of a soluble uranyl tricarbonate complex and has low particle reactivity. Thorium-234, unlike its parent isotope, is present as the Th 4+ ion, is particle-reactive under most conditions, is readily scavenged on to available particle surfaces (K_d = 1–

50×10^5), and may settle through the water column (Baskaran and Santschi, 1993; Feng et al., 1999a). Removal of ^{234}Th from the water column creates disequilibrium between ^{234}Th and ^{238}U, leaving the water column depleted in ^{234}Th.

In coastal systems where suspended sediment concentrations may be high, the ^{234}Th produced in the water column is effectively scavenged onto particle surfaces leaving little in the dissolved form. Once scavenged onto particles, ^{234}Th may remain suspended in the water column until it decays or it may be advected or deposited (Aller and Cochran, 1976; Feng et al., 1999a; Feng et al., 1999b).

Coastal lagoons are typically geologically ephemeral, shallow, and separated from the ocean by a barrier island. These systems are often thought to be sinks for organic and inorganic sediments and can be highly impacted by anthropogenic processes (Kjerfve, 1994). Sediment is carried into coastal lagoons by rivers, by tidal currents from an ocean source, and by winds. Additional material deposited within lagoons may include material of organic origin, such as shells and peat. Increased sediment yield to lagoon may be caused by the reduction of vegetative cover and the onset of soil erosion in the surrounding river catchment. Although lagoons serve primarily as sediment sinks, the sediment is often extensively modified, recycled, and reworked (Bird, 1994). In this study we used the patterns of ^{234}Th in an urban coastal lagoon and the seasonal and spatial variation of $^{234}Th_{xs}$ in surficial, subtidal sediments to evaluate sediment transport and deposition.

3. Methods

3.1 Study Site

Jamaica Bay (see Chapter 1, Fig. 1-1) is a small coastal lagoon (53 km^2; Benotti, et al., 2007) located along the southern coast of western Long Island (O'Shea and Brosnan, 2000). The bay is shallow (mean depth ~5 m), has no significant riverine input, and contains numerous salt marsh islands. Ocean water enters the bay through Rockaway Inlet, which serves as a pathway for particle and water exchange between the Bay and the New York Bight. The dominant supply of freshwater is wastewater from four sewage treatment facilities in New York City. Due to its location, Jamaica Bay has been subjected to many of the impacts that come with heavy urbanization, such as extensive dredging, marsh ditching, marsh filling, bulkheading, and landfill construction (Black, 1981; Botton et al., 2006).

3.2 Field Methods

Subtidal sediment samples were collected in Jamaica Bay during cruises in September-2004, May-2005, November-2005, and July-2006. The timing of the sampling cruises was structured to compare changes in spring, summer and fall conditions due to changes in seasonal wind patterns, precipitation and frequency of storm events. The sample sites were distributed throughout the bay with emphasis on regions of interest after the initial sampling. Surficial sediment samples used for $^{234}Th_{xs}$ inventories were collected using an Ekman bottom grab. Each grab sample was examined to insure the sediment surface was preserved and then the top 5 cm of the grab

sample were sub-sampled with a plastic cylindrical cone and returned to the lab for radiometric analysis. This sampling strategy was designed to obtain the entire sediment inventory of ^{234}Th in a single sample at each site and thus maximize the number of sites sampled at any given time. Generally, 60-70 sites were sampled during each cruise and initial gamma counting was completed within ~3 weeks.

Additional subtidal sediment samples were taken in August-2008. Grabs were taken in areas dominated by fine sediments at 5 locations to determine the $^{234}Th_{xs}$ inventory in the upper 2 mm compared with the total inventory in the upper 5 cm at these sites (Fig. 2-1). Samples were taken in sand-dominated areas to determine the total $^{234}Th_{xs}$ inventory at these sites and the inventory of $^{234}Th_{xs}$ associated with sand-sized sediments (Fig. 2-1).

In August-2008 the activities of ^{234}Th associated with particles in the water column entering the bay and within the bay were measured by filtering large volumes (>100 liters) of bay water through ship-powered in-situ pumps equipped with a polypropylene filter cartridge (CUNO Micro-Wynd II® D-CCPY, nominal 1 μm) at select sites (Fig. 2-2). Additional water samples were also taken at these sites to determine total ^{234}Th (particulate + dissolved), salinity, and dissolved ^{238}U in the water column. An additional 30 L water sample was taken in June-2009 at the inlet and filtered through a polypropylene filter cartridge to determine particle bound ^{234}Th activity.

3.3 Laboratory Methods

The surficial sediment samples were returned to the lab, homogenized, and weighed. Samples were analyzed for ^{234}Th (63 keV) by counting the wet samples on a

Canberra 3800 mm^2 germanium gamma detector for ~ 24 hours. To determine counting efficiencies and to correct for the self-absorption that occurs below 200 keV, liquid standards of varying densities were spiked with ^{238}U and counted several times on each detector. Sediment samples were recounted after 4 months to determine the ^{234}Th supported by the ^{238}U within the samples; this value was used in calculation of excess ^{234}Th ($^{234}Th_{xs}$) activities.

To compare the total $^{234}Th_{xs}$ inventory in a grab sample with that contributed by the sand-sized fraction of sediments alone, grab samples were taken at 3 sites and a subsample was analyzed for $^{234}Th_{xs}$. A larger subsample was taken, dried, and then soaked in a 0.5% sodium hexametaphosphate saltwater solution, agitated, and then wet sieved through a 63 µm sieve. The sand fraction was then dried and analyzed for $^{234}Th_{xs}$.

Cartridges from the high-volume water sampling were ashed in a furnace at 450°C for 24 hours. The remaining ash (comprised of inorganic particles) was counted on Canberra 3800 mm^2 germanium gamma detectors for 24 hours to determine activities of ^{234}Th on inorganic, filterable particles. Samples were recounted after five months to determine the supported ^{234}Th on filterable particles. Total suspended solids (TSS) for the water column stations were determined by normalizing the ash weight to the liters filtered through the cartridge.

Total ^{234}Th at the water column stations was determined using the basic small volume (2 – 20 L) procedure described by Rutgers van der Loeff and Moore (1999) as refined for use in smaller volume samples by Buesseler et al (2001) and Benitez-Nelson (2001). In this method ^{234}Th is co-precipitated with MnO_2 by increasing the pH of the 2-L sample to ~9 by adding NaOH, adding 250 µl of $KMnO_4$ and then adding 100 µl of

$MnCl_2$. After 8 hours the sample was filtered through a 1 µm, 25 mm diameter, microquartz filter. The filter was dried, mounted and then counted on a RISØ muticounter, low-level betacounter. Mounted samples were counted 6 times over a 3 month period to differentiate ^{234}Th activity in the sample from other, longer-lived radionuclides (e.g. ^{210}Pb). ^{238}U activity in the water column was determined by aging 2-L of water for 5 months, allowing time for in-growth of ^{234}Th and equilibrium between ^{234}Th and ^{238}U. The ^{234}Th activity (assumed to be in equilibrium with ^{238}U) was then measured by the procedure previously outlined.

4. Results

4.1 Excess ^{234}Th in Subtidal Sediments

Inventories of $^{234}Th_{xs}$ in sediments were calculated using the equation:

$$I_{Th} = A_{Th} \times \rho_i \times 5 \text{ cm} \qquad (2\text{-}1)$$

where I_{Th} is the $^{234}Th_{xs}$ inventory (dpm cm^{-2}), A_{Th} is the $^{234}Th_{xs}$ activity (dpm g^{-1}), ρ_i is the dry bulk density of the sample (g cm^{-3}), and 5 cm is the depth of each sample. As noted above, the sampling scheme was designed to obtain the entire excess ^{234}Th inventory in a single sample. This assumption was tested and found to be reasonable by measuring the ^{7}Be activity (half-life = 53.3 days) in the upper 6 cm of gravity cores taken separately (see Chapter 3). ^{7}Be activity was confined to the upper 2 cm, except in core 1 where ^{7}Be was measured to 4 cm (see Chapter 3, Fig. 3-13).

Sediment samples were collected in August-2008 with the purpose of comparing the inventory of excess ^{234}Th in the upper 2 mm of bottom sediments with the inventory

in the upper 5 cm of the same sediments. At the sample sites selected the activity of ^{234}Th in the upper 2 mm dominated the samples (80 -100%; Fig 2-1; Table 2-1).

There were spatial and seasonal variations in the inventories of $^{234}Th_{xs}$ within Jamaica Bay during the sampling cruises (Fig. 2-3). The range of inventories of $^{234}Th_{xs}$ measured during four sampling cruises in 2004-2006 and the bay-wide means of activities and inventories are given in Table 2-2.

4.2 General Patterns of Radionuclides in the Subtidal Sediments

The spatial and seasonal variation of $^{234}Th_{xs}$ in the bottom sediments during the sampling cruises are shown in Fig. 2-3. In September-2004 the high inventories of $^{234}Th_{xs}$ were measured near the marsh islands in the western part of the bay and in the southern channel adjacent to the Rockaway waste-water treatment plant and the combined-sewer overflow outfall (Fig. 2-3A). High inventories also were observed in the southeastern part of the bay (Fig. 2-3A). Inventories of $^{234}Th_{xs}$ from the May-2005 cruise were also high near the marsh islands in the western portion of the bay, however there were also high inventories near the inlet (Fig. 2-3B). In November-2005 instances of high inventories were found in all areas of the bay, with the highest $^{234}Th_{xs}$ inventories in the eastern part, particularly near the marsh islands, and in the southeastern deep channel (Fig. 2-3C). During the July-2006 sampling cruise, the $^{234}Th_{xs}$ inventory pattern was similar to November-2005 with highest $^{234}Th_{xs}$ in the bottom sediment near the eastern marshes and in the southeastern channel (Fig. 2-3D).

To better visualize the general spatial trends in $^{234}Th_{xs}$ inventories, Jamaica Bay was divided into a western and eastern areas, divided by broad channel island (see

Chapter 1, Fig. 1-1). The mean $^{234}Th_{xs}$ inventories of sites sampled in western and eastern part of the bay were 5.2 ± 0.9 and 3.7 ± 0.9 dpm cm^{-2}, respectively (Fig. 2-4A). Mean inventory of sites measured during the May-2005 sampling cruise were significantly lower in the eastern half of the bay (2.4 ± 0.6 dpm cm^{-2}) than in the western half of the bay (6.0 ±0.8; Fig. 2-4B). During the November-2005 sampling cruise the mean inventory of the western and eastern half of the bay were similar (4.2 ± 0.7 and 5.2 ± 0.6 dpm cm^{-2}, respectively; Fig. 2-4C). During the July-2006 cruise the mean inventory in the western bay (2.5 ± 0.5 dpm cm^{-2}) was significantly lower than in the eastern part of the bay (5.2 ± 0.6 dpm cm^{-2}; Fig. 2-4D).

4.3 Inventories of $^{234}Th_{xs}$ in Sand Dominated Sediments

A summary of the total inventory of $^{234}Th_{xs}$ in the subtidal sediments, compared with the inventory of $^{234}Th_{xs}$ contributed by the sand fraction, is given in Table 2-3. The 3 sites sampled were dominated by sand (> 95%). $^{234}Th_{xs}$ inventory was low at sites JB8-08-27 and JB-08-28, with no measurable $^{234}Th_{xs}$ present in the sand fraction of the sediment (Table 2-3, Fig. 2-1). In contrast, site JB8-08-26 had a higher $^{234}Th_{xs}$ inventory in the upper 5 cm than the other two sites, and the sand fraction had a measurable $^{234}Th_{xs}$ inventory (Table 2-3, Fig. 2-1).

4.4 Activity of ^{234}Th in the Water Column

A summary of total $^{234}Th_{xs}$ and the activity of $^{234}Th_{xs}$ on suspended mineral particles in the water column are given in Table 2-4. Total $^{234}Th_{xs}$ and $^{234}Th_{xs}$ associated with particles was highest at the station closest to the inlet and in the deep water just within the bay (Fig. 2-2). Lowest total $^{234}Th_{xs}$ and activity were measured on inorganic filterable particles in the interior of the bay near the marsh islands in the east. Salinity measured at the water column station varied only slightly from 28.5 at the inlet station to 26.6 in Grassy Bay (Table 2-4; Fig. 2-2). The activity of ^{238}U in the water column at these sites also showed little variation, ranging from 1.9 to 2.0 dpm L^{-1} (Table 2-4).

5. Discussion

5.1 Variations in Spatial Distribution of $^{234}Th_{xs}$ and Storm Events

The differences in spatial distribution and magnitude of $^{234}Th_{xs}$ inventories in the surficial bottom sediments as measured during September-2004, May-2005, November-2006 and July-2006 cruises (Figs. 2-3, 2-4) may, in part, reflect redistribution of surficial sediment within the bay. Indeed, the results of the subtidal samples taken in August-2008 show that >75% of the $^{234}Th_{xs}$ inventory was within the upper 2 mm (Table 2-1). These results suggest that while mean $^{234}Th_{xs}$ inventories did not vary greatly between sampling cruises (Table 2-2), changes in spatial distribution within the bay between cruises may be a result of the resuspension, transport and re-deposition of a thin veneer of sediments at the sediment-water interface.

The spatial distribution and magnitude of $^{234}Th_{xs}$ inventories in the surficial bottom sediments as measured during the May-2005 and November-2005 cruises (Figs. 2-3B, C) may also, in part, reflect changes in the import of fine-grained particles from the ocean (see section 5.2). In general there is a seasonal pattern of storm activity off the coast of Long Island, with more frequent storms occurring during winter and early spring, resulting in higher significant wave heights (Fig. 2-5). Storm activity and the increase in significant wave heights off the coast may also be observed within the bay. While ocean waves would not impact the bay directly, storm winds, especially from the southwest, would produce wind-driven waves in the bay and resuspend bottom sediment. Tidal, estuarine and wind-driven currents would then redistribute suspended sediments, allowing them to deposit in deeper waters of the bay, and, possibly, onto salt marshes (see Chapter 5). There are two tidal gauges in Jamaica Bay, one at Inwood Park and the other at Rockaway Inlet (Fig. 2-6). The rate of change of the difference in mean daily tidal height between these two stations indicates flow of water between the eastern and western bay. If the mean daily tidal height at the eastern station (Inwood) is increasing with respect to that at Rockaway, water is being pushed into the bay from the ocean by wind and waves.

Mean $^{234}Th_{xs}$ inventories of in the surficial bottom sediments of the western and eastern parts of the Bay during the September-2004 and November-2005 sampling cruise did not vary significantly. However, the May-2005 cruise the mean $^{234}Th_{xs}$ inventory in the western part of the bay was significantly higher than in the eastern bay (Fig. 2-4). Prior to the sampling cruise in May-2005, winds recorded at JKF Airport were from the south (Fig. 2-7). These dominant winds may have prevented transport of sediment and

associated ^{234}Th to the eastern part of the bay, particularly Grassy Bay, and may have even resulted in transport of ^{234}Th produced by the decay of ^{238}U in the eastern part of the bay to the western bay.

$^{234}Th_{xs}$ inventories in subtidal sediments in November-2005 were high near the western marshes, but were also high in Grassy Bay (Fig. 2-3C). In July-2006 the mean $^{234}Th_{xs}$ inventories were significantly higher in the eastern part of bay than the western (Fig. 2-4). In contrast to May-2005, there was a large storm event prior to the November-2005 sampling cruise. This storm event resulted in higher significant wave heights offshore at the ALSN6 buoy station (Fig. 2-5). Offshore waves were also consistently higher than normal prior to the July-2006 cruise. Strong local winds out of the southwest, along the long axis of the bay and oriented with the two channels of exchanges between the western and eastern bay, prior to both the November-2005 and July-2006 sampling cruises, would have likely resulted in increased wave action in the bay (Figs. 1-1, 2-7). These conditions may have contributed to an increase in the import of ocean-derived sediment and associated ^{234}Th into the bay, as well as increased the ^{234}Th and sediment transport to the eastern part of the bay. Overall, the spatial patterns of $^{234}Th_{xs}$ inventories in bottom sediments of Jamaica Bay suggest following periods of storm activity and winds out of the southwest, the transfer of particles and associated ^{234}Th to the eastern, deeper parts of the bay can occur.

5.2 Mass Balance of $^{234}Th_{xs}$

5.2.1 In Situ Production

^{234}Th is produced within Jamaica Bay by the decay of its parent isotope, ^{238}U, which has generally been found to be conservative with salinity. Water column sampling was conducted in Jamaica Bay in August-2008 at four sites (Fig. 2-2). Salinity at these sites ranged from 26.6 to 28.5 and the activity of ^{238}U at these sites ranged from 1.9 to 2.0 dpm L^{-1} (Table 2-4). These results agree with to the relationship found between salinity and ^{238}U (^{238}U (dpm L^{-1}) = 0.0707 × salinity + 0.0276, r^2 = 0.955) by Feng et al. (1999a) in the Hudson River estuary. The relationship between ^{238}U and salinity allows for production of ^{234}Th in the water column to be estimated from salinity:

$$\text{Expected } ^{234}Th_{xs} \text{ inventory} = A_{238} \times H \qquad (2\text{-}2)$$

where A_{238} is the dissolved ^{238}U activity (dpm cm^{-3}) estimated from the salinity and H is the water depth in cm. The observed salinity of Jamaica Bay has been reported to vary 23 up to 28.5 (mean depth ~ 26; R.E. Wilson Pers. Comm.), and the subtidal depth ranges from 2 to 10 meters (mean depth ~ 5 m; Benotti et al., 2007). The estimated production of ^{234}Th within the bay from the decay of dissolved ^{238}U ranges from ~0.3 – 2.0 dpm cm^{-2} based on the variation of salinity and depth observed in the bay, while the average production of ^{234}Th based on a mean bay depth of 5 m over the observed salinities ranges from ~0.8 – 1.0 dpm cm^{-2}. Thus complete scavenging of ^{234}Th produced within the bay should result in sediment inventories of $^{234}Th_{xs}$ of ~0.3 - 2.0 dpm cm^{-2} (mean ~ 0.9 dpm cm^{-2}). However, the mean $^{234}Th_{xs}$ inventories in the bottom sediments of Jamaica Bay

during all sampling cruises range from 3.4 – 5.6 dpm cm^{-2} (Table 2-2). The sampling intensity is sufficient to indicate that this phenomenon of "surplus" inventory relative to that expected from ^{238}U decay within the bay occurs bay-wide. Such surplus inventories can be produced in only two ways: import of particles with associated $^{234}Th_{xs}$ into the bay and/or tidal exchange of water with dissolved ^{234}Th that is transported into the bay, scavenged onto particles and deposited.

5.2.2 Import of ^{234}Th from the Ocean

To assess the possible import of dissolved ^{234}Th and $^{234}Th_{xs}$ in association with particles, total ^{234}Th activity in the water column and ^{234}Th activities on particles filtered from the water column were measured at 4 stations in September-2008 during a flooding tide (Fig. 2-2; Table 2-4). Total ^{234}Th activity in the water column (dissolved + particulate) was highest at the inlet station (0.5 ± 0.1 dpm L^{-1}). $^{234}Th_{xs}$ activity on particles was also highest at the inlet station (0.3 ± 0.02 dpm L^{-1} or 20 ± 1.4 dpm g^{-1}; ~ 65% of the total activity) and just within the bay in the deep water (0.11 ± 0.01 dpm L^{-1} or 7.8 ±0.8 $dpmg^{-1}$; ~ 58% of the total ^{234}Th). The high activity on the suspended particles at near the bay inlet suggests that excess ^{234}Th is imported into the bay from the ocean associated with particles. However, the presence of "dissolved" ^{234}Th near the inlet suggests that dissolved ^{234}Th can also be imported in solution into the bay, where it can be scavenged. At all the water column stations sampled there was already substantial scavenging of ^{234}Th, as the ratio of $^{234}Th/^{238}U$ ranged from ~0.07 to 0.24.

If we assume that sediment inventories of $^{234}Th_{xs}$ that are greater than production in the overlying water column represent the import and deposition of dissolved ^{234}Th

entering the inlet that can be scavenged onto particles as well as $^{234}Th_{xs}$ associated with particulate material that enters the system, we can estimate the contribution of dissolved ^{234}Th (entering through the inlet) to the surplus inventory in the subtidal sediments from:

$$\text{Dissolved } ^{234}\text{Th Import} = (V_{in} \times t_d \times Th_D) / (\lambda_{Th} \times \text{Subtidal Bay Area}) \qquad (2\text{-}3)$$

where V_{in} is the tidal prism (difference in the volume of water in an estuary between mean high and low tide)of Jamaica Bay (6.06×10^{10}L; Beck et al., 2007), t_d is the tidal cycles per day (1.91), Th_D is the dissolved ^{234}Th measured in the water column at the inlet station in August-2008 (0.17 ± 0.1 dpm L^{-1}; Table 2-4), λ_{Th} is the decay constant of ^{234}Th (0.029 day^{-1}), and the area of the subtidal bay is ~ 39 km^2 (3.9×10^{11} cm^2). The assumption in this calculation is that the dissolved ^{234}Th activity measured at the inlet station represents the typical dissolved ^{234}Th activity at Rockaway Inlet. This calculation yields a dissolved ^{234}Th input into the bay of 2.1 dpm cm^{-2} which represents 30 - 50% of the observed inventories of $^{234}Th_{xs}$ in the subtidal sediments. The remaining surplus inventory is likely imported into the bay as particulate $^{234}Th_{xs}$.

The import of particulate ^{234}Th through the inlet can be calculated from:

$$\text{Particulate } ^{234}\text{Th Import} = (V_{in} \times t_d \times Th_P) / (\lambda_{Th} \times \text{Subtidal Bay Area}) \qquad (2\text{-}4)$$

where V_{in} is the tidal prism of Jamaica Bay (6.06×10^{10}L; Beck et al., 2007), t_d is the tidal cycles per day (1.91), Th_P is the mean particulate ^{234}Th measured in the water column at the inlet station in August-2008 (0.31 ± 0.02 dpm L^{-1}; Table 2-4), λ_{Th} is the decay constant of ^{234}Th (0.029 day^{-1}), and the area of the subtidal bay is ~ 39 km^2 (3.9×10^{11} cm^2). The assumption in this calculation is that the particulate ^{234}Th activity

measured at the inlet station represents the typical particulate ^{234}Th activity at Rockaway Inlet. This calculation yields a particulate input into the Bay of 3.2 dpm cm^{-2}. Thus, the import of particulate ^{234}Th alone accounts for 57 – 94% of the $^{234}Th_{xs}$ inventory in the subtidal sediments.

The input terms of ^{234}Th in to Jamaica Bay (in situ production + dissolved and particulate ^{234}Th import through the inlet) would result in a ^{234}Th inventory of 5.9 dpm cm^{-2}. This is 0.3 to 2.5 dpm cm^{-2} in surplus to the $^{234}Th_{xs}$ inventory measured in the subtidal sediments and suggests there is not complete retention within the subtidal Bay of all imported ^{234}Th. Surficial samples were taken on select salt marsh islands in September-2004 and May-2005. $^{234}Th_{xs}$ inventories for September-2004 and May-2005 were 5.4 ± 0.9 and 2.7 ± 1.0 dpm cm^{-2}, respectively, suggesting that deposition on the salt marshes is one pathway of loss of ^{234}Th from the subtidal Bay. However, sampling density on the marsh islands was insufficient to quantify this loss term (see Chapter 5 for details). Another possible pathway of loss ^{234}Th from Jamaica Bay is exportation through the inlet.

5.2.3 Loss of ^{234}Th from the Bay

Jamaica Bay is a flood dominated coastal lagoon with baroclinic driven estuarine flow (Swanson and Wilson, 2008; Wilson pers comm.), making it likely there is loss of ^{234}Th from Jamaica Bay in the outflow of fresher, surface waters. Loss of ^{234}Th from the Bay can be calculated if we assume that the activity of ^{234}Th, just within the bay (Station JB-WS-2-Shallow and Deep, Table 2-4) characterizes the water lost from the Bay:

$$\text{Export of } ^{234}\text{Th} = [(Th_{D,P}) \times V_{out} \times t_d] \div (\lambda_{Th} \times \text{subtidal bay area}) \qquad (2\text{-}5)$$

where $Th_{D,P}$ is the mean activity of particulate ^{234}Th (0.10 dpm L^{-1}) or dissolved ^{234}Th just within the bay (0.14 dpm L^{-1}), just within the bay (JB-WS-2-Shallow; Table 2-4), subtidal bay area is 3.9×10^{11} cm^2, V_{out} is the tidal prism of Jamaica Bay (6.06×10^{10} L ; Beck et al., 2007) plus the average daily water discharge from the wastewater treatment plants in the bay (7.5×10^8 L d^{-1}; Beck et al., 2007), t_d is the tidal cycles per day (1.91) and (λ_{Th}) is the radiometric mean-life of ^{234}Th (0.029 d^{-1}). This calculation yields a particulate ^{234}Th and dissolved ^{234}Th loss from the Bay of 1.0 and 1.4 dpm cm^{-2}, respectively. Like the previous calculations, this calculation assumes that dissolved and particulate ^{234}Th activities in the upper water column August-2008 are representative of typical conditions in the bay. In addition, the average daily flow from the wastewater treatment plants includes the Coney Island plant located near the mouth of the bay (Fig. 1-1). Much of the wastewater discharge from this plant may not enter the bay, thus the ^{234}Th loss through the inlet is most likely an overestimation.

The terms for the mass balance of ^{234}Th are compiled in Table 2-5. The predicted inventory of $^{234}Th_{xs}$ in the subtidal sediments that would result from this mass balance is 3.5 dpm cm^{-2}. This is 63 – 100% of the inventories measured during all the sampling cruises and 97 - 100% of the inventories measured in May-2005 and July-2006. Water column sampling used in the mass balance was in August-2008 and may very well reflect the ^{234}Th balance during the spring/summer. Additional measurements in the water column would be needed to determine the averaged import and export of ^{234}Th into the Bay. Also note that $^{234}Th_{xs}$ inventories were measured on marsh islands in September-2004 and May-2005 the sampling coverage was not sufficient to extrapolate these inventories over the entire marsh surface area and include them in the mass balance.

5.2.4 Mass Estimate of Sediment from the Ocean

Using the mass balance of $^{234}Th_{xs}$ an estimate of annual net sediment import (g y^{-1}) can be made using the equation:

$$\text{Sediment import} = [I_{Th}' \div (Th_P \div TSS)] \times \lambda_{Th} \times \text{subtidal bay area} \qquad (2\text{-}6)$$

where I_{Th}' is the mean $^{234}Th_{xs}$ inventory in the bottom sediments in surplus relative to that produced within the bay (maximum ~ 1.0 dpm cm^{-2}) and the ^{234}Th imported as dissolved ^{234}Th using the averaged dissolved activity at the inlet station (2.1 dpm cm^{-2}; see eqn. 2-3) for the four sampling cruises (0.3 – 2.5 dpm cm^{-2}), Th_P is the mean activity of $^{234}Th_{xs}$ on filterable particles at the inlet station (~ 0.38 dpm L^1; Table 2-4), TSS is the mean concentration of total suspended solids at the inlet station (0.0133 g L^{-1}), λ_{Th} is the decay constant of ^{234}Th (10.5 yr^{-1}), and the area of the subtidal bay is 39 km^2 (3.9×10^{11} cm^2). Using the mean inventory during each of the sampling cruises, estimates of particle import from the ocean to the subtidal bay range from $4.3 – 35.8 \times 10^{10}$ g y^{-1}.

We can compare these estimates of sediment import to Jamaica Bay based on the mass balance of $^{234}Th_{xs}$ with other estimates. An earlier attempt at a sediment budget for inorganic silt and clay in Jamaica Bay (Bokuniewicz and Ellsworth, 1986) required an input of 1.5 – 2.9 x 10^{10} g y^{-1} (15 – 29 thousand MT y^{-1}) to bring the Bay's sediment budget into balance. This sediment budget included an estimate of sediment sources due to *in situ* production (0.1 x 10^{10} g y^{-1}), and sewage treatment plants (0.5 x 10^{10} g y^{-1}). Significantly, the importation of fine-grained sediment through Rockaway Inlet seemed to be the dominant sediment source. Sediment sinks included deposition in dredged channels (0.1 x 10^{10} g y^{-1}) subtidal areas (0.6 – 1.5 x 10^{10} g y^{-1}) and marshes (1.5 – 2.0 x

10^{10} g y^{-1}). Evidence for the importation of sediment has been documented in other estuaries in the region, such as Long Island Sound (Bokuniewicz et al., 1976), Newark Bay (Suszkowski, 1978), the Hudson River estuary (Ellsworth, 1986), and the Raritan River estuary (Renwick and Ashley, 1984).

Direct evidence of sediment import into Jamaica Bay was based on simultaneous measurements of water velocity by ADCP and suspended sediment concentrations across Rockaway Inlet over one tidal cycle on 30 September/1 October, 1995 (Lwiza and Bokuniewicz, unpublished data); a single tide can import 3.6×10^6 g of sediment into the Bay under the right conditions, resulting in an estimated yearly import of 2.6×10^9 g y^{-1}. The difference in the estimated annual import of sediment from direct measurement and the $^{234}Th_{xs}$ mass balance and the sediment budget, may suggest enhanced import of suspended sediments from the ocean during spring tides, favorable wind conditions and storm events (see section 5.1, this chapter). As well, because conditions vary, some tides will carry in less material and some will export sediment from the bay to the ocean. However, all estimates strongly indicate that sediment is imported into Jamaica Bay from the ocean. ^{234}Th-based estimates that are at the high end of the values estimated for sediment import are greater than other estimates and this likely reflects the fact that a limited sampling of total ^{234}Th in the water column and ^{234}Th associated with suspended particles was carried out. As well, ^{234}Th integrates over relatively short time intervals (a few months) and extrapolating to annual time scales on the basis of a few seasonal samplings may exaggerate sediment importation.

5.3 Spatial Patterns in the Deposition of Imported Sediment

The spatial pattern of deposition rates of sediment imported from the ocean into Jamaica Bay may be estimated by modifying equation 2-6 to:

$$\text{Sediment deposition rate} = [I_{Th}' \div (Th_P \div TSS)] \times \lambda_{Th} \qquad (2\text{-}7)$$

where I_{Th}' is the $^{234}Th_{xs}$ inventory in surplus of local production within the bay (maximum ~ 1.0 dpm cm^{-2}) and the averaged import of dissolved ^{234}Th through the inlet (2.1 dpm cm^{-2}; see eqn. 2-3), Th_P is the mean activity of ^{234}Th on suspended particles at Rockaway Inlet (0.38 dpm L^{-1}), TSS is the averaged particle concentration at the inlet (0.0133 g L^{-1}) and λ_{Th} is the decay constant of ^{234}Th (10.5 y). This calculation assumes that each site will have a minimum $^{234}Th_{xs}$ inventory equal to the production in the overlying water column, and that this inventory is maintained by resuspension, scavenging, and re-deposition rates by the net input of sediment. The surplus inventory is assumed to result from deposition of new sediment to the site. The resulting deposition at each sample site is then given in g cm^{-2} y^{-1}. Using this method, the mean mass deposition rates of sediment imported from the ocean varied by a factor of 8× and are 0.9, 0.1, 0.5, and 0.2 g cm^{-2} y^{-1} for the September-2004, May-2005, November-2005, and July-2006 cruises, respectively. The mass accumulation rates derived from the ^{210}Pb geochronologies of gravity cores taken in the bay varied similarly from 0.1 to 0.9 g cm^{-2} y^{-1} (see Chapter 3). These results suggest that although $^{234}Th_{xs}$ may be best used as a tracer for shorter-term processes due to its half-life, these short-term processes may be consistent and heavily influence the long-term accumulation with the bay.

Deposition rates of imported sediment (g cm^{-2} y^{-1}) naturally reflect the distribution of $^{234}Th_{xs}$ inventories for the sampling cruises. High deposition rates of sediment imported from outside the bay occurred near the western marshes during September-2004, May-2005, and November-2006 (Figs. 2-8A, B, C). High deposition occurred in the eastern part of the bay during November-2005 and July-2006 cruises (Figs. 2-8C, D). As noted in section 5.1, prior to both of these cruises high significant wave heights were observed at the ALSN6 buoy (Fig. 2-5). These results suggest that storm events are likely important in transporting sediments from the oceans to the far eastern part of the bay, particularly Grassy Bay.

6. Conclusions

Multiple seasonal samplings of inventories of $^{234}Th_{xs}$ in the subtidal sediments of Jamaica Bay showed significant spatial and temporal variations, likely as a result of resuspension and redistribution of bottom sediments, partly in response to winds and storm events. Despite these seasonal variations of the mean inventory of $^{234}Th_{xs}$ in the sediments there was a consistent surplus of $^{234}Th_{xs}$ relative to production of ^{234}Th within the bay from the decay of ^{238}U in the overlying water column suggesting that there is an additional source of ^{234}Th in to Jamaica Bay. An estimation of sediment import from the ocean into the bay was made assuming that the surplus of $^{234}Th_{xs}$ inventory in the sediments relative to in situ production resulted from the import of dissolved ^{234}Th through the inlet and the activity of ^{234}Th on particles measured at the inlet. Apparently 38 to 62% of the surplus could be explained by the import of dissolved ^{234}Th through the inlet, followed by its scavenging onto particles in the Bay. The remaining surplus would be imported as particulate ^{234}Th, resulting an annual sediment import of 4.3 – 35.8 x 10^{10}

g y^{-1}. Previous attempts to derive a sediment budget for Jamaica Bay using ^{210}Pb geochronologies included an import of $1.5 – 2.9 \times 10^{10}$ g y^{-1} to bring the bay into balance. The short-lived radionuclide based estimates are roughly an order of magnitude greater than previous estimates from suspended sediment concentrations and water velocity of a single tidal cycle, but the difference between the two estimates may reflect the fact that the radionuclides integrate over longer time scales and would include the effects of storm events. Indeed, the patterns of $^{234}Th_{xs}$ inventories in the subtidal sediment of the bay are consistent with transport of ^{234}Th–labeled particles to the northeast Bay (e.g. Grassy Bay) following storm events when winds were out of the southwest.

7. References

Aller, R.C., Benninger, L.K. and J.K. Cochran (1980) Tracking particle-associated processes in nearshore environments by use of Th-234 and U-238 disequilibrium. *Earth Planet. Sci. Lett.* 47: 161-175.

Aller, R.C. and J.K. Cochran (1976) $^{234}Th/^{238}U$ disequilibrium in near-shore sediment: Particle reworking and diagenetic time scales. *Earth Planet. Sci. Lett.: 29: 37-50.*

Baskaran, M. and P.H. Santchi (1993) The role of particles and colloids in the transport of radionuclides in the coastal environments of Texas. *Marine Chemistry:* 43: 95-114.

Beck, A.J., J.P. Rapaglia, J.K. Cochran and H.J. Bokuniewicz (2007) Radium mass-balance in Jamaica Bay, NY: Evidence for substantial flux of submarine groundwater. *Marine Chemistry:* 106: 416-441.

Benitez-Nelson, C.R., K.O. Buesseler, M.M. Rutgers van der Loeff, J.A. Andrews, L. Ball, G. Crossin and M.A.Charette (2001) Testing a new small-volume technique for determining thorium-234 in seawater, *Journal of Radioanalytical and Nuclear Chemistry* 248: 795-799.

Benotti, M.J. and B.J. Brownawell (2007) Distriubtion of pharmaceuticals in an urban estuary during both dry- and wet-weather conditions. *Environmental Science and Technology* 41: 5795-5802.

Bird, E.C. (1994) Physical Setting and Geomorphology of Coastal Lagoons. In *Coastal Lagoon Processes*, Björn Kjerfve (ed). Coastal Lagoon Processes, Elsevier, Amsterdam: 9-39.

Black, F.R. (1981) *Jamaica Bay: A History*. Gateway National Recreation Area New York, New Jersey.

Botton, M.L., R.E. Loveland, J.T. Tanacredi, and T. Itow (2006) Horseshoe Crabs (*Limulus polyphemus*) in an urban estuary (Jamaica Bay, New York) and the potential for ecological restoration. *Estuaries and Coasts* 29: 820-830.

Bokuniewicz, H., and J. Ellsworth (1986) Sediment budget for the Hudson system, *Journal of Northeastern Geology* 8: 158-164.

Bokuniewicz, H. J., J. A. Gebert and R. B. Gordon (1976) Sediment mass balance in a large estuary: Long Island Sound. *Estuarine and Coastal Marine Science* 4: 523-536.

Buesseler, K.O., C. Benitez-Nelson, M.M. Rutgers van der Loeff, J. Andrews, L. Ball, G. Crossin and M.A. Charette (2001) An intercomparison of small-and large-volume techniques for thorium-234 in seawater. *Marine Chemistry* 74: 15-28.

DeMaster,D.J., B.A. McKee, C.A. Nittrouer, J.C. Quian and G.D. Cheng (1985) Rates of sediment accumulation and particle reworking based on radiochemical measurements from continental-shelf deposits in the East China Sea. *Continental Shelf Research* 4, 143-158.

DeMaster, D.J., S.A. Kuehl and C.A. Nittrouer (1986) Effects of suspended sediments on geochemical processes near the mouth of the Amazon River: Examination of biological silica uptake and the fate of particle-reactive elements. *Continental Shelf Research* 6, 107-125.

Ellsworth, J. (1986) Shore erosion as a source of fine-grained sediment to the lower Hudson River. M.S. Thesis, Stony Brook University, Stony Brook, NY, 96pp.

Feng, H., J.K. Cochran and D.J. Hirschberg (1999a) ^{234}Th and ^{7}Be as tracers for the sources of particles to the turbidity maximum of the Hudson River Estuary. *Estuarine, Coastal, and Shelf Science* 49: 629-645.

Feng, H., J.K. Cochran, and D.J. Hirschberg (1999b) ^{234}Th and ^{7}Be as tracers for the transport and dynamics of suspended particles in a partially mixed estuary. *Geochimica et Cosmochimica Acta* 63: 2487-2505.

Giffen, D. and.R. Corbett (2003) Evaluation of sediment dynamics in coastal systems via short-lived radioisotopes. *Journal of Marine Systems 42: 83-96.*

Kjerfve, B. (1994) Coastal lagoons. In *Coastal Lagoon Processes*, Björn Kjerfve (ed). Coastal Lagoon Processes, Elsevier, Amsterdam: 1-7.

McKee, B.A.,C.A. Nittrouer and D.J. DeMaster (1983) Concepts of sediment deposition and accumulation applied to the continental shelf near the mouth of the Yangtze River. *Geology* 11,631-633.

O'Shea, M.L. and T.M. Brosnan (2000) Trends in indicators of eutrophication in western Long Island Sound and the Hudson-Raritan Estuary. *Estuaries* 23: 877-901.

Renwick, W. H. and G. M. Ashley (1984) Sources, storages and sinks of fine-grained sediment in a fluvial-estuarine system. *Geological Society of America Bulletin* 94: 1343-1348.

Roman, C.T., J.A. Peck, J.R. Allen, J.W. King and P.G. Appleby (1997) Accretion of a New England (USA) salt marsh in response to inlet migration, storms and sea-level rise. *Estuarine, Coastal and Shelf Science.* 45: 717-727.

Rutgers van der Loeff, M.M. and W.S. Moore (1999) The analysis of natural radionuclides in seawater. In: Grasshoff, K.,M.Ehrhardt, K. Kremling (Eds.), Methods of Seawater Analysis. VerlagChemie, Weinhim, pp. 365-397.

Rutgers van der Loeff, M. R., M. M. Sarin, M. Baskaran, C. Benitez-Nelson, K. O. Buesseler, M. Charette, M. Dai, O. Gustafsson, P. Masqué, P. J. Morris, K. Orlandini, A. Rodriguez y Baena, N. Savoye, S. Schmidt, R. Turnewitsch, I. Vöge and J. T. Waples (2006) A review of present techniques and methodological advances in analyzing ^{234}Th in aquatic systems. *Marine Chemistry* 100: 190-212.

Stumpf, R.P. (1983) The process of sedimentation on the surface of a salt-marsh. *Estuarine, Coastal and Shelf Science.* 17: 495-508.

Suszkowski, D. J. (1978) Sedimentology of Newark Bay, New Jersey: an urban estuary, Ph.D. Thesis, University of Delaware, 222 pp.

Swanson, L.R. and R. E. Wilson (2008) Increased tidal ranges coinciding with Jamaica Bay development contribute to marsh flooding. *Jounral of Coastal Research* 24: 1565-1569.

Table 2-1. Inventory of $^{234}Th_{xs}$ in the upper 2 mm and upper 5 cm taken in August-2008

Sample ID	Latitude (°N)	Longitude (°W)	Mud Fraction (%)	Specific Activity of excess ^{234}Th (dpm g^{-1}) in 0 – 2 mm	Specific Activity of excess ^{234}Th (dpm g^{-1}) in 0 -5 cm	Excess ^{234}Th (dpm cm^{-2}) in 0 - 2 mm	Excess ^{234}Th (dpm cm^{-2}) in 0 - 5 cm	% of Inventory in upper 2 mm
JB8-08-1	40.6120	73.8108	77	1.1 ± 0.3	0.04 ± 0.1	0.8 ± 0.2	0 ± 0.4	~100
JB8-08-4	40.6021	73.7950	73	4.1 ± 0.4	0.6 ± 0.1	2.2 ± 0.7	1.8 ± 0.4	~100
JB8-08-8	40.6152	73.7778	66	12.3 ± 2.5	1.1 ± 0.1	4.4 ± 1.1	4.1 ± 0.4	~100
JB8-08-20	40.6313	73.8348	72	0.3 ± 0.05	0.1 ± 0.1	0.5 ± 0.1	0.6 ± 0.1	83
JB8-08-23	40.6293	73.8742	57	3.1 ± 0.5	0.7 ± 0.4	2.7 ± 0.9	3.4 ± 0.4	79

Table 2-2. Summary table of excess ^{234}Th data from September-2004, May-2005, November-2005, and July-2006 sampling cruises.

	Mean $^{234}Th_{xs}$ Activity (dpm g^{-1})	Range of $^{234}Th_{xs}$ Inventories (dpm cm^{-2})	Mean $^{234}Th_{xs}$ Inventory (dpm cm^{-2})	Mean $^{234}Th_{xs}$ Inventory /Production*	"Surplus" $^{234}Th_{xs}$ Inventory (dpm cm^{-2})
September-04	1.4 ± 0.2	0 – 20.2	5.6 ± 0.8	6.2	4.5
May-05	1.5 ± 0.6	0 – 17.9	3.4 ± 0.7	3.8	2.3
November-05	1.8 ± 0.2	0 – 13.2	4.5 ± 0.4	5.0	3.4
July-06	1.8 ± 0.2	0 – 13.0	3.6 ± 0.4	4.0	2.5

* ^{234}Th production in the water column of 0.9 dpm cm^{-2} based on a salinity of 32 and a water depth of 5 meters.

Table 2-3. Excess ^{234}Th Inventory in the sand fraction of 0 – 5 cm sediments.

Sample ID	Latitude (°N)	Longitude (°W)	$^{234}Th_{xs}$ (dpm cm^{-2}) in Sand fraction	$^{234}Th_{xs}$ (dpm cm^{-2}) Total	% Sand	% Mud	Specific Activity of Sand Fraction (dpm g^{-1})	Specific Activity of $^{234}Th_{xs}$ in the Mud Fraction (dpm g^{-1})	Specific Activity of Mud Fraction (dpm g^{-1})	Specific Activity of ^{7}Be in the Mud Fraction (dpm g^{-1})
JB8-08-26	40.6008	73.879	1.9 ± 0.2	7.8 ± 1.2	96.2	3.8	0.2	22.5	16.3	8.2
JB8-08-27	40.5881	73.8446	0 ± 0.3	0.8 ± 0.2	97.6	2.4	0	10.1	4.2	10.1
JB8-08-28	40.5757	73.8699	0 ± 0.2	0.7 ± 0.2	97.5	2.5	0	6.9	3.5	6.7

Table 2-4. ^{234}Th activities of filterable (> 1 μm) particles in the water column

Sample ID	Description	Depth (m)	Salinity	TSS (mg L^{-1})	^{238}U (dpm L^{-1})	Total ^{234}Th (dpm L^{-1})	^{234}Th/^{238}U	Particulate $^{234}Th_{xs}$ (dpm L^{-1})	Particulate $^{234}Th_{xs}$ (dpm g^{-1})
JB-WS-1	Inlet Station	3.0	28.5	15.5	2.0 ± 0.06	0.48 ± 0.1	0.24	0.31 ± 0.02	20.0 ± 1.4
JB-WS-1*	Inlet Station	1.0	28.3	11.1	_	0.69 ± 0.2	_	0.45 ± 0.1	40.7 ± 7.3
JB-WS-2-Shallow	Bay Interior	1.0	28.3	13.1	2.0± 0.05	0.24 ± 0.1	0.12	0.10 ± 0.01	7.8 ± 0.9
JB-WS-2-Deep	Bay Interior	5.0	28.5	16.5	2.0 ± 0.05	0.19 ± 0.1	0.10	0.11 ± 0.01	7.8 ± 0.8
JB-WS-3	Grassy Bay	5.0	26.6	15.0	1.9 ± 0.06	0.15 ± 0.1	0.08	0.13 ± 0.02	7.5 ± 1.3
JB-WS-4	Near eastern marshes	2.0	27.5	15.2	2.0 ± 0.06	0.13 ± 0.1	0.07	0.08 ± 0.02	5.2 ± 1.3

* Additional sample (28 L) was taken at inlet in June-2009

Table 2-5 Mass Balance of $^{234}Th_{xs}$

	Total ^{234}Th (dpm, $\times 10^{10}$)	^{234}Th (dpm cm^{-2})
Inputs		
Production in the Water Column	39	1.0
Import from the Ocean		
Aqueous phase	66	1.7
On suspended particles	125	3.2
Total Import	191	4.9
Export		
Loss via Inlet		
Aqueous phase	55	1.4
On suspended particles	39	1.0
Total Export	94	2.4
Predicted ^{234}Th Inventory from Mass Balance	136	3.5
^{234}Th Inventory Measured in Subtidal Sediments	133 – 218	3.4- 5.6

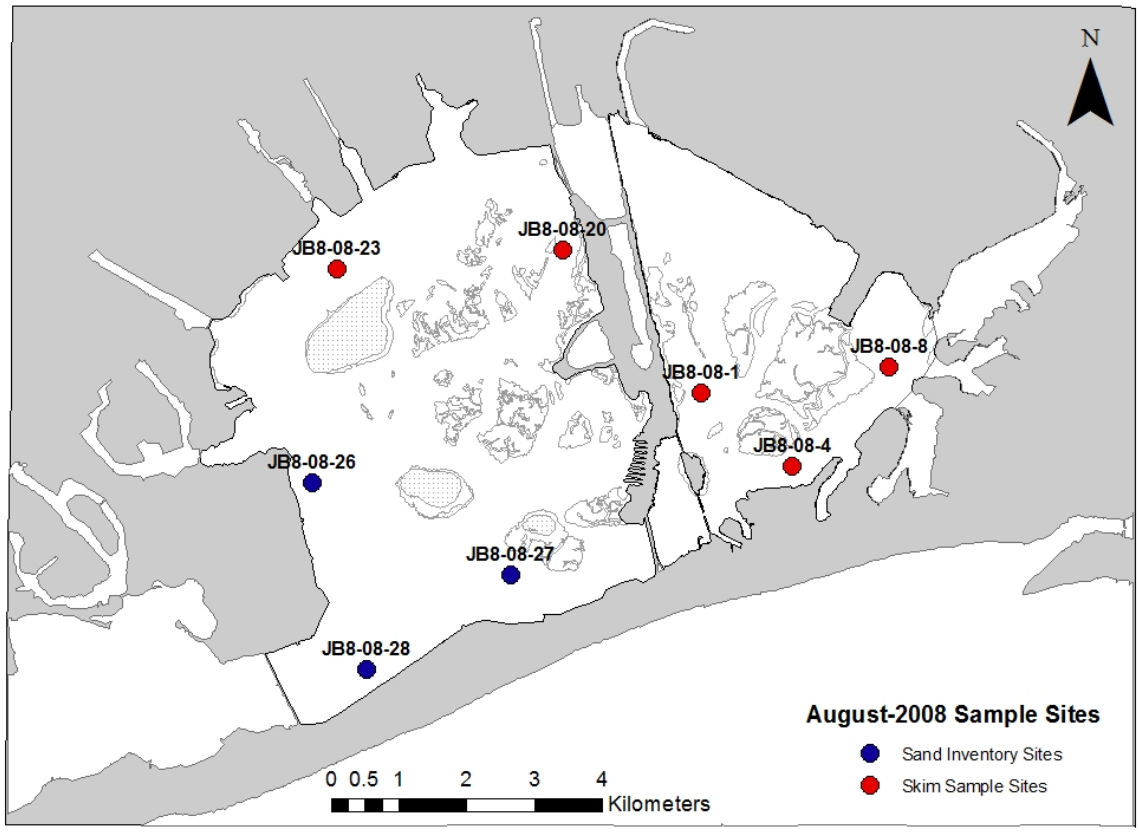

Figure 2-1. Location sites of August-2008 samples

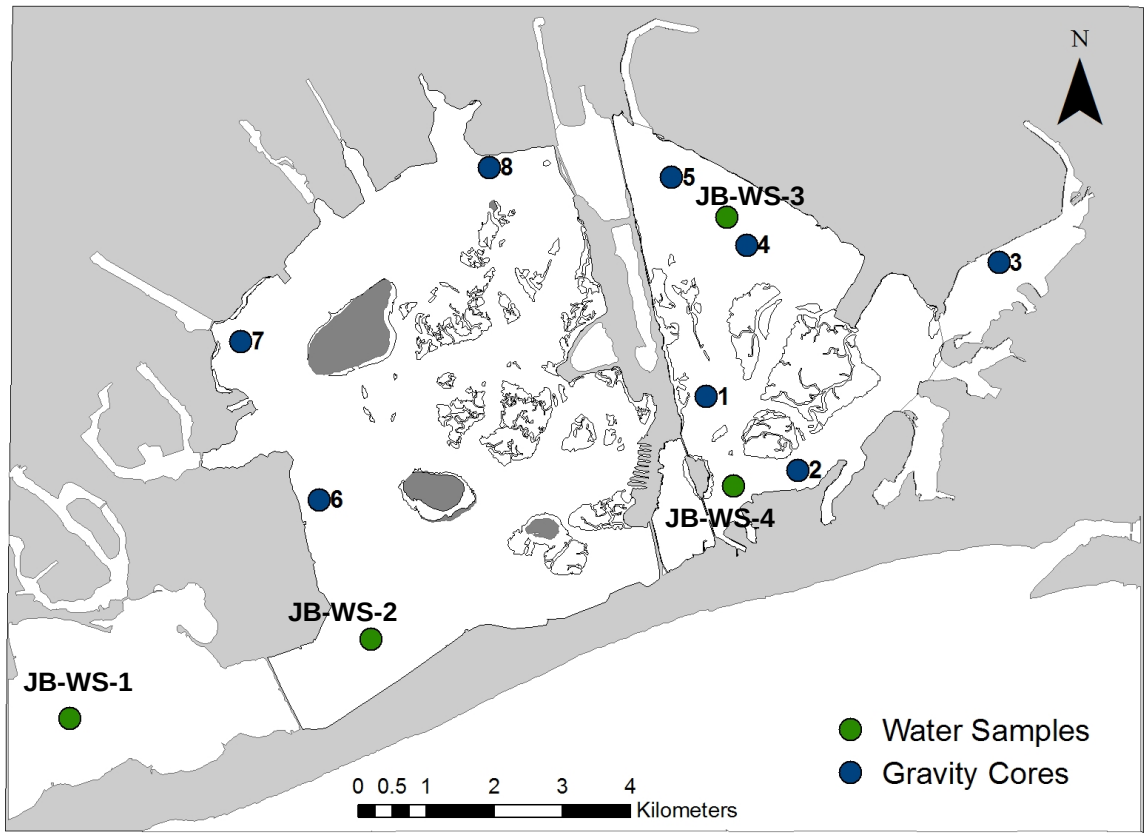

Figure 2-2. Gravity core and water column filtering location site map

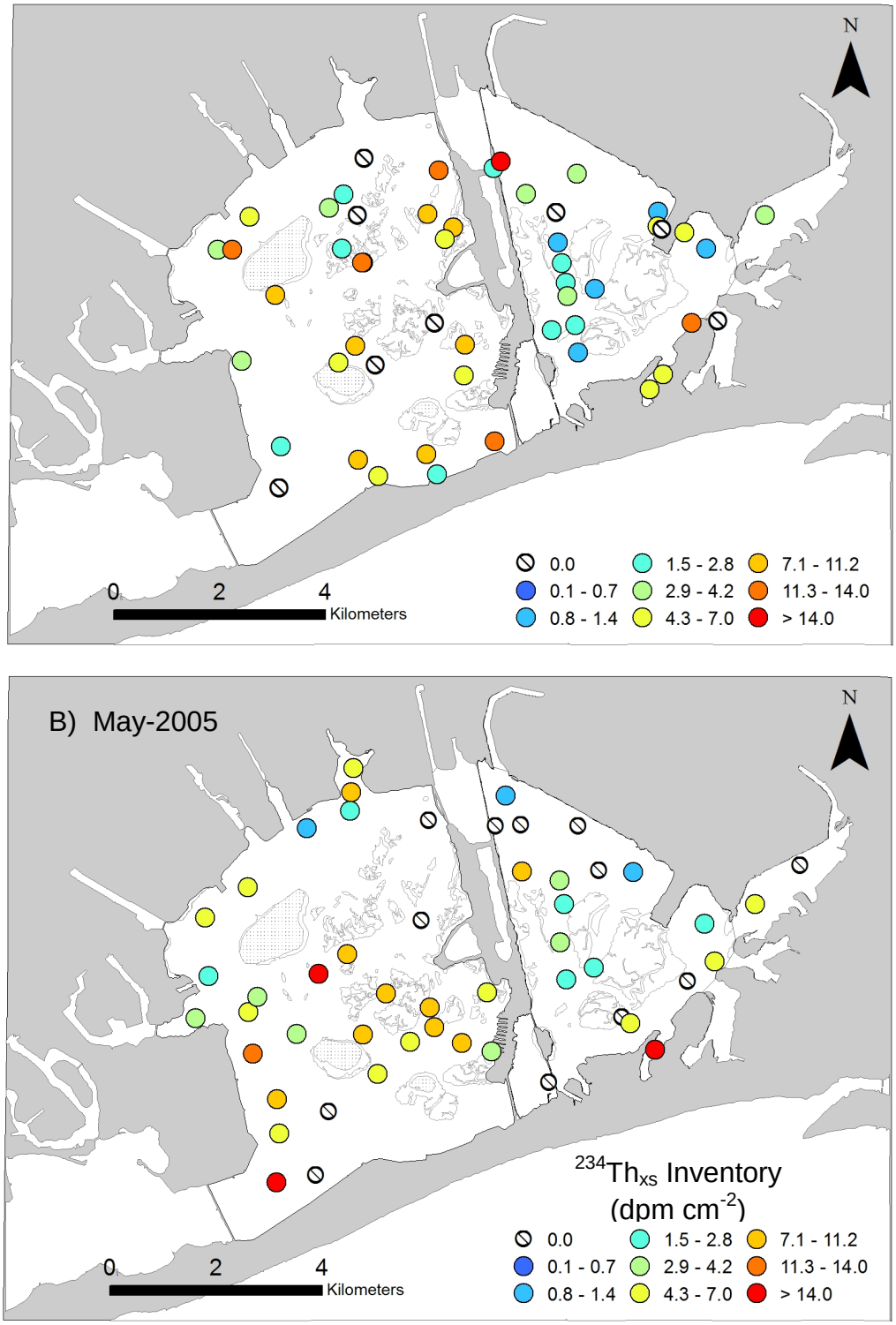

Figure 2-3. $^{234}Th_{xs}$ Inventory of surficial bottom sediments (0-5 cm) during A) September-2004, B) May-2005, C) November-2005 and D) July-2006 cruises.

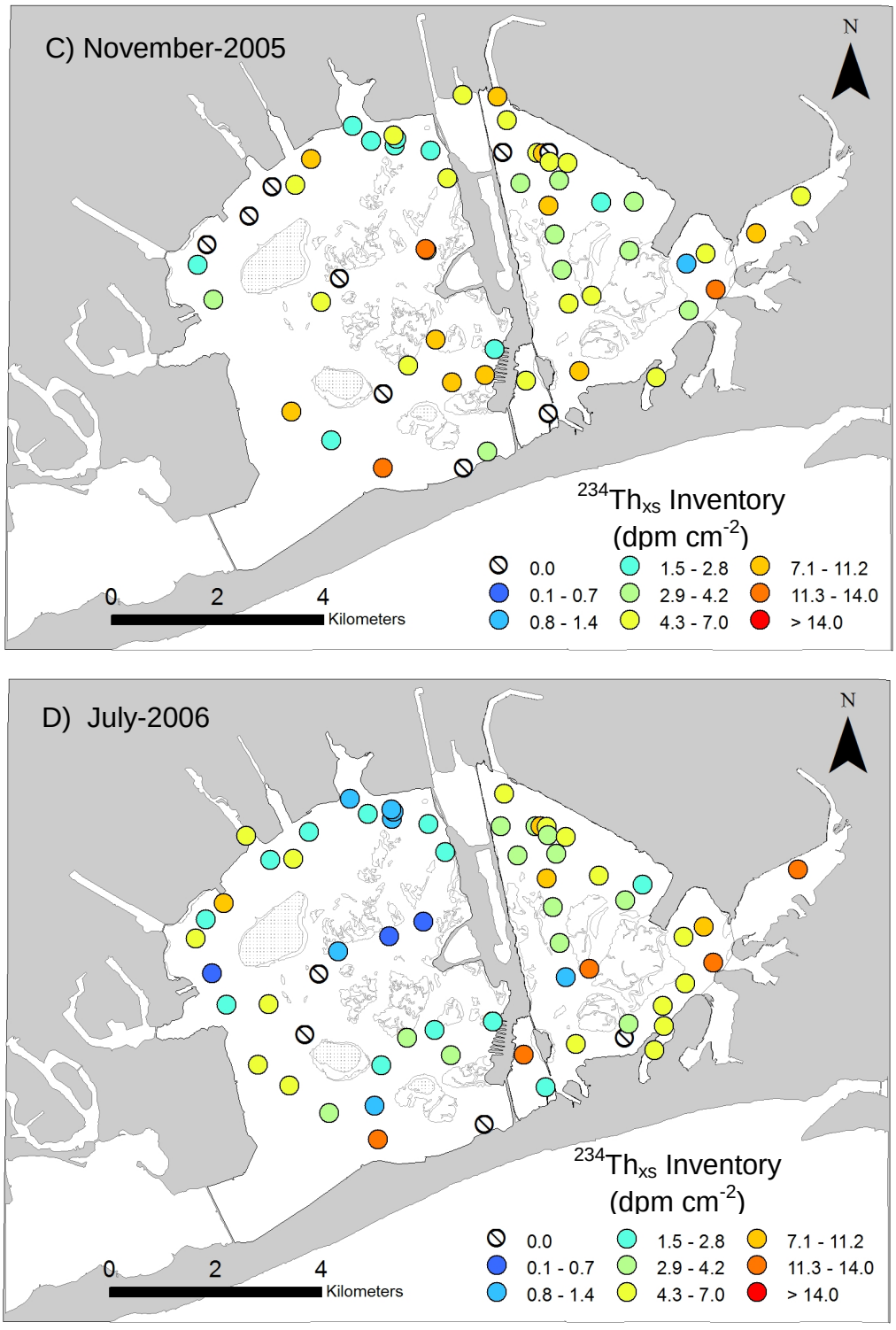

Figure 2-3. Continued.

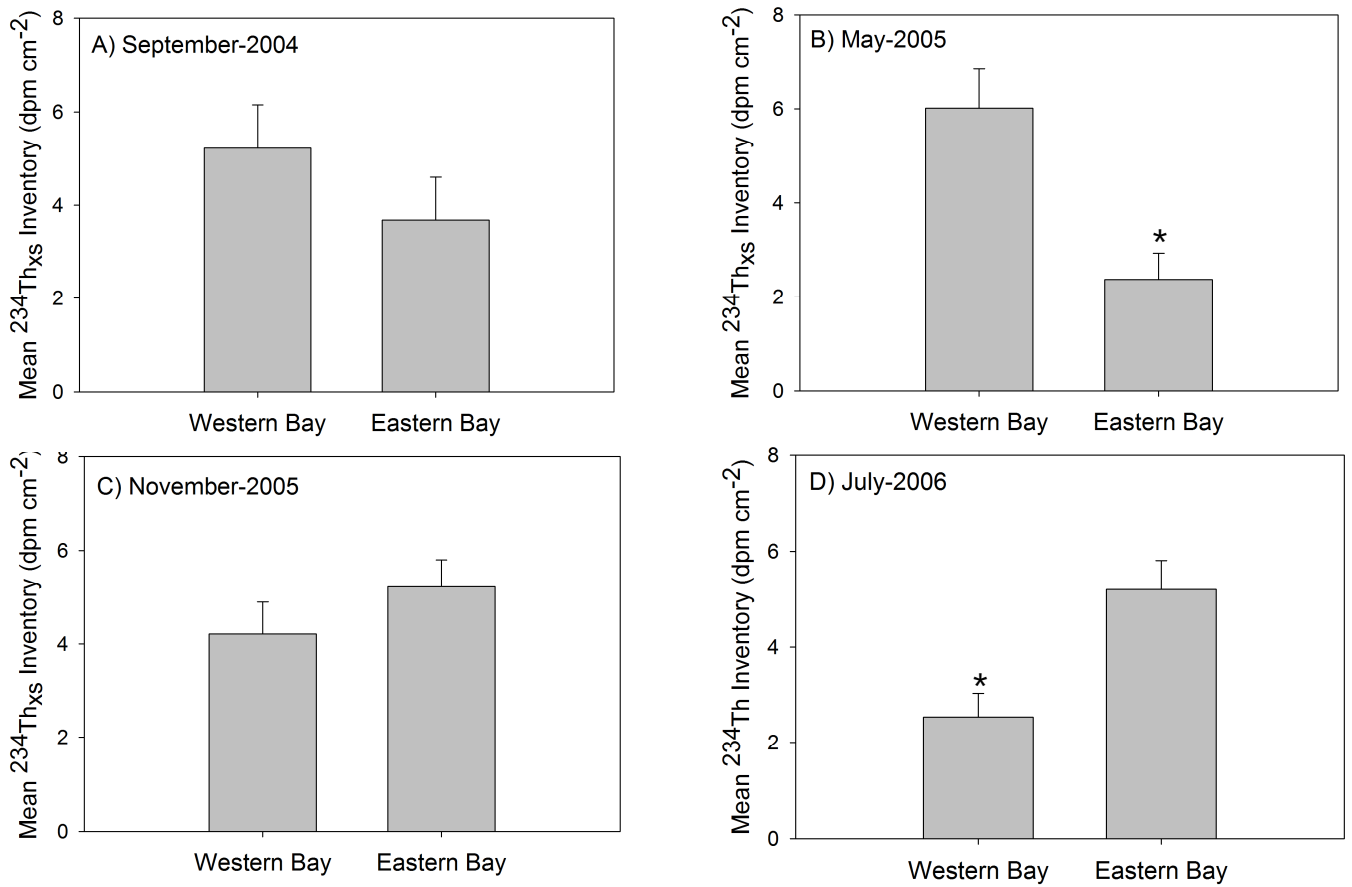

Figure 2-4. Mean $^{234}Th_{xs}$ inventory in western and eastern Jamaica Bay during A) September-2004, B) May-2005, C) November-2005, and D) July-2006. * denotes mean $^{234}Th_{xs}$ inventories that are significantly lower ($p < 0.05$) than the other half of the bay during that sampling cruise.

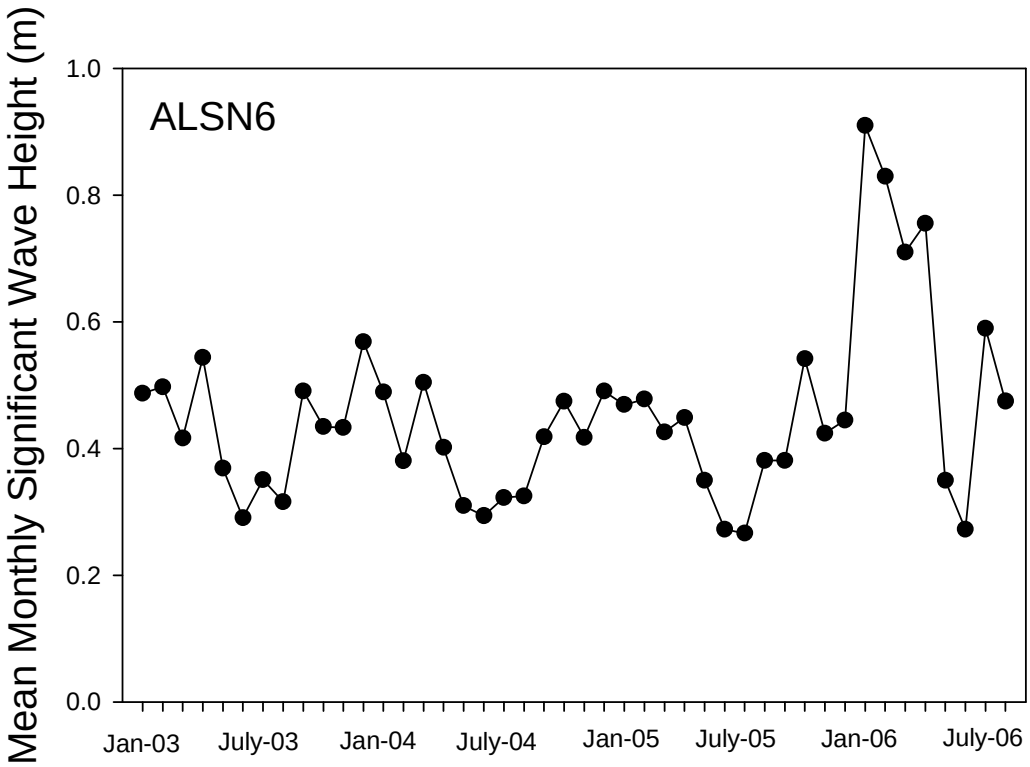

Figure 2-5. Significant wave height at the NOAA ALSN6 Buoy from January 2003 to August 2006.

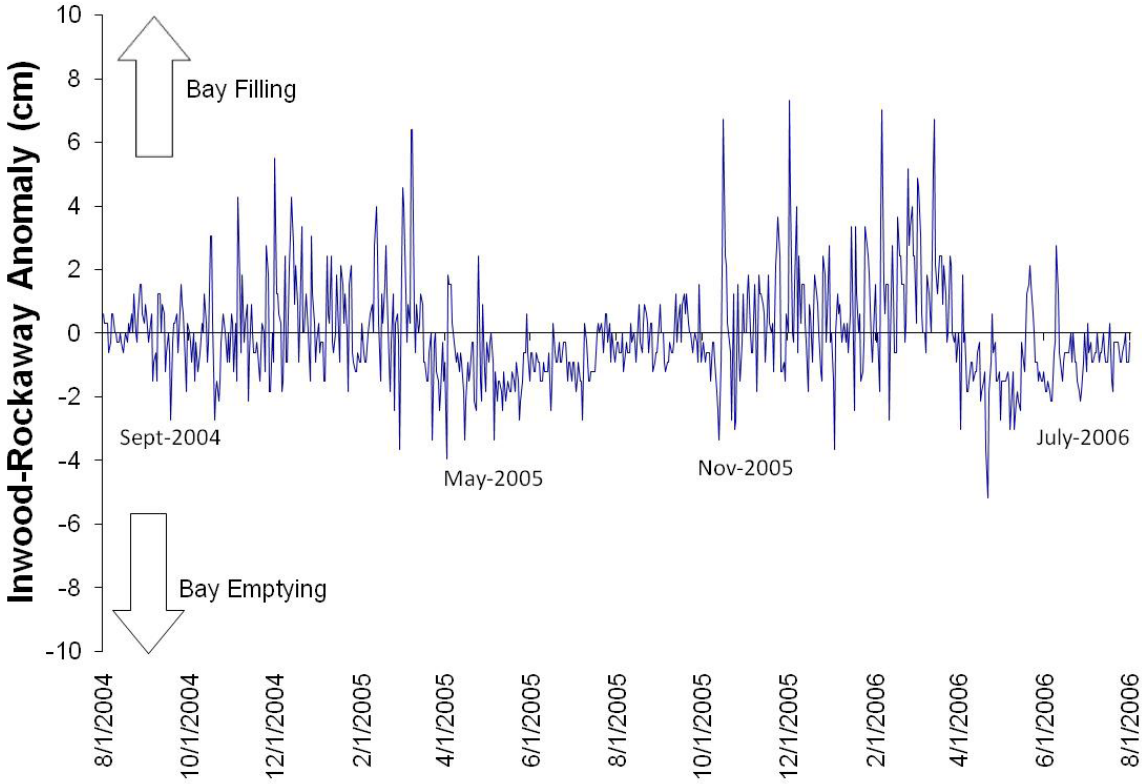

Figure 2-6. Mean daily tidal height difference between Inwood and Rockaway tidal stations.

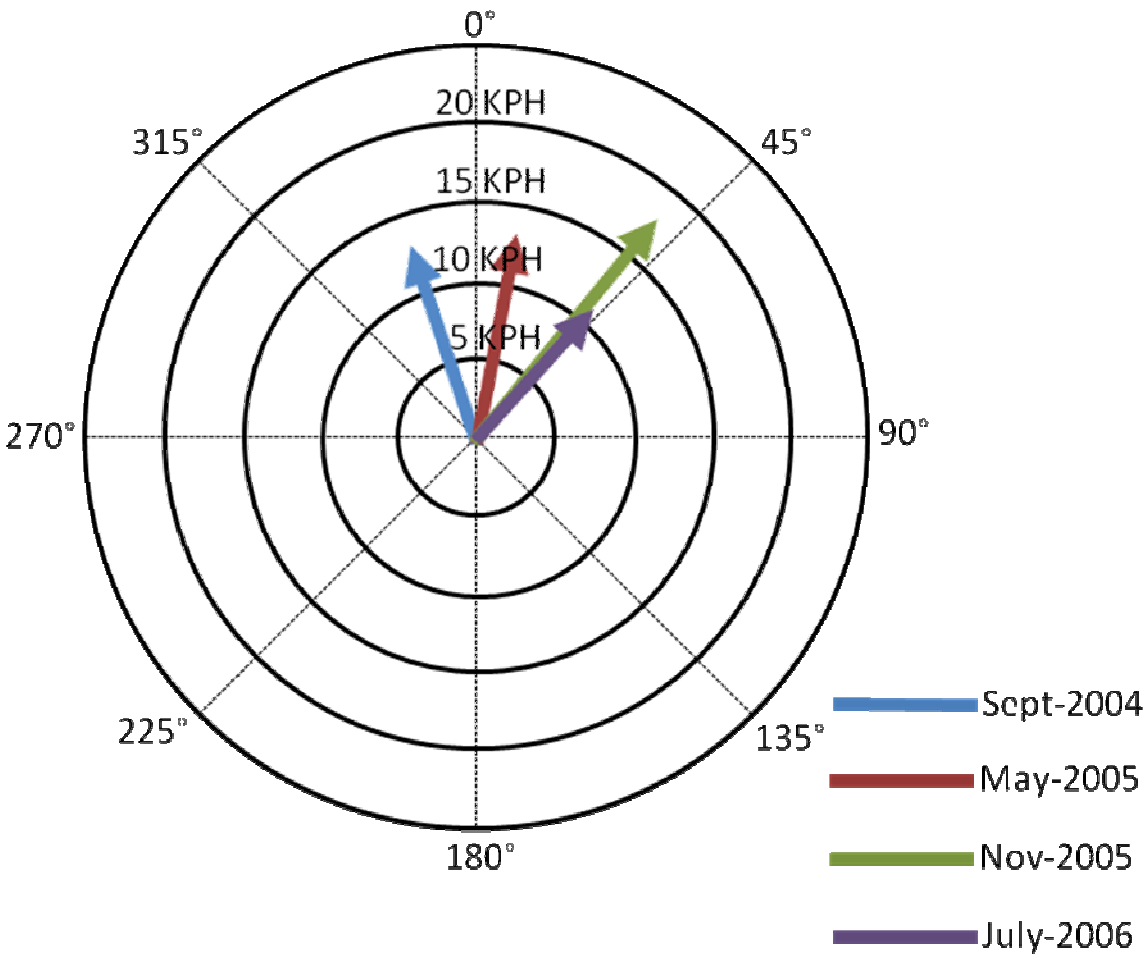

Figure 2-7. Mean wind speed (kph) and wind direction for the 24 days preceding the sampling cruises in September-2004, May-2005, November-2005, and July-2006.

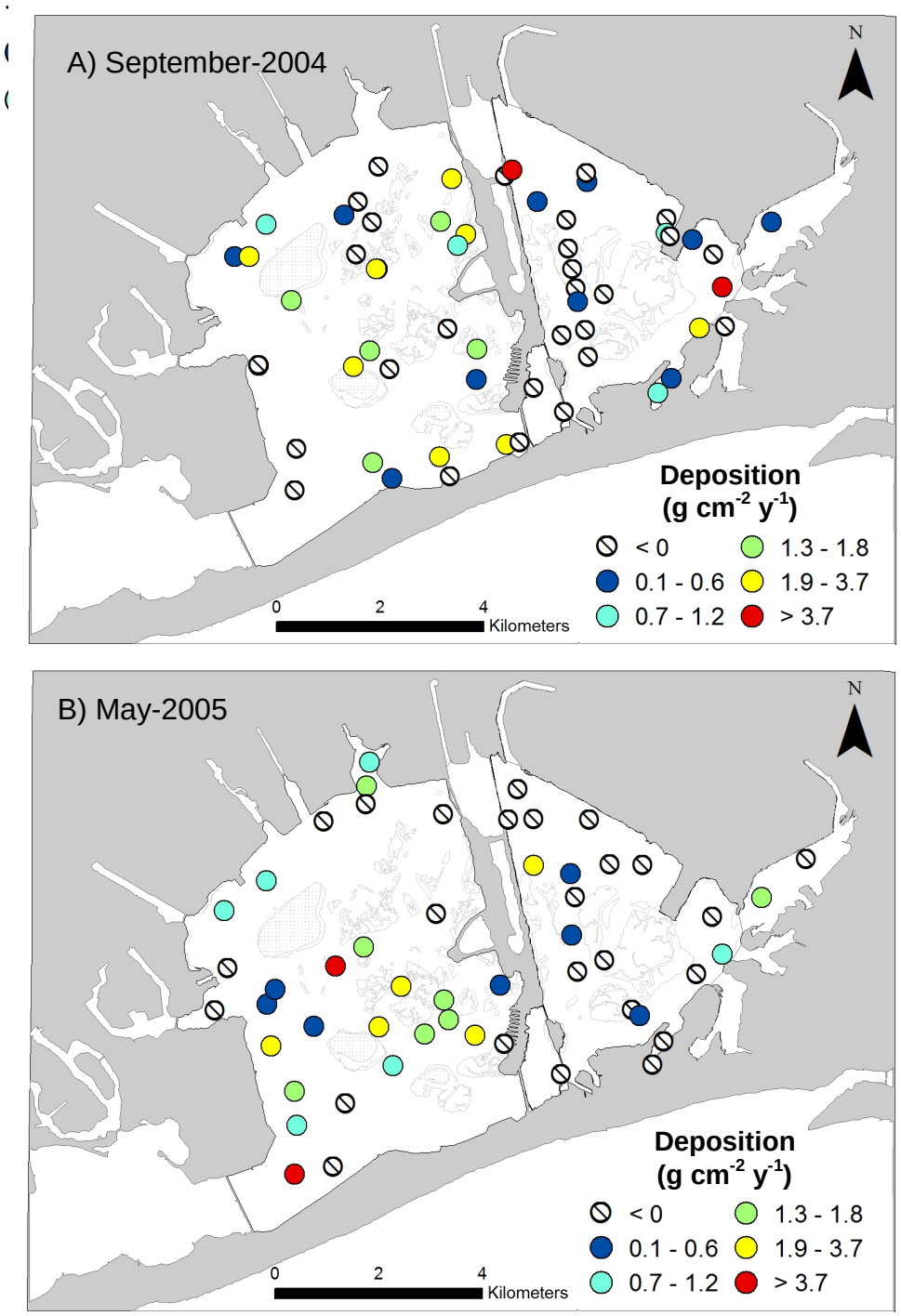

Figure 2-8. Estimation of deposition of sediment imported into the bay using $^{234}Th_{xs}$ inventories in surplus to production within the bay and dissolved import (see section 5.3) during A) September-2004, B) May-2005, C) November-2005 and D) July-2006.

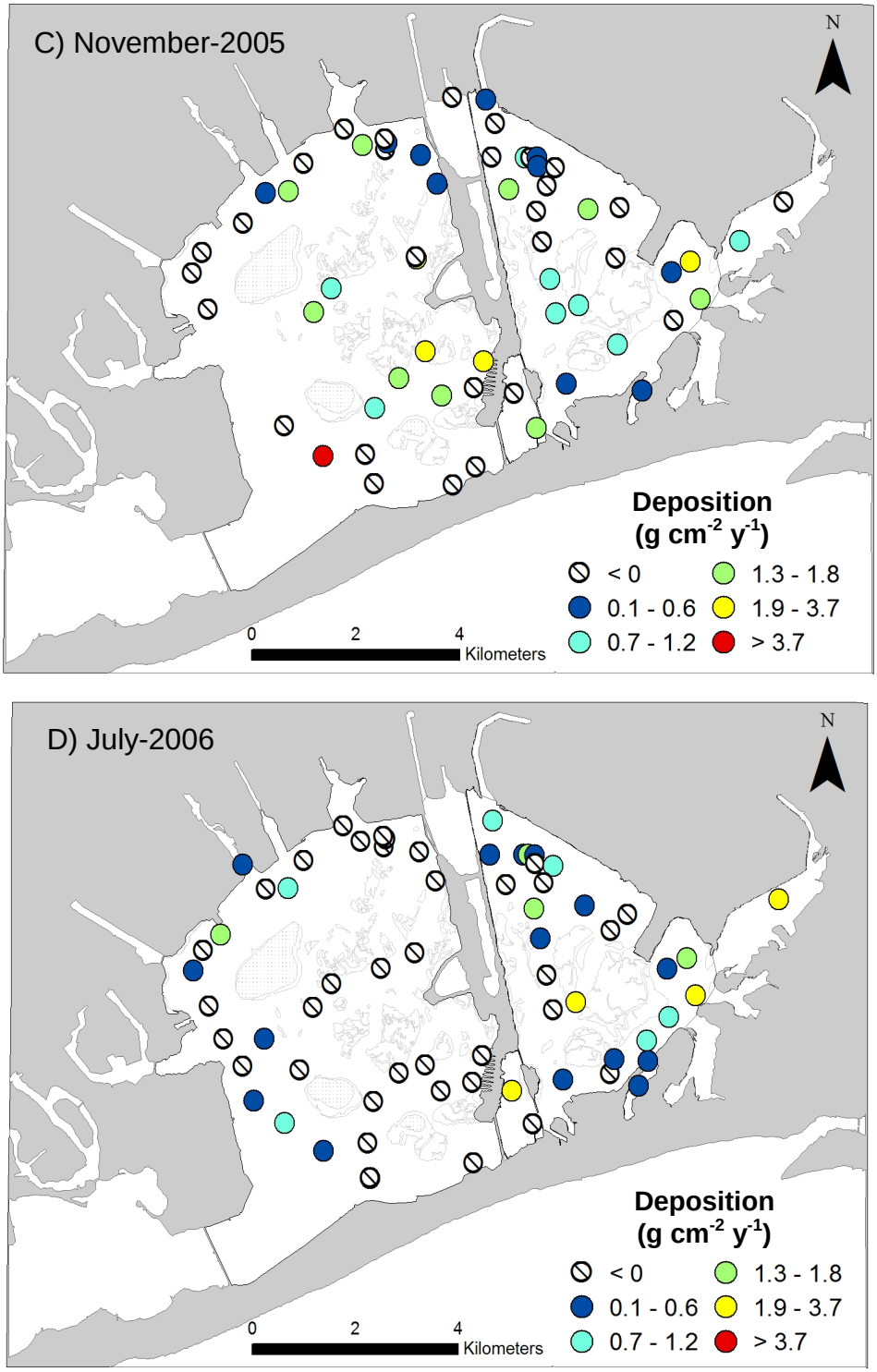

Figure 2-8. Continued.

CHAPTER 3

Geochemistry of ^{210}Pb in an urban coastal lagoon (Jamaica Bay, NY)

1. Abstract

Jamaica Bay is a highly impacted urban coastal lagoon that has had significant modifications to its hydrodynamics in the past century, which may have lasting effects on the patterns of sediment accumulation in the subtidal bay. The spatial pattern of fine-particle sediment accumulation has been evaluated through excess ^{210}Pb geochronologies of gravity cores taken throughout the bay. Accumulation rates vary from 0.1 to 1.1 cm y^{-1}, with the highest sediment accumulation rates in the northwestern part of the bay in a dredged channel. Mass accumulation rates vary from 0.1 to 0.9 g cm^{-2} y^{-1} and are comparable to the $^{234}Th_{xs}$ derived mass accumulation rates given in Chapter 2. The accumulation rates derived from $^{210}Pb_{xs}$ agree well with those inferred from ^{137}Cs, suggesting that bioturbation does not significantly alter the excess ^{210}Pb profiles. Inventories of excess ^{210}Pb in the sediment cores range from 168 ± 20 to 351 ± 39 dpm cm^{-2}. The direct atmospheric input adjusted for focusing with the fine sediments is 80 dpm cm^{-2}, and accounts for only 22 – 48% of the total inventory. Additional sources of ^{210}Pb into Jamaica Bay are combined sewer overflow events (15 dpm cm^{-2}), in situ production (0.2 dpm cm^{-2}), groundwater (7 dpm cm^{-2}) and import from the ocean. Using the ^{210}Pb inventory in surplus of that expected from other sources (direct atmospheric input, CSO discharge, in situ production and groundwater discharge) to estimate the import of sediment via Rockaway Inlet gives 6.8 ± 1.6 × 10^{10} g y^{-1}. A sediment budget for Jamaica Bay also is constructed using the annual sediment accumulation in the

subtidal bay ($7.6 \pm 1.6 \times 10^{10}$ g y^{-1}) and the annual mass accumulation on the marsh islands ($0.2 - 0.4 \times 10^{10}$ g y^{-1}). The sediment import needed to balance the sediment sinks in the bay is $5.8 - 8.8 \times 10^{10}$ g y^{-1}. This estimated import is comparable to that derived from the "surplus" $^{234}Th_{xs}$ inventory in the subtidal Bay ($4.3 - 35.8 \times 10^{10}$ g y^{-1}; see Chapter 2), the mass balance of $^{210}Pb_{xs}$ ($6.8 \pm 1.6 \times 10^{10}$ g y^{-1}) and by Bokuniewicz and Ellsworth (1986; $1.5 - 2.9 \times 10^{10}$ g y^{-1}). These results suggest that sediment importation is an important factor in balancing the bay's sediment budget.

2. Introduction

^{210}Pb is a naturally occurring radionuclide that is produced in the ^{238}U decay series. It is preceded by its grandparents. ^{222}Rn (half-life = 3.83 days), radon is a noble gas, that can escape from soils and rocks into the atmosphere. The ^{222}Rn that escapes to the atmosphere decays eventually into ^{210}Pb, which becomes associated with aerosols and is removed through wet and dry precipitation. ^{210}Pb also can be added to subtidal sediments by scavenging following its production from dissolved ^{226}Ra. Thus, ^{210}Pb is added to coastal sediments by scavenging of that produced in situ and added from the atmosphere (Appleby and Oldfield, 1992; Le Cloarec et al., 2007; Matisoff et al., 2005).

Appleby and Oldfield (1992) observed that the atmospheric ^{210}Pb flux varies with the amount of precipitation over short-term scales. However, over longer time scales (several years), the ^{210}Pb flux at a given location appears to be relatively constant (±10%), although its input from the atmosphere is regionally variable (Baskaran, 1995; Turekian et al., 1977). Atmospherically deposited ^{210}Pb is scavenged on to particle

surfaces ($K_d = 10^3–10^6$). These particles can then remain suspended in the water column, settle, be deposited, eroded, or advected (see Chapter 1, Fig. 1-4).

^{210}Pb has been frequently used as a chronometer for estimating sediment accumulation and mixing rates in the marine environment (Appleby and Oldfield, 1992; Sharma et al., 1987). Profiles of excess ^{210}Pb ($^{210}Pb_{xs}$; measured ^{210}Pb – ^{226}Ra) in sediments can reflect both sediment accumulation and bioturbation, and the latter process must be considered in reporting sediment accumulation rates (DeMaster et al., 1985). Here we use the distribution of excess ^{210}Pb in the sediments of an urban coastal lagoon to evaluate the spatial variability of sediment accumulation and bioturbation, as well as the mass balance of sediment in the system.

3. Methods

3.1 Study Site

Jamaica Bay (see Chapter 1, Fig. 1-1) is a highly urbanized coastal lagoon (53 km^2; Benotti, et al., 2007) located along the southern coast of western Long Island (O'Shea and Brosnan, 2000). Extensive modifications have been made to the bay throughout the 20^{th} century, including dredging of the channel in the northwestern bay, infilling of marshes on the bay periphery, shoreline armoring and creation of a large borrow pit in Grassy Bay to build John F. Kennedy Airport (formerly known as Idlewild Airport; Black, 1981). These changes to the bay have increased the mean depth from 3 to 5 meters. While the depth of the bay has increased, the area of the bay has remained approximately the same resulting in tidal amplification, particularly in the eastern part of the bay (Swanson and Wilson, 2008). In addition, Jamaica Bay has changed from a

slightly ebb-dominated to a flood-dominated estuary. These modifications to the bay may have severe repercussions for sediment delivery, deposition, and net accumulation with the bay (Swanson and Wilson, 2008). There is no significant riverine input directly in to the bay which may limit the upland source of sediment to the bay. Instead, the dominant supply of freshwater is from the four wastewater treatment plants (Benotti et al., 2007). The sewer system of New York City is such as to allow for bypassing of wastewater treatment facilities during times of high rainfall. At such times, storm water (and associated ^{210}Pb and ^{7}Be) and wastewater enter the estuary simultaneously. The combined sewer overflow outlets are located throughout the Bay (Fig. 1-1). Combined sewer overflow (CSOs) events that occur after heavy rainfalls may be an important input of freshwater, as well as nutrients, into the bay (Botton et al., 2006; O'Shea and Brosnan, 2000).

3.2 Field Methods

Sediment samples were taken in Jamaica Bay in September-2004, May-2005, November-2005 and July-2006. Surficial sediment samples (0 – 5 cm) were collected using an Ekman bottom grab at 60-70 sites during each cruise. This intensity of sampling, plus the fact that all sediment provinces were sampled on each cruise, makes it possible to make meaningful temporal comparisons of bay-wide distribution of fine sediments.

Down-core distribution of ^{210}Pb were obtained in 8 gravity cores (> 30 cm) taken in Jamaica Bay in August, 2008 (see Chapter 2, Fig. 2-2). Cores were then returned to the lab for radiometric analysis.

The activities of ^{210}Pb associated with particles in the water column entering the bay and within the bay were measured by filtering large volumes (> 100 liters) of bay water through ship-powered in-situ pumps equipped with a polypropylene filter cartridge (CUNO Micro-Wynd II® D-CCPY, nominal 1 μm) at selected sites (see Chapter 2, Fig. 2-2).

3.3 Laboratory Methods

An aliquot of each surficial sediment sample was taken to determine water content and then combusted in a furnace at 450°C for > 6 hours to determine loss-on-ignition (LOI). The remainder of the dried sample was soaked in a 0.5% sodium hexametaphosphate solution, sonicated for 10 minutes, and then wet-sieved through a 63 micron sieve to determine the percentages of the mud and sand.

The gravity cores were returned to the lab and immediately frozen. Later the cores were extruded and sectioned. The upper 20 cm of each core was sectioned into 2-cm intervals, from 20 cm to 48 cm the cores were sectioned into 4-cm intervals, and the remainder of the core was sectioned into 8-cm intervals. Each interval was counted wet on a Canberra 3800 mm^2 germanium gamma detector for ~ 24 hours to determine ^{210}Pb, ^{214}Pb, and ^{137}Cs activities, as described above. An aliquot of each sample was combusted in a furnace at 450° for > 6 hours to determine LOI.

Cartridges from the high-volume water column sampling were ashed in a furnace at 450°C for 16 hours. The ash was analyzed for ^{210}Pb (46-keV) and the granddaughter of ^{226}Ra, ^{214}Pb (353-keV) on Canberra 3800 mm^2 germanium gamma detectors for 24

hours to determine activities of $^{210}Pb_{xs}$ on inorganic, filterable particles. Counting efficiencies for the detectors were determined using the method outlined previously.

4. Results

4.1 Sediment Organic Content and Grain Size

A compilation of wet sieve results and LOI results for the subtidal, bottom samples from the four sampling cruises was used to create the contour maps shown in Figs. 3-1, 3-2. The mud content of the sediments varied from 0 to 95% (Fig. 3-1). Fine-grained sediments (mud content > 50%) dominated the eastern part of the bay, in particular Grassy Bay, but coarser sediments were found in the western bay adjacent to the marsh islands. Fine-grained sediments also dominated in the northwestern channel of the bay near the combined sewage overall outfalls. Organic content of the sampled sediments ranged from 0 to 25%. Organic content (determined from LOI) shows a similar distribution to mud content, with high organic content (LOI > 10%) in the eastern part of the bay and low in LOI the western bay near the marsh islands (Fig. 3-2).

Water content, LOI and bulk density were measured for each of the gravity core intervals. The highest water content was generally measured at the top of the core and values decreased with depth (Fig. 3-3). However, in cores 4 and 5 (located in Grassy Bay) water content was high and less variable with depth (Fig. 3-3). LOI was also generally highest near the sediment-water interface of each core and decreased with depth (Fig 3-3). Core 6 was an exception, with the lowest LOI measured at the sediment-water interface (Fig. 3-3) and overall low LOI throughout this core.

4.2 *Activities of ^{210}Pb on Suspended Particles*

Activities of ^{210}Pb on suspended particles measured in August-2008 ranged from 0.6 ± 0.3 to 9.3 ± 1.0 dpm g^{-1} (0.01 ± 0.01 to 0.1 ± 0.03 dpm L^{-1}; Table 3-1). The highest excess ^{210}Pb particulate activities were measured at the station closest to the inlet and in deep water just within the inlet (Table 3-1). At the interior stations, away from the inlet, the ^{210}Pb activity on particles decreased.

4.3 Down Core ^{210}Pb Distributions: Inventories and Decadal-Scale Sediment Accumulation Rates

Plots of excess ^{210}Pb activity versus depth in each of the gravity cores are shown in Fig. 3-4. Inventories of $^{210}Pb_{xs}$ were calculated for all cores using the equation:

$$I_{Pb} = \sum (A_i \rho_i x_i) \quad (3\text{-}1)$$

where I_{Pb} is the inventory of excess ^{210}Pb within the core (dpm cm^{-2}), A_i is the excess ^{210}Pb activity (dpm g^{-1}) of the i^{th} interval of the core, ρ_i is the bulk density of that interval, and x_i is the thickness of the interval. The $^{210}Pb_{xs}$ inventories of the cores collected in the bay ranged from 167 to 351 dpm cm^{-2} (Table 3-2).

Sediment accumulation rates were calculated using a "constant initial activity" model which assumes that initial $^{210}Pb_{xs}$ activity in the sediments has been constant with time and that bioturbation is negligible. The change of $^{210}Pb_{xs}$ activity with depth is then described by the following equation

$$A = A_0 \exp(-\lambda x/S) \quad (3\text{-}2)$$

where A is the $^{210}Pb_{xs}$ activity at depth, A_0 is the initial activity (at x = 0), λ is the decay constant of ^{210}Pb, x is depth in the core (cm), and S is the sedimentation rate (cm yr^{-1}). The accumulation rate is determined by a best-fit line through a plot of ln A vs. x (Fig. 3-5). This model can be affected by the compositional change that change the initial activity and thus provides only an average accumulation rate. In addition, bioturbation can alter the ^{210}Pb gradient with depth in a core, such that the sediment accumulation rate obtained from eqn (3-2) is a maximum.

One approach to evaluate the importance of bioturbation on ^{210}Pb-derived sediment accumulation rates is to compare the results with those determined from ^{137}Cs. In five of the cores, a clear ^{137}Cs peak was detected (Fig. 3-6). The value of S may be estimated by assuming that this peak corresponds to the 1963 maximum in global ^{137}Cs fallout (Ritchie and McHenry, 1990). The accumulation rates estimated by $^{210}Pb_{xs}$ and ^{137}Cs for the cores taken within the bay are summarized in Table 3-2. In general the agreement is good. However, in core 6 the core length was too short to reach the 1963 ^{137}Cs peak if the accumulation rate was 1.1 cm yr^{-1}, as the peak would then be located at 50 cm deep and the core was only 36 cm long. In core 2 the 1963 peak would be ~ 23 cm deep, and while there appears to be high ^{137}Cs around this depth, it is at the bottom of the core at cannot be unambiguously discerned. In core 3, given the $^{210}Pb_{xs}$-derived accumulation rate, the 1963 ^{137}CS peak should be ~ 5 cm in depth, but given the slow accumulation rate that appears to occur at this site, the sub-sectioned intervals are too coarse to for it to be clear.

Accumulation rates ranged from 1.1 to 0.1 cm yr^{-1}, with high values in the western part of the bay, near a CSO outfall (cores 6 and 7; Table 3-2). In Grassy Bay, the

northeastern part of Jamaica Bay, accumulation rates at two sites were 0.79 to 1.04 cm yr^{-1} (cores 4 and 5; Table 3-2). The lowest accumulation rate measured at core 3 site, located in the northeastern part of the bay in the Thurston Basin (Table 3-2).

Mass accumulation rates were determined from the $^{210}Pb_{xs}$ profiles using:

$$S_M = S \times \rho \quad (3\text{-}3)$$

where S is the sediment accumulation rate (cm y^{-1}) estimated from the excess ^{210}Pb of the gravity core using the "constant initial activity" model and ρ is the mean bulk density (g cm^{-3}) of the sediment in each core. The mass accumulation values ranged from 0.01 to 0.89 g cm^{-2} y^{-1} (Table 3-2).

5. Discussion

5.1 Mud Content and LOI Contour Maps

Contour maps of the percent mud and organic content were constructed from the results of the 220 sites sampled in Jamaica Bay over the course of this study (Figs. 3-1, 3-2). The contour maps show a general trend of sediment dominated by fine-grained particles and high LOI in the eastern part of the bay, while in the western part of the bay sediments had a higher proportion of sand-size particles and lower LOI.

The validity of the contour maps created from the mud content and LOI data using ArcMap Raster interpolation were compared to previous measurements of mud content in Jamaica Bay by the EPA in 1993-1994 (Adams et al., 1998) and NOAA in 1995 (Iocco et al., 2000). The mud content distribution predicted by the contour map was similar to that found by those previous studies (Fig. 3-7). Deviation from the predicted

mud content distribution was rare, but was observed in Grassy Bay where the mud content was typically > 50%. However, a site in Grassy Bay where the measured mud content was 20-30% was also the site where a clam bed was found in the 1995 NOAA study (Iocco et al., 2000; Fig. 3-7). The good agreement between the distribution predicted by the mud content contour map and the sites previously sample by the EPA (Adams et al., 1998) and NOAA (Iocco et al., 2000) suggests that the contour map prepared in the present study is a reasonable representation of the fine sediment distribution within Jamaica Bay.

The contour map created from the distribution of organic content measured in this study was compared to the organic content of sites measured by the EPA in 1993-1994 and NOAA in 1995 (Fig. 3-8). The distribution of organic content mapped in the present study is generally similar to the previous measurements, although previous measurements of organic content are often greater than those measured by us. This may be due to the relatively small size (3%) of each interval. Nevertheless, the general correlation of organic content with mud content suggests that the present map is a reasonable pattern of organic content in the Bay's sediments.

5.2 Sediment Accumulation Rates and Bioturbation

Bioturbation of sediments by the burrowing and feeding of benthic macrofauna can disturb the record of sediment accumulation by redistributing the radionuclide activities with depth. For example deposit feeders consume from a variety of sediment depths and may excrete "older" (i.e. low $^{210}Pb_{xs}$) sediment at the sediment-water interface. Other organisms, such as large crustaceans can create deep burrows, which

subsequently can be filled with surficial ("young") sediment. Physical mixing processes, such as bottom currents, waves and tides, as well as episodic events, such as storms and floods, can also disturb the continuity of the sediment record by causing mass deposition or erosion (Carroll and Lerche, 2003). In estuaries, particle mixing has been found to extend to depths of one meter or more into the sediment column (Benninger et al., 1979).

In the mid-19th century the oyster and clam fisheries of Jamaica bay became major industries and provided significant employment, with the peak of these fisheries occurring in the early 20^{th} century. After this time, production steadily decreased; however the end of the shellfish industry in Jamaica Bay was not due to a disappearance of oysters and clams, but rather increased contamination of bay water and shellfish (Black, 1981). Benthic surveys using sediment profile images were conducted by Iocco et al. (1995) in June-1995 and October-1995; no oyster beds were found within the bay but isolated clam and mussel beds were recorded. During both surveys, mats of the tube-dwelling amphipod *Ampelisca* were the dominant benthic organism in the western and in the far eastern parts of the bay (Fig. 3-9). Macrofauna were not recorded in Grassy Bay. Indeed, during the June-1995 survey Grassy Bay sediments were soft, silty-muds with gas voids, and bacterial mats were observed there in October-1995. Although the benthic communities of Jamaica Bay were not surveyed as a part of the present study, the distributions of mud and organic content of sediments measured by us are similar to those of Iocco et al. (1995; Figs. 3-7 and 3-8), and thus we assume that the benthic communities have not changed drastically since 1995.

The distribution of short-lived particle reactive radionuclides can be use as an indicator of bioturbation rates. ^{7}Be (half-life = 53.3 d) is a useful tracer for characterizing

particle mixing in the sediments. This radionuclide is produced in the atmosphere and enters the bay through direct atmospheric input (Baskaran and Santchi, 1993; Feng, et al., 1999; Giffen and Corbett, 2003; Kaste et al., 2002). As shown in Chapter 4 there may be an additional input of ^{7}Be into Jamaica Bay through combined-sewer overflow events (CSOs) which transport ^{7}Be deposited on impervious surfaces (e.g. roads) in the Bay's drainage area ("sewershed"; see Chapter 4 for details). Profiles of ^{7}Be in cores are compared with ^{210}Pb in Fig. 3-10. Sediment cores taken in the nearby Peconics Estuary by Cochran et al. (2000) had ^{7}Be inventories in the upper 5 cm ranging from 0.23 to 7.05 dpm cm^{-2} and measurable ^{7}Be was typically found down to 5 cm in depth. More recent work in the Peconics has measured ^{7}Be down to 10 cm (R.C. Aller, pers. comm.). In contrast, in Jamaica Bay the ^{7}Be activities are confined to the top interval (0-2 cm) in all the cores, with the exception of core 1 where it is detectable to 4 cm. With the 53-day half-life of ^{7}Be, the ^{7}Be distribution reflects short-term mixing processes. This may reflect the average particle mixing in Jamaica Bay; during the summer higher benthic activity would be expected when water temperatures increased and in the winter mixing would be expected to be reduced as water temperatures decreased (Cochran et al., 2000).

In cores 1, 2 and 8 the $^{210}Pb_{xs}$ profiles have a subsurface maximum (Fig. 3-4). These cores were taken in areas where *Ampelisca* mats were the dominant benthic habitat during the 1995 benthic survey (Fig. 3-9; Iocco, et al., 2000). *Ampelisca* are tube-building, filter feeding amphipods that appear to thrive in area of good water quality and high organic input (Strickney and Stringer, 1957). They have been found to have sensitivity to pollutants (Wolfe et al., 1996). A study in Boston Harbor (1993-2006), a

highly impacted, urban estuary, found an increase in the depth of the redox potential discontinuity down to 5 cm with the presence of *Ampelisca* mats (Diaz et al., 2008).

Bioturbation does not appear to affect the mean accumulation rate of cores determined from $^{210}Pb_{xs}$ profile in cores 1, 7 and 8 in Jamaica Bay. At these core sites the 1963 ^{137}Cs peak was reached (Fig. 3-6) and similar accumulation rates comparable to those from $^{210}Pb_{xs}$ (Table 3-2). The 1963 ^{137}Cs was not identifiable in the core 2 profile (Fig. 3-8). The accumulation rate determined for core 2 from the $^{210}Pb_{xs}$ profile was 0.5 cm y^{-1} which would result in the 1963 ^{137}Cs peak being found in the 20-24 interval. The activity of ^{137}Cs is slightly higher near this depth interval but a pronounced peak may be obscured by the coarse interval taken this depth (4 cm) coupled with the overall low ^{137}Cs activity found in this core (Fig. 3-6).

5.3 Long-Term Sediment Accumulation Rates

Upper limits on sediment accumulation rates can be determined from $^{210}Pb_{xs}$ profiles, assuming no bioturbation; values range from 0.1 ± 0.01 to 1.1 ± 0.1 cm yr^{-1}. Mass accumulation rates have been calculated from multiplying the accumulation rate at each site by the mean dry bulk density at that site (Table 3-2). The highest accumulation rates were measured in cores 6 and 7 in the western part of the bay, and these two sites also had the deepest water depth (13.0 m) of all stations sampled (Table 3-2). This suggests that once sediment settles into these deep sites, it is not likely to be resuspended and transported to other locations within the bay. The high accumulation rates at these locations are consistent with high ^{7}Be inventories during all sampling cruises (see

Chapter 4) and high $^{234}Th_{xs}$ inventories during the May-2005 and July-2006 sampling cruises (see Chapter 2).

High accumulation rates are also observed in the eastern part of the bay at stations 1, 4 and 5 (Table 3-2). The accumulation rate measured in core 4 is (1.0 cm y^{-1}), which is consistent with a previous accumulation rate (0.9 cm y^{-1}) measured nearby by Ferguson et al. (2003). The eastern part of the bay, particularly Grassy Bay, has limited connection to the western bay, and in turn, the ocean. However, high accumulation rates within and near Grassy Bay suggest that sediment is, at least periodically, transported to the eastern bay. Inventories of the short-lived radionuclide ^{234}Th were low in Grassy Bay during the September-2004 and May-2005 cruises, but high in November-2005 and July-2006 (see Chapter 2). Significant wave height outside the bay at buoy station ALSN6 increased prior to both of these sampling cruises (see Chapter 2, Fig. 2-5). These results suggest that storm events may play an important role in moving sediment to the eastern part of the bay. Once deposited in this deep area of the bay it is unlikely that sediment would be resuspended and transported elsewhere in the bay.

The lowest accumulation measured was at site 3 in Thurston Basin, in the far eastern part of the bay (Fig. 3-11). At this site there seems to be a distinct change in deposition rate with depth in the core, as seen in the change in the slope of the $^{210}Pb_{xs}$ vs. depth plot at ~7 cm (Fig. 3-4). In the upper 7 cm, the accumulation rate was low (0.1 ± 0.01 cm y^{-1}), while deeper in the core (9 – 30 cm) the accumulation rate was higher (0.80 ± 0.02 cm y^{-1}). A significant change in the organic content of the core also occurs in the upper 7 cm: LOI is high (> 20%) in this zone, but below this depth, the organic content is consistently < 10% (Fig. 3-3). These results suggest that a change in sediment delivered

to this site occurred ~50 years ago. This change may reflect increased development (e.g. paving) in the upland region surrounding this site, limiting the inorganic sediment transported to the bay from runoff. The change in accumulation rate and sediment type at this location is perhaps more noticeable due to the site's isolation from much of the rest of the bay.

The mass accumulation rates derived from excess ^{210}Pb profiles may be compared with the accumulation rates derived from surplus $^{234}Th_{xs}$ inventories (0.1 – 0.9 g cm^{-2} y^{-1}). For example, in Grassy Bay the ^{210}Pb-derived mass accumulation rate is ~0.3 – 0.4 g cm^{-2} y^{-1}. Rates derived from mean $^{234}Th_{xs}$ inventories are in close agreement in this region ranging from 0.1 to 1.0 g cm^{-2} y^{-1}. The average mass accumulation rate in the bay determined from the ^{210}Pb data (mean ± 1σ = 0.47 ± 0.27 g cm^{-2} y^{-1}) yields an annual sediment input of 18.3 × 10^{10} g y^{-1} when extrapolated over the entire bay subtidal area (39 km^2). This is in agreement with the annual sediment import estimate derived from the ^{234}Th balance (4.3 × 10^{10}- 35.8 × 10^{10} g yr^{-1}; see Chapter 2, section 5.2). This calculation assumes that the sediment is distributed uniformly over the subtidal portion of the bay (39 km^2). While the two estimates are in reasonable agreement given the assumptions of the methods, it is likely that the ^{234}Th estimates are high because they represent short-term patterns of deposition which cannot be extrapolated to a full year. This is consistent with the pattern evident in the sediment $^{234}Th_{xs}$ inventories of seasonal transport of sediment into Grassy Bay and other eastern portions of Jamaica Bay. ^{210}Pb profiles in the sediments, with a sampling resolution of ~2-8 years, effectively integrate over these seasonal sediment transport events.

Annual deposition (g y^{-1}) in the subtidal Bay dominated by fine sediments can be derived from the mass accumulation measured in the gravity cores using the equation:

$$\text{Sediment Deposition} = S_M \times (\text{Subtidal Bay Area} \times M_F) \quad (3\text{-}4)$$

where S_M is the mean mass accumulation of the gravity cores (0.5 ± 0.1 g cm^{-2} yr^{-1}), subtidal bay area is 3.9×10^{11} cm^{-2} and M_F is the fraction of bay area dominated by fine-grained sediments (~ 0.40; Fig. 3-1). Using the mass accumulation rates derived from the gravity cores taken in Jamaica Bay, the sediment deposition in the Bay was ~ $7.6 \pm 1.4 \times 10^{10}$ g y^{-1}.

A sediment budget was constructed for Jamaica Bay by Bokuniewicz and Ellsworth (1986). This sediment budget included an estimate of sediment sources due to *in situ* production (0.1×10^{10} g y^{-1}) and sewage treatment plants (0.5×10^{10} g y^{-1}). They estimated a sediment deposition of $0.6 - 1.5 \times 10^{10}$ g y^{-1} in the subtidal bay from the ^{210}Pb geochronologies of 2 cores. They also estimated an annual deposition on the marshes of $1.5 - 2.0 \times 10^{10}$ g y^{-1} based on the ^{210}Pb geochronologies of 2 cores with accumulation rates of 0.7 to 0.9 cm y^{-1} and a marsh area of 17 km^2. A sediment importation through the inlet of $1.5 - 2.9 \times 10^{10}$ g y^{-1} would be needed to balance the other sediment sources and sinks.

A contemporary sediment budget can be constructed for Jamaica Bay using the previously estimated input due to *in situ* production (0.1×10^{10} g y^{-1}) and waste water (0.5×10^{10} g y^{-1}) and an annual sediment deposition in the bay subtidal derived from the geochronologies of 8 cores ($7.6 \pm 1.4 \times 10^{10}$ g y^{-1}). A revised estimate of annual sediment deposition on the marshes can be calculated from:

Deposition on the Marsh Islands = S_M × marsh area

where marsh area is the area of vegetated marsh in the bay in 2003 (~ 3.5 km^2; Update on the Missing Marshes of Jamaica Bay, 2007) and S_M is the mass accumulation rate measured on select marsh islands by Kolker (0.05 – 0.1 g cm^{-2} y^{-1}; 2005). This calculation yields an annual deposition on the marsh islands of ~ 0.2 – 0.4 × 10^{10} g y^{-1}. The annual sediment import needed to bring the input (*in situ* production and waste-water) and deposition terms (subtidal and marshes) into balance would be ~ 5.8 – 8.8 × 10^{10} g y^{-1}. This import estimate is similar to that found from "surplus" $^{234}Th_{xs}$ inventories (4.3 – 35.8 × 10^{10} g y^{-1}, see Chapter 2). However, although sediment deposition has been measured on marsh islands within the bay there has been 1.1 km^2 loss of vegetated marsh from 1974-1989 (0.07 km^2 loss y^{-1}) and 1.9 km^2 loss from 1989-2003 (0.13 km^2 loss y^{-1}; Update from the disappearing salt marshes of Jamaica Bay, NY, 2007). Some of this vegetated marsh loss includes interior ponding, fragmentation, slumping and edge erosion (Hartig et al., 2002), but to date there has been no work differentiating the vegetated marsh loss in Jamaica Bay between edge erosion and slumping and vegetation loss due to ponding. Sediment is deposited on the marsh islands and counted as a sediment sink in this budget, but there may be an unaccounted for source of sediment from erosion of the marsh islands. Thus, the calculated import of sediment via Rockaway Inlet needed to balance this budget should still be regarded as a high end estimate and the calculation of marsh loss due to edge erosion can further refine the bay's sediment budget.

5.4 Mass Balance of ^{210}Pb in Jamaica Bay

5.4.1 Atmospheric Deposition of ^{210}Pb

A 21 month record of atmospheric ^{210}Pb flux at Stony Brook, NY is shown in (see Chapter 4, Fig. 4-2 for details). Annual deposition was 0.87 ± 0.08 dpm cm^{-2} y^{-1} which is consistent with other measurements of direct atmospheric ^{210}Pb flux in New Haven, CT (Turekian et al., 1983; 0.86 – 1.04 dpm cm^{-2} y^{-1}), Norfolk, VA (Olsen et al., 1985; 0.90 dpm cm^{-2} y^{-1}) and Oak Ridge, TN (Olsen et al., 1985; 1.03 dpm cm^{-2} y^{-1}). Soil profiles from undisturbed sites have also been used to estimate annual atmospheric ^{210}Pb flux. Profiles from Connecticut (McCaffrey, 1977), Pennsylvania (Lewis, 1976) and Maryland (Fisenne, 1968) yielded annual atmospheric fluxes of 0.83, 1.0, 1.2 dpm cm^{-2} y^{-1}, respectively. Measurements of the excess ^{210}Pb in a soil profile taken in Jamaica Bay, on Broad Channel Island, yielded an annual flux of 1.1 dpm cm^{-2} yr^{-1} (Zeppie, 1977).

Based on a 1.0 dpm cm^{-2} yr^{-1} atmospheric flux of ^{210}Pb the expected steady state inventory of ^{210}Pb$_{xs}$ in a core that reflects only atmospheric input should be ~ 32.0 dpm cm^{-2} (annual ^{210}Pb flux × mean life of ^{210}Pb). ^{210}Pb inventories higher than 32 dpm cm^{-2} suggests additional sources or sediment focusing within Jamaica Bay. Indeed, inventories of ^{210}Pb$_{xs}$ in the Jamaica Bay cores were much higher than expected from direct atmospheric deposition (168 -351 dpm cm^{-2}). However, these cores were taken in areas dominated by fine sediments (mud fraction > 50%) which only comprise ~ 40% of the subtidal Bay (Fig. 3-1).

Since atmospherically derived ^{210}Pb is likely focused into these fine-grained sediment areas, the inventory expected from direct input can be adjusted using the equation:

Atmospheric Contribution =

$$(I^{Atm}_{Pb} \times \text{Subtidal Bay Area}) \div (\text{Subtidal Bay Area} \times 0.40) \qquad (3\text{-}5)$$

where I^{Atm}_{Pb} is the inventory of $^{210}Pb_{xs}$ in the sediments from an annual atmospheric ^{210}Pb flux of 1.0 dpm cm^{-2} yr^{-1} (~ 32 dpm cm^{-2}), Subtidal Bay Area is 3.9×10^{11} cm^{-2} and 0.4 is the fraction of the subtidal bay that is dominated by mud (Fig. 3-1). This adjustment increases the expected $^{210}Pb_{xs}$ inventory in the sediment cores due to direct input from the atmosphere from 32 to 80 dpm cm^{-2}. Even with this modification inventories of $^{210}Pb_{xs}$ in the sediment cores taken in Jamaica Bay are far in surplus to the adjusted expected inventory with the atmospheric source of $^{210}Pb_{xs}$ accounting for only 23- 48% of the observed $^{210}Pb_{xs}$ inventory. This suggests that there are sources of $^{210}Pb_{xs}$ into Jamaica Bay in addition to direct atmospheric input.

5.4.2 Freshwater Supply of ^{210}Pb

Previous studies of unsupported ^{210}Pb in Chesapeake Bay (Helz et al., 1985) and Long Island Sound (Benninger, 1978) showed that while the direct atmospheric input was the dominant source of ^{210}Pb, riverine input of ^{210}Pb also an important source. Jamaica Bay is a "sewershed" with the dominant freshwater source (90%) coming primarily from four wastewater treatment plants – Coney Island, Jamaica, 26th Ward and Rockaway (Beck et al., 2007; Bennoti et al., 2007). These wastewater treatment plants are connected to a

combined sewer system which combines sewage with street water runoff. During periods of heavy rainfall or frequent rainfall the inflow of wastewater exceeds the treatment plant capacity and untreated wastewater pours into the Bay.

The combined drainage area of these four wastewater plants is ~ 2.1×10^{12} cm^2 and the plants service a population of ~ 1.6 million people (Table 3-3). Due to the highly urbanized setting, impervious surface cover dominates the drainage area. The prevalence of impervious surface may allow the drainage area of these plants to act as a large atmospheric collector of $^{210}Pb_{xs}$. During light to moderate rainfall events the $^{210}Pb_{xs}$ can be rinsed off the roads (as well as sediments) and into the combined sewer where it is transported to the wastewater treatment plants. Due to the affinity of ^{210}Pb for fine-particles ($K_d = 10^3$–10^6), the ^{210}Pb from minor rainfall events is likely be removed from the wastewater during the primary treatment stage (sedimentation stage) and never enter Jamaica Bay. In contrast, during heavy rainfall events when a combined-sewer overflow occurs, $^{210}Pb_{xs}$ can enter Jamaica Bay directly with untreated sewage and wastewater. Thus, CSO events may be an important source of $^{210}Pb_{xs}$ into the subtidal sediments of Jamaica Bay and contribute to the elevated ^{210}Pb inventories measured in this study.

The concentration of ^{210}Pb in rainfall was measured from April-2008 to December-2009 in Stony Brook, NY and ranged from 4.0 to 15.0 dpm L^{-1} (see Chapter 4 for details). These values are consistent with those measured in New Haven, CT (1.8 – 17.1 dpm L^{-1}; Turekian et al., 1983) and Norfolk, VA (2.7 – 20.6 dpm L^{-1}; Todd et al., 1989). The contribution of CSO events to the $^{210}Pb_{xs}$ inventory measured in Jamaica Bay can be assessed using the equation:

$$\text{CSO Contribution} = [(R_{Pb} \times F_{CSO}) \div (\text{Subtidal Bay Area} \times 0.40)] \times (1/\lambda) \quad (3\text{-}6)$$

where R_{Pb} is the mean concentration of ^{210}Pb measured in rainfall (mean = 7.9 dpm L^{-1}; see Chapter 4 for details), F_{CSO} is the estimated average annual CSO flow into Jamaica Bay (32.0×10^9 L y^{-1}; Table 3-3; The Jamaica Plan: Final Environmental Impact Statement, 2007), the Subtidal Bay Area is 3.9×10^{11} cm^2, 0.40 is the fraction of subtidal of the Bay dominated by fine sediments (Fig. 3-1), and $1/\lambda$ (32 yr) is the radioactive mean life of ^{210}Pb. This calculation yields a CSO contribution to the total ^{210}Pb inventory in Jamaica Bay of 52 dpm cm^{-2}. This is a high estimate of ^{210}Pb input from CSO event because it assumes that all of the annual CSO flow into Jamaica Bay is surface water runoff from the streets. The CSO contribution of ^{210}Pb to the Bay accounts for 14 – 29% of the inventory measured in the sediment cores. This suggests that CSO events may be a significant, but not the dominant source of ^{210}Pb to Jamaica Bay.

5.4.3 In Situ Production of ^{210}Pb

^{210}Pb is produced in the water column by the in situ decay of dissolved ^{226}Ra, but this source is likely trivial to the ^{210}Pb budget of the Bay. The mean activity of ^{226}Ra in the water column was measured by Beck et al. (2007) in four sampling cruises in 2004-2006 and found to be ~ 0.15 dpm L^{-1}. Production of ^{210}Pb from the decay of ^{226}Ra, assuming no loss of ^{222}Rn, would result in an annual in situ production of 4.7×10^{-3} dpm L^{-1} y^{-1}. The inventory that can then be attributed to production in the water column can be calculated from:

$$\text{In Situ Production} = (A_{Pb} \times (1/\lambda) \times \text{Bay Volume}) \div (\text{Subtidal Bay} \times M_F) \quad (3\text{-}7)$$

where A_{Pb} is the annual activity of ^{210}Pb in the water column produced by the decay of ^{226}Ra (4.7×10^{-3} dpm L^{-1} y^{-1} or 4.7×10^{-6} cm^3 y^{-1}), $1/\lambda$ is the mean half-life of ^{210}Pb (32 y), the bay volume, assuming a mean depth of 500 cm, is 2.0×10^{14} cm^3, the subtidal bay area is 3.9×10^{11} cm^{-2} and M_F is the fraction of the subtidal bay dominated by muddy sediments (0.40). In situ production of ^{210}Pb in the water column assuming a complete scavenging and then deposition to the Bay bottom sediments would only account for an inventory of ~ 0.20 dpm cm^{-2}, less 1% of the $^{210}Pb_{xs}$ inventory measured in the sediment cores.

5.4.4 Groundwater Supply of ^{210}Pb

Groundwater may potentially be a source of ^{210}Pb into Jamaica Bay, the ^{210}Pb supplied by groundwater can be scavenged on to particles and deposited in the subtidal bay sediments. Few studies have examined the behavior of ^{210}Pb in groundwater (Porcelli, 2008). In contrast, the grandparent of ^{210}Pb, ^{226}Ra, has been measured and used, along with the other radium isotopes (^{224}Ra, ^{223}Ra, ^{228}Ra), to characterize and estimate submarine groundwater discharge in several coastal and estuarine systems (Moore, 1996; Charette et al., 2001, Beck et al., 2007). The concentration of ^{226}Ra in Jamaica Bay's groundwater was measured by Beck et al. (2007) and found to be 0.83 ± 0.39 dpm L^{-1}.

If we use the ground-water input of ^{226}Ra as a upper limit of the input of ground-water derived ^{210}Pb to Jamaica Bay, the inventories supplied from this source can be estimated from:

$$\text{Groundwater Contribution} = (C_{226} \times J_{GW} \times (1/\lambda)) \div (\text{Subtidal Bay Area} \times M_F) \quad (3\text{-}8)$$

where C_{226} is the concentration of ^{226}Ra in groundwater (0.83 dpm L^{-1}; Beck et al., 2007), J_{GW} is the discharge of ground-water to Jamaica Bay (~ 4.16×10^{10} L y^{-1}; Misut and Voss, 2004), $1/\lambda$ is the mean half-life of ^{210}Pb (32 y), subtidal bay area is 3.9×10^{11} and M_F is the fraction of the subtidal bay dominated by fine-grained sediments (~0.40). This calculation, assuming complete scavenging and subsequent deposition in the subtidal bay, yields a ^{210}Pb inventory of 7.1 dpm cm^{-2} which would account for 2 – 4% of the total $^{210}Pb_{xs}$ inventory in the sediments. This is likely an overestimation of ^{210}Pb input from groundwater as it does not account for scavenging of ^{210}Pb onto aquifer surfaces or in the subterranean estuary. In addition the ^{226}Ra concentration measured in Jamaica Bay reflects both the input of fresh ground-water to the bay and recirculation of saline water through the sediments and thus, likely further contributes to an overestimation of ^{210}Pb input from groundwater. However for the purposes of this mass balance study, even this a high end estimate of ^{210}Pb via ground-water input does not explain the high $^{210}Pb_{xs}$ inventories measured in the sediment cores.

5.4.5 Import of ^{210}Pb from the Ocean

Previous studies indicate that sediment is imported into Jamaica Bay through Rockaway Inlet (Bokuniewicz and Ellsworth, 1986; Swanson and Wilson, 2008; see Chapter 2); the various estimates of sediment import into Jamaica Bay are compiled in Table 4-3. To assess the possible import of ^{210}Pb from the ocean associated with particles, the activities of ^{210}Pb on filterable particles were measured at 4 sites, in August-2008, during a flooding tide (Table 3-1). The $^{210}Pb_{xs}$ activity on particles was highest at the inlet station (0.1 dpm g^{-1}) and in the deep water just within the bay (2.8 ± 0.6 dpm g^{-}

[1]). High $^{210}Pb_{xs}$ activities on filterable particles at the inlet suggest that $^{210}Pb_{xs}$ may be imported from the ocean into the bay associated with particles.

The concentration of dissolved $^{210}Pb_{xs}$ was not measured in this study. Total ^{210}Pb concentrations (particulate + dissolved) in the water column at the eastern end of Long Island Sound were found to be ~ 0.04 dpm L^{-1} (Benninger, 1978) and total ^{210}Pb concentrations measured in the waters of the New York Bight were ~ 0.05 dpm L^{-1} (Li, Y-H et al., 1981). $^{210}Pb_{xs}$ activity on filterable particles at the inlet station in Jamaica Bay was 0.12 dpm L^{-1}; higher than the total activity measured in the water column in the New York Bight. Similar conditions were observed in Tampa Bay, FL where within the Bay the mean concentration of total ^{210}Pb was 0.14 dpm L^{-1} (Baskaran and Swarzenski, 2007), while total ^{210}Pb concentration in the surface waters of the shelf and slope of the Gulf of Mexico were ~ 0.05 dpm L^{-1} (Basakaran and Satschi, 2006). In addition, the work conducted in Tampa Bay found that at salinities greater than 27.0 the dissolved ^{210}Pb concentrations were below detection limits, leaving all measurable ^{210}Pb in the water column associated with particles. Thus, for the purposes of this study we assume that ^{210}Pb is predominantly imported into Jamaica Bay associated with particles and that the import of dissolved ^{210}Pb through the inlet is negligible.

The inventory of ^{210}Pb supported by the ^{210}Pb activity imported via Rockaway Inlet can be calculated from:

Input of ^{210}Pb from the Ocean =

$$[Pb_P \times V_{in} \times t_d \times (1/\lambda_{Pb})] \div (\text{Subtidal Bay Area} \times M_F) \qquad (3\text{-}9)$$

where Pb_P is the activity of particulate ^{210}Pb at the inlet station (0.09 dpm L^{-1}; Table 3-1), V_{in} is the tidal prism of Jamaica Bay (6.06×10^{10} L; Beck et al., 2007), t_d is the tides per day (1.91 d^{-1}; Beck et al., 2007), $(1/\lambda_{Pb})$ is the radioactive mean half-life of ^{210}Pb (1.2×10^4 d), the subtidal bay area is 3.9×10^{11} cm^2 and M_F is the fraction of the bay area dominated by fine-grained sediments (~ 0.40; Fig. 3-1). The calculated $^{210}Pb_{xs}$ inventory supported by import of $^{210}Pb_{xs}$ associated with particles from the ocean is 801 dpm cm^{-2} which is 100% of the $^{210}Pb_{xs}$ inventory measured in the Jamaica Bay sediment cores (Table 3-2). However, as suggested by the mass balance of ^{234}Th and ^{7}Be (see Chapters 2 and 4 for details) there may be loss of ^{210}Pb from the Bay.

If we assume that the activity of ^{210}Pb at station JB-WS-2-Shallow (Table 3-1) characterizes the activity of the water lost from the Bay, the ^{210}Pb export can be calculated from:

$$\text{Export of } ^{210}Pb = [Pb_P \times (V_{out} \times t_d + F_{WW}) \times (1/\lambda_{Pb})] \div (\text{Subtidal Bay Area} \times M_F) \quad (3\text{-}10)$$

where Pb_P is the activity of particulate ^{210}Pb in the surface water within the Bay (0.06 dpm L^{-1}; Table 3-1), V_{out} is the tidal prism of Jamaica Bay (6.06×10^{10} L; Beck et al., 2007), t_d is the tides per day (1.91 d^{-1}; Beck et al., 2007), F_{WW} is the mean daily wastewater discharge (7.5×10^8 L d^{-1}; Beck et al., 2007), $(1/\lambda_{Pb})$ is the radioactive mean half-life of ^{210}Pb (1.2×10^4 d), the subtidal bay area is 3.9×10^{11} cm^2 and M_F is the fraction of the bay area dominated by fine-grained sediments (~ 0.40; Fig. 3-4). This calculation yields an export of ^{210}Pb of 538 dpm cm^{-2} and net import of ^{210}Pb from the ocean of 263 dpm cm^{-2}. This net import estimate of ^{210}Pb is 76-100% of the inventory

measured in the gravity cores. The mass balance terms for ^{210}Pb are compiled in Table 3-4.

In the mass balances of ^{234}Th and ^{7}Be the predicted inventories were comparable to those measured in the subtidal sediments over the sampling period. (see Chapters 2 and 4 for details). In contrast, the mass balance of ^{210}Pb predicts inventories 1 to 2.0× higher than that measured in the cores. This may in part reflect overestimation in the inputs of ^{210}Pb to Jamaica Bay (e.g. CSO input and groundwater input). In addition, with a half-life of 22.2 years, ^{210}Pb integrates over much longer periods of time, compared to ^{234}Th and ^{7}Be, thus a single set of water column measurements appear to be insufficient for balancing ^{210}Pb in Jamaica Bay.

The sediment import required to bring the ^{210}Pb budget of Jamaica Bay into balance can be calculated from:

$$\text{Sediment Import} = [I_{Pb}\square \div (Pb_P \div TSS)] \times \lambda_{Pb} \times (\text{Subtidal Bay Area} \times M_F) \quad (3\text{-}11)$$

where $I_{Pb}\square$ is the $^{210}Pb_{xs}$ inventory is surplus to that supplied through other sources (66 – 249 dpm cm^{-2}; Table 3-2), Pb_P is the activity of ^{210}Pb on particles measured at the inlet (0.1 dpm L^{-1}; Table 3-1), TSS is the particle concentration in the water column at the inlet station (0.0133 g L^{-1}), λ_{Pb} is the decay constant of ^{210}Pb (0.0312 y^{-1}), subtidal bay area is (3.9×10^{11} cm^{-2}) and M_F is the fraction of the subtidal bay dominated by fine sediments (0.40; Fig. 3-1). From this calculation the annual sediment import required to account $^{210}Pb_{xs}$ inventory of the bay ranges from $4.2 – 15.8 \times 10^{10}$ g y^{-1}. This import range agrees with that determined from ^{210}Pb-derived mass accumulation rates ($5.8 – 8.8 \times 10^{10}$ g y^{-1};

see Section 5.3). The good agreement between the estimates of sediment input to Jamaica Bay for ^{210}Pb (this study) and sediment mass balance (1.5 – 2.9 × 10^{10} g y^{-1}; Bokuniewicz and Ellsworth, 1986) contrasts with the input estimate based on ^{234}Th (4.3 – 35.8 ×10^{10} g y^{-1}; see Chapter 2). This suggests that seasonal differences in sediment import can affect the ^{234}Th-derived estimates, dissolved ^{234}Th import, scavenging and production. Although there are differences in the estimates of sediment importation into Jamaica Bay from these various methods indicate that sediment import is significant.

^{210}Pb mass balances have been constructed for Long Island Sound by Benninger (1978) and for the Chesapeake Bay (Helz, 1985). In Long Island Sound the direct atmospheric input accounted for ~ 100% of the unsupported ^{210}Pb measured in cores taken within the Bay (Benninger, 1978). In the Chesapeake Bay, the direct atmospheric input of ^{210}Pb accounted for 91% and 97% of the ^{210}Pb inventory in the middle and lower bay, respectively. In the upper Chesapeake, direct atmospheric input accounted for 48% of the ^{210}Pb inventory and riverine input from the Susquehanna accounted for 46% (Helz, 1985). In contrast, the direct atmospheric input of ^{210}Pb into Jamaica Bay only accounts for ~ 22 – 30 % of the $^{210}Pb_{xs}$ inventory measured in the cores (Table 3-4), while the importation of ^{210}Pb associated with particles via Rockaway Inlet accounts for 62 – 72 % of the ^{210}Pb inventory measured. This suggests that importation and trapping of sediments is an important consideration in the overall sediment budget of Jamaica Bay.

6. Conclusions

Extensive modification have been made since the mid-1800s such as, dredging for shipping channels and the creation of deep borrow pits within the bay. These

modification have resulted in a change of the bay's hydrodynamics, switching it from a slightly ebb dominated to flood dominated estuary. Sediment accumulation rates, determined from ^{210}Pb profile in 8 gravity cores taken in the bay in August-2008, were highest in the dredged channel in the northwestern part of the bay and in the borrow pit in the northeastern bay (Grassy Bay). Annual deposition in the subtidal bay derived from the gravity cores ranged from $7.6 \pm 1.4 \times 10^{10}$ g y^{-1}. To balance the sediment budget of the bay a sediment import of $5.8 - 8.8 \times 10^{10}$ g y^{-1} was required. This may be a high end estimate for sediment import as the sediment budget does not account for an input of sediment in the subtidal bay from the erosion of marsh islands in the bay. Further research is needed to differentiate vegetated marsh loss due to interior ponding and edge erosion to further refine this budget.

Inventories of ^{210}Pb in the 8 gravity cores were in surplus to the direct atmospheric input of ^{210}Pb (32 dpm cm^{-2}), even when adjusted for focusing of sediment deposition into fine-particle dominated area (80 dpm cm^{-2}), suggesting that there are additional sources of ^{210}Pb in to Jamaica Bay. Additional input of ^{210}Pb was from CSO discharge (15 dpm cm^{-2}), in situ production (0.2 dpm cm^{-2}) and groundwater input (7 dpm cm^{-2}). Using a mass balance of $^{210}Pb_{xs}$ in Jamaica Bay the import of sediment needed to balance the ^{210}Pb budget was estimated ($4.2 - 15.8 \times 10^{10}$ g y^{-1}). This import estimate based on surplus ^{210}Pb inventories is comparable to that suggested by Bokuniewiz and Ellsworth to balance the Bay's sediment budget.

7. References

Adams, D.A., J.S. O'Connor, and S.B. Weisberg (1998) *Sediment Quality of the NY/NJ Harbor System*. U. S. Environmental Protection Agency, Report No. 902-R-98-001.

Appleby, P.G. and F. Oldfield (1992) Applications of Lead-210 to sedimentation studies. M. Ivanovich and R.S. Harmon (eds), Uranium-Series Disequilibrium: Applications to Environmental Problems, Clarendon Press, Oxford, pp. 731-778

Baskaran, M. (1995) A search for the seasonal variability on the depositional fluxes of ^{7}Be and ^{210}Pb. *Journal of Geophysical Research* 100: 2833-2840.

Baskaran, M. and P. H. Santchi (1993) The role of particles and colloids in the transport of radionuclides in the coastal environments of Texas. *Marine Chemistry* 43: 95-114.

Baskaran, M. and P.W. Swarzenski (2006) Seasonal variations on the residencetimes and partitioningof short-lived radionuclides (^{234}Th, ^{7}Be and ^{210}Pb) and depositional fluxes of ^{7}Be and ^{210}Pb in Tampa Bay, Florida. *Marine Chemistry* 104: 27-42.

Beck, A.J., J.P. Rapaglia, J.K. Cochran and H.J. Bokuniewicz (2007) Radium mass-balance in Jamaica Bay, NY: Evidence for substantial flux of submarine groundwater. *Marine Chemistry*, 106: 416-441.

Benninger, L.K. (1978) ^{210}Pb balance in Long Island Sound. *Gechimica et Cosmochimica Acta*, 42: 1165-1174.

Benninger, L.K., R.C. Aller, J.K. Cochran and K.K. Turekian (1979) Effects of biological mixing on the 210Pb chronology and trace metal distribution in a Long Island sound sediment core. *Earth Planetary Science Letters*, 43: 241-259.

Benotti, M. J., M. Abbene and S. A Terracciano (2007) Nitrogen Loading in Jamaica Bay, Long Island, New York: Predevelopment to 2005. USGS Open File Report SIR 2007-5051, 17 pp.

Black, F.R. (1981) *Jamaica Bay: A History*. Gateway National Recreation Area New York, New Jersey.

Botton, M.L., R.E. Loveland, J.T. Tanacredi, and T. Itow (2006) Horseshoe Crabs (*Limulus polyphemus*) in an urban estuary (Jamaica Bay, New York) and the potential for ecological restoration. *Estuaries and Coasts* 29: 820-830.

Bokuniewicz, H., and J. Ellsworth (1986) Sediment budget for the Hudson system, *Journal of Northeastern Geology* 8: 158-164.

Carroll, J. and I. Lerche (2003) Sedimentary processes: Quantification using radionuclides (M.S. Baxter ed.), Radioactivity in the Environment, vol. 5.

Charette, M.A. K.O. Buesseler, J.E. Andrews (2001) Utility of radium isotopes for evaluating the input and transport of groundwater-derived nitrogen to a Cape Cod estuary. *Limnology and Oceanography* 46: 465-470.

Cochran, J.K., D.J. Hirschberg and D. Amiel (2000) Particle mixing and sediment accumulation rates of Peconic Estuary sediments: A sediment accretion study in support of the Peconic Estuary Program. Report #: 0014400498181563

DeMaster, D.J., B.A. McKee, C.A. Nittrouer, Q. Jiangchu and C. Guodong (1985) Rates of sediment accumulation and particle reworking based on radiochemical measurements from continental shelf deposits in the East China Sea. *Continental Shelf Research* 4: 143-158.

Diaz, R.J., D.C. Rhoads, J.A. Blake, R.K. Kropp and K.E. Keay (2008) Long-term trends of benthic habitats related to a reduction in wastewater discharge to Boston Harbor. *Estuaries and Coasts,* 31: 1184-1197.

Feng, H., J.K. Cochran and D.J. Hirschberg (1999) ^{234}Th and ^{7}Be as tracers for the sources of particles to the turbidity maximum of the Hudson River Estuary. *Estuarine, Coastal, and Shelf Science* 49: 629-645.

Ferguson, P.L., R.F. Bopp, S.N. Chillrud, R.C. Aller and B.J. Brownawell (2003) Biogeocehmistry of nonylphenol ethoxylatesin urban estuarine sediments. *Environment Science and Technology* 37: 3499-306.

Fisenne, I.M. (1968) Distribution of lead-210 and radium-226 in soil. Rep. UCRL-18140, pp. 145-158. Washington, D.C.: US At. Energy Comm.

Giffin, D. and D. R. Corbett (2003) Evaluation of sediment dynamics in coastal systems via short-lived radioisotopes. *Journal of Marine Systems* 42: 83-96.

Hartig, E. K., V. Gornitz, A. Kolker, F. Mushacke and D. Fallon (2002) Anthropogenic and climate-change impacts on salt marshes of Jamaica Bay, New York City. Wetlands 22: 71-89.

Helz, G.R., G.H. Setlock, A.Y. Cantillo and W.S. Moor (1985/86) Processes controlling the regional distribution of ^{210}Pb, ^{226}Ra and anthropogenic zinc in estuarine sediments. *Earth and Planetary Science Letters* 76: 23-34.

Interstate Environmental Commission, 2008 Annual Report, New York, NewJersey Connecticut, 99 pp.

Iocco, L.E., P. Wilber, R.J. Diaz, D.G. Clarke and R.J. Will (2000) *Benthic Habitats of New York/New Jersey Harbor: 1995 Survey of Jamaica, Upper, Newark, Bowery and Flushing Bays Final Report*.

Jamaica Plan: Final Environmental Impact Statement (2007) Appnedix I: WPCP and CSO impact analysis. 27 pp.

Kaste, J. M., S. A. Norton and C. T. Hess (2002) Environmental chemistry of beryllium-7. In: Beryllium: Mineralogy, petrology, and geochemistry (P. H. Ribbe and J. J. Rosso, eds.), Reviews in Mineralogy and Geochemistry, vol. 50, pp. 291-312.

Kolker, A. (2005) The Impacts of Climate Variability and Anthropogenic Activities on Salt Marsh Accretion and Loss on Long Island. Stony Brook, New York: Stony Brook University Ph.D. thesis, 278p.

LeCloarec, M-F., P. Bonté, I. Lefèvre, J-M Mouchel, S. Colbert (2007) Distribution of ^{7}Be, ^{210}Pb, and ^{137}Cs in watersheds of different scales in the Seine River basin: Inventories and residence times. *Science of the Total Environment* 375: 125-139.

Lewis, D.M. (1976) The geochemistry of manganese, iron, uranium, lead-210 and major ions in the Susquehanna River. PhD Thesis. New Haven, CT. 272 pp.

Li, Y-H, P.H. Santschi, A. Kaufman, L.K. Benninger and H.W. Feely (1981) Natural radionuclides in waters of the New York Bight. *Earth and Planetary Science Letters* 55: 217-228.

Matisoff, G., C.W. Wilson, and P.J. Whiting (2005) The ^{7}Be/^{210}Pb ratio as an indicator of suspended sediment age or fraction new sediment in suspension. *Earth Surface Processes and Landforms* 30: 1191-1201.

McCaffrey, R.J. (1977) A record of the accumulation of sediment and trace metals in a Connecticut, USA, salt marsh. PhD Thesis, New Haven, CT, 156 pp.

Moore, W.S. (1996) Large groundwater inputs to coastal waters revealed by Ra-226 enrichments. *Nature* 380: 612-614.

Olsen, C.R., I.L. Larsen, P.D. Lowry, N.H. Cutshall, J.F. Todd, G.T.F. Wong and W.H. Casey (1985) Atmospheric fluxes and marsh-soil inventories of ^{7}Be and ^{210}Pb. *Journal of Geophysical Research* 90: 10487-10495.

O'Shea, M.L. and T.M. Brosnan (2000) Trends in indicators of eutrophication in western Long Island Sound and the Hudson-Raritan Estuary. *Estuaries* 23: 877-901.

Ritchie, J.C. and J.R. McHenry (1990) Application of radioactive fallout cesium-137 for measuring soil erosion and sediment accumulation rates and patterns: A review. *Journal of Environmental Quality* 19: 215-233.

Sharma, P., L.R. Gardner, W.S. Moore, and M.S. Bollinger. (1987) Sedimentation and bioturbation in a salt marsh as revealed by ^{210}Pb, ^{137}Cs, and ^{7}Be studies. *Liminology and Oceanography* 32: 313-326.

Strickney, A.P. and L.D. Stringer (1957) A study of the invertebrate bottom fauna Greenwich Bay, Rhode Island. *Ecology* 38: 111-122.

Suszkowski, D. J. (1978) Sedimentology of Newark Bay, New Jersey: an urban estuary, Ph.D. Thesis, University of Delaware, 222 pp.

Swanson, L.R. and R. E. Wilson (2008) Increased tidal ranges coinciding with Jamaica Bay development contribute to marsh flooding. *Jounral of Coastal Research* 24: 1565-1569.

Todd, J.F., G.T.F. Wong, C. Olsen and I.L. Larsen (1989) Atmospheric depositional characteristics of Beryllium 7 and Lead 210 along the southeastern Virginia coast. *Journal of Geophysical Research* 94: 11106-11116.

Turekian, K.K., L.K. Benninger, and E.P. Dion (1983) ^{7}Be and ^{210}Pb total depositional fluxes at New Haven, Connecticut, and Bermuda. *Journal of Geophysical Research* 88: 5411-5415.

Turekian, K.K., Y. Nozaki, and L. Benninger (1977) Geochemistry of atmospheric radon and radon products. *Annual Review of Earth and Planetary Science* 5: 227-255.

An update on the disappearing salt marshes of Jamaica Bay, NY (2007) http://nbii-nin.ciesin.columbia.edu/jamaicabay/jbwppac/JBAC_NPS_SaltMarshReport_080207.pdf.

Wolfe, D.A., E.R. Long and G.B. Thursby (1996) Sediment toxicity in the Hudson-Raritan estuary: Distribution and correlations with chemical contaminations. *Estuaries* 19: 901-912.

Zeppie, C.R. (1977) Vertical profiles and sedimentation rates of Cd, Cr,Cu, Ni and Pb in Jamaica Bay, New York. M.S. Thesis. Stony Brook, NY. 85pp.

Table 3-1. ^{210}Pb activities of filterable (> 1 mm) particles in the water column

Sample ID	Description	Depth (m)	Salinity	TSS (mg L^{-1})	Particulate $^{210}Pb_{xs}$ (dpm L^{-1})	Particulate $^{210}Pb_{xs}$ (dpm g^{-1})
JB-WS-1	Inlet Station	3.0	28.5	15.5	0.09 ± 0.01	9.3 ± 1.0
JB-WS-1*	Inlet Station	1.0	28.3	11.1	0.1 ± 0.03	8.2 ± 2.6
JB-WS-2-Shallow	Bay Interior	1.0	28.3	13.1	0.06 ± 0.01	2.8 ± 0.6
JB-WS-2-Deep	Bay Interior	5.0	28.5	16.5	0.05 ± 0.01	2.7 ± 0.5
JB-WS-3	Grassy Bay	5.0	26.6	15.0	0.01 ± 0.01	0.6 ± 0.3
JB-WS-4	Near eastern marshes	2.0	27.5	15.2	0.01 ± 0.01	0.7 ± 0.2

Table 3-2. Inventory of $^{210}Pb_{xs}$ in gravity core and accumulation rates estimated from $^{210}Pb_{xs}$ and ^{137}Cs

Core #	Description	Water Depth (m)	$^{210}Pb_{xs}$ Inventory (dpm cm^{-2})	Accumulation Rate (cm y^{-1}) estimated from $^{210}Pb_{xs}$	Accumulation Rate (cm y^{-1}) estimated from ^{137}Cs	Mean Bulk Density (g cm^{-3})	Mass Accumulation Rate (g cm^{-2} y^{-1})
1	Eastern Marshes	4.7	245.5 ± 21.3	0.9 ± 0.1	0.9*	0.8 ± 0.07	0.7
2	Southeastern Channel	5.8	167.5 ± 20.4	0.5 ± 0.1	-	0.9 ± 0.06	0.5
3	Thurston Basin	8.0	332.5 ± 56.1	0.1 ± 0.01	-	1.2 ± 0.05	0.1
4	Grassy Bay	11.4	187.3 ± 35.4	1.0 ± 0.1	1.0*	0.3 ± 0.05	0.3
5	Grassy Bay	9.3	193.1 ± 25.1	0.8 ± 0.1	0.7*	0.5 ± 0.02	0.4
6	Floyd Bennett Field	13.0	269.6 ± 25.8	1.1 ± 0.1	-	0.8 ± 0.05	0.9
7	Northwestern Bay	12.7	350.9 ± 39.2	1.0 ± 0.1	1.2	0.6 ± 0.04	0.6
8	Northern Bay	9.6	205.6 ± 23.1	0.5 ± 0.1	0.4	0.7 ± 0.09	0.4

* estimated from 1963 ^{137}Cs peak

Table 3-3. Characteristics of the waste-water treatment plants that discharge to Jamaica Bay, NY.

Waste-water Treatment Plants	Drainage Basin Area ($\times 10^{11}$ cm^2)	Population Served*	Design Flow (10^6 L d^{-1})*	Annual CSO Flow ($\times 10^9$ L)**	Annual Input of ^{210}Pb from CSO events ($\times 10^{10}$ dpm)***	Expected ^{210}Pb Inventory (dpm cm^{-2}) from CSO events
Coney Island	6.1	602,100	409	2.4	1.9	3.5
26th Ward	10.2	271240	316	8.1	6.4	11.9
Jamaica	2.4	632150	372	21.6	17.1	31.4
Rockaway	2.5	94,500	167	0	0	0
Total	**21.2**	**1,599,990**	**1287**	**32.1**	**25.4**	**52.1**

* data from Interstate Environmental Commission, 2008
** data from The Jamaica Plan: The Final Environmental Impact Statement, 2007.
*** estimated using the mean atmospheric ^{210}Pb flux of 7.9 dpm L^{-1} (see Chapter 4 for details).

Table 3-4. Mass balance of $^{210}Pb_{xs}$ in Jamaica Bay

		Total $^{210}Pb_{xs}$ ($\times 10^{11}$ dpm)	$^{210}Pb_{xs}$ (dpm cm^{-2})
Inputs			
	Atmospheric Deposition	125	80
	CSO Discharge	81	52
	In Situ Production from ^{226}Ra	0.3	0.2
	Groundwater Discharge	11	7
	Import from the Ocean	1250	801
	Total	1466	940
Export	Loss via Inlet	839	538
	Predicted $^{210}Pb_{xs}$ Inventory	627	402
	Measured $^{210}Pb_{xs}$ Inventory of Subtidal Sediment Cores	418 – 563	168 – 351

Table 3-5. Estimates of sediment import into Jamaica Bay.

Estimated Sediment Import ($g\ y^{-1}$)	Method of Estimate	Reference
$1.5 – 2.9 \times 10^{10}$	Sediment Budget Balance	Bokuniewicz and Ellsworth, 1986
$4.3 – 35.8 \times 10^{10}$	$^{234}Th_{xs}$ Mass Balance	This Study (see Chapter 2)
$5.8 – 8.8 \times 10^{10}$	Based on mass accumulation rates (^{210}Pb Geochronology)	This Study (see Chapter 3)
$4.2 – 15.8 \times 10^{10}$	^{210}Pb Mass Balance	This Study (see Chapter 3)

* import estimate calculated from unaccounted for ^{210}Pb inventory in the gravity cores

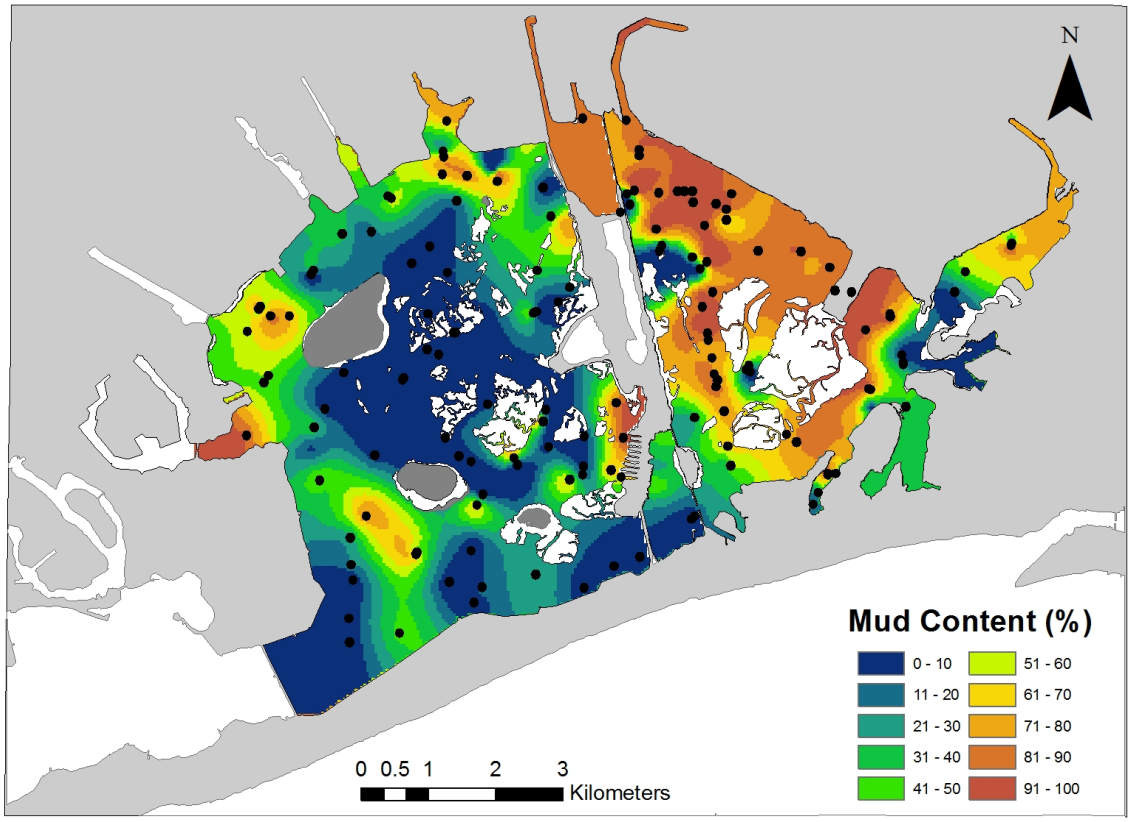

Figure 3-1. Contour map of mud content of the surficial, subtidal sediments of Jamaica Bay. The black circles indicate sites sampled and measured for mud content.

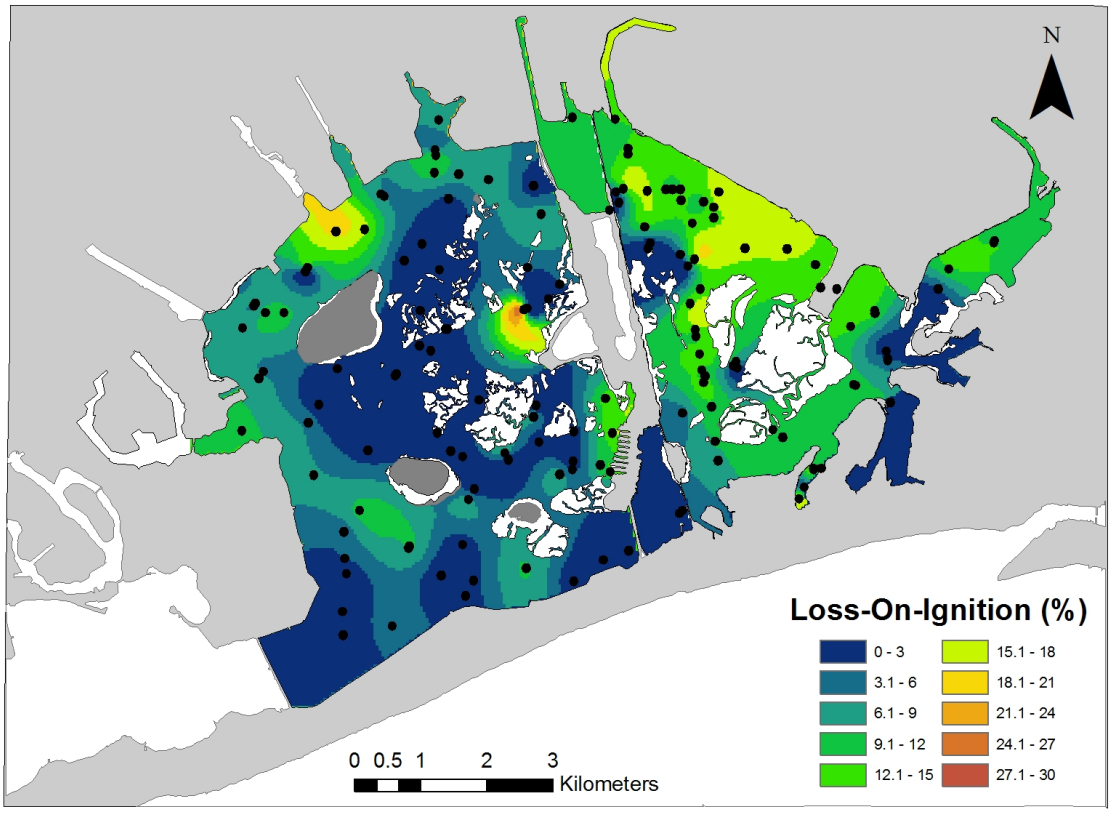

Figure 3-2. Contour map of organic content (determined from loss-on-ignition, LOI) of the surficial, subtidal sediments of Jamaica Bay. The black circles indicate sites sampled and measured for organic content.

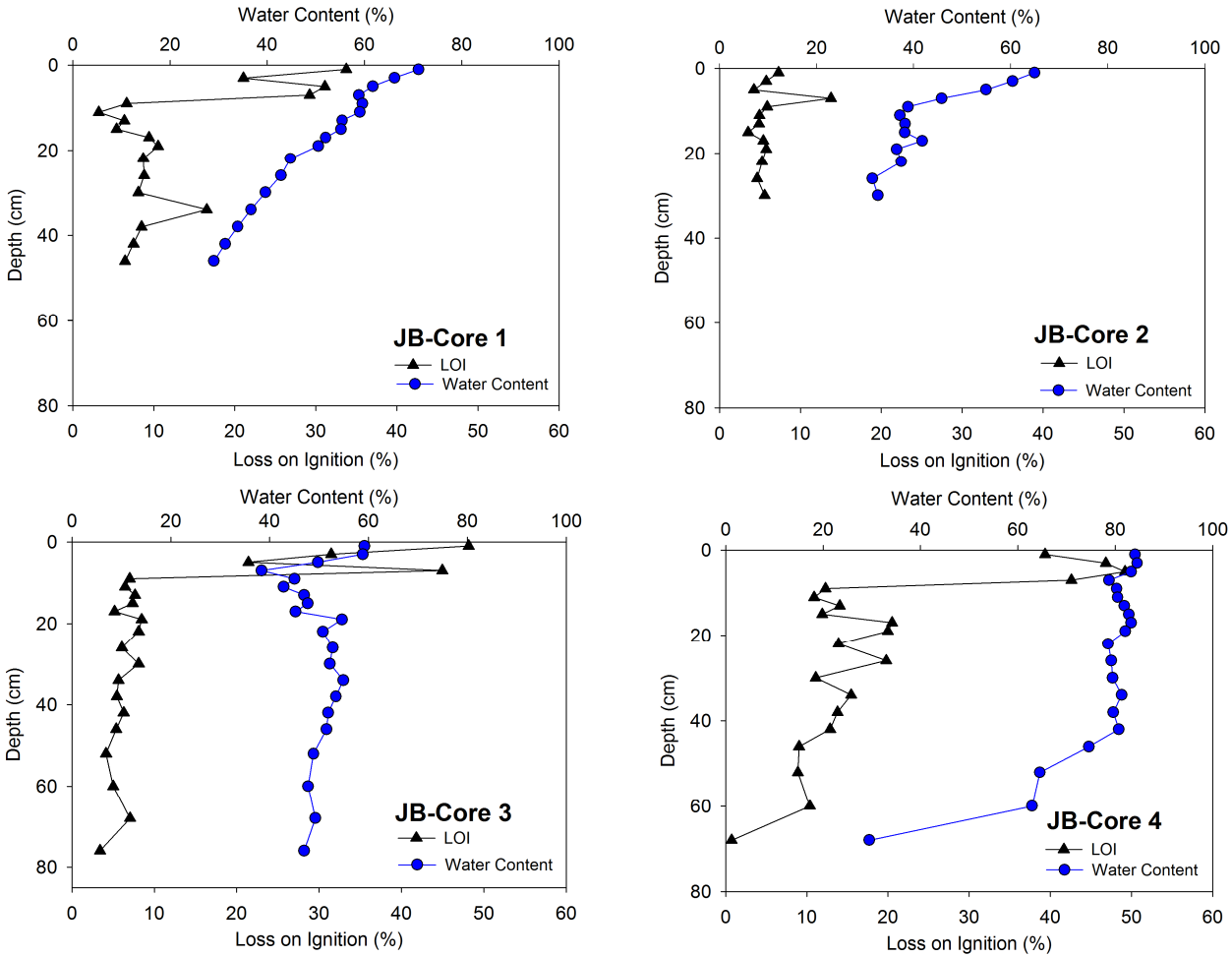

Figure 3-3 Water content and Loss-on-Ignition (LOI) vs depth for the gravity cores taken in Jamaica Bay

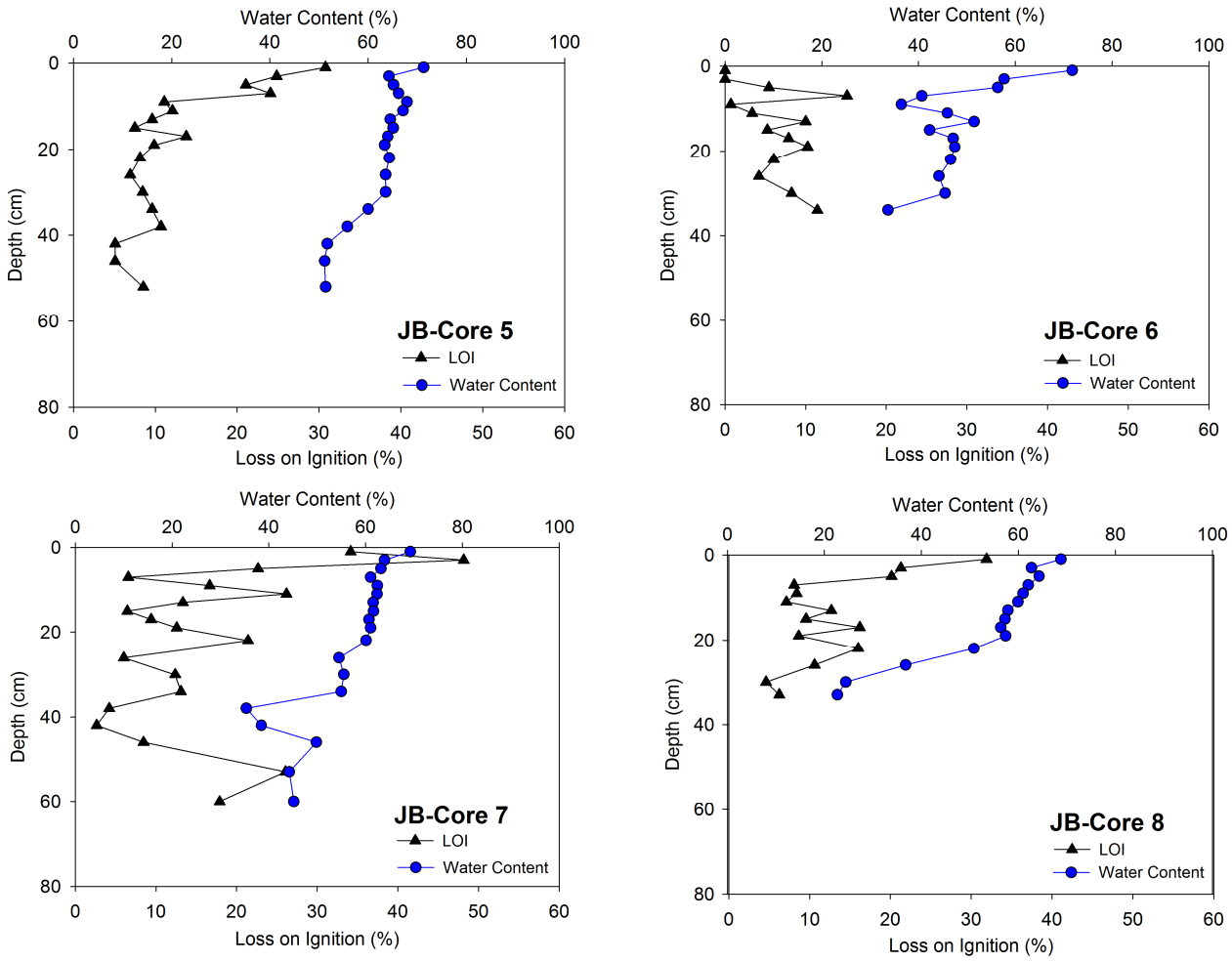

Figure 3-3 Continued

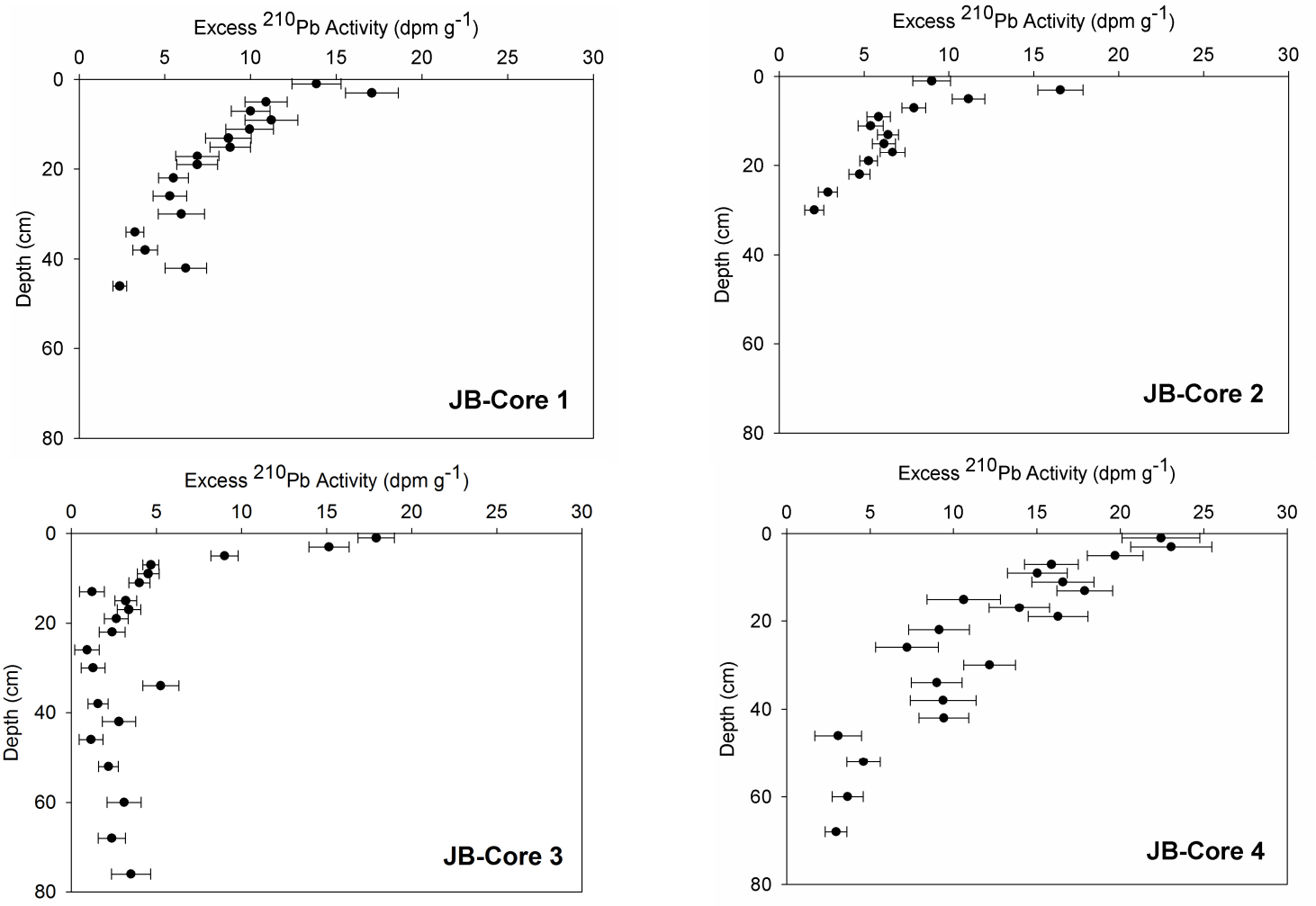

Figure 3-4 Excess ^{210}Pb activity with depth for the gravity cores taken in Jamaica Bay

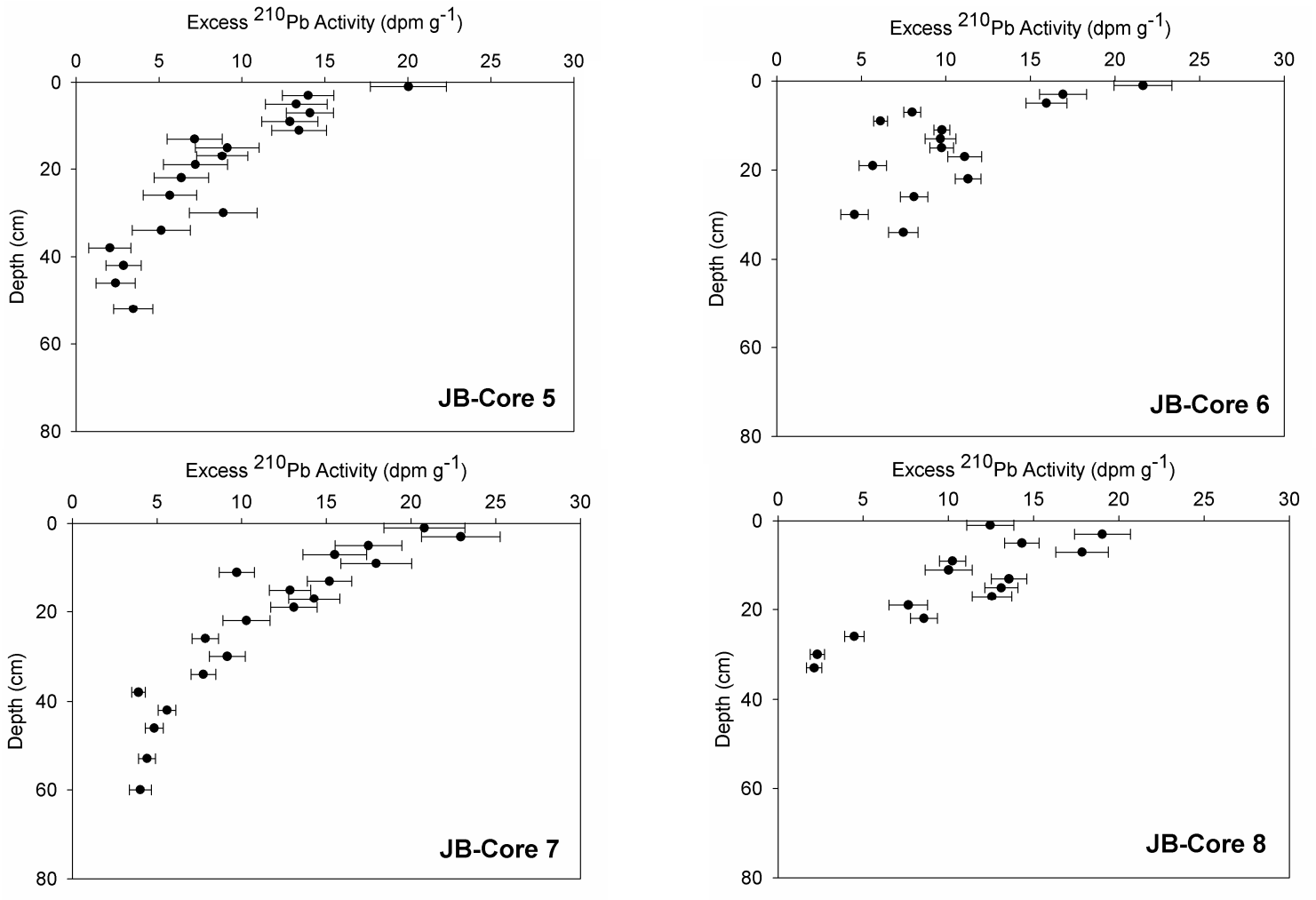

Figure 3-4 Continued

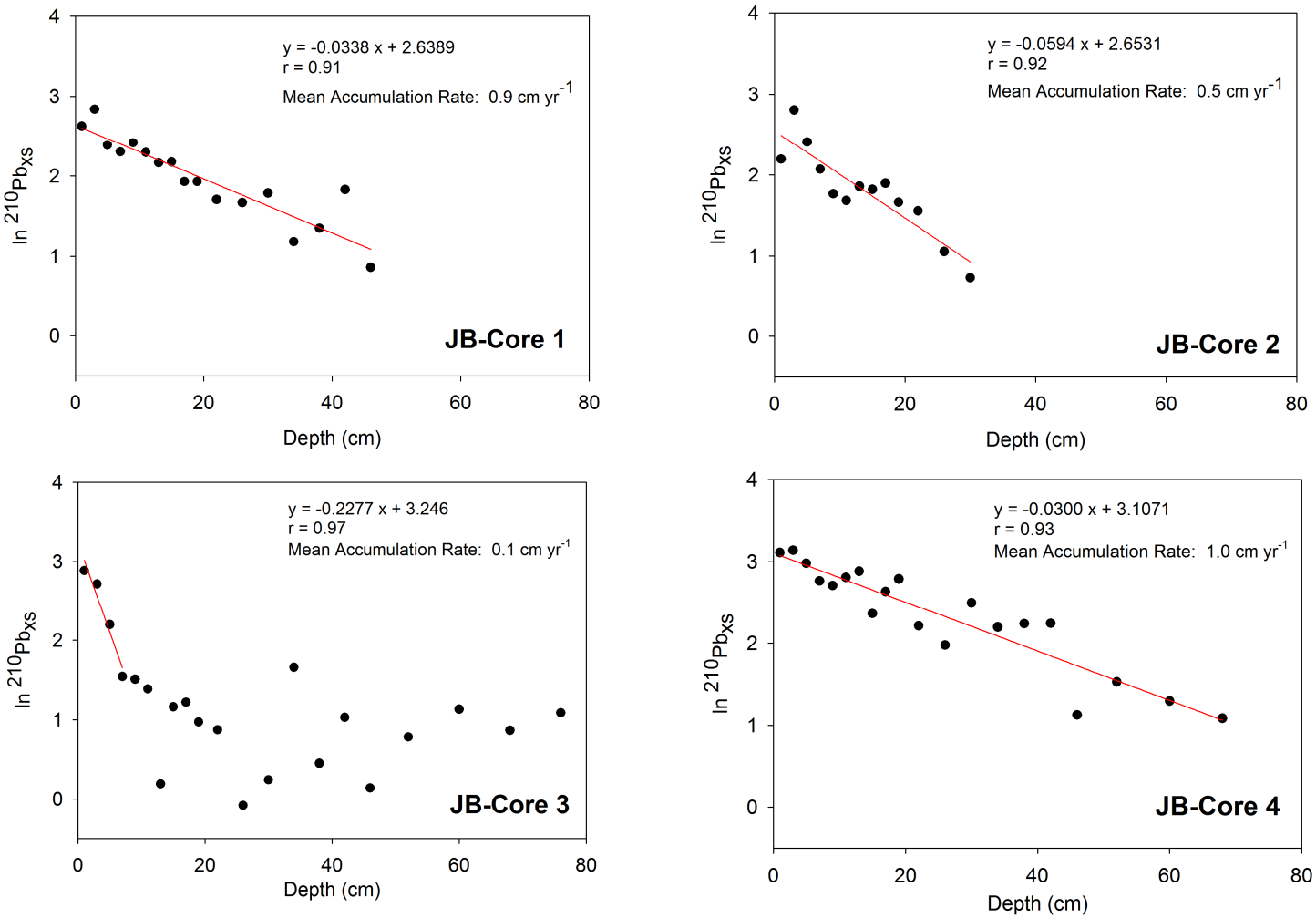

Figure 3-5 Ln $^{210}Pb_{xs}$ vs depth for the gravity cores taken in Jamaica Bay

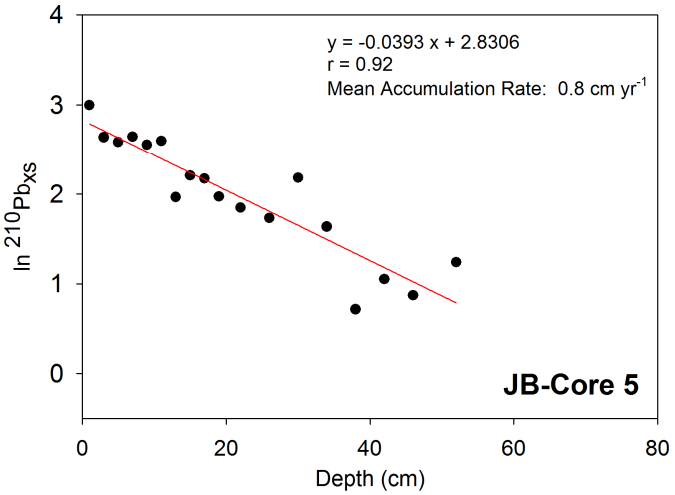

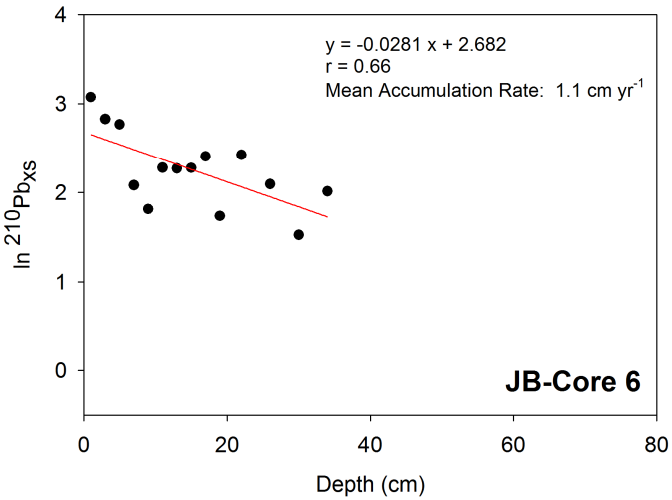

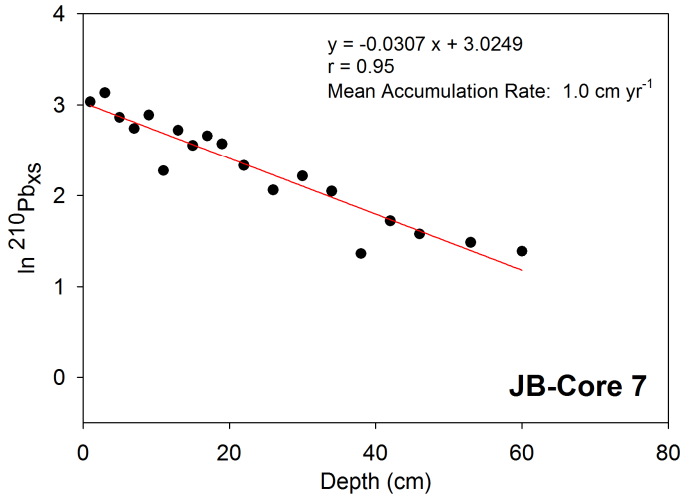

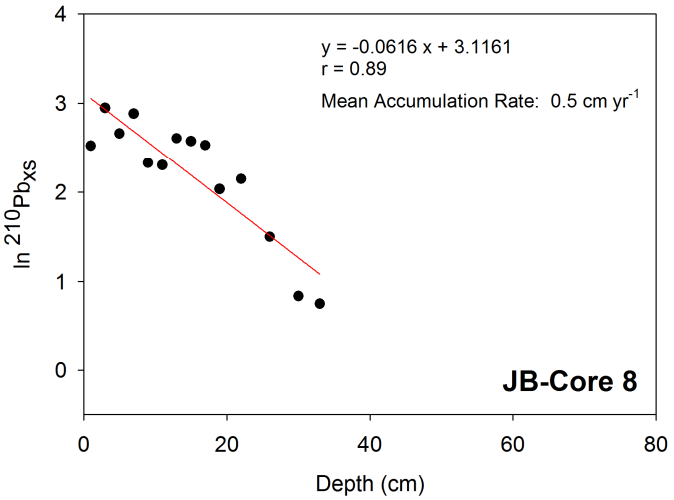

Figure 3-5 Continued

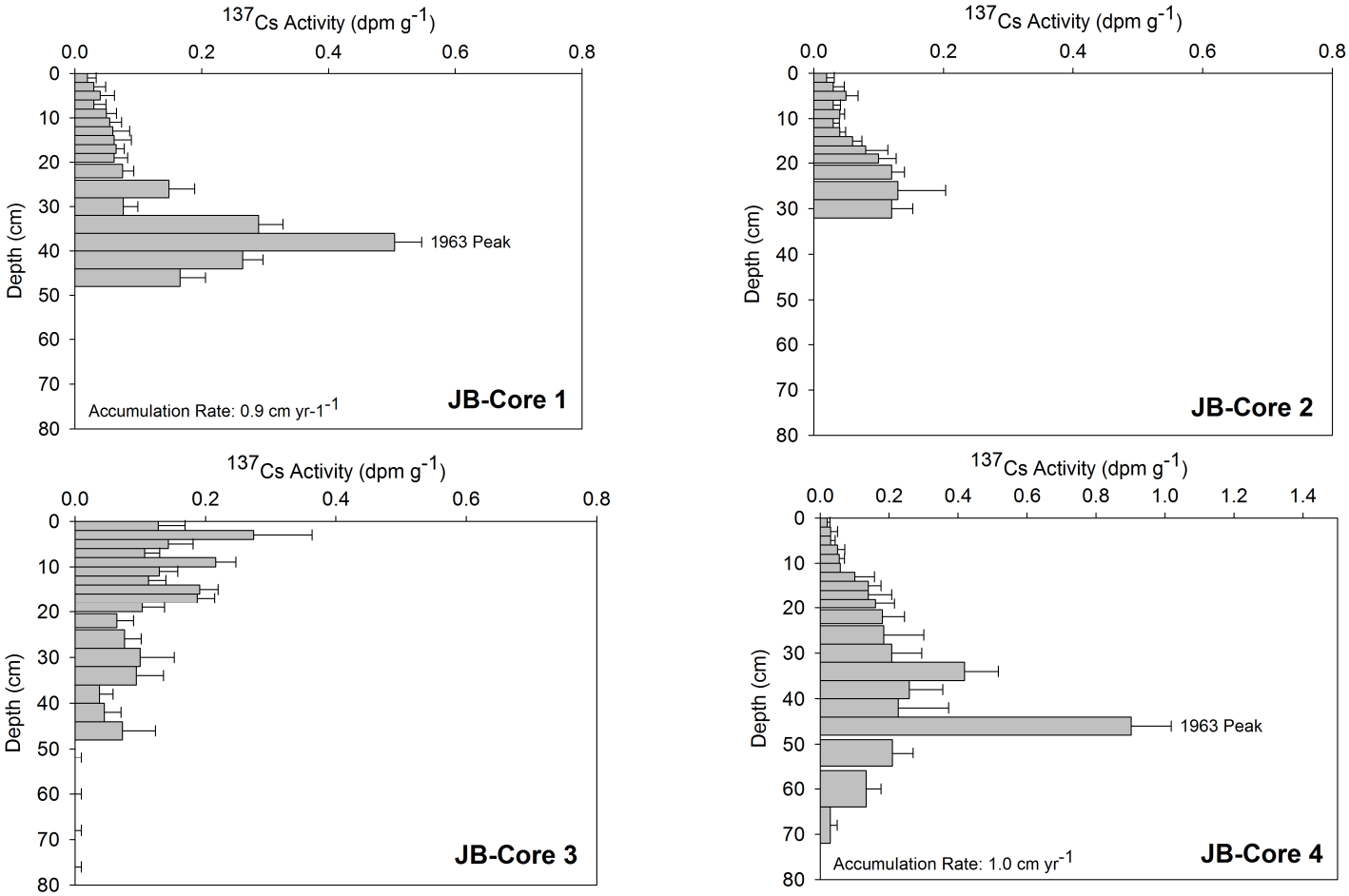

Figure 3-6 Activity of ^{137}Cs with depth for gravity cores taken in Jamaica Bay

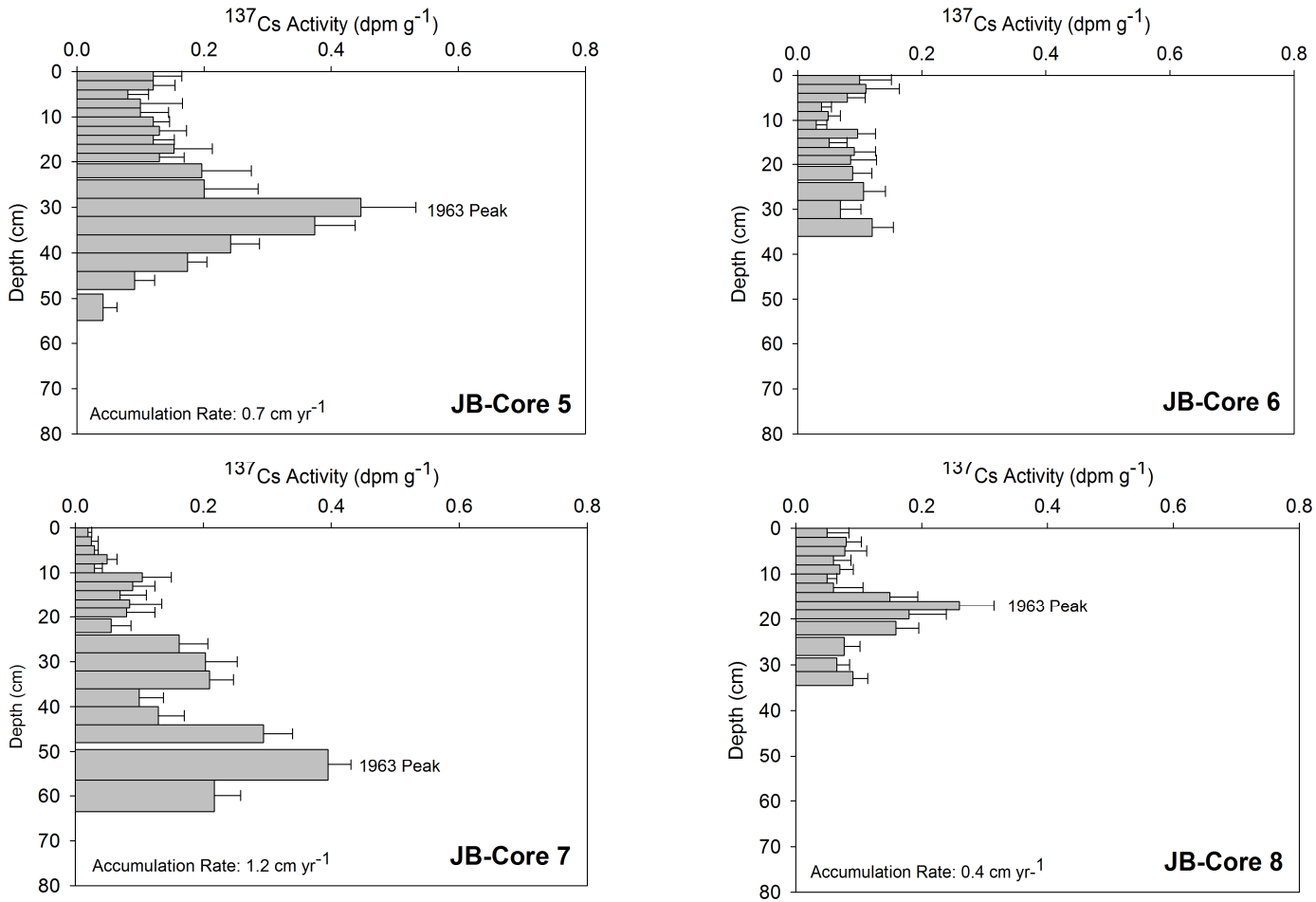

Figure 3-6 Continued

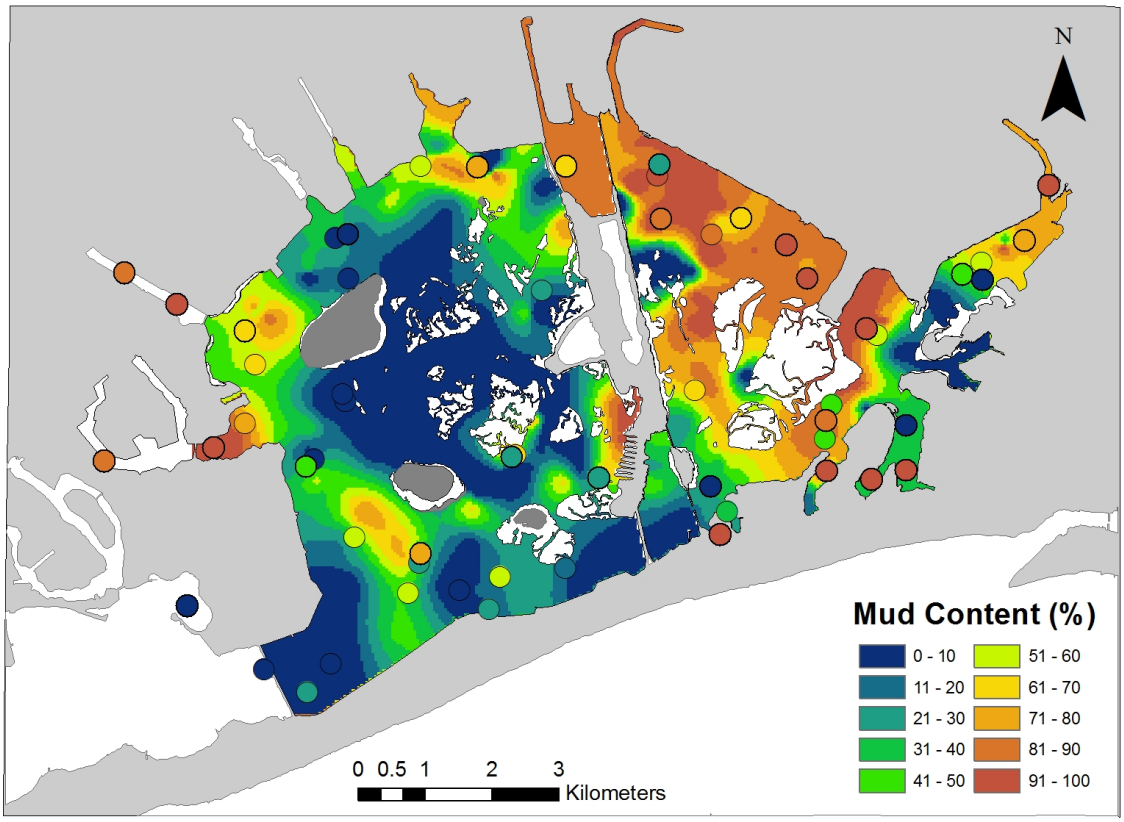

Figure 3-7 Contour map of mud content created from measurement made in this study. The circles represent mud content measurement made by the EPA in 1993-1994 (Adams et al., 1998) and by NOAA in 1995 (Iocco et al., 2000).

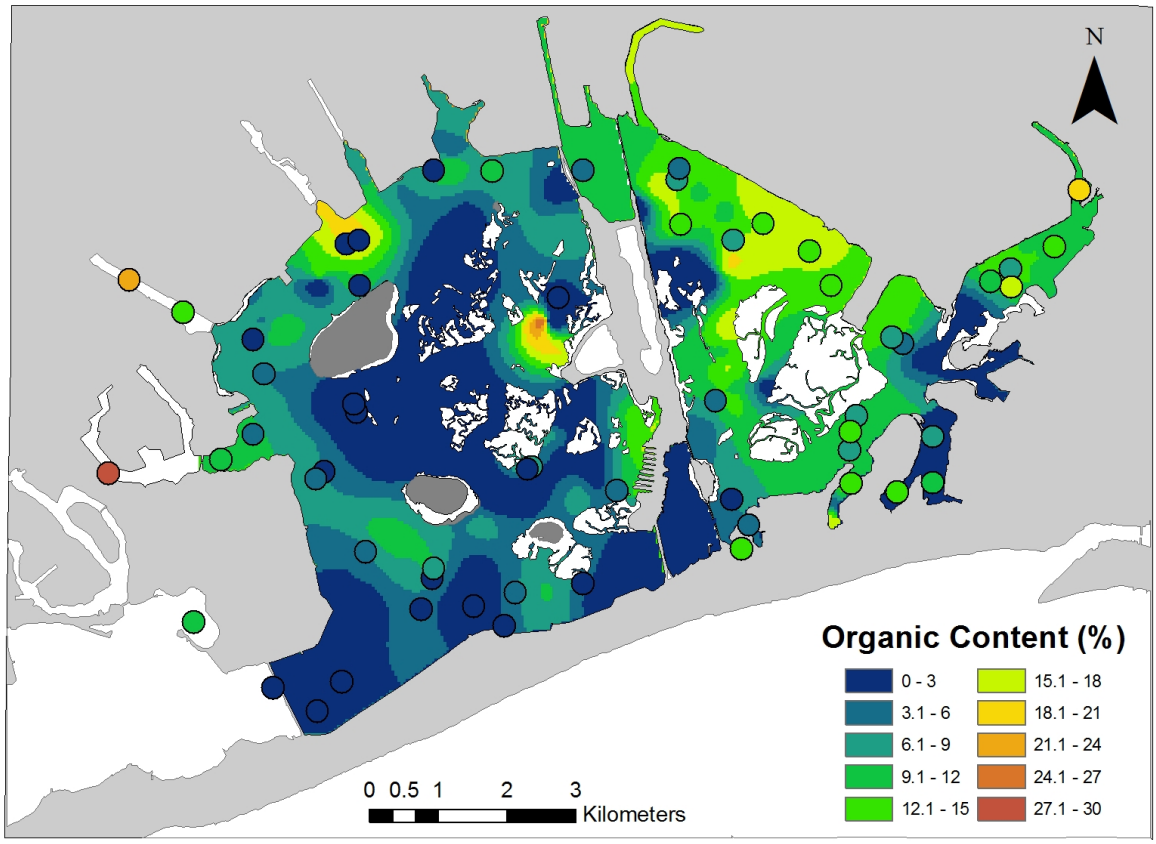

Figure 3-8 Contour map of LOI created from measurement made in this study. The circles represent mud content measurement made by the EPA in 1993-1994 (Adams et al., 1998) and by NOAA in 1995 (Iocco et al., 2000).

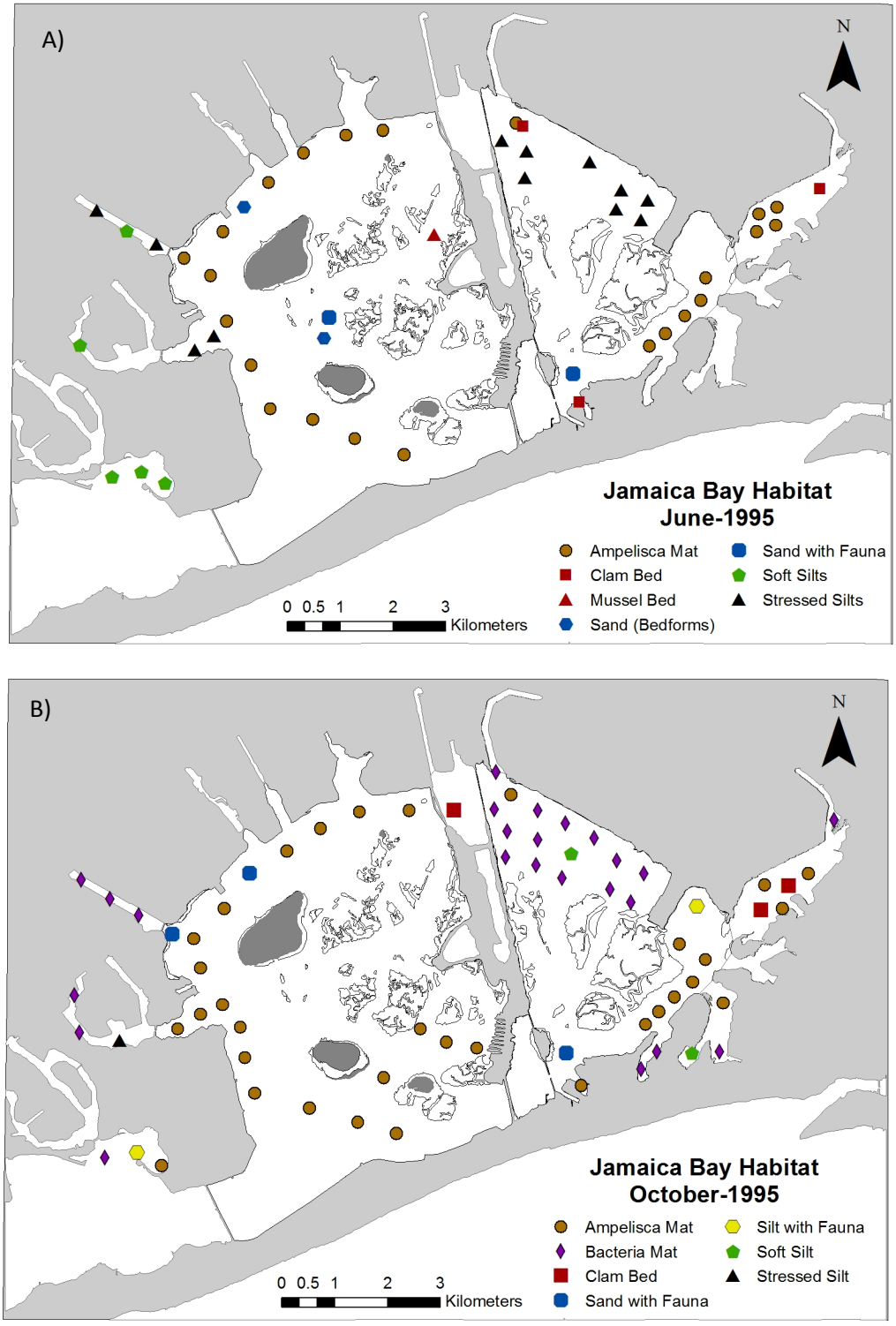

Figure 3-9 Benthic habitats of Jamaica Bay in A) June 1995 and B) October 1995 (reproduced from Iocco et al., 2000).

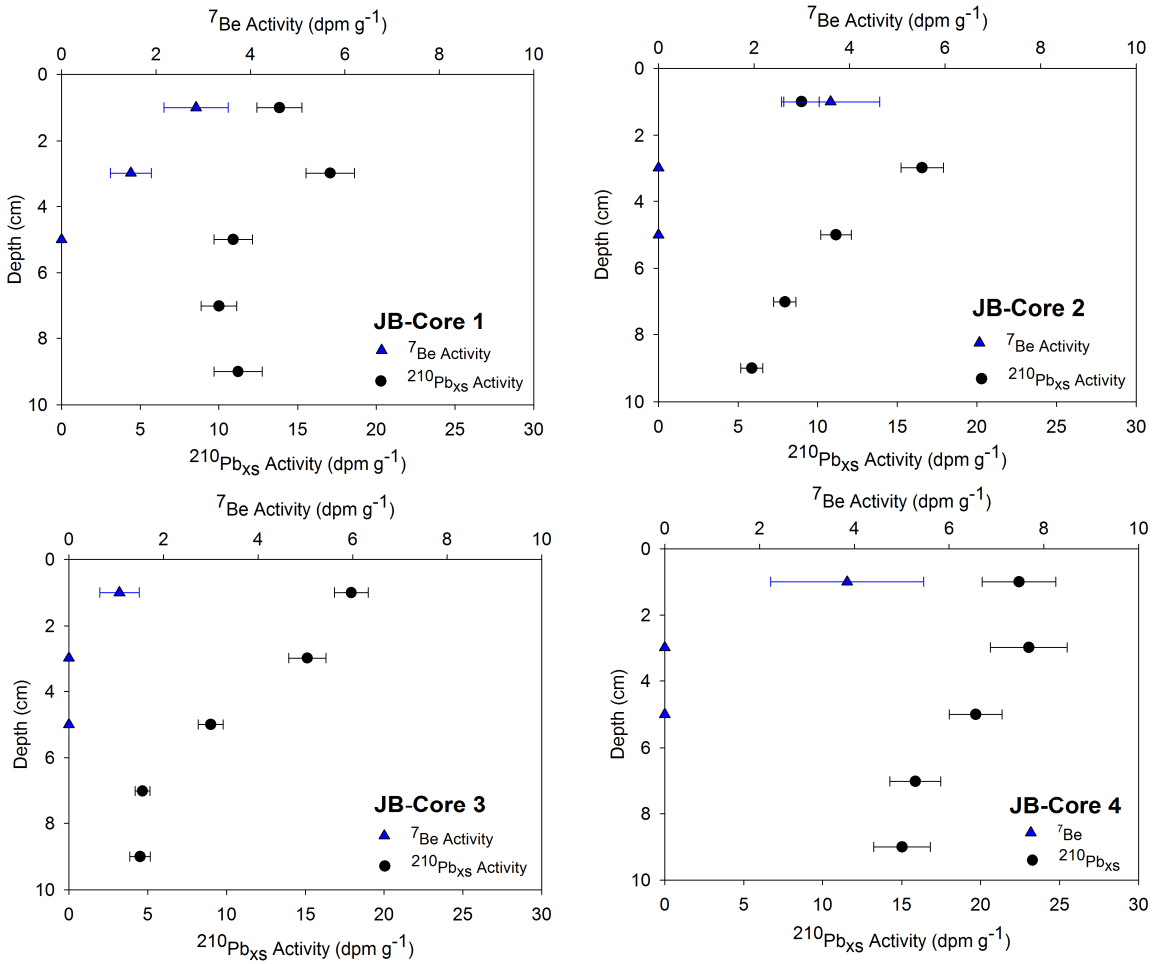

Figure 3-10 Activity of ^{7}Be and excess ^{210}Pb in the upper 10 cm of gravity cores taken in Jamaica Bay.

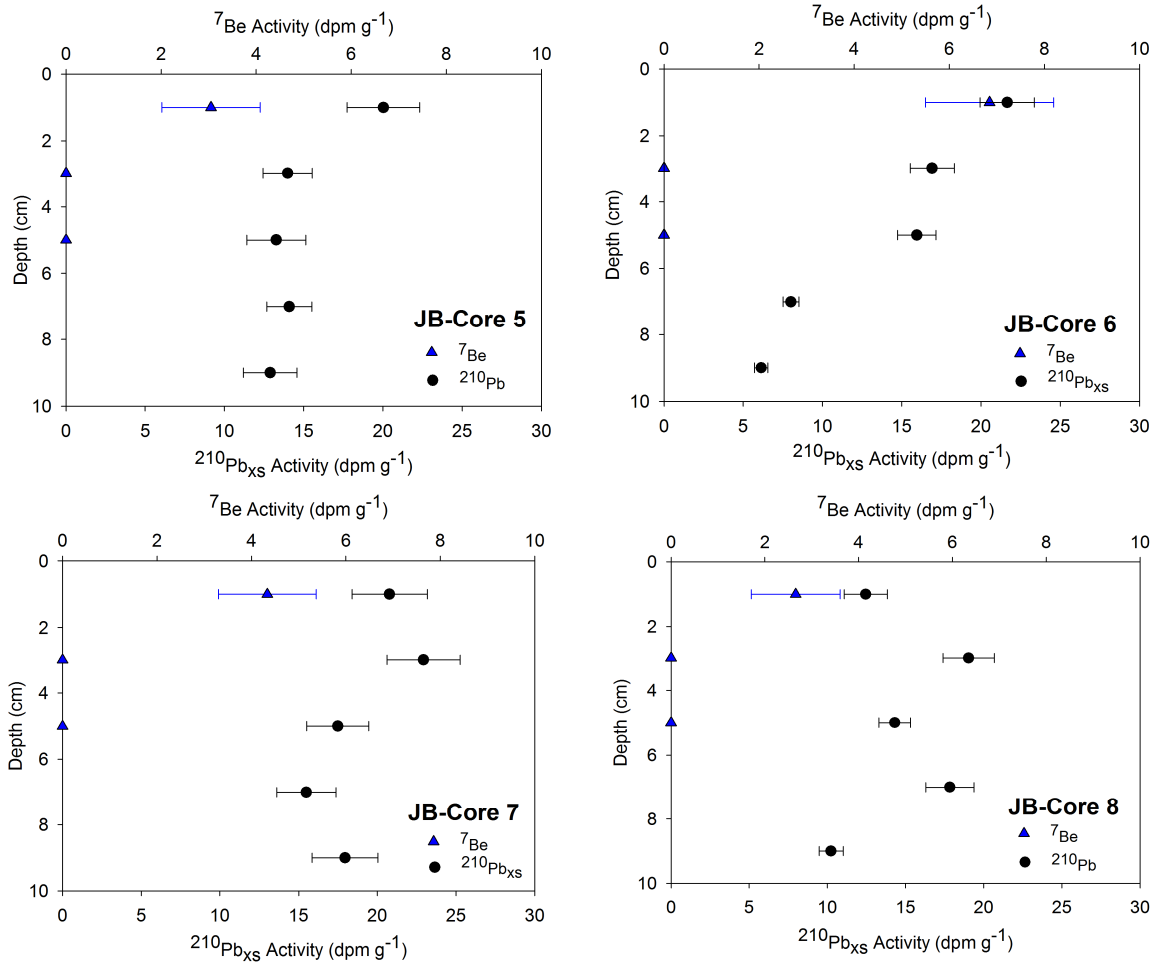

Figure 3-10 Continued

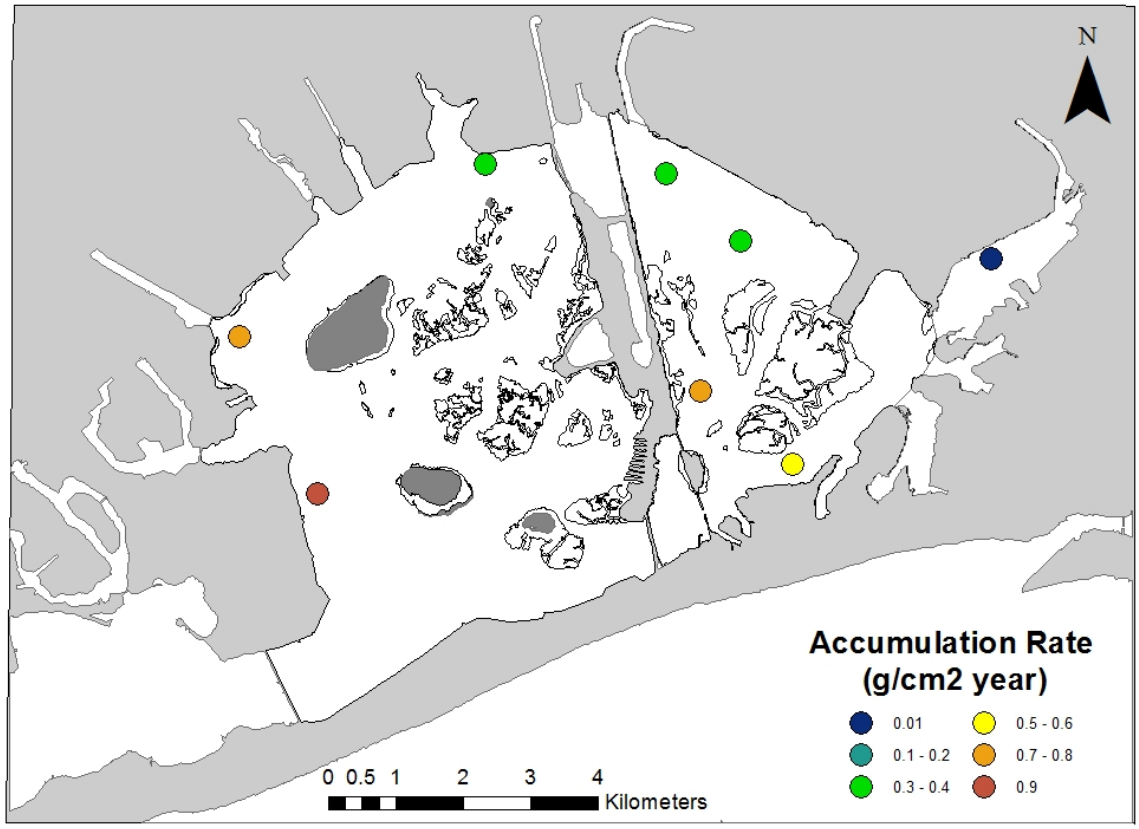

Figure 3-11 Sediment accumulation rate (g cm^{-2} yr^{-1}) determined from ^{210}Pb accumulation rates and sediment bulk density.

CHAPTER 4

The Mass Balance of ^{7}Be in Subtidal Sediments in an Urban Coastal Lagoon (Jamaica Bay, NY)

1. Abstract

Beryllium-7 (half-life = 53.3 days) is a naturally occurring radionuclide produced in the lower stratosphere and upper troposphere through a cosmic-ray spallation reaction. The monthly atmospheric flux of ^{7}Be, measured at Stony Brook, NY from April-2008 to December-2009 ranged from 0.4 to 2.3 dpm cm^{-2} with an annual flux of 16.4 dpm cm^{-2}. The monthly atmospheric flux of ^{210}Pb ranged from 0.04 to 0.11 dpm cm^{-2} and the annual ^{210}Pb flux was ~ 1.0 dpm cm^{-2}. Monthly atmospheric fluxes of both ^{7}Be and ^{210}Pb were positively correlated with rainfall. The activity of ^{7}Be and ^{210}Pb in rainfall ranged from 80 to 273 and 4 to 15 dpm L^{-1}, respectively. ^{7}Be flux was also correlated with precipitation during four rainfall events that were sampled during the summer of 2009, but ^{210}Pb was not. The relationship between ^{7}Be and precipitation was used to estimate atmospheric ^{7}Be flux for the sampling cruises conducted in September-2004, May-2005, November-2005 and July-2006. During these cruises ^{7}Be inventories in the subtidal sediment varied spatially, with mean inventories ranging from 2.6 ± 0.5 to 4.1 ± 0.7 dpm cm^{-2}, which were 10 - 30% in excess to the estimated direct atmospheric input of ^{7}Be into the bay. The mass balance of ^{7}Be in Jamaica Bay suggests that much of the inventory in the subtidal sediments can be explained by direct atmospheric input of ^{7}Be (77 – 92%). However, periodic combined sewer overflow events (CSOs) may also serve as an important source of ^{7}Be to the Bay. The additional CSO source of ^{7}Be complicates its

use in the Bay, but may reveal the fate of particles introduced into the Bay during these CSO events.

2. Introduction

Beryllium-7 is produced in the lower stratosphere and upper troposphere through a cosmic-ray spallation reaction involving nitrogen and oxygen. Production of ^{7}Be varies with latitude, altitude and solar activity. Production is highest between 12 and 20 km altitude and decreases exponentially nearer to the Earth's surface (Lal et al., 1958; Bhandari et al., 1970). Production is also higher near the poles and decreases nearer to the equator (Lal. et a., 1958). Solar activity, and consequently ^{7}Be production, varies over an 11-year solar cycle with high solar activity increasing deflection of cosmic rays, thus decreasing ^{7}Be production.

While ^{7}Be concentrations in the stratosphere remain fairly constant, ^{7}Be in the troposphere exhibits seasonal fluctuations (Feely et al., 1989). Seasonal fluctuations in the troposphere may be a result of increased mixing between the stratosphere and troposophere that occurs during the spring at mid-latitudes. In addition, intense thunderstorms may also mix stratospheric air downward, increasing ^{7}Be concentrations in the troposphere. This mixing may increase the ^{7}Be concentration in the upper troposphere. In the troposphere, ^{7}Be adsorbs electrostatically to aerosols and is delivered through wet and dry precipitation to the Earth's surface (Baskaran and Santchi, 1993; Feng, et al., 1999; Giffen and Corbett, 2003; Kaste et al., 2002).

Despite the variations in production within the troposphere and stratosphere, a major control on ^{7}Be flux to the Earth's surface appears to be delivery through wet precipitation (+ dry deposition; Turekian et al., 1983). ^{7}Be delivered through wet

precipitation to the Earth's surface is in the 2+ valence state (Kaste et al., 2002) and it can be scavenged onto particles in terrestrial soils or aquatic (freshwater or marine) environments. ^{7}Be has an affinity for fine-grained particles and in estuarine systems has a K_d of 1-10x10^4 (Kaste et al., 2002). Olsen et al. (1986) observed that ^{7}Be activities on suspended particles were highest in high-energy environments where particle residence time in the water column was long and lowest in low-energy environments where sedimentation rates were high. Once ^{7}Be is scavenged on to particle surfaces, the particles may remain suspended in the water column, be advected or deposited (Fig. 1-4). In this study, we use the geochemistry of ^{7}Be in an urban coastal lagoon and the seasonal and spatial variation of ^{7}Be in surfical, subtidal sediments to evaluate sediment transport and deposition.

3. Methods

3.1 Study Site

Jamaica Bay is a small coastal lagoon (53 km^2; Benotti, et al., 2007) located along the southern coast of western Long Island (O'Shea and Brosnan, 2000). The bay is shallow (mean depth ~5 m), has no significant riverine input, and contains numerous salt marsh islands. Ocean water enters the bay through Rockaway Inlet, which serves as a pathway for particle and water exchange between the Bay and the New York Bight. The dominant supply of freshwater is wastewater from three sewage treatment facilities in New York City. The sewer system of New York City is such as to allow for bypassing of wastewater treatment facilities during times of high rainfall. At such times, storm water and wastewater enter the estuary simultaneously. The combined sewer overflow pipes

are located throughout the bay (Fig. 1-2). Combined sewer overflow (CSOs) events that occur after heavy rainfalls are an important input of freshwater, as well as nutrients, into the bay (Botton et al., 2006; O'Shea and Brosnan, 2000). Due to its location, Jamaica Bay has been subjected to many of the impacts that come with heavy urbanization, such as extensive dredging, marsh ditching, marsh filling, bulkheading, and landfill construction (Botton et al., 2006).

3.2 Field Methods

Subtidal sediment samples were collected in Jamaica Bay during cruises in September-2004, May-2005, November-2005, and July-2006. The sample sites were distributed throughout the bay with emphasis on regions of interest after the initial sampling. Surficial sediment samples used for ^{7}Be inventories (dpm cm^{-2}) were collected using an Ekman bottom grab. Each grab sample was examined to insure the sediment surface was preserved and then the top 5 cm of the grab sample were sub-sampled and returned to the lab for radiometric analysis. This sampling strategy was designed to obtain the entire sediment inventory of ^{7}Be in a single sample at each site and thus maximize the number of sites sampled at any given time. Generally, 60-70 sites were sampled during each cruise and initial gamma counting was completed within ~3 weeks.

The activities of ^{7}Be associated with particles in the water column entering the bay and within the bay were measured by filtering large volumes (>100 liters) of bay water through ship-powered in-situ pumps equipped with a polypropylene filter cartridge (CUNO Micro-Wynd II® D-CCPY, nominal 1 μm) at select sites (see Chapter 2; Fig. 2-2).

3.3 Laboratory Methods

The surficial sediment samples were returned to the lab, homogenized, and weighed. Samples were analyzed for ^{7}Be (477 keV) by counting the wet samples on a Canberra 3800 mm^2 germanium gamma detector for ~ 24 hours. The counting efficiency of each detector was determined for ^{7}Be by counting well-analyzed sediment standards (IAEA-300 and IAEA-375) and using a linear regression of calculated efficiencies from radioisotopes within the standard sample between 200 keV and 662 keV. Initial ^{7}Be counts were then corrected for detector efficiency and isotope decay between collected and counting.

Cartridges from the high-volume water sampling were ashed in a furnace at 450°C for 24 hours and the ash was counted on Canberra 3800 mm^2 germanium gamma detectors for 24 hours to determine activities of ^{7}Be filterable particles.

3.4 Atmospheric Deposition Collector

An atmospheric deposition collector for ^{7}Be and ^{210}Pb, consisting of a large funnel (diameter = 53.3 cm) connected to a 20-L glass bottle, was deployed from April, 2008 to December-2009 on the roof of a building at the School of Marine and Atmospheric Sciences at Stony Brook University (40°54′17”N, 73°07′06”W). Atmospheric deposition was sampled monthly by rinsing the funnel thoroughly three times (first with distilled water, then HCL, and then again with distilled water). The amount of precipitation was monitored by a rain gauge and compared with respective measurements at Long Island’s McArthur Airport and John F. Kennedy International Airport.

Atmospheric deposition of ^{7}Be and ^{210}Pb also were measured during four rainfall events - two steady rainfall events (6/20/2009 and 7/23/09) and two thunderstorm events (6/26/09 and 7/29/2009). Rainfall was collected in 1-L Nalgene beakers, distributed 0.5 meter above the ground. Rainfall samples were collected as a cumulative time series. During long rainfall events samples were collected hourly for the duration of the rainfall (6/20/2009 and 7/23/09). During the large thunderstorm event occurring on 6/26/09 samples were collected at 10, 15, 20, 25, 30, 40, 50 and 60 minutes, while during the 7/29/09 thunderstorm samples were collected at 10 minute intervals.

In the laboratory 1 ml Fe (10% wt/vol solution of $FeCl_3$ in dilute HCl) was stirred into the sample which was then allowed to stand for at least 6 hours. The ^{7}Be and ^{210}Pb of the sample were concentrated by a co-precipitation with Fe by raising the pH to 9.5 with NaOH (Olsen et al., 1986). The precipitate was left to settle for several hours and was then carefully decanted and dried. The dried precipitate was counted in a glass vial on a Canberra 54 mm^2 germanium Well detector for ~ 24 hours. Detector efficiency at 477-keV was calculated by counting a sediment standard (IAEA-375) and using a linear interpolation between the 351-keV ^{214}Pb and 661-keV ^{137}Cs photopeaks. Samples were corrected for decay between sampling mid-point and counting date.

4. Results

4.1 Atmospheric Deposition Collector

Between April 2008 and December-2009, 21 monthly, atmospheric deposition samples were collected. Rainfall during the sampling period ranged from 2.0 to 19.7 cm (Table 4-1; Fig. 4-1). ^{7}Be activities over the sampling period ranged from 0.4 ± 0.01 to

2.3 ± 0.05 dpm cm^{-2} (Table 4-2) with a mean monthly flux of 1.4 dpm cm^{-2}. The highest ^{7}Be flux was measured in June-2009 and the lowest was measured in February-2009. The monthly atmospheric flux of ^{7}Be was positively correlated with precipitation ($R = 0.81$; $p < 0.01$; Fig. 4-3A). The activity of ^{7}Be in precipitation ranged from 80 ± 1.2 to 273 ± 1.6 dpm L^{-1}, but was not correlated with precipitation (Fig. 4-4A). Monthly atmospheric ^{210}Pb flux over the sampling period ranged from 0.04 ± 0.002 to 0.11 ± 0.005 dpm cm^{-2} and the activity of ^{210}Pb in the sampled rainwater ranged from 4 ± 0.2 to 15 ± 0.3 dpm L^{-1} (Table 4-1). Annual atmospheric flux over the sampling period was ~ 0.9 dpm cm^{-2}. Atmospheric ^{210}Pb flux was positively correlated with precipitation ($R = 0.55$; $p < 0.05$; Fig. 4-3B), but the activity of ^{210}Pb in rainwater was negatively correlated with precipitation ($R = 0.75$; $p < 0.01$; Fig. 4-4B).

Individual rainfall events were sampled as a cumulative time series on 6/20/09, 6/26/09, 7/23/09 and 7/29/09. The rainfall event on 6/20/09 lasted for 18 hours, resulted in 1.4 cm of rain and a flux of ^{7}Be and ^{210}Pb of 0.7 ± 0.04 and 0.0025 ± 0.0006 dpm cm^{-2}, respectively (Figs. 4-5A, 4-6A). A short, intense thunderstorm event followed a few days later, when 2.0 cm of rain fell in 1 hour; the ^{7}Be and ^{210}Pb flux were 0.7 ± 0.3 and 0.002 ± 0.0005 dpm cm^{-2}, respectively (Figs. 4-5B, 4-6B). Two rainfall events were also sampled in July. A long rainfall event was measured 7/23/09 and lasted 16 hours. This event resulted in 3.9 cm of precipitation, total ^{7}Be flux from the atmosphere was 0.2 ± 0.02 dpm cm^{-2} (Fig. 4-5C) and the total ^{210}Pb flux from the atmosphere was 0.002 ± 0.0004 dpm cm^{-2} (Fig. 4-6C). A short thunderstorm event was measured on 7/29/09 which resulted in 0.75 cm of rainfall, a total atmospheric ^{7}Be flux of 0.3 ± 0.04 dpm cm^{-2} (Fig. 4-5D), and a total atmospheric ^{210}Pb flux of 0.002 ± 0.0005 dpm cm^{-2} (Fig. 4-6D).

4.2 Activity of ^{7}Be in the Water Column

The summary of the activity of ^{7}Be measured on particles in the water column is given in Table 4-2. There was little variation in the activity on particles measured at the inlet in August-2008 and just within the Bay. Higher ^{7}Be was measured in the Bay's interior in the eastern Bay, near the eastern marshes and in Grassy Bay. An additional sample taken at the inlet in June-2009 had a slightly higher particle activity than the previous sample.

4.3 ^{7}Be in Subtidal Sediments

Inventories of ^{7}Be in sediments were calculated using the equation:

$$I_{Be} = A_{Be} \times \rho_i \times 5 \text{ cm} \qquad (4\text{-}1)$$

where I_{Be} is the ^{7}Be inventory (dpm cm^{-2}), A_{Be} is the ^{7}Be activity (dpm g^{-1}) of ^{7}Be, ρ_i is the dry bulk density of the sample (g cm^{-3}), and 5 cm is the depth of each sample. This sampling scheme was designed to obtain the entire excess ^{7}Be inventory in a single sample. This procedure was checked through sub-sampling the gravity cores and found to be valid (see Chapter 3 for details). Mean inventories in the subtidal sediments ranged from 2.6 ± 0.3 to 4.1 ± 0.7 dpm cm^{-2} (Table 4-3).

Sediment samples were collected in August-2008 with the purpose of comparing the inventory of ^{7}Be in the upper 2 mm of bottom sediments with the inventory in the upper 5 cm of the same sediments. At the sample sites selected the activity of ^{7}Be in the upper 2 mm accounted for 63 – 100% of the total inventory (Table 4-4).

^{7}Be inventories in the surficial bottom sediments are shown in Fig. 4-7. In September-2004 the highest ^{7}Be inventories in the bottom sediments were measured in the northwestern part of the bay, in the southern channel near combined-sewer overflow outfalls, and near the marsh islands in the eastern part of the bay (Fig. 4-7A). In May-2005 mean ^{7}Be inventories in the bay sediments were lower than the previous sampling cruise, with the highest inventories located in the eastern part of the bay near JoCo marsh and the western part of the bay near sites of combined-sewer overflow outfall and the 26th Ward waste-water treatment plant (Figs. 4-7B). In November-2005, ^{7}Be inventories were highest in the northwestern part of the bay adjacent to combined-sewer overflow outfall (Figs. 4-7C), in the eastern portion of the bay near the marsh islands, and in Grassy Bay. In July-2006 the highest inventories were found in the northwest near combined-sewer overflow outfall and the 26th Ward treatment plant and in the southeastern channel (Figs. 4-7D).

5. Discussion

5.1 Atmospheric ^{7}Be and ^{210}Pb Fluxes

^{7}Be is produced in the stratosphere and troposphere through a cosmic-ray spallation reaction involving nitrogen and oxygen. It can then be scavenged onto particles in the atmosphere and can then be removed predominantly through precipitation (Turekian et al., 1983). Enhanced mixing between the stratosphere and troposphere with the mid-latitude folding during the spring has been shown to increase ^{7}Be in the troposphere (Feely et al., 1989; Heikkilä, et al., 2008). Intense thunderstorms, typically in the spring and summer, can also enhance mixing between the stratosphere and

troposphere, increasing the availability of ^{7}Be that can then be scavenged through precipitation (Noyce et al., 1971). As a result, atmospheric flux of ^{7}Be is often higher during the spring and summer months (Doering and Akber, 2008; Feely et al., 1989; Gonzalez-Gomez et al., 2006; Zhu and Olsen, 2009) and this is indicated in the results collected at Stony Brook, NY (40°54′17”N, 73°07′06”W). Over the 22-month sampling period, the mean atmospheric flux of ^{7}Be during spring and summer (March-August) was 1.6 ± 0.2dpm cm^{-2} and the mean flux during the fall and winter (September-February) was 1.2 ± 0.2 dpm cm^{-2}, but the mean precipitation did not vary (Table 4-1).

The mean atmospheric flux of ^{7}Be measured at Stony Brook, NY over the entire sampling period was 1.4 ± 0.1 dpm cm^{-2} resulting in an annual flux of 16.8 dpm cm^{-2} yr^{-1}. The annual flux at the Stony Brook site is within the range of 4.3 – 22.7 dpm cm^{-2} yr^{-1} tabulated for the latitude range 19° - 52° N by Turekian et al. (1983). In addition, the mean monthly flux of 1.4 dpm cm^{-2} is consistent with measurements at geographically comparable sites: Boston, MA (1.4 dpm cm^{-2}; Zhu and Olsen, 2009), New Haven, CT (1.9 dpm cm^{-2}, CT, Turekian et al., 1983), Solomons, MD (1.1 dpm cm^{-2}, Dibb, 1989), Norfolk, VA (1.0 dpm cm^{-2}; Todd et al., 1989) and Morehead City, NC (1.3 dpm cm^{-2}; Canuel et al., 1990).

The relationship between atmospheric ^{7}Be flux and rainfall along the east coast of the U.S. has been explored by several researchers and found to be significantly correlated (Turekian et al., 1983; Dibb, 1989; Todd et al., 1989; Canuel et al., 1990; Zhu and Olsen, 2009; Fig 4-8). A significant, positively correlated relationship was found in this study at Stony Brook, NY (Fig. 4-8C; R = 0.81). Although a significant correlation between precipitation and atmospheric ^{7}Be flux has been found at several locations along the east

coast of U.S. the flux of ^{7}Be with precipitation generally decreases with decreasing latitude (Fig 4-8). This is consistent with increased production of ^{7}Be in the troposphere and stratosphere with increasing latitude (Bhandari et al., 1970; Lal et al., 1958).

The production of ^{7}Be varies over the 11-year solar cycle, with increasing solar activity resulting in increased deflection of cosmic rays from the solar system which decreases cosmic-ray flux to the Earth (Lal and Peters, 1967). The decrease in cosmic rays to the Earth results in a decrease in the production of beryllium and thus a decrease in ^{7}Be that can be removed through rainfall (Beer et al., 1990, Ioannidou et al., 2005). In general, atmospheric flux data collected by researchers from 42 - 34° N shows a decrease in ^{7}Be flux from the atmosphere with decreasing latitude (Fig. 4-8). However, the data collected in New Haven, CT (Turekian et al., 1983) indicates a higher ^{7}Be flux than at the Boston, MA site (Zhu and Olsen, 2009; Figs. 4-8A, 4-8B). This may reflect the longer collection time in the Zhu and Olsen study Boston, MA site, the higher sunspot activity during collection at that site (Figs. 4-9) and higher removal of ^{7}Be from the atmosphere due to higher mean precipitation during Turekian's et al., (1983) sampling in New Haven, CT than Zhu and Olsen's in Boston, MA (11.6 and 9.2 cm, respectively). These results suggest that in addition to latitude, sunspot activity and precipitation should be considered when estimating ^{7}Be flux from the atmosphere at a particular location, at a specific time.

^{210}Pb is produced in the atmosphere through the decay of its parent isotope ^{222}Rn (half-life 3.82 d), an inert noble gas. ^{222}Rn is released to the atmosphere predominantly from continental sources. Once formed ^{210}Pb, like ^{7}Be, can be scavenged on to submicron-sized aerosol particles and removed from the atmosphere through wet or dry

deposition (Ioannidou et al., 2005; Todd et al., 1989). Monthly atmospheric ^{210}Pb flux at Stony Brook, NY over the 22-month sampling period ranged from 0.04 to 0.1 dpm cm^{-2} with a mean flux of 0.08 dpm cm^{-2}, and an annual ^{210}Pb flux of 01.0 dpm cm^{-2} y^{-1}. This annual flux is consistent with annual ^{210}Pb fluxes measured at New Haven, CT (1.2 dpm cm^{-2} y^{-1}; Turekian et al., 1983) and Norfolk, VA (0.9 dpm cm^{-2} y^{-1}; Todd et al., 1989). Soil profiles from undisturbed sites have also been used to estimate annual atmospheric ^{210}Pb flux. Profiles from Connecticut (McCaffrey, 1977), Pennsylvania (Lewis, 1976) and Maryland (Fisenne, 1968) yielded annual atmospheric fluxes of 0.83, 1.0, 1.2 dpm cm^{-2} y^{-1}, respectively. Measurements of the excess ^{210}Pb in a soil profile taken in Jamaica Bay, on Broad Channel Island, yielded an annual flux of 1.1 dpm cm^{-2} y^{-1} (Zeppie, 1977).

The mechanism for removing ^{210}Pb from the atmosphere is "washout" from rainfall and dry deposition (Appleby and Oldfield, 1992). The relationship between precipitation and atmospheric ^{210}Pb flux at Stony Brook, NY was found to be significantly and positively correlated ($R = 0.62$; $p < 0.0$; Fig. 4-3B). Precipitation was also positively correlated to ^{210}Pb flux in New Haven, CT (Turekian et al., 1983) and Norfolk, VA (Todd et al., 1989). In contrast, the activity of ^{210}Pb in precipitation was negatively correlated with the amount of precipitation at Stony Brook, NY varying from 4 to 15 dpm L^{-1} (mean ~ 7.9 dpm L^{-1}; Fig. 4-4B). ^{210}Pb activities were also negatively correlated with precipitation in New Haven, CT (Turekian et al., 1983) and Norfolk, VA (Todd et al., 1989) with ^{210}Pb activities ranging from 1.8 - 17.1 dpm L^{-1} (mean ~ 9.6 dpm L^{-1}) and 2.8 – 18.2 dpm L^{-1} (mean ~ 7.3 dpm L^{-1}), respectively.

5.2 ^{7}Be and ^{210}Pb Flux in Individual Rainfall Events

Individual rainfall events were sampled in the summer of 2009 to determine whether ^{7}Be and ^{210}Pb are washed out of the atmosphere during the initial fall of rain or over course of the entire event. Long rainfall events (> 8 hours) were sampled on 6/20/09 and 7/23/09 and short, intense, thunderstorm events were sampled on 6/26/09 and 7/29/09. During all the sampled events the flux of ^{7}Be from the atmosphere (dpm cm^{-2}) was correlated with precipitation (Fig. 4-10) suggesting that ^{7}Be is removed from the atmosphere throughout the rainfall event and not just in the initial rainfall.

Atmospheric flux of ^{7}Be during the rainfall events sampled in June-2009 had a more gradual increase over the event with ^{7}Be flux in the first hour of the 6/23/09 event and the first 10 minutes of the 6/26/09 rainfall event comprising 5% and 17%, respectively, of the total ^{7}Be flux from the atmosphere of the entire event (Figs. 4-10A, 4-10B). In contrast, the events sampled in July-2009 the initial ^{7}Be flux from the atmosphere in the first hour of the 7/23/09 event and the first 10 minutes of the 7/29/09 event comprised 41% and 68% of the total ^{7}Be flux from the atmosphere, respectively, although the total ^{7}Be flux was much lower than the June-2009 events (Figs. 4-10C, 4-10D). These results may be due to higher than normal precipitation in June-2009 and in early July-2009 (19.6 and 16.4 cm, respectively) washing most of the ^{7}Be out of the troposphere throughout June and into early July. When the rainfall events were then sampled in second part of July-2009, little ^{7}Be may have been left in the troposphere, the result of which was the total ^{7}Be removed during the events sampled was lower than the previous month.

In contrast to the ^{7}Be, the ^{210}Pb flux from the atmosphere was not significantly correlated with precipitation during any of the sampled rainfall events. Plots of the atmospheric flux of ^{210}Pb and precipitation during these events show little difference in the ^{210}Pb over time. In addition, the activity of ^{210}Pb in rainfall also had no correlation with precipitation. However, the atmospheric flux of ^{210}Pb, as well as the activities of ^{210}Pb in rain-water were significantly correlated with rainfall on monthly scales (Figs. 4-3B, 4-4B).

5.3 Mass Balance of ^{7}Be

The inventory of ^{7}Be in the subtidal sediments of Jamaica Bay for the four sampling cruises ranged from 2.6 to 4.1 dpm cm^{-2}, with a subtidal bay area of 3.9×10^{11} cm^2 ($1.0 – 1.6 \times 10^{12}$ dpm). However, the ^{7}Be in the sediment does not represent the entirety of ^{7}Be in the Bay, as ^{7}Be would also be found in the water column dissolved or associated with particles. The activity of ^{7}Be on particles in the water column within the Bay were measured in August-2008 and found to be ~ 0.097 dpm L^{-1}. Assuming a subtidal bay area of 3.9×10^{11} cm^2 and a mean depth of 5 m (~ 2.0×10^{11} L), an estimated total activity of ^{7}Be associated with particles in the water column would be 2.0×10^{10} dpm or 0.05 dpm cm^{-2}.

5.3.1 Direct Atmospheric Input

Typically, the dominant source of ^{7}Be into an estuarine system with little riverine input, such as Jamaica Bay, is directly atmosphere during rainfall events (Olsen et al., 1986; Dibb, 1989; Dibb and Rice, 1989). In an idealized estuary, where no lateral

transport of water or particles occurs, the ^{7}Be inventory measured in the sediments will likely reflect the atmospheric input, with the only factors causing deviation between the atmospheric input and the bottom sediments being the time required for ^{7}Be to be scavenged on to suspended particle surfaces and then these particles to settle to the bottom. However, in many estuaries, lateral transport of water and particles are important and may result in focusing in localized areas where ^{7}Be inventories in the bottom sediments exceed the inventory supported by the direct input (Dibb and Rice, 1989).

Atmospheric flux of ^{7}Be into Jamaica Bay prior to the sampling cruises was estimated using the correlation between rainfall and ^{7}Be observed at Stony Brook University from April-2008 to December-2009:

$$I_{Be} = 0.0983 \times \text{Rainfall (cm)} + 0.3543 \qquad (4\text{-}3)$$

where I_{Be} is the ^{7}Be inventory (dpm cm^{-2}, or alternatively, the ^{7}Be flux in atoms min^{-1} cm^{-2}) that enters the bay directly from the atmosphere and rainfall is the precipitation in cm that fell in the 53 days prior to sampling and decay corrected. In the 53 days prior to the September-2004, May-2005, November-2005 and July-2006 sampling cruises there were 34, 19, 39, and 22 cm of precipitation, resulting in an estimated 3.1, 2.0, 3.6 and 2.4 dpm cm^{-2} of ^{7}Be entering the bay directly from the atmosphere, respectively. Mean ^{7}Be inventories in the bottom sediments during the September-2004, May-2005, November-2005, and July-2006 cruises were in balance or slightly in excess (8 – 30%) of the estimated ^{7}Be entering the bay directly from the atmosphere, prior to sampling (Table 4-3). Sampling density was sufficient to suggest that the inventories in “surplus” to the

atmospheric input were not a result of focusing of fine sediments. Instead, these results suggest that there is a source of ^{7}Be in addition to direct atmospheric input.

5.3.2 CSO Input

Another possible source of "surplus" ^{7}Be measured in the subtidal sediments of Jamaica Bay is from runoff during CSO events. The dominant source of freshwater into Jamaica bay is from wastewater treatment plants (Botton et al., 2006; O'Shea and Brosnan, 2000). There are four primary wastewater treatment plants on the bay – Coney Island, 26th Ward, Jamaica, and Rockaway. During dry conditions and light rainfall events ^{7}Be may be deposited on the impervious surfaces in the bay watershed. Then during heavy rainfall events the previously deposited ^{7}Be, as well as that supplied from the rain event itself, can be rinsed off of the roads and into the combined sewers. During heavy or frequent rainfall events, the waste water treatment plants become overloaded with water, particularly from street runoff, causing the plants to be bypassed and dumping untreated wastewater and storm water, including ^{7}Be, directly in to the bay.

The activity of ^{7}Be in precipitation was measured from April-2008 to December-2009 in Stony Brook, NY and ranged from 80 to 273 dpm L^{-1} (mean ~ 143 dpm L^{-1}; Table 4-1). These values are consistent with those reported for New Haven, CT (65 - 339 dpm L^{-1}; Turekian et al., 1983) and Norfolk, VA (29 – 191 dpm L^{-1}). The contribution of CSO events to the ^{7}Be inventory of Jamaica Bay can be estimated from:

$$\text{CSO Contribution} = [R_{Be} \times F_{CSO} \times (1/\lambda)] \div \text{Subtidal Bay Area} \qquad (4\text{-}4)$$

where R_{Be} is the mean activity of ^{7}Be measured in rainfall (mean ~ 143 dpm L^{-1}; Table 4-1), F_{CSO} is the estimated average annual CSO flow into Jamaica Bay (32.1×10^{9} L yr^{-1}; Table 3-1; The Jamaica Plan: Final Environmental Impact Statement, 2007), the subtidal bay area is 3.9×10^{11} cm^{2} and 1/λ (0.21 yr) is the mean life of ^{7}Be. This calculation yields a possible contribution of 2.5 dpm cm^{-2} to the inventory of ^{7}Be in the subtidal sediments. This estimation of the contribution of ^{7}Be from CSO events in Jamaica Bay is a high end estimate, as it assumes that 100% of the water entering the Bay was from street-water runoff and not waste-water.

5.3.3 Import from the Ocean

Once possible source of additional ^{7}Be it to Jamaica Bay is import of atmospherically derived ^{7}Be from the ocean either dissolved or associated with particles. The ^{7}Be activity on filterable particles at the inlet was ~ 0.091 dpm L^{-1} and an activity of ~ 0.090 dpm L^{-1} was measured just within the Bay (Table 4-2). The import of ^{7}Be associated with particles through the inlet can be estimated using the equation:

$$\text{Input of Particulate } ^{7}Be = [Be_P \times V_{in} \times t_d \times (1/\lambda)] \div \text{subtidal bay area} \qquad (4\text{-}5)$$

where Be_P is the activity of ^{7}Be measured on particles at the inlet station (0.09 dpm L^{-1}), V_{in} is the tidal prism of Jamaica Bay (6.06×10^{10}L; Beck et al., 2007), t_d is the tidal cycles per day (1.91), (1/λ) is the mean half-life of ^{7}Be (77 d) and the area of the subtidal bay is 39 km^{2} (3.9×10^{11} cm^{2}). This calculation yields an import of ^{7}Be associated with particles of 2.1 dpm cm^{-2} (7.8×10^{11} dpm) which accounts for 49 – 78% of the total ^{7}Be inventory in the subtidal sediments.

5.3.4 Loss from the Bay

Prior to the 20th century, when the entrance of Jamaica Bay, Rockaway Inlet, was shorter, the Bay was characterized as ebb dominated. During the 20th century hardening of the Bay's periphery, stabilization of the inlet and deepening of the Bay have modified the hydrodynamics of the Bay, making it flood dominated (Swanson and Wilson, 2008). The mass balances of ^{234}Th and ^{210}Pb indicate that import of these radionuclides associated with particles is a significant input term in Jamaica Bay (see Chapters 2 and 3). However, there does also appear to be loss of these radionuclides from the bay as a result of stratification and estuarine circulation (see Chapters 2 and 3; R.E. Wilson Pers. Comm.). If we assume the ^{7}Be activity in the water column characterizes that water lost from the bay the loss of ^{7}Be can be estimated from:

$$^{7}\text{Be Export} = [Be_P \times (V_{out} \times t_d\ F_{ww}) \times 1/\lambda\ ] \div \text{Subtidal Bay Area} \qquad (4\text{-}8)$$

where Be_P is the ^{7}Be activity in the surface waters near the inlet (0.1 dpm L^{-1}), V_{out} is the tidal prism of Jamaica Bay (6.06×10^{10}L; Beck et al., 2007), t_d is the tidal cycles per day (1.91 d^{-1}), F_{ww} is the wastewater discharge (7.5×10^{8} L d^{-1}), ($1/\lambda$) is the mean half-life of ^{7}Be (77 d) and subtidal bay area is 3.9×10^{11} cm^2. This calculation yields an export of particulate ^{7}Be of 2.3 dpm cm^{-2}.

The mass balance terms for ^{7}Be are compiled in Table 4-5. The expected inventory in the subtidal sediments ranges from 4.3 to 5.9 dpm cm^{-2}, which is > 100% of the ^{7}Be inventory measured in the subtidal sediments. The overestimation of ^{7}Be in the subtidal sediments may reflect incomplete scavenging and deposition of ^{7}Be-derived from CSO events. The direct atmospheric flux of ^{7}Be to Jamaica Bay can account for ~

77 – 92% of the ^{7}Be inventory measured in the subtidal sediments (Table 4-5). ^{7}Be mass balances made for the James River Estuary by Olsen et al. (1986) and Chesapeake Bay by Dibb and Rice (1989) indicated that the direct atmospheric flux of ^{7}Be accounted for > 90% of the ^{7}Be inventory in the subtidal sediments. In Jamaica Bay, while atmospheric flux can account for most of the measured ^{7}Be in to the Bay, periodic CSO events may also make a sizeable contribution.

5.4 Accumulation Patterns and Inventories

Sediment accumulation patterns in Jamaica Bay are heterogeneous, with long-term sediment accumulation rates, as determine by ^{210}Pb geochronology, ranging from 0.1 to 1.1 cm yr^{-1} (see Chapter 3). The highest accumulation rates were measured in the deeper northwestern channel and in northeastern part of the Bay, known as Grassy Bay (see Chapter 3). ^{7}Be inventory was consistently high in the northwestern part of the Bay, but were generally low in Grassy Bay (Fig 4-7). In November-2005 and July-2006 mean ^{7}Be inventories were significantly higher in the western part of the bay than in the eastern (Fig. 4-11). In contrast, in November-2005 there was no difference in the mean $^{234}Th_{xs}$ inventory between the western and eastern parts of the Bay. In May-2005 the mean $^{234}Th_{xs}$ inventory was significantly higher in the eastern part of the Bay than in the western part of the bay, whereas in July-2006 $^{234}Th_{xs}$ inventory was significantly higher in the eastern bay than the western (see Chapter 2 for details).

The difference in the patterns of high ^{234}Th and ^{7}Be inventories in subtidal sediments may reflect the different sources of these radionuclides to Jamaica Bay. The dominant source of ^{234}Th into the Bay is imported associated with particles via Rockaway

Inlet. The difference in the spatial distribution of $^{234}Th_{xs}$ inventories in the subtidal sediments suggests that deposition is focused in the western bay during quiescent periods and in the eastern bay following periods of storm activity (see Chapter 2 for details). In contrast, high ^{7}Be inventories in the subtidal sediments in the western part of the Bay (where CSO outfalls are concentrated; Fig. 1-1) were measured during the November-2005 sampling cruise, which followed a storm event in mid-October that produced 27 cm of precipitation over a 3-day period. High inventories in the western bay, particularly near the CSO outfalls in the northwestern Bay indicates that CSO events may be an episodic source of ^{7}Be to the subtidal sediments in Jamaica Bay and the ^{7}Be associated with particles from these events are predominantly deposited in the deep, dredged channel in the northwestern Bay. During periods with lower precipitation, where CSO events are less likely, ^{7}Be inventories appear to be more evenly distributed throughout the Bay which likely reflects the direct atmospheric input of ^{7}Be.

6. Conclusions

A significant correlation was found between precipitation and the atmospheric flux of ^{7}Be and ^{210}Pb at Stony Brook, NY. The annual flux of ^{7}Be and ^{210}Pb were also similar to previous studies in the region. Comparisons to previous studies suggest that differences in the atmospheric flux of ^{7}Be are most dependent on difference in latitude. In addition, individual rainfall events measured showed that ^{7}Be was removed from the atmosphere throughout the rainfall, but the total atmospheric flux of ^{7}Be may be quite dependent on the standing stock in the atmosphere. ^{7}Be inventories in surficial, subtidal sediments varied spatially and temporally over the course of this study. Highest mean

inventories were measured following periods of higher rainfall (September-2004 and November-2005). However, during all sampling cruises, mean ^{7}Be inventories were in excess to the estimated direct atmospheric input into the bay suggesting there was an additional source of ^{7}Be into Jamaica Bay. An attempt at a mass balance of ^{7}Be within the Bay suggests that while the atmospheric flux of ^{7}Be would account for much of the ^{7}Be reflected in the subtidal sediments, combined sewer overflow events induced by high rainfall have the potential to contribute significantly to the ^{7}Be budget of the Bay. During periods of lower rainfall (May-2005) ^{7}Be inventories were evenly distributed throughout the Bay, but following a period of high rainfall (November-2005), mean ^{7}Be inventories in the western Bay, near the highest concentration of CSO outfalls was significantly higher.

7. References

Appleby, P.G. and F. Oldfield (1992) Applications of Lead-210 to sedimentation studies. M. Ivanovich and R.S. Harmon (eds), Uranium-Series Disequilibrium: Applications to Environmental Problems, Clarendon Press, Oxford, pp. 731-778

Baskaran, M. and P. H. Santchi (1993) The role of particles and colloids in the transport of radionuclides in the coastal environments of Texas. *Marine Chemistry* 43: 95-114.

Beck, A.J., J.P. Rapaglia, J.K. Cochran and H.J. Bokuniewicz (2007) Radium mass-balance in Jamaica Bay, NY: Evidence for substantial flux of submarine groundwater. *Marine Chemistry,* 106: 416-441.

Beer, J., A. Blinov, G. Bonani, R.C. Finkel, H.J. Hofmann, B. Lehmann, H. Oeschger, A. Sigg, J. Schwander, T. Saffelbach, M. Suter and W. Wolfi (1990) Use of 10Be in polar ice to trace the 11-year cycle of solar activity. *Nature* 347: 164-166.

Benitez-Nelson, C.R. and K.O. Buesseler (1999) Phosphorus 32, phosphorus 37, beryllium 7, and lead 210: Atmospheric fluxes and utility in tracing stratosphere/troposphere exchange. *Journal of Geophysical Research* 104: 11745-11754.

Benotti, M.J., M. Abbene, and S.A. Terracciano (2007) Nitrogn Loading in Jamaica Bay, Long Island, New York: Predevelopment to 2005.

Bhandari, N., D. Lal, Rama (1970) Vertical structure of the troposphere as revealed by radioactive tracer studies. *Journal of Geophysical Research* 75: 2974-2980.

Botton, M. L., R. E. Loveland, J. T. Tanacredi, and T. Itow (2006) Horseshoe Crabs (*Limulus polyphemus*) in an urban estuary (Jamaica Bay, New York) and the potential for ecological restoration. *Estuaries and Coasts* 29: 820-830.

Canuel,, E.A., C.S. Martens, and L.K. Benninger (1990) Seasonal variations in ^{7}Be activity in the sediments of Cape Lookout Bight, North Carolina. *Geochimica et Cosmochimica Acta* 54: 237-245.

Dibb, J. E. (1989) Atmospheric deposition of beryllium-7 in the Chesapeake Bay region. *Journal of Geophysical Research* 94: 2261-2265.

Dibb, J.E. and D.L. Rice (1989) Temporal and spatial distribution of beryllium-7 in the sediments of Chesapeake Bay. *Estuarine, Coastal and Shelf Science* 28: 395-406.

Doering, C. and R. Akber (2008) Beryllium-7 in near-surface air and deposition at Brisbane, Australia. *Journal of Environmental Radioactivity* 99: 461-467.

Feely, H.W., R.J. Larsen, C.G. Sanderson (1989) Factors that causes seasonal variations in beryllium-7 in surface air. *Journal of Environmental Radioactivity* 9: 223-249.

Feng, H., J.K. Cochran and D.J. Hirschberg (1999) ^{234}Th and ^{7}Be as tracers for the sources of particles to the turbidity maximum of the Hudson River Estuary. *Estuarine, Coastal, and Shelf Science* 49: 629-645.

Fisenne, I.M. (1968) Distribution of lead-210 and radium-226 in soil. Rep. UCRL-18140, pp. 145-158. Washington, D.C.: US At. Energy Comm.

Giffin, D. and D. R. Corbett (2003) Evaluation of sediment dynamics in coastal systems via short-lived radioisotopes. *Journal of Marine Systems* 42: 83-96.

González-Gómez, M. Azahra, J.J. López-Peñalver, A. Camacho-García, T.El. Bardouni and H. Boukhal (2006) Seasonal variability in ^{7}Be depositional fluxes at Granada, Spain. *Applied Radiations and Isotopes* 64: 228-234.

Heikkilä, U., J. Beer and V. Alfimov (2008) Beryllium-10 and beryllium-7 in precipitation in Düberdorf (440 m) and Jungfraujoch (3580 m), Switzerland (1998-2005). *Journal of Geophysical Research – Atmosphere* doi: 10.1029/2007JD009160.

Ioannidou, A., M. Manolopoulou and C. Papastefanou (2005) Temporal changes in ^{7}Be and ^{210}Pb concentrations in surface air at temperate latitudes (40° N). *Applied Radiation and Isotopes* 63: 277-284.

Kaste, J. M., S. A. Norton and C. T. Hess (2002) Environmental chemistry of beryllium-7. In: Beryllium: Mineralogy, petrology, and geochemistry, (P. H. Ribbe and J. J. Rosso, eds.), Reviews in Mineralogy and Geochemistry, vol. 50, pp. 291-312.

Lal, D., P.K. Malhotra and B. Peters (1958) On the production of radioisotopes in the atmosphere by cosmic radiation and their application to meteorology. *Journal of Atmospheric and Solar-Terrestrial Physics* 12: 306-328.

Lal, D. and B. Peters (1967) Cosmic ray produced radioactivity on earth. In: Handbuch der Physik 46: 551-612.

LeCloarec, M-F., P. Bonté, I. Lefèvre, J-M Mouchel, S. Colbert. (2007) Distribution of ^{7}Be, ^{210}Pb, and ^{137}Cs in watersheds of different scales in the Seine River basin: Inventories and residence times. *Science of the Total Environment* 375: 125-139.

Lewis, D.M. (1976) The geochemistry of manganese, iron, uranium, lead-210 and major ions in the Susquehanna River. PhD Thesis. New Haven, CT. 272 pp.

Matisoff, G., C.W. Wilson, and P.J. Whiting (2005) The $^{7}Be/^{210}Pb$ ratio as an indicator of suspended sediment age or fraction new sediment in suspension. *Earth Surface Processes and Landforms* 30: 1191-1201.

McCaffrey, R.J. (1977) A record of the accumulation of sediment and trace metals in a Connecticut, USA, salt marsh. PhD Thesis, New Haven, CT, 156 pp.

Noyce, J.R., T.S. Chen, D.T. Moore, J.N. Beck and P.K. Kuroda (1971) Temporal distributions of radioactivity and Sr-87/Sr-86 ratios during rainstorms. *Journal of Geophysical Research* 76: 646-656.

Olsen, C.R., I.L. Larsen, P.D. Lowry, and N.H. Cutshall (1986) Geochemistry and deposition of ^{7}Be in river-estuarine and coastal waters. *Journal of Geophysical Research* 91: 896-908.

O'Shea, M. L. and T. M. Brosnan (2000) Trends in indicators of eutrophication in western Long Island Sound and the Hudson-Raritan Estuary. *Estuaries* 23: 877-901.

Swanson, L.R. and R. E. Wilson (2008) Increased tidal ranges coinciding with Jamaica Bay development contribute to marsh flooding. *Jounral of Coastal Research* 24: 1565-1569.

Todd, J.F., G. T.F. Wong, C.R. Olsen and I.L Larsen (1989) Atmospheric ceositional characteristics of Beryllium 7 and Lead 21 along the Southeastern Virginia coast. *Journal of Geophysical Research* 94: 11106-11116.

Turekian, K.K., Y. Nozaki, and L. Benninger (1977) Geochemistry of atmospheric radon and radon products. *Annual Review of Earth and Planetary Science* 5: 227-255.

Turekian, K. K., L. K. Benninger and E. P. Dion (1983) ^{7}Be and ^{210}Pb total depositional fluxes at New Haven, Connecticut, and Bermuda. *Journal of Geophysical Research* 88: 5411-5415.

Zeppie, C.R. (1977) Vertical profiles and sedimentation rates of Cd, Cr,Cu, Ni and Pb in Jamaica Bay, New York. M.S. Thesis. Stony Brook, NY. 85pp.

Zhu, J. and C.R. Olsen (2009) Beryllium-7 atmospheric deposition and sediment inventories in the Neponset River estuary, Massachusetts, USA. *Journal of Environmental Radioactivity* 100: 192-197.

Table 4-1 Fluxes of precipitation, ^{210}Pb and ^{7}Be at the Marine Science Research Center in Stony Brook, NY (40°54 ´17”N, 73°07 ´06”W).

Month	Rainfall (cm)	^{210}Pb Flux (dpm cm^{-2})	^{210}Pb (dpm L^{-1})	^{7}Be Flux (dpm cm^{-2})	^{7}Be (dpm L^{-1})
April-08	10.0	0.07 ± 0.003	1.1 ± 0.3	2.0 ± 0.04	199 ± 4.0
May-08	12.9	0.07 ± 0.002	5.6 ± 0.2	2.0 ± 0.02	156 ± 1.7
June-08	7.1	0.07 ± 0.002	9.8 ± 0.4	1.6 ± 0.02	219 ± 2.4
July-08	10.1	0.09 ± 0.003	9.2 ± 0.3	2.1 ± 0.02	207 ± 1.8
August-08	7.2	0.10 ± 0.003	13.2 ± 0.2	0.5 ± 0.01	273 ± 1.6
September-08	19.0	0.11 ±0.005	5.8 ± 0.3	2.1 ± 0.03	110 ± 1.9
October-08	7.6	0.04 ± 0.002	5.2 ± 0.3	0.8 ± 0.02	102 ± 24
November-08	8.1	0.08 ± 0.002	9.9 ± 0.3	0.7 ± 0.01	152 ± 2.8
December-08	17.0	0.07 ± 0.002	4.2 ± 0.1	1.7 ± 0.02	98 ± 1.1
January-09	8.1	0.06 ± 0.003	7.4 ± 0.3	0.7 ± 0.02	80 ± 1.2
February-09	4.6	0.04 ± 0.003	8.8 ± 0.7	0.4 ± 0.01	88 ± 2.2
March-09	6.2	0.07 ± 0.004	11.3 ± 0.7	0.8 ± 0.01	122 ± 3.2
April-09	12.3	0.10 ± 0.003	8.0 ± 0.2	2.0 ± 0.02	164 ± 1.3
May-09	14.9	0.06 ± 0.001	4.0 ± 0.2	1.3 ± 0.03	87 ± 2.3
June-09	19.7	0.10 ± 0.005	5.1 ± 0.3	2.3 ± 0.05	118 ± 2.5
July-09	16.6	0.08 ± 0.004	8.2 ± 0.4	1.7 ± 0.02	134 ± 2.2
August-09	9.0	0.07 ± 0.03	7.8 ± 0.3	1.3 ± 0.03	148 ± 3.3
September-09	8.0	0.06 ± 0.003	7.5 ± 0.4	1.0 ± 0.03	129 ± 3.8
October-09	15.0	0.09 ± 0.005	5.7 ± 0.3	1.9 ± 0.03	127 ± 2.0
November-09	3.6	0.05 ± 0.001	15.0 ± 0.3	0.7 ± 0.01	180.6 ± 8.3
December-09	15.9	0.10 ± 0.005	6.0 ± 0.3	1.8 ± 0.03	110.1 ± 1.9

Table 4-2. ^{7}Be activities on filterable (> 1 μm) particles in the water column

Sample ID	Description	Depth (m)	Salinity	TSS (mg L^{-1})	Particulate ^{7}Be (dpm L^{-1})	Particulate ^{7}Be (dpm g^{-1})
JB-WS-1	Inlet Station	3.0	28.5	15.5	0.09 ± 0.01	5.8 ± 0.6
JB-WS-1*	Inlet Station	1.0	28.3	11.1	0.1 ± 0.1	9.0 ± 2.4
JB-WS-2-Shallow	Bay Interior	1.0	28.3	13.1	0.1 ± 0.01	7.6 ± 0.9
JB-WS-2-Deep	Bay Interior	5.0	28.5	16.5	0.09 ± 0.01	5.5 ± 0.7
JB-WS-3	Grassy Bay	5.0	26.6	15.0	0.09 ± 0.02	6.7 ± 1.1
JB-WS-4	Near eastern marshes	2.0	27.5	15.2	0.1 ± 0.02	6.6 ± 1.4

* Additional sample (28 L) was taken at inlet in June-2009

Table 4-3. ^{7}Be inventories in subtidal sediments and atmospheric inputs for September-2004, May-2005, November-2005, and July-2006 sampling cruises.

	Mean Sediment ^{7}Be Inventory (dpm cm^{-2})	**Direct ^{7}Be flux from atmosphere* (dpm cm^{-2})**	**^{7}Be Inventory /Atmospheric Input****	**Direct ^{7}Be flux from atmosphere*** (dpm cm^{-2})**	**^{7}Be Inventory /Atmospheric Input*****
September-04	3.8 ± 0.6	3.1	1.2	3.3	1.2
May-05	2.6 ± 0.5	2.0	1.3	2.0	1.3
November-05	4.1 ± 0.7	3.6	1.1	3.8	1.1
July-06	2.6 ± 0.3	2.4	1.1	2.6	1.0

*Estimated using data collected at Stony Brook University

**Relative to direct atmospheric input of ^{7}Be.

***Estimated using data from Zhu and Olsen, 2009.

Table 4-4. Inventory of ^{7}Be in the upper 2 mm and upper 5 cm taken in August-2008

Sample ID	Latitude (°N)	Longitude (°W)	Specific Activity of ^{7}Be (dpm g^{-1}) in 0 – 2 mm	Specific Activity of ^{7}Be (dpm g^{-1}) in 0 -5 cm	^{7}Be Inventory (dpm cm^{-2}) in 0 - 2 mm	^{7}Be Inventory (dpm cm^{-2}) in 0 - 5 cm	% of Inventory in upper 2 mm
JB8-08-1	40.6120	73.8108	4.0 ± 0.4	1.3 ± 0.2	4.2 ± 0.4	4.3 ± 0.5	98
JB8-08-4	40.6021	73.7950	9.1 ± 0.8	1.1 ± 0.1	3.7 ± 0.3	3.3 ± 0.4	~100
JB8-08-8	40.6152	73.7778	1.9 ± 0.2	1.1 ± 0.3	1.0 ± 0.1	1.6 ± 0.5	63
JB8-08-20	40.6313	73.8348	0.8 ± 0.1	0.6 ± 0.1	1.8 ± 0.2	2.4 ± 0.3	75
JB8-08-23	40.6293	73.8742	2.8 ± 0.4	0.7 ± 0.1	3.0 ± 0.4	3.3 ± 0.3	91

Table 4-5. Mass Balance of ^{7}Be in Jamaica Bay

	Total ^{7}Be ($\times 10^{10}$ dpm)	^{7}Be (dpm cm^{-2})
Input		
Atmospheric deposition	78 – 140	2.0 – 3.6
Import		
Particulate Phase	78	2.1
Input from CSO events	98	2.5
Total	254 - 316	6.6 – 8.2
Export of ^{7}Be		
Particulate Phase	90	2.3
Predicted ^{7}Be Inventory in Subtidal Sediments	164 - 226	4.3 – 5.9
Measured ^{7}Be Inventory in Subtidal Sediments	101 – 160	2.6 – 4.1

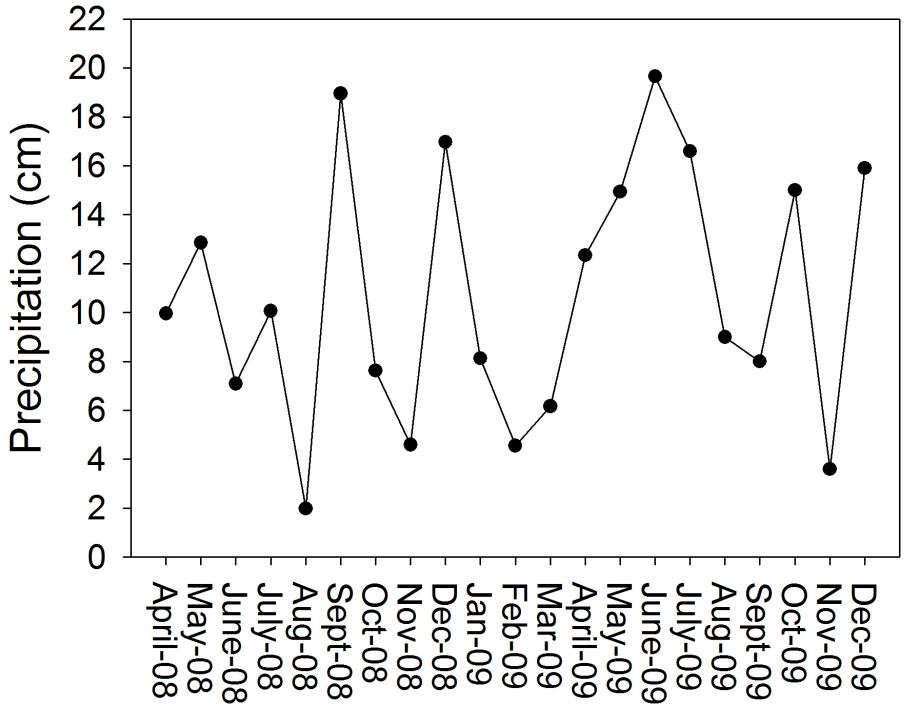

Figure 4-1 Monthly precipitation at Stony Brook, NY from April-2008 to December-2009

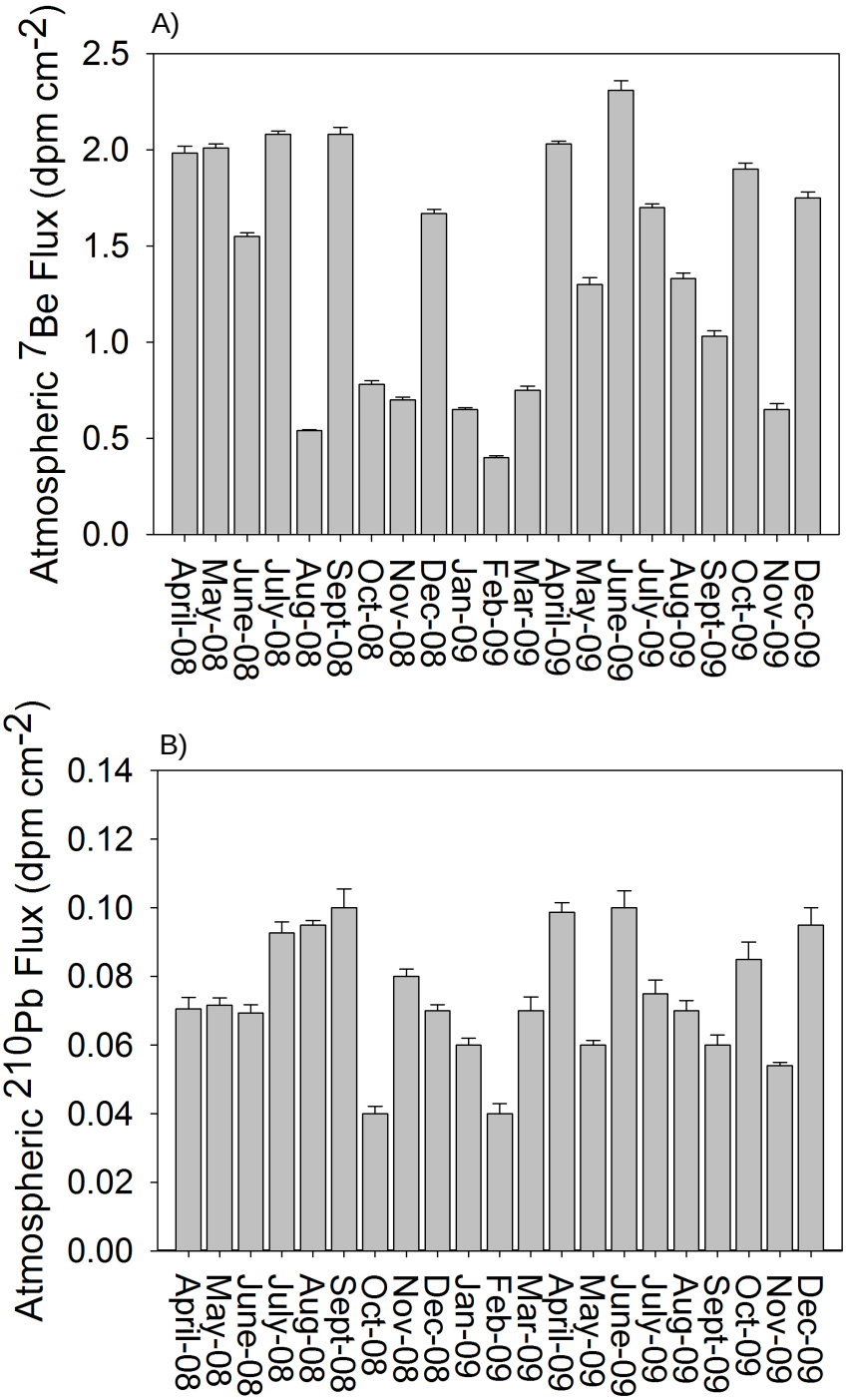

Figure 4-2. Monthly atmospheric flux of A) ^{7}Be and B) ^{210}Pb at Stony Brook, NY from April-2008 to December-2009

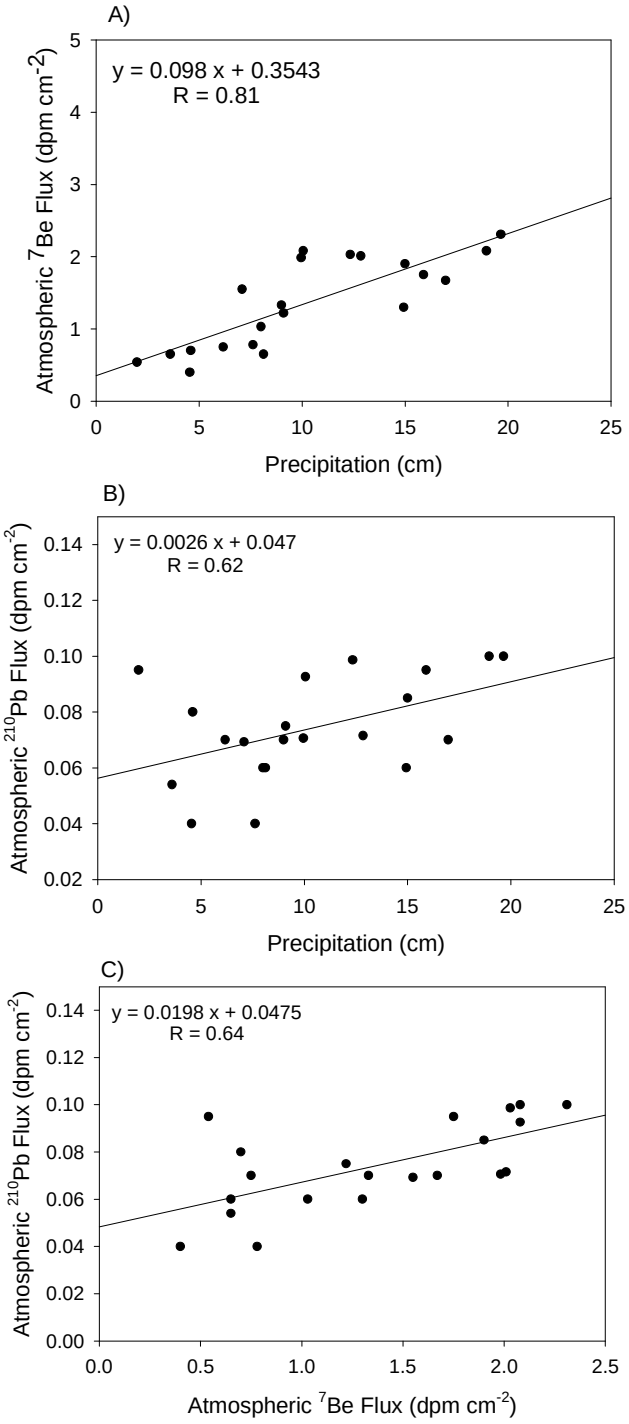

Figure 4-3. Scatter plot illustrating the linear correlation between precipitation (cm) and the atmospheric fluxes of A) ^{7}Be (dpm cm^{-2}), B) ^{210}Pb (dpm cm^{-2}) and C) atmospheric flux of ^{210}Pb (dpm cm^{-2}) and ^{7}Be (dpm cm^{-2}) collected at Stony Brook University from April-2008 to December-2009.

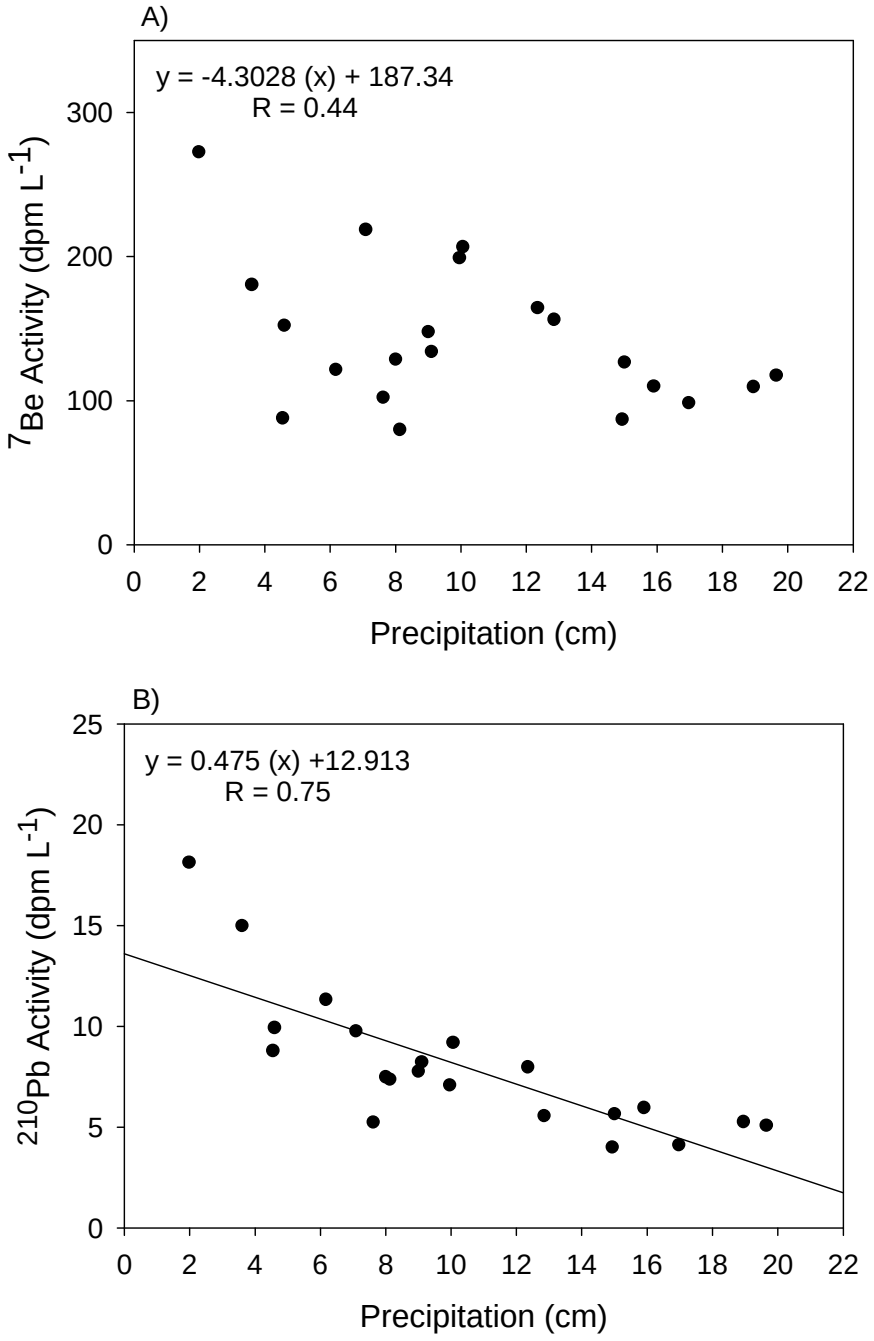

Figure 4-4. Scatter plot illustration the relationship between precipitation and A) ^{7}Be activity and B) ^{210}Pb activity at Stony Brook, NY from April-2009 to December-2009

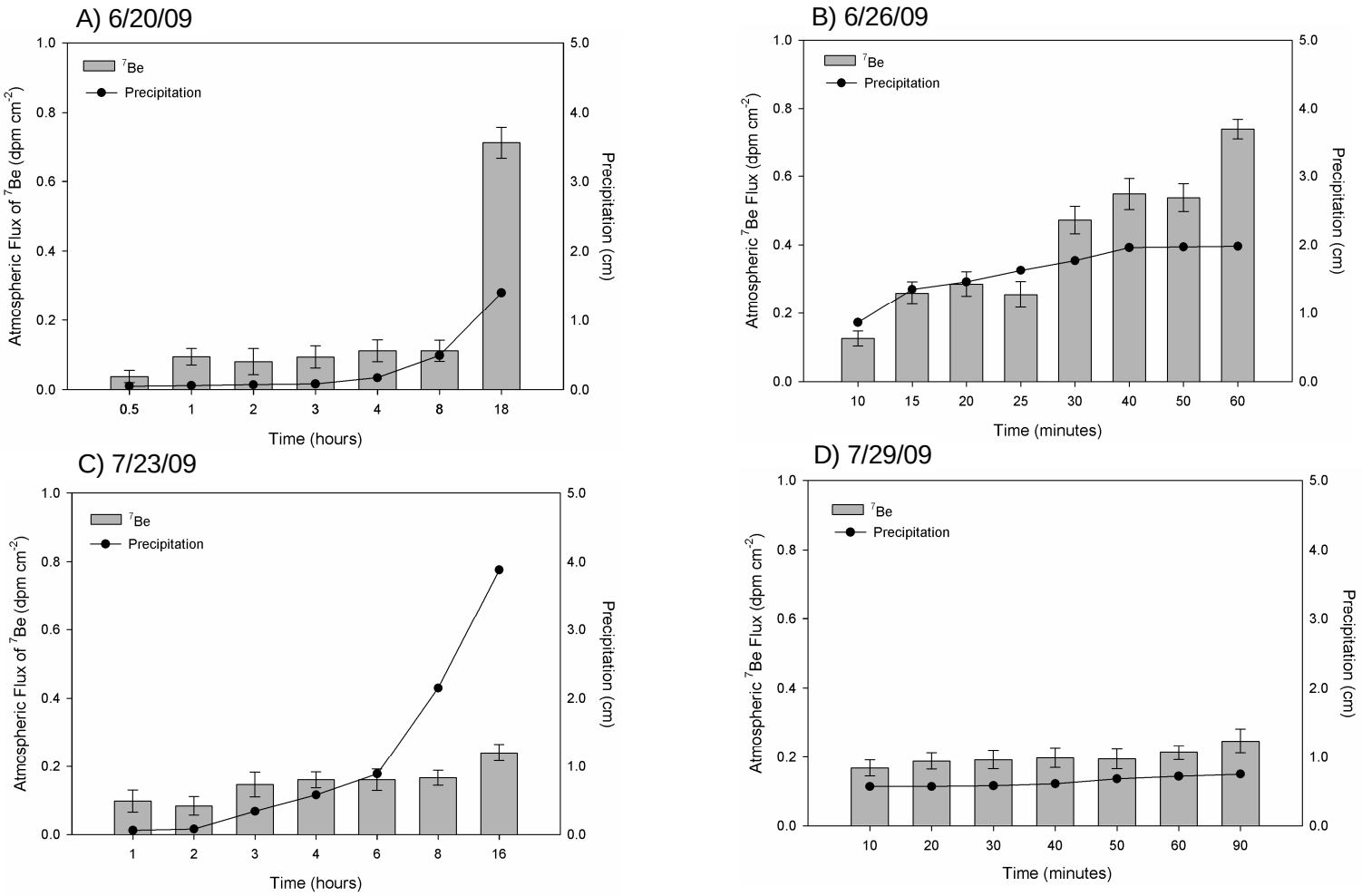

Figure 4-5. Atmospheric flux of ^{7}Be (dpm cm^{-2}) and precipitation (cm) versus time for rainfall events occurring on A) 6/20/09, B) 6/26/09, C) 7/23/09 and D) 7/29/09.

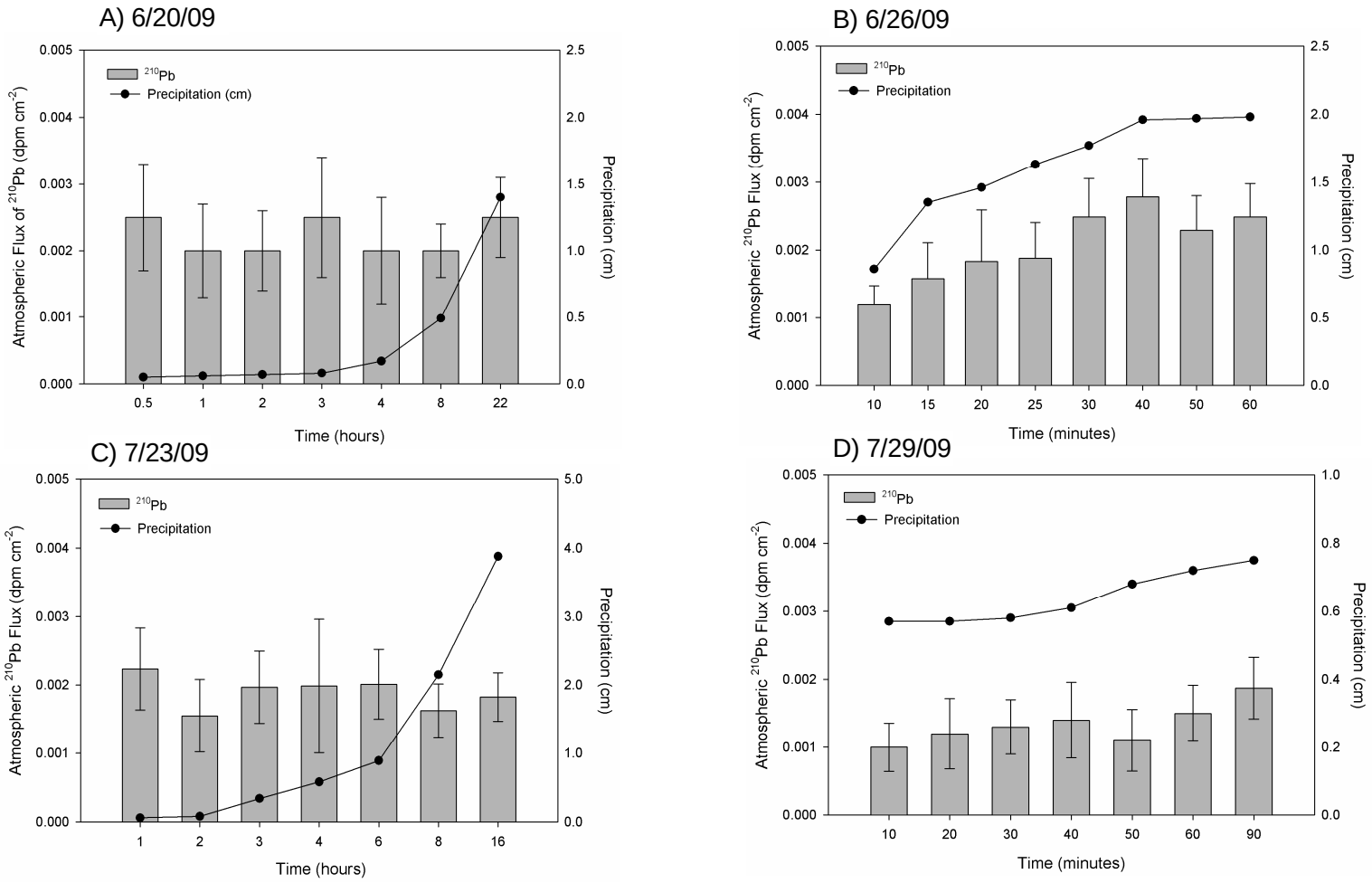

Figure 4-6. Atmospheric flux of ^{210}Pb (dpm cm^{-2}) and precipitation (cm) versus time for rainfall events occurring on A) 6/20/09, B) 6/26/09 and C) 7/23/09 and D) 7/29/09.

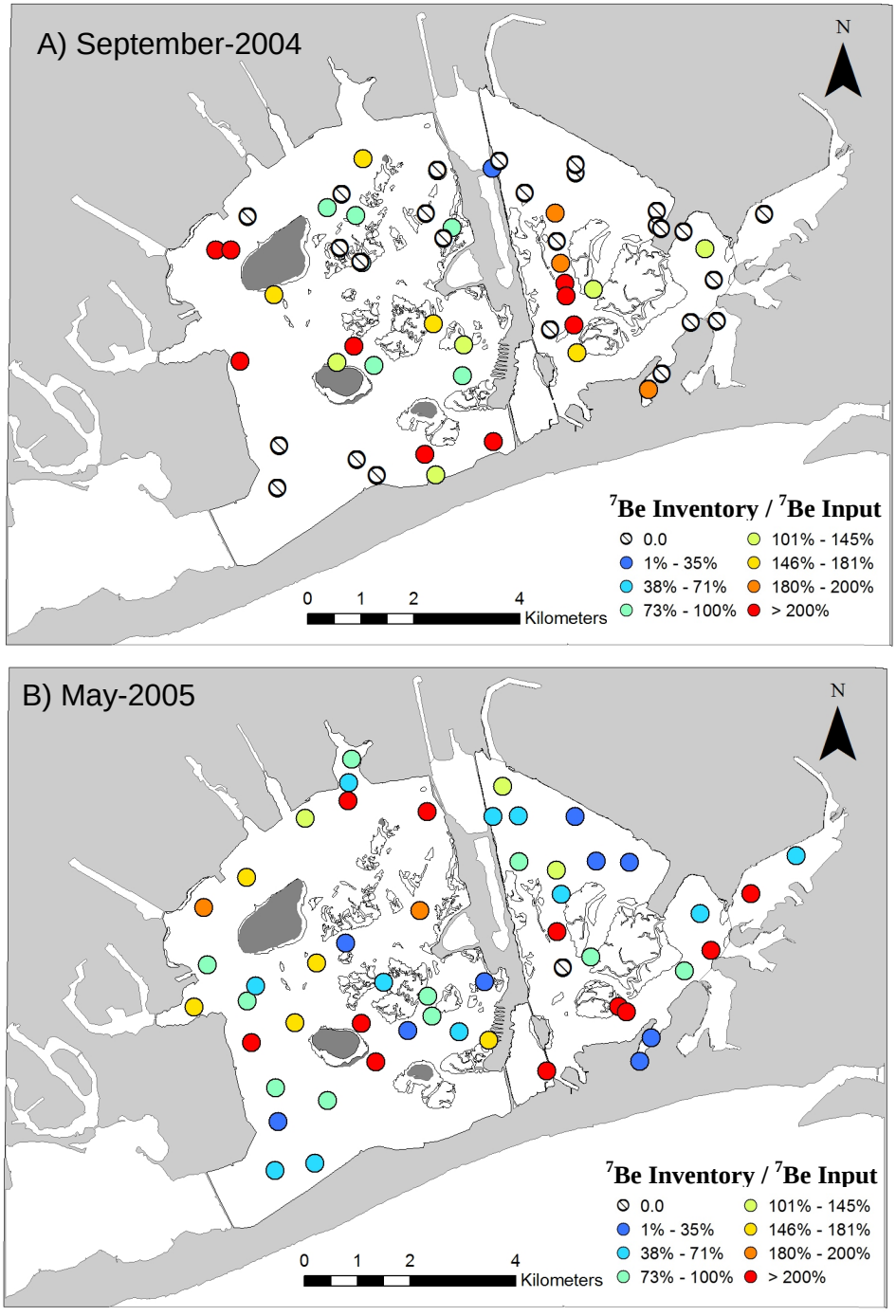

Figure 4-7. ^{7}Be Inventories of surficial bottom sediments during cruises in A) Sept-2004, B) May-2005, C) Nov-2005, D) July-2006. Estimated ^{7}Be inputs from the atmosphere for September-2004, May-2005, November-2005, and July-2006 cruises were 3.6, 2.3, 4.2, and 2.9 dpm cm^{-2}, respectively.

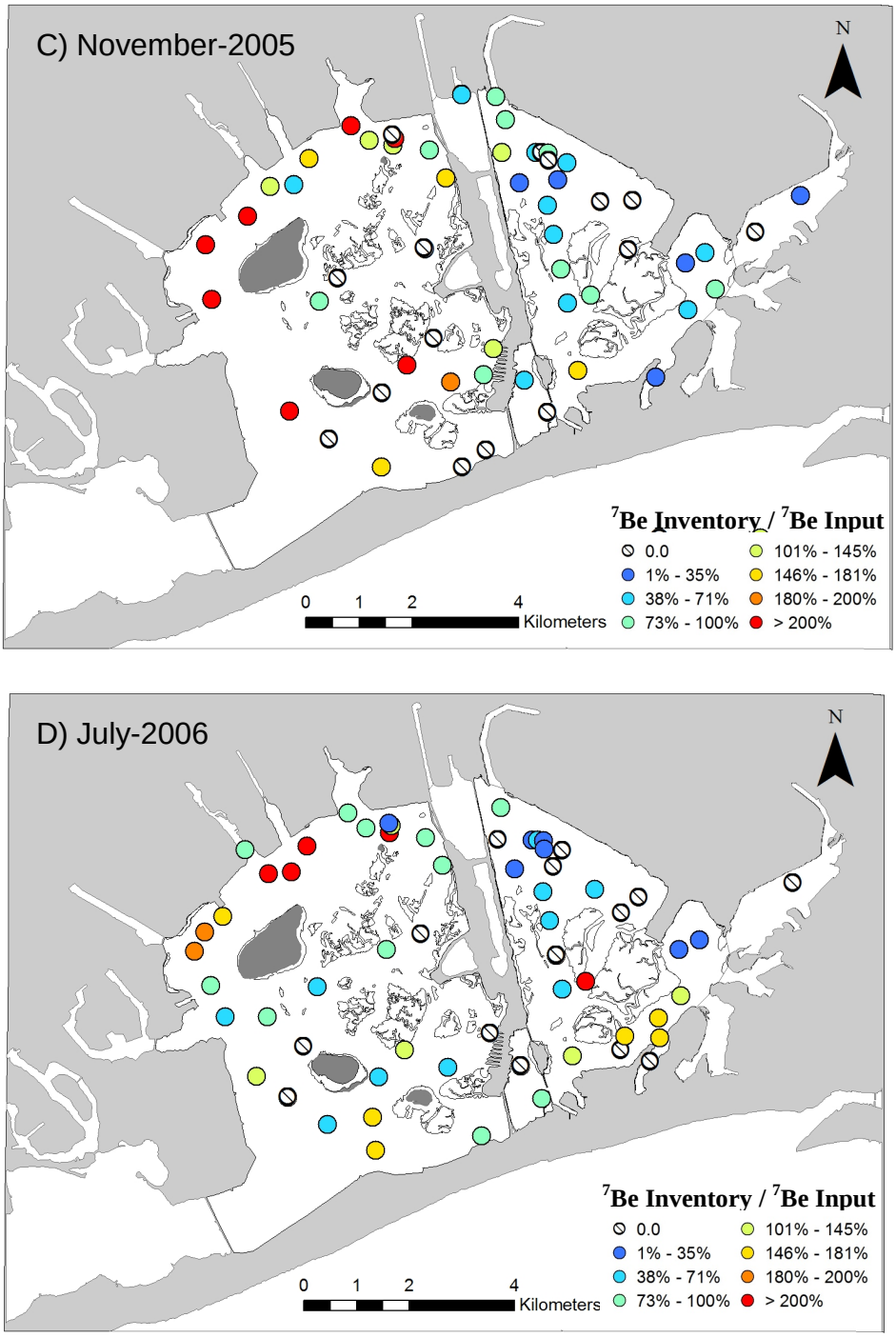

Figure 4-7. Continued

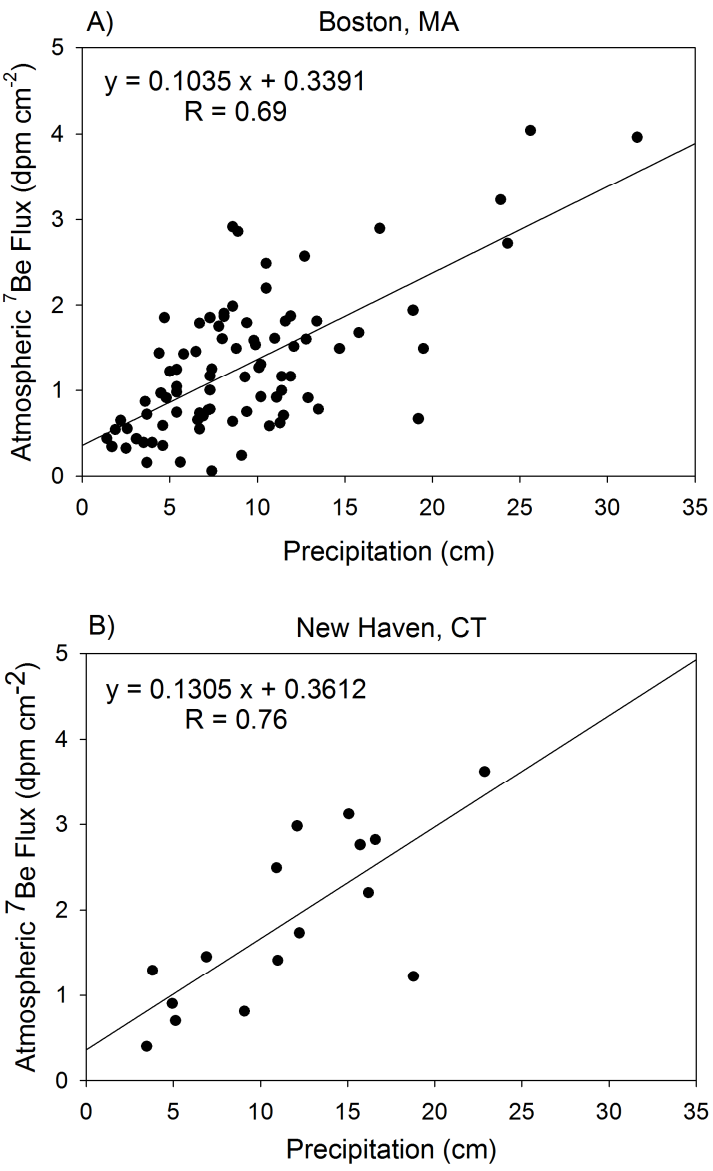

Figure 4-8. Relationship between atmospheric ^{7}Be flux (dpm cm^{-2}) and precipitation from data collected at A) Boston, MA (42°N; Zhu and Olsen, 2009), B) New Haven, CT (41°N; Turekian et al., 1983), C) Stony Brook, NY (41°N; This work), D) Solomons, MD (38°N; Dibb, 1989), E) Norfolk, VA (37°N; Todd et al., 1989) and F) Morehead, NC (34°N; Canuel et al., 1990).

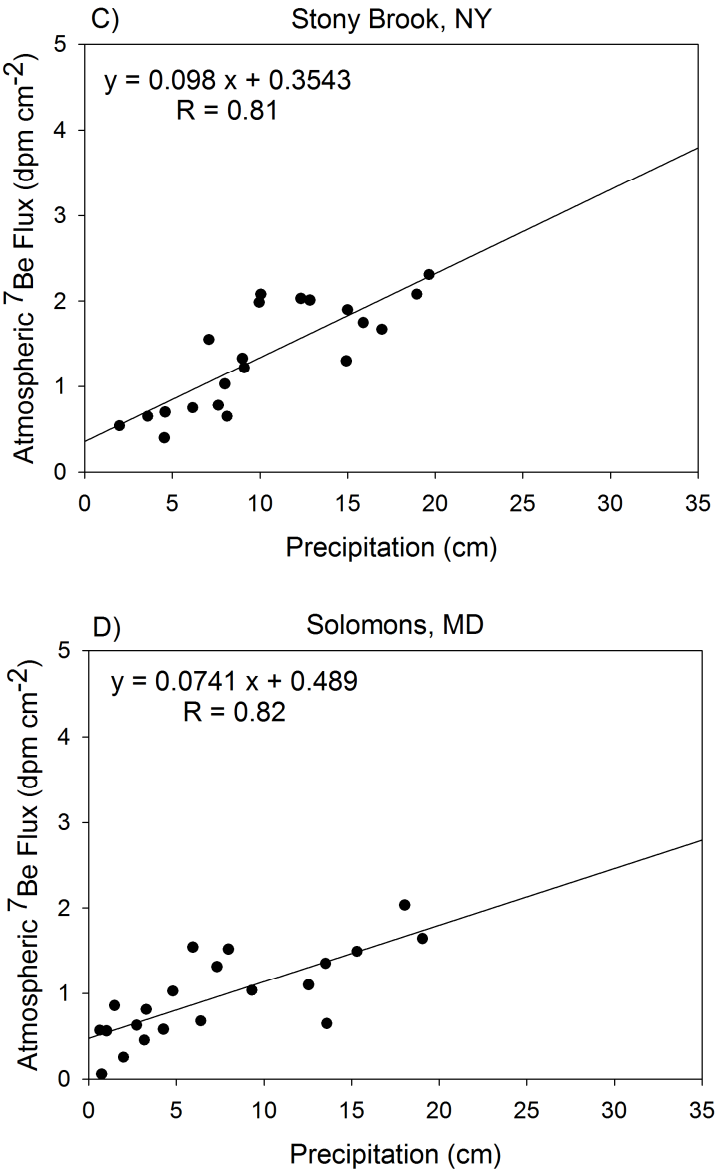

Figure 4-8. Continued

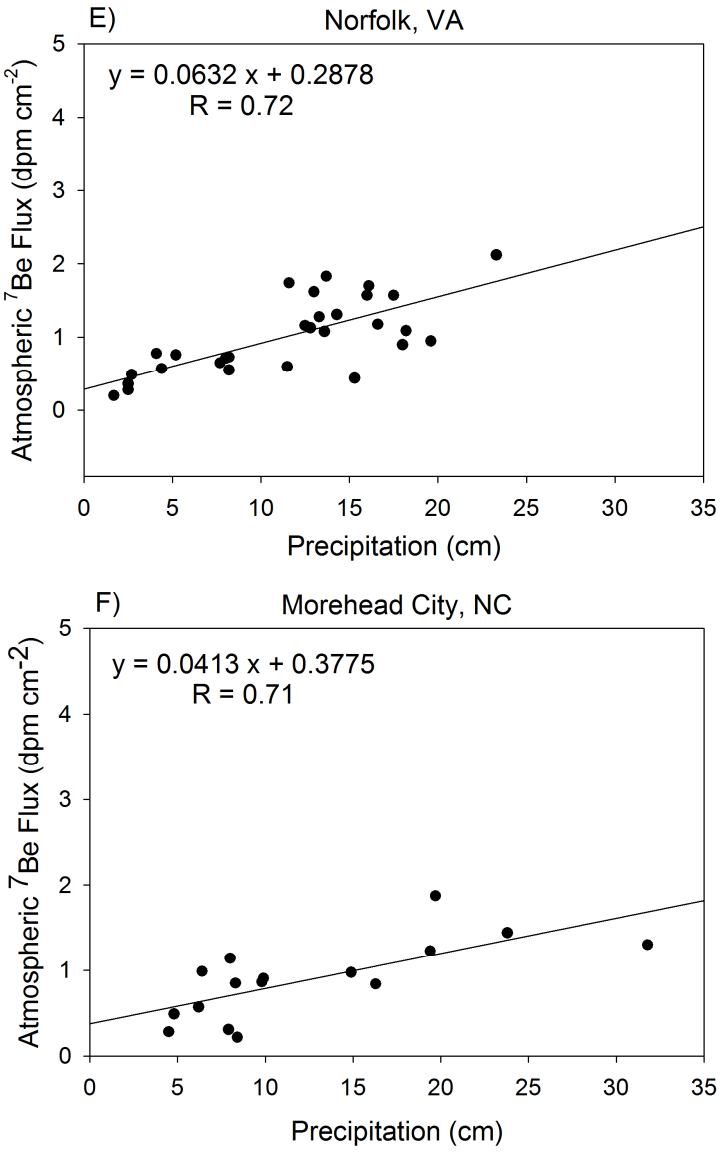

Figure 4-8. Continued

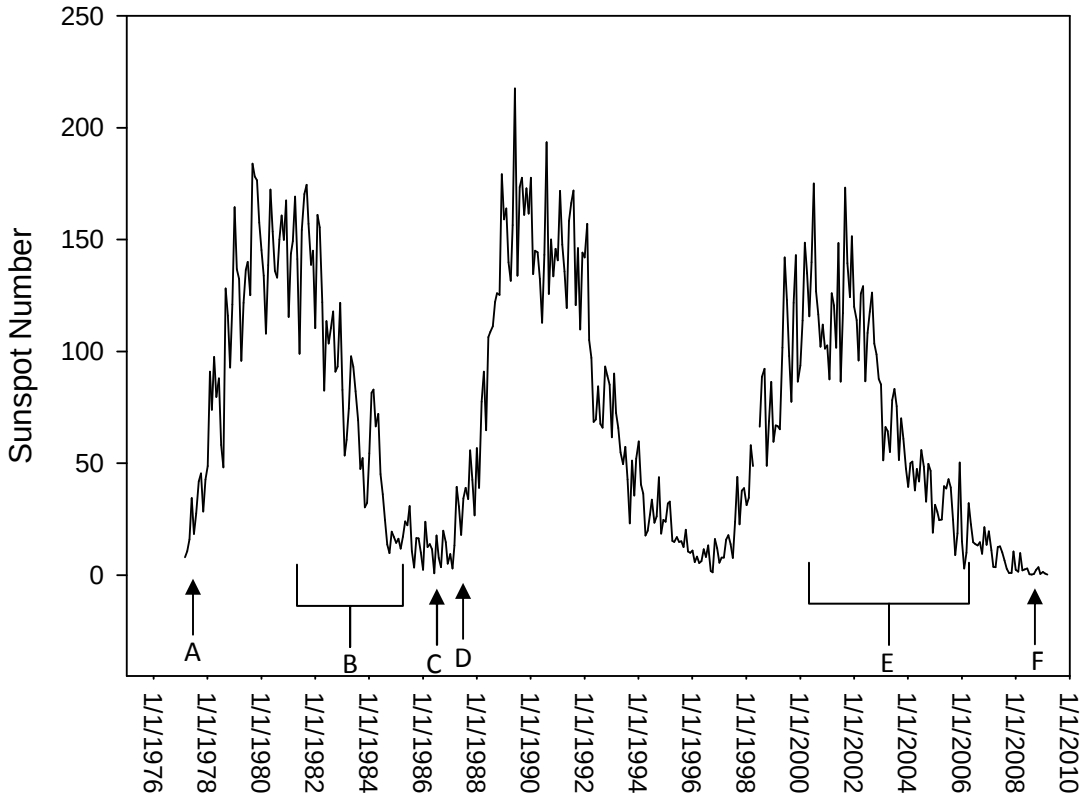

Figure 4-9. Sunspot activity over the last 34 years. Letters denote the mid-point of monthly rainfall collection at A) New Haven, CT by Turekian et al., 1983 from 1977-1978, B) Norfolk, VA by Todd et al., 1989 from 1982-1985, C) Solomons, MD by Dibb, 1989 from 1986-1987, D) Morehead, NC by Canuel et al., 1990 from 1987-1988, E) Boston, MA by Zhu and Olsen, 2009 from 2000-2007 and F) Stony Brook, NY from 2008-2009

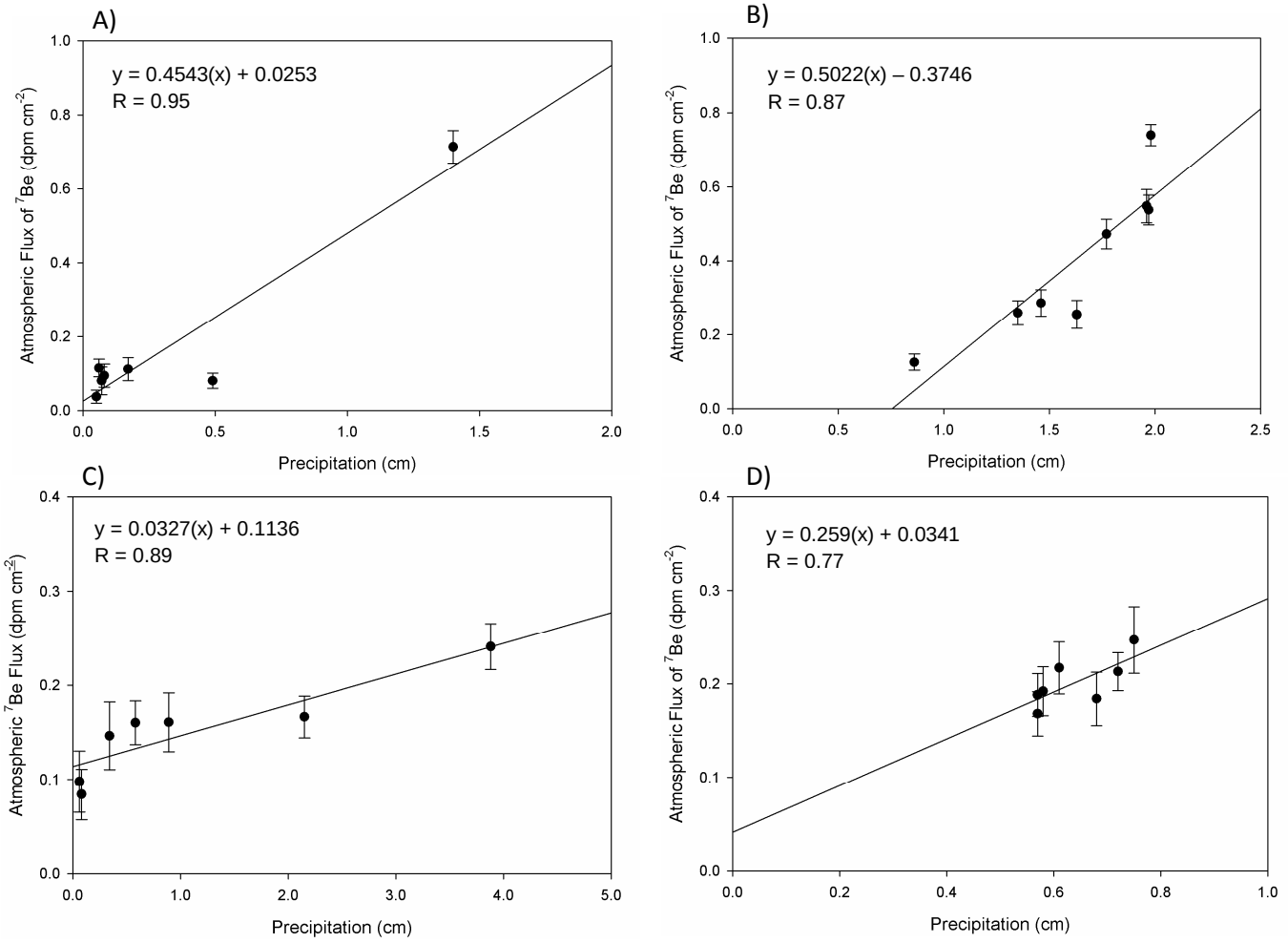

Figure 4-10. Relationship between atmospheric ^{7}Be flux (dpm cm-2) and Precipitation for individual rainfall events occurring on A) 6/20/09, B) 6/26/09, C) 7/23/09 and D) 7/29/09.

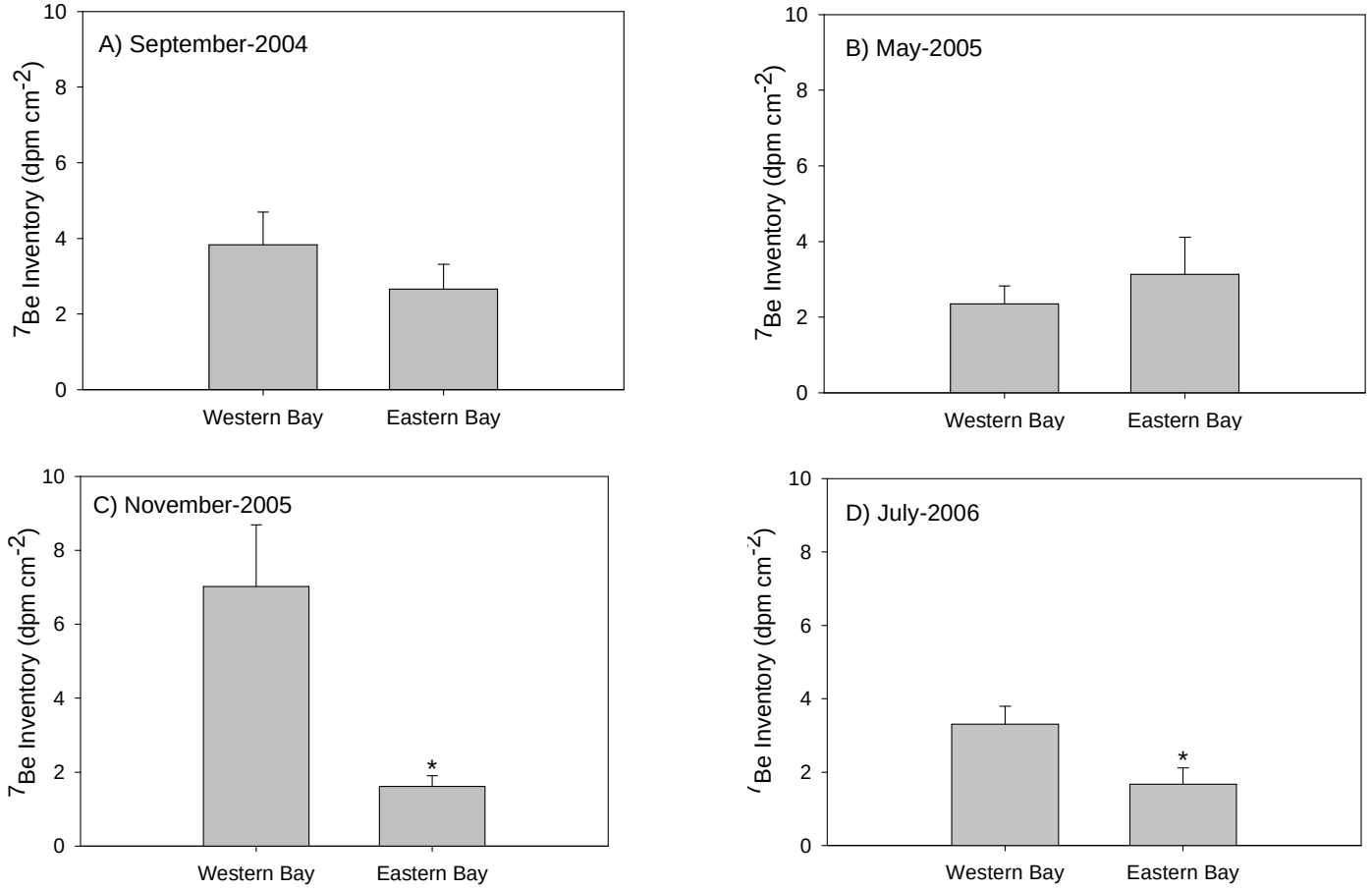

Figure 4-11. Mean ^{7}Be inventory in western and eastern Jamaica Bay during A) September-2004, B) May-2005, C) November-2005, and D) July-2006. * denotes mean ^{7}Be inventories that are significantly lower ($p < 0.05$) than the other half of the bay during that sampling cruise.

CHAPTER 5

Short-Lived Radionuclides and Sediment Deposition in the Salt Marsh Islands of Jamaica Bay, NY

1. Abstract

The ability of a salt marsh to keep pace with sea-level is heavily dependent of sediment accretion on the marsh surface. The marshes of Jamaica Bay, a coastal lagoon in New York, have undergone a rapid decrease in area over the last 25 years. Sediment deposition and retention on the marsh surface was evaluated using short-lived radionuclides $^{234}Th_{xs}$ (half-life = 24.1 days) and ^{7}Be (half-life = 53.3 days). Samples collected on marsh islands during September-2004, May-2005, May-2007, August-2007 and October-2007 had significant excess ^{234}Th inventories, with highest values measured in the salt marshes in the western half of the bay. These results indicate that sediment is transported from the subtidal bay is, at least temporarily, deposited and stored on these marsh islands. Mass accumulation rates estimated from the $^{234}Th_{xs}$ on the marsh sediments ranged from 0 to 2.5 g cm^{-2} y^{-1}. These values are higher than those determined using ^{210}Pb chronologies (0.05 - 0.1 g cm^{-2} y^{-1}) from a previous study, suggesting that the high deposition rates are not sustained over time. ^{7}Be inventories measured on the marsh islands were, in general, highest at JoCo marsh (generally considered the healthiest marsh in Jamaica Bay). At this site, ^{7}Be inventories were higher than the expected from direct atmospheric input of ^{7}Be, suggesting there was input and retention of subtidal sediments to the marsh. In contrast, the salt marshes (in September-2004) in the western part of the bay were depleted in ^{7}Be relative to the direct atmospheric input which may reflect the prevalence of non-vegetated areas in the western marshes where sediment (and ^{7}Be) was not retained due to erosion.

2. Introduction

Salt marshes are among some of the most productive ecosystems in the world, serving as important habitats for fish and birds, as well as areas high primary productivity. The coastal marshes of the Northeastern United States were formed as post-glacial sea-level rise slowed 4000 to 7000 years ago (Teal and Teal, 1969; Redfield, 1972). These marshes are typically built on marine sediments and are dominated by *Spartina alterniflora* (Mitsch and Gosselink, 2000). Long-term marsh stability is dependent on marsh accretion, which causes the marsh to increase outward and upward and submergence of the marsh due to relative sea-level rise and marsh surface subsidence (Mitsch and Gosselink, 2000; Friedrichs and Perry, 2001).

These processes are, to an extent, self-regulating in a salt marsh. If accretion rates are high, submergence of the marsh during a normal tidal cycle decreases, decreasing sediment deposition on the marsh surface, and thus reducing one mode of marsh accretion (Mitsch and Gosselink, 2000; Friedrichs and Perry, 2001). In addition, less frequent flooding of the marsh surface oxidizes more peat, allowing for faster degradation of the organic material (Mitsch and Gosselink, 2000). In contrast, if the marsh accretion rate slows, the marsh surface is inundated more frequently and for longer periods of time, increasing the sediment deposition on the surface, as well as increased storage of peat due to anoxic conditions (Mitsch and Gosselink, 2000; Friedrichs and Perry, 2001). Regional conditions, such as sediment type and concentration in the water column and amplitude and frequency of tides can unbalance this feedback between marsh accretion and submergence.

The marsh islands of Jamaica Bay have decreased significantly in size and total acreage between 1951 and 2003 (An update on the disappearing salt marshes of Jamaica Bay, NY, 2007). The geomorphological changes in the marsh islands of the Bay include erosion of the marsh island perimeter, widening of tidal creeks, and expansion of internal tidal pools (Hartig et al., 2002). The decreases in marsh area and health are also marked by pronounced die-offs of marsh vegetation (Hartig et al., 2002, Kolker, 2005). It has been suggested that this is a result of increases in organic and nutrient loading to the marsh causing enhanced rates of sulfate reduction within the plant root zone, and inducing sulfide toxicity in the marsh plants and their subsequent death (Kolker, 2005). However, sediment deposition, or rather the lack thereof, may also be important as either a driver of the process of degradation or as a factor that may simply exacerbate the problem once it begins. If surficial sediment deposition combined with below-ground biomass production is not sufficient to maintain a steady marsh elevation relative to sea level rise, the marsh will be inundated for longer periods of time. This may increase the delivery of nutrients and of organic material to the marsh surface and lead to the rapid vegetation loss, as has been observed (Mitsch and Gosselink, 2000; Friedrichs and Perry, 2001).

Previous studies have used particle reactive radionuclides in a range of environments in order to understand mixing in the water column, sediment transport, deposition and resuspension. Naturally occurring radionuclides, such as ^{234}Th and ^{7}Be have been useful in studies within coastal areas due to their high particle reactivity, well-established decay rates and well constrained sources (e.g. Feng et al., 1999). The short-lived radionuclides, ^{234}Th (half-life = 24.1 days) and ^{7}Be (half-life = 53.3 days) are

particularly useful in studying processes that operate over seasonal time scales. In addition, the sources of these radionuclides differ: ^{234}Th has an oceanic source (via production from its dissolved parent, ^{238}U), while ^{7}Be has an atmospheric source (Baskaran and Swarenski, 2006; Feng et al., 1999; Vogler et al., 1996)

The particle affinities of both ^{234}Th and ^{7}Be make these radionuclides useful tracers for sediment transport and deposition. Our goal in this study was to use these tracers to understand better the retention of sediment on the marsh islands of Jamaica Bay and the exchange of sediment between the subtidal salt marsh environments.

3. Methods

3.1 Study Site

Jamaica Bay is a back-barrier coastal lagoon located on the southwestern coast of Long Island surrounded by the New York City boroughs of Brooklyn and Queens. Jamaica Bay provides an important habitat for a variety of waterfowl, reptiles, amphibians, and small mammals (Hartig et al., 2002). In 1972, Jamaica Bay became a Gateway National Recreation Area. However, despite this protection an analysis of wetland acreage between 1959 and 1999 indicated that 38-75% of the wetland area has been lost during this time (Hartig et al., 2002). Jamaica Bay and its marshes are impacted by point and non-point sources of pollution, including wastewater treatment plants, combined sewer outfalls, numerous large roadways, landfills, and the densely populated communities of Brooklyn and Queens. During high rainfall events, wastewater treatment plants can become overloaded and bypassed, allowing for storm water and wastewater to enter the bay simultaneously. These combined sewer overflow (CSOs) events may be an

important input of freshwater and nutrients into the bay (Botton et al., 2006; O'Shea and Brosnan, 2000). Previous studies in this region have suggested that modification to the bay's hydrodynamics and nutrient input may be important contributing factors to the decreased health and area of the marsh islands.

3.2 Field Methods

Sediment samples were collected on selected marsh islands in September-2004, May-2005, May-2007, August-2007 and October-2007 (Fig. 5-1). Samples were taken by inserting a ~5 cm core tube into the marsh peat. In the laboratory, the sample was extruded, homogenized and counted by gamma spectrometry. In September-2004, 24 surficial sediment samples were taken on Duck Point, Ruffle Bar, Little Egg, JoCo, and East High marshes (Fig.5-1). In May-2005, 29 marsh samples were taken on the marsh islands of West Elders Point, Yellow Bar, Little Egg, Big Egg, JoCo, and East High (Fig. 5-1). In part, the sampling sites were selected to follow up on previous sampling at three of the sites (Big Egg, East High and JoCo) by Kolker (2005). Sampling in the marshes was determined by accessibility and state of the tide. Thus it was not possible to sample the same sites in both Septermber-2004 and May-2005. However, JoCo and East High marshes were sampled during both these sampling periods. Marsh samples were also taken in May-2007, August-2007 and October-2007; 28 marsh samples were taken on these marsh islands: Elders Point West, Elders Point East and JoCo (Fig. 5-1). For the 2007 samplings the same stations were re-occupied along transects in each marsh. The sampling in Elders Point West spanned the restoration efforts in this marsh, undertaken by the Army Corps of Engineers and the National Park Service.

Subtidal sediments were collected throughout the bay during September-2004 and May-2005 using an Ekman bottom grab (see Chapter 2); 60-70 samples were collected. Each grab sample was examined to insure the sediment surface was preserved and then the top 5 cm of the grab sample were sub-sampled and returned to the lab for radiometric analysis. Further details of the subtidal sampling are presented in Chapter 2.

3.3 Laboratory Methods

The surficial marsh samples and subtidal sediment samples were returned to the lab, homogenized, and weighed. Samples were analyzed for ^{234}Th (63.3 keV) and ^{7}Be (477 keV) by counting the wet samples on a Canberra 3800 mm^2 germanium gamma detector for ~ 24 hours. The counting efficiency of each detector was determined for ^{7}Be by counting well-analyzed sediment standards (IAEA-300 and IAEA-375) and using a linear regression of calculated efficiencies from radioisotopes with gamma emissions between 200 keV and 662 keV in the standard. Initial ^{7}Be counts were then corrected for detector efficiency and decay between collection and counting. Gamma measurements of ^{234}Th require a correction for self-absorption. For this purpose, liquid standards of varying densities were spiked with ^{210}Pb and ^{238}U (^{234}Th in equilibrium) and counted several times on each detector. Densities were "calibrated" via the transmission of a gamma source corrected through both standards and samples. Sediment samples were recounted after 4 months to determine the ^{234}Th supported by the decay of ^{238}U within the samples; this value was used in calculation of excess ^{234}Th ($^{234}Th_{xs}$ = measured total ^{234}Th – supported ^{234}Th) activities.

4. Results

4.1 Radionuclide Activities and Inventories in Salt Marshes

Inventories of $^{234}Th_{xs}$ and ^{7}Be on the marsh islands were calculated from:

$$I_R = A_R \times \rho_i \times 5 \text{ cm} \quad (5\text{-}1)$$

where I_R is the $^{234}Th_{xs}$ or ^{7}Be inventory (dpm cm^{-2}), A_R is the $^{234}Th_{xs}$ activity (dpm g^{-1}) or ^{7}Be activity (dpm g^{-1}), ρ_i is the dry bulk density of the sample (g cm^{-3}), and 5 cm is the depth of each sample.

Mean $^{234}Th_{xs}$ and ^{7}Be inventories on marsh islands sampled in September-2004 and May-2005 are summarized in Table 5-1. In September-2004 the mean $^{234}Th_{xs}$ inventories on the marsh sampled ranged from 3.7 ± 2.2 to 6.9 ± 4.8 dpm cm^{-2} (Table 5-2). In May-2005 the mean $^{234}Th_{xs}$ inventories on the marsh islands sampled ranged from 0 ± 0 to 9.8 ± 4.3 dpm cm^{-2} (Table 5-3). Mean $^{234}Th_{xs}$ inventories in May, August and October-2007 ranged from 0.4 ± 0.3 to 1.0 ± 0.5, 0.5 ± 0.3 to 1.1 ± 0.6 and 0.6 ± 0.3 to 1.5 ± 0.7 dpm cm^{-2}, respectively (Fig. 5-4). The same marshes were not sampled during the September-2004 and May-2005 samplings; however, there still appears to be a general trend such that marshes in the western bay had higher $^{234}Th_{xs}$ inventories than the eastern marshes (Table 5-1).

In September-2004 the mean ^{7}Be inventories on the sampled marsh islands ranged from 1.1 ±0.3 to 3.2 ± 1.0 dpm cm^{-2}(Table 5-2), while in May-2005 the mean ^{7}Be inventories ranged from 0.7 ±0.4 to 2.3 ± 1.5 dpm cm^{-2}. During the September-2004 and

May-2005 marsh samplings, in contrast to the trends in $^{234}Th_{xs}$ inventories, the ^{7}Be inventories were generally higher in the eastern bay than the western (Table 5-1).

In September-2004, Duck Point marsh had the highest mean $^{234}Th_{xs}$ inventory, while JoCo marsh had the lowest mean inventory (Table 5-2, Fig. 5-2). The mean ^{7}Be inventory in the surficial marsh sediments had the reverse of this trend, with the highest activity in JoCo and the lowest at Little Egg marsh (Table 5-2). Sample location sites for May-2005 are shown in Fig. 5-3. $^{234}Th_{xs}$ inventories were highest at Yellow Bar marsh and lowest at East High marsh in the east and Elders Point West marsh in the west, where no $^{234}Th_{xs}$ was measured (Table 5-3). ^{7}Be inventories were highest in the eastern bay at JoCo marsh and lowest in the west on Yellow Bar marsh. In May-2007, Elders Point West had the highest $^{234}Th_{xs}$ inventory and the nearby Elders Point East had the lowest (Table 5-4). Mean ^{7}Be inventories were highest inventories on JoCo marsh and the lowest on Elders Point West (Table 5-4). In August-2007, Elders Point East had the highest $^{234}Th_{xs}$ inventory and JoCo marsh had the lowest inventory. In contrast, in October-2007 the highest mean $^{234}Th_{xs}$ inventory was measured on Elders Point East, but the lowest was measured on Elders Point West (Table 5-4). ^{7}Be inventory was highest on Elders Point East and lowest on Elders Point West in August-2007 (Table 5-4). In October-2007, mean ^{7}Be inventory was similar between the sampled marsh islands (Table 5-4).

5. Discussion

The ability of salt marshes to keep pace with rapidly rising sea level is partially dependent on the rate of sediment supply to the marsh (Redfield, 1965). The rate of

sediment deposition on marshes is affected by sediment availability, frequency with which the marsh surface is inundated by water, length of the inundation, and proximity to the source of material (Friedrichs and Perry, 2001). Kolker (2005) measured ^{210}Pb profiles in East High, Big Egg and JoCo marshes and found recent (~1999 - 2001) accretion rates of 0.25, 0.41 and 0.35 cm y^{-1}, respectively. Marsh surface elevation changes, tracked using sediment elevation tables (SETs) on JoCo and Black Bank marsh islands are 0.4 and 0.5 cm y^{-1}, respectively (2003 – 2009; Cahoon and Lynch, unpublished data). These accumulation rates and changes in marsh elevation suggest that, over the long-term, these three marsh sites are keeping pace with rising sea level (~0.3 cm y^{-1}). The dry bulk densities of these marsh sediments are all ~ 0.2 g cm^{-3}, yielding mass accretion rates of ~0.05 – 0.1 g cm^{-2} y^{-1}. The use of short-lived radionuclides ^{234}Th and ^{7}Be may provide a means to evaluate the exchange of environment between salt marshes and the surrounding subtidal sediments on seasonal scales and at higher resolution that has been possible in previous studies.

5.1 *$^{234}Th_{xs}$ as a Tracer of Sediment Supply to Marsh Islands*

The presence of $^{234}Th_{xs}$ in marsh sediments provides a tracer for the supply of subtidal sediment to the marsh surface. This is because ^{234}Th is produced in the water of the bay by the decay of it parent isotope ^{238}U, and the inventory of ^{234}Th expected in the sediments is thus a function of salinity and water depth. Although some production of ^{234}Th may occur in water overlying a flooded marsh surface, the length of time the marsh is flooded, and more importantly the depth of the water, would be minimal. Salinity in Jamaica Bay has been reported to range from 23 to 28.5 and the ^{238}U measured in the bay

was ~ 2.0 dpm L^{-1} (see Chapter 2, Table 2-4). ^{234}Th production in the water overlying the marshes can be calculated from:

$$\text{Subtidal } ^{234}Th_{xs} \text{ Production} = A_{238} \times H \qquad (5\text{-}2)$$

where A_{238} is the dissolved ^{238}U activity (0.002 dpm cm^{-3}) and H is the depth of the water overlying the salt marshes during inundation in cm. The tidal range of Jamaica Bay is 1.4 m and even if we assume a 24-hour inundation of the marshes by 50 cm of water, the production in the overlying water is only ~ 0.1 dpm cm^{-2}.

$^{234}Th_{xs}$ inventories in the marshes often were substantial, greatly exceeding the ^{234}Th produced during high water (Figs. 5-2 to 5-6). However, there is both temporal and spatial variation in $^{234}Th_{xs}$ inventories within a marsh site (Figs. 5-2 to 5-6). Stations on the marsh edge often displayed higher $^{234}Th_{xs}$ inventories (e.g. East High and Duck Point in September-2004, Fig. 5-2; JoCo in May-2007, August-2007 and October-2007, Figs. 5-4, 5-5, 5-6), while the interior of a marsh often displays low inventories (e.g. Little Egg and Duck Point in September-2004, Fig. 5-2; JoCo, Big Egg and East High in May-2005, Fig. 5-3; JoCo marsh in May-2007, August-2007 and October-2007, Fig. 5-4, 5-5, 5-6). In addition, the mean $^{234}Th_{xs}$ inventory (as well as the ^{7}Be inventory; see below) of all sampling periods at sites that were unvegetated (dead zone or ponding areas, typically in the marsh interior) was significantly lower ($p < 0.01$) than that characterized by dense vegetation (Fig. 5-7A). Mean $^{234}Th_{xs}$ inventory at the marsh edge and at vegetated sites in the marsh interior were significantly higher than the mean inventory at the non-vegetated sites (Fig. 5-7).

This spatial pattern of $^{234}Th_{xs}$ inventories is consistent with patterns of sedimentation observed in marshes by several researchers (UK, French and Spencer, 1993; Louisiana, Wang et al., 1993; Florida, Leonard et al., 1995; North Carolina, Leonard, 1997; Virginia, Christiansen et al., 2000). Typically, high sedimentation rates are observed at the marsh edge and decrease into the interior. This pattern is a result of proximity to the sediment source (the bay) and the interaction between marsh grasses and the flooding water. The marsh grasses slow the flooding water velocity and allows for suspended material in the water column to settle out of the water onto the marsh surface. The distance from the sediment source increases as the water moves over the marsh and the decrease in suspended sediment concentration results in decreased deposition within the marsh interior (French and Spencer, 1993; Wang et al., 1993; Leonard et al., 1995; Leonard, 1997, Christiansen et al., 2000; Friedrichs and Perry, 2001). Exceptions to this pattern include the supply of sediment via channels or ditches within the marsh. They can serve as conduits for bringing sediment to the interior of the marsh. The link between previously observed patterns of sedimentation on marshes and the $^{234}Th_{xs}$ inventories measured in this study suggests a similar delivery mechanism and that $^{234}Th_{xs}$ has the potential to be used as a proxy for short-term sediment transport into the marsh.

In addition to spatial trends in $^{234}Th_{xs}$ on the marsh island of Jamaica Bay, there are also temporal differences, with greater $^{234}Th_{xs}$ inventories observed, on average, during the September-2004 sampling (Table 5-1). These sampling show that marshes in the western bay have higher mean inventories than marshes in the eastern bay (Table 5-1). Indeed, $^{234}Th_{xs}$ inventories in 2004 and 2005 subtidal sediments show similar general trends, with higher inventories in the western part of the bay near the marsh islands and

in the deep channel in the northern part of the bay (see Chapter 2; Fig. 2-4). These subtidal $^{234}Th_{xs}$ inventories also are in surplus to the in situ production of ^{234}Th in the water column (~ 1.0 dpm cm^{-2}), and in Chapter 2, it was argued that these surplus inventories are produced by the import of $^{234}Th_{xs}$ associated with sediment brought into the bay through Rockaway Inlet. Thus, while some of the material may have be the result of direct deposition of material transported into the bay from the ocean via Rockaway Inlet, much of the elevated $^{234}Th_{xs}$ observed on the western marsh islands is likely the result of transport of resuspended subtidal sediment onto the marsh surface Fig. 5-8).

The $^{234}Th_{xs}$ and ^{7}Be activities in the subtidal sediments near the sampled marsh islands are summarized in Tables 5-5 and 5-6. These activities reflect a bulk sample of the upper 5 cm of subtidal sediments. In August-2008, subtidal samples were taken to compare the $^{234}Th_{xs}$ and ^{7}Be activity in the surficial 0 - 2 mm of the sediments to that in the 0 – 5 cm and found that the activity in the upper 2 mm was 67 – 100 and 25 – 88% of the total activity (0 – 5 cm), respectively (see Chapter 2; Table 2-1). This highly activity surficial layer of sediment is likely to be easily resuspended and transported throughout the subtidal bay (see Chapter 2), but it is also likely to characterize the subtidal sediment that is mobilized and deposited on the marsh surface. Additional subtidal samples were taken in August-2008 in sand dominated sediments to compare the specific activity of $^{234}Th_{xs}$ and ^{7}Be on the sand fraction to the mud fraction (see Chapter 2; Table 2-1). Activity of $^{234}Th_{xs}$ on the sand fraction was low, ranging from 0.2 to 0.9 dpm g^{-1} and the mud fraction was higher, ranging from 6.7 to 22.5 dpm g^{-1}. This is unsurprising, as both ^{234}Th and ^{7}Be have an affinity for fine particles.

The higher specific activities in the upper 2 mm sediments and in the fine sediments suggests that the activity of $^{234}Th_{xs}$ (and ^{7}Be) measured in the 0 – 5 cm of subtidal sediments underestimates the activity of the material that would be resuspended, transported and deposited on the marsh. To compensate for the "dilution" of the specific activity in the subtidal samples with sand-sized particles each sample can be concentrated in the upper 5 mm and normalized to the mud fraction. The mud fraction was measured for each subtidal sample taken (see Chapter 3). The $^{234}Th_{xs}$ activity was concentrated in the upper 5 mm and then normalized to the mud fraction from:

$$A_{Th}^{MF} = (I^{R} \div 0.5\ cm) \div (\rho \times M_{F}) \qquad (5\text{-}3)$$

where I^{r} is the total activity of the bulk sample (0 – 5 cm), ρ is the bulk density of the sample and M_F is the fraction of mud for each sample. The mud fraction normalized specific $^{234}Th_{xs}$ and ^{7}Be activity of the subtidal sediments, near the marshes sampled in September-2004 and May-2005 are shown in Table 5-5.

In general, sediments with low mud content dominated the subtidal bay near the marsh islands in the western bay and high mud content sediments were found near the eastern marshes. Thus, the normalization of specific $^{234}Th_{xs}$ activity to mud content resulted in greater specific activity of $^{234}Th_{xs}$ (in dpm g^{-1}) in the western bay, while the normalization resulted in little change in the eastern bay. Interestingly, the mean $^{234}Th_{xs}$ inventories are greater in the western marshes in both September-2004 and May-2005, consistent with the higher ^{234}Th inventories in the fine-grained fraction of the subtidal sediments in the western bay. If we assume that the subtidal sediments near the marsh

islands is the source of $^{234}Th_{xs}$ to these marshes, then the short-term mass accretion rates of mud (R_{Th}) in marsh sites can be estimated using the equation:

$$R_{Th} = (I_{Th}/A_{Th}^{MF}) \times \lambda_{Th} \quad (5\text{-}4)$$

where I_{Th} is the $^{234}Th_{xs}$ inventory measured on the marsh islands, A_{Th}^{MF} is the mud fraction normalized activity of $^{234}Th_{xs}$ in the upper 5 mm of subtidal sediments near the marsh islands (Table 5-5)and λ_{Th} is the decay constant of ^{234}Th (10.5 y^{-1}). The resulting deposition rate at each sample site is then given in g cm^{-2} y^{-1}. Mass accretion rates on the marsh islands range from ~ 0 to 2.5 g cm^{-2} y^{-1} (mean ~ 0.6 ± 0.2 g cm^{-2} y^{-1}; Figs 5-14, 5-15). These mass accretion rates, extrapolated to a year are higher than previous estimates of ~0.05 – 0.1 g cm^{-2} y^{-1} made by Kolker (2005) from ^{210}Pb profiles in cores. This suggests that accretion estimates based on ^{234}Th inventories are not representative of long-term conditions or do not apply to large areas of the marsh surface. Indeed, the marsh samples, particularly those sampled in September-2004 and May-2005, were biased toward the marsh edge where sedimentation is likely higher, whereas the deposition rates derived from ^{210}Pb cores and SETs reflect deposition in the interior, high marsh.

5.2 Times-Series Sampling of ^{234}Th – JoCo and Elders Point

In 2006-2007 a major restoration project took place on Elders Point East. The project placed 2.5 × 10^5 m^3 of dredged material on the marsh, creating ~ 0.1 km^2 of marsh. In addition, native vegetation was planted throughout the restored marsh (P. Rafferty, National Park Service pers. comm.). Prior to the restoration project, what little

marsh vegetation that remained on Elders Point East was confined to hummocks of vegetation surrounded by mussels. Elders Point West at the time of sampling was characterized as a tidal flat with sparse vegetation, much of which was elevated and surrounded by mussels. The marsh sampling in this study took place in 2007 after this restoration project was complete. The marsh islands sampled in 2007 include the restored Elders Point East and the nearby unrestored Elders Point West (Fig. 5-1).

In May-2007, early in the marsh vegetation growing season, mean $^{234}Th_{xs}$ inventory on the restored marsh (Elders Point East) was low (0.4 ± 0.3 dpm cm^{-2}), but in August and October, later in the growing season mean $^{234}Th_{xs}$ inventories were higher (1.1 ± 0.6 and 1.5 ± 0.7 dpm cm^{-2}, respectively; Table 5-4). As was discussed in section 5.1 $^{234}Th_{xs}$ production in the overlying water column when the marsh surface is flooded is negligible and significant $^{234}Th_{xs}$ inventories on the marsh are likely the result of resuspension and transport of material from the surrounding subtidal bay to the marsh island. Thus, the increase in $^{234}Th_{xs}$ inventory as the growing season progresses may indicate enhanced trapping of sediment (and associated $^{234}Th_{xs}$) as the vegetation increased in density. However, it should also be noted that during the 2007 samplings fencing was in place on Elders Point East as part of the construction and monitoring project and that may also have enhanced sediment trapping. These results indicate that despite the increase in elevation due to the dredge fill placement, sediment was still delivered to the marsh surface.

On the nearby unrestored marsh Elders Point West, mean $^{234}Th_{xs}$ inventories varied little between May, August and October (Table 5-4). Unlike post-restoration Elders Point East, Elders Point West has little vegetation remaining and, instead, is in

general, a tidal flat with patches of vegetation elevated and surrounded by mussel beds. Thus, the mean $^{234}Th_{xs}$ inventory on Elders Point West is not as heavily influenced by the marsh vegetation growing season than might be expected on the restored Elders Point East. Future plans for restoration of Elders Point West are in place that will likely alter this pattern.

JoCo marsh in the eastern bay is generally considered the healthiest marsh in Jamaica Bay and was used as the control marsh in the Elders Point restoration project. Mean $^{234}Th_{xs}$ inventories on JoCo were generally lower than on Elders Point West and East which reflects the $^{234}Th_{xs}$ inventories measured in the subtidal sediments near these marsh islands in September-2004, May-2005, November-2005 and July-2006 (see Chapter 2, Fig. 2-2). $^{234}Th_{xs}$ inventories of sites sampled in May, August and October-2007 on JoCo were consistently high at the edge (sites 9 and 10) and generally low in the marsh interior (Fig. 5-6). However, $^{234}Th_{xs}$ was also present at a few sites in the marsh interior, suggesting that tidal creeks may also serve as conduits for sediment and $^{234}Th_{xs}$ to this marsh island.

JoCo marsh was also sampled in September-2004 and May-2005. $^{234}Th_{xs}$ inventories were higher in September-2004 and May-2005 (3.7 ± 2.2 and 3.2 ± 2.9 dpm cm^{-2}, respectively) than those measured in May-2007, August-2007 and October-2007 (0.7 ± 0.4, 0.5 ± 0.3 and 0.6 ± 0.3 dpm cm^{-2}, respectively). The higher inventories in September-2004 and May-2005 may be, in part, due to sampling bias to the marsh edge during these sampling cruises. In addition, sites sampled in September-2004 and May-2005 were on the western side of JoCo marsh while the 2007 sites were on the eastern side of the marsh (Fig. 5-16). On the western side of JoCo marsh the subtidal bay is

shallow (< 0.5 m), but the subtidal bay on the eastern side of JoCo is much deeper (~ 9 m). $^{234}Th_{xs}$ inventories in the subtidal bay near JoCo marsh was typically slightly higher on the eastern side of the marsh than the western side (see Chapter 2; Fig. 2-3). However, the sediment and ^{234}Th in the subtidal on the western side of JoCo may be more easily mobilized and transported on to the marsh under normal conditions in contrast to the eastern side of the marsh.

5.3 ^{7}Be Source to Marshes

^{7}Be serves as an independent tracer of short-term processes in salt marshes. The radionuclide is produced in the lower stratosphere and upper troposphere through a cosmic ray spallation reaction involving oxygen and nitrogen. Production of ^{7}Be in the atmosphere varies with latitude and sunspot activity. Cosmogenic ^{7}Be becomes associated with aerosols and can be removed from the atmosphere to the Earth's surface through wet and dry precipitation. Wet precipitation has been found to be significantly correlated with atmospheric ^{7}Be flux in New Haven, CT by Turekian et al., (1983) and in Boston, MA by Zhu and Olsen (2009). The atmospheric flux of ^{7}Be was measured in Stony Brook, NY from April-2008 to December-2009 was also found to be significantly correlated with rainfall (R = 0.81, see Chapter 4 for details). Using the relationship between atmospheric ^{7}Be flux and rainfall, the ^{7}Be inventories produced by the direct atmospheric input of ^{7}Be into Jamaica Bay prior to September-2004, May-2005, May-2007, August-2007 and October-2007 sampling cruises were estimated to be 3.1, 2.0, 1.6, 2.4 and 1.3 dpm cm^{-2}, respectively. ^{7}Be inventories on the individual marsh islands were

spatially variable (Fig. 5-9) and ^{7}Be inventories in relation to the direct atmospheric input varied between marsh islands (Tables 5-1 to 5-4).

In addition to direct atmospheric deposition, ^{7}Be also can be supplied to the marsh via resuspension and transport of subtidal sediments (Fig. 5-8). The mean ^{7}Be inventories at the marsh edge sites were in surplus to the direct atmospheric input (by 40%), vegetated areas in the marsh interior showed lower surplus inventories (~ 10% greater than the direct atmospheric input; Fig. 5-7). This pattern is consistent with the $^{234}Th_{xs}$ inventories measured on the marsh islands (see section 5.1)

Although the ^{7}Be is supplied uniformly to the marsh surface from the atmosphere, it may not be retained uniformly. Variation in inventory with a marsh may be due to variation in retention possibly caused by vegetative coverage. In general, the ^{7}Be inventory to each site within a marsh is nearly in balance with the atmospheric flux.

Work conducted by Hartig et al. (2002) analyzed aerial photographs and found that since 1974 the mean vegetation loss in the low marsh was ~ 38%. Loss of vegetation from the marsh islands of Jamaica Bay can be caused by erosion of the marsh along the margins and tidal channels, expansion of non-vegetated tidal pools and increased fragmentation of marsh vegetation (Hartig et al., 2002). Indeed, the mean ^{7}Be inventory at marsh sites where no vegetation was present had markedly lower than sites where vegetation was present (Fig. 5-7). This suggests that ^{7}Be (and associated particles) is either not being retained in non-vegetated regions of the marsh or is being lost to tidal creeks and the surrounding bay or is transported to vegetated areas by wind and water during the flooding tide. At sites where vegetation was present (but not at the marsh edge), the ^{7}Be inventory was ~ 10% greater than the direct atmospheric input. Marsh

vegetation may enhance removal of ^{7}Be from the atmosphere or trapping of sediment (and the associated ^{7}Be; Olsen et al., 1986; Leonard et al., 1995; Friedrichs and Perry, 2001; Neubauer et al., 2002).

Previous studies in marshes have also observed enhanced ^{7}Be inventories in vegetated areas in comparison with non-vegetated areas (Olsen et al., 1986; Neubauer et al., 2002). However, other studies have also found that plants may intercept the direct atmospheric fallout and reduce its delivery to the underlying sediments (Ruseell et al., 1981; Wallbrink and Murray, 1996). Frequent flooding of the marsh surface over a tidal cycle may be mechanism of transferring the ^{7}Be from the plant to the underlying sediment, but the ^{7}Be inventories measured in the marsh vegetation in the present study should be considered minimum ^{7}Be inventories. This suggests that the atmospheric flux of ^{7}Be to the sediment surface of the marshes may be reduced during the early to mid summer when the plant biomass and coverage is greatest (Neubauer et al., 2002). The ratio between ^{7}Be inventory and atmospheric flux in 2007 was highest on JoCo marsh in May-2007 (during the plant growing season) and lowest in August (when biomass was likely the greatest; Table 5-4).

6. Conclusions

The marshes of Jamaica Bay have experienced extensive loss of vegetative area and a decline in marsh health over the last 25 years. Previous work has suggested that increased nutrient input to the marshes may induce sulfide toxicity and ultimately lead to plant die-offs and marsh loss. However, accretion of salt marshes may also be an important indicator of marsh health and the ability to sustain its elevation with rising sea-

level. ^{234}Th is an effective tracer of short term deposition of subtidal sediments on the marsh and retention or the loss of this material. $^{234}Th_{xs}$ inventories were generally higher in the western marshes than the eastern marshes during sampling in September-2004and May-2005. Estimates of deposition derived from inventories of $^{234}Th_{xs}$ on the marsh islands ranged from ~0 – 2.5 g cm^{-2} y^{-1}, which are higher than previous estimates on Jamaica Bay marsh islands from ^{210}Pb-derived measurements of ~0.05 – 0.1 g cm^{-2} y^{-1}. The difference between these two measurement methods may reflect temporary storage affect on marsh islands on seasonal time scales, as well as sampling bias during the September-2004 and May-2005 at the edge of the marshes. Indeed, $^{234}Th_{xs}$ inventories for all samplings are significantly higher at the marsh edge than in the marsh interior suggesting transport and deposition of material from the subtidal bay. These results suggest that the $^{234}Th_{xs}$ inventory is a useful as a tracer for short-term deposition on salt marsh islands. ^{7}Be inventories on the marsh islands are dominated by the atmospheric supply of this cosmogenic radionuclide to the marsh surface. However, ^{7}Be inventories also were higher at the marsh edges suggesting some transport from the subtidal bay to the marsh surface. In addition, both $^{234}Th_{xs}$ and ^{7}Be inventories were higher in vegetated areas of the interior marshes than in unvegetated areas. This suggests either erosion in areas where vegetation no longer exists or preferential trapping in vegetated areas of the marsh.

7. References

Baskaran, M. and P.W. Swarzenski (2006) Seasonal variations on the residence times and partitioning of short-lived radionuclides (^{234}Th, ^{7}Be and ^{210}Pb) and depositional fluxes of ^{7}Be and ^{210}Pb in Tampa Bay, Florida. *Marine Chemistry*, 104: 27-42.

Benotti, M.J., M. Abbene, and S.A. Terracciano (2007) Nitrogen Loading in Jamaica Bay, Long Island, New York: Predevelopment to 2005.

Botton, M. L., R. E. Loveland, J. T. Tanacredi and T. Itow (2006) Horseshoe Crabs (*Limulus polyphemus*) in an urban estuary (Jamaica Bay, New York) and the potential for ecological restoration. *Estuaries and Coasts* 29: 820-830.

Bokuniewicz, H., and J. Ellsworth (1986) Sediment budget for the Hudson system, *Journal of Northeastern Geology* 8: 158-164.

Christiansen, T., P.L. Wiberg and T.G. Milligan (2000) Flow and sediment transport on a tidal salt marsh surface. *Estuarine, Coastal and Shelf Science* 50: 315-331.

Feng, H., J. K. Cochran and D. J. Hirschberg (1999) ^{234}Th and ^{7}Be as tracers for the sources of particles to the turbidity maximum of the Hudson River Estuary. *Estuarine, Coastal, and Shelf Science* 49: 629-645.

French, J.R. and T. Spencer (1993) Dynamics of sedimentation in a tide-dominated back barrier salt marsh, Norfolk, UK. *Marine Geology* 110: 315-331.

Friedrichs, C. T., and J. E. Perry (2001) Tidal marsh morphodynamics, *Journal of Coastal Research* SP 27: 7-37.

Giffin, D. and D. R. Corbett (2003) Evaluation of sediment dynamics in coastal systems via short-lived radioisotopes. *Journal of Marine Systems* 42: 83-96.

Hartig, E. K., V. Gornitz, A. Kolker, F. Mushacke and D. Fallon (2002) Anthropogenic and climate-change impacts on salt marshes of Jamaica Bay, New York City. Wetlands 22: 71-89.

Ioannidou, A. and C. Papastefanou (2006) Precipitation scavenging of ^{7}Be and ^{137}Cs radionuclides in air. Journal of Environmental Radioactivity. 85, 121-136.

Kaste, J.M., S.A. Norton, C.T. Hess (2002) Environmental chemistry of beryllium-7. P.H. Ribbe and J.J. Rosso (eds). Beryllium: Mineralogy, petrology, and geochemistry, Reviews in Mineralogy and Geochemistry, vol. 50, pp. 291-312.

Kolker, A. (2005) The impacts of climate variability and anthropogenic activities on salt marsh accretion and loss on Long Island. PhD Thesis, Stony Brook University, Stony Brook, NY, 261 pp.

Leonard, L.A. (1997) Controls of sediment transport and deposition in an incised mainland marsh basin, southeastern North Carolina. *Wetlands* 17: 263-274.

Leonard, L.A., A.C. Hine and M.E. Luther (1995) Surficial sediment transport and deposition processes in a *Juncus roemerianus* marsh, west-central Florida. *Journal of Coastal Research* 11: 322-336.

Mitsch, W.J. and G. Gosselink (2000) *Wetlands.* John Wiley & Sons, Inc.: New York, 920pp.

Neubauer, S.C, I.C. Anderson, J.A. Constantine and S.A.Kuehl (2002) Sediment deposition and accretion in a mid-Atlantic (U.S.A) tidal freshwater marsh. *Estuarine, Coastal and Shelf Science* 54: 713-727.

Olsen, C.R., I.L. Larsen, P.D. Lowry, and N.H. Cutshall (1986) Geochemistry and deposition of ^{7}Be in river-estuarine and coastal waters. *Journal of Geophysical Research* 91: 896-908.

O'Shea, M. L. and T. M. Brosnan (2000) Trends in indicators of eutrophication in western Long Island Sound and the Hudson-Raritan Estuary. *Estuaries* 23: 877-901.

Redfield, A. C. (1972) Development of a New England salt marsh. *Ecological Monographs* 42:201–237.

Russell, I.J., C.E. Choquette, S.L. Fang, W.P. Dundulis, A.A. Pao and A.A. Pszenny (1981) Forest vegetation as a sink for atmospheric particulates: Quantitative studies in rain and dry deposition. *Journal of Geophysical Research* 86: 5247-5363.

Swanson, L.R. and R. E. Wilson (2008) Increased tidal ranges coinciding with Jamaica Bay development contribute to marsh flooding. *Jounral of Coastal Research* 24: 1565-1569.

Teal, J. and M. Teal. (1969) Life and Death of the Salt Marsh. Ballantine Books, New York, NY, USA.

Turekian, K.K., L.K. Benninger, and E.P. Dion (1983) ^{7}Be and ^{210}Pb total depositional fluxes at New Haven, Connecticut, and Bermuda. *Journal of Geophysical Research* 88: 5411-5415.

An update on the disappearing salt marshes of Jamaica Bay, NY (2007) http://nbii-nin.ciesin.columbia.edu/jamaicabay/jbwppac/JBAC_NPS_SaltMarshReport_080207.pdf.

Vogler, S., M. Jung, and a. Mangini (1996) Scavenging of ^{234}Th and ^{7}Be in Lake Constance. *Limnol. Oceanogr*. 41: 1384-1393.

Walbrink, P.J. and A.S. Murray (1996) Distribution and variability of 7Be in soils under different surface cover conditions and its potential for describing soil redistribution processes. *Water Resources Research* 32: 467- 476.

Wang, F.C., T. Lu and W.B. Sikora (1993) Intertidal marsh suspended sediment transport processes, Terrebonne Bay, Louisiana, U.S.A. *Journal of Coastal Research* 9: 209-220.

Zhu, J. and C.R. Olsen (2009) Beryllium-7 atmospheric deposition and sediment inventories in the Neponset River estuary, Massachusetts, USA. *Journal of Environmental Radioactivity* 100: 192-197.

Table 5-1. Mean $^{234}Th_{xs,}$ ^{7}Be inventories in Jamaica Bay marshes during September-2004 and May-2005 samplings.

Sample Period		Mean $^{234}Th_{xs}$ Inventory (dpm cm^{-2})	Mean ^{7}Be Inventory (dpm cm^{-2})	^{7}Be inventory /Input*
September-2004	Total	5.4 ± 0.9	2.1 ± 0.3	0.7
	West Marshes	6.0 ± 1.3	1.8 ± 0.3	0.6
	East Marshes	4.1 ± 1.2	2.7 ± 0.7	0.9
May-2005	Total	2.7 ± 1.0	1.7 ± 0.5	0.9
	West Marshes	3.4 ± 1.3	1.4 ± 0.4	0.7
	East Marshes	1.8 ± 1.7	2.1 ± 1.1	1.1

* Relative to direct atmospheric input of ^{7}Be estimated from the relationship between rainfall and atmospheric ^{7}Be flux measured at Stony Brook University (September-2004 ~ 3.1 dpm cm^{-2} and May-2005 ~ 2.0 dpm cm^{-2} (see Chapter 4 for details).

Table 5-2. Mean $^{234}Th_{xs}$ inventory and ^{7}Be inventory in the surficial sediments on Jamaica Bay marsh islands in September-2004.

Marsh Island	Mean $^{234}Th_{xs}$ Inventory (dpm cm^{-2})	Mean ^{7}Be Inventory (dpm cm^{-2})	^{7}Be inventory /Input*
Duck Point (n = 3)	6.9 ± 4.8	2.4 ± 1.5	0.8
Ruffle Bar (n = 5)	6.1 ± 1.3	2.6 ± 0.5	0.8
Little Egg (n = 8)	5.6 ± 1.9	1.1 ± 0.3	0.4
East High (n = 4)	4.6 ± 2.3	2.2 ± 1.1	0.7
JoCo (n = 4)	3.7 ± 2.2	3.2 ± 1.0	1.0

*Relative to direct atmospheric input of ^{7}Be estimated from the relationship between rainfall and atmospheric ^{7}Be flux measured at Stony Brook University (3.1 dpm cm^{-2}; see Chapter 4 for details).

Table 5-3. Mean $^{234}Th_{xs}$ inventory and ^{7}Be inventory in the surficial sediments on Jamaica Bay marsh islands in May-2005.

Marsh Island	Mean $^{234}Th_{xs}$ Inventory (dpm cm^{-2})	Mean ^{7}Be Inventory (dpm cm^{-2})	^{7}Be inventory /Input*
Elders Point West (n = 4)	0 ± 0	1.8 ± 1.1	0.9
Big Egg (n = 5)	2.6 ± 1.1	1.9 ± 1.0	1.0
Yellow Bar (n = 3)	9.8 ± 4.3	0.7 ± 0.4	0.4
Little Egg (n = 3)	2.1 ± 2.1	0.8 ± 0.2	0.4
East High (n = 3)	0 ± 0	1.3 ± 0.7	0.7
JoCo (n = 7)	3.2 ± 2.9	2.3 ± 1.5	1.2

* Relative to direct atmospheric input of ^{7}Be estimated from the relationship between rainfall and atmospheric ^{7}Be flux measured at Stony Brook University (2.0 dpm cm^{-2}; see Chapter 4 for details).

Table 5-4. Mean $^{234}Th_{xs}$ inventory and ^{7}Be inventory in the surficial sediments on Jamaica Bay marsh islands in May-2007, August-2007 and October-2007.

Marsh Island	Mean $^{234}Th_{xs}$ Inventory (dpm cm^{-2})	Mean ^{7}Be Inventory (dpm cm^{-2})	^{7}Be inventory /Input*
May-2007			
Elders Point West (n = 8)	1.0 ± 0.5	1.4 ± 0.3	0.9
Elders Point East (n = 10)	0.4 ± 0.3	1.4 ± 0.6	0.9
JoCo (n = 10)	0.7 ± 0.4	2.1 ± 0.3	1.3
August-2007			
Elders Point West (n = 8)	1.0 ± 0.4	1.9 ± 0.3	0.8
Elders Point East (n = 10)	1.1 ± 0.6	2.5 ± 0.4	1.0
JoCo (n = 10)	0.5 ± 0.3	1.9 ± 0.4	0.8
October-2007			
Elders Point West (n = 8)	0.8 ± 0.4	1.2 ± 0.1	0.9
Elders Point East (n = 10)	1.5 ± 0.7	1.3 ± 0.2	1.0
JoCo (n = 10)	0.6 ± 0.3	1.3 ± 0.2	1.0

Table 5-5 Summary of mean $^{234}Th_{xs}$ in the subtidal sediments near the marsh islands sampled in September-2004 and May-2005.

	Mean $^{234}Th_{xs}$ Activity (dpm g^{-1}) 0 – 5 mm	Mean Mud Fraction (%)	Mean $^{234}Th_{xs}$ Activity (dpm g^{-1}) normalized to mud fraction
September-2004			
Duck Point (n = 3)	33.6 ± 14.7	5	385.8 ± 186.2
Ruffle Bar (n = 3)	17.7 ± 8.9	4	170.7 ± 87.1
Little Egg (n = 2)	19.4 ± 6.3	3	147.8 ± 25.1
East High (n = 5)	1.1 ± 0.2	76	19.7 ± 7.7
JoCo (n = 3)	2.1 ± 0.6	76	22.3 ± 13.7
May-2005			
Big Egg (n = 4)	15.2 ± 5.2	43	159.2 ± 53.0
Elders Point West (n = 4)	18.8 ± 11.5	35	172.7 ± 98.5
Yellow Bar (n = 3)	14.7 ± 3.7	21	180.6 ± 104.3
Little Egg (n = 3)	2.8 ± 1.4	30	106.2 ± 85.1
East High (n = 3)	1.2 ± 0.7	53	14.4 ± 10.2
JoCo (n = 2)	1.1 ± 0.3	58	60.1 ± 1.2

*

Table 5-6 Deposition rates derived from $^{234}Th_{xs}$ inventories on Jamaica Bay marsh islands.

Marsh Island	$^{234}Th_{xs}$ Derived Deposition ($g\ cm^{-2}\ y^{-1}$)
September-2004	
Duck Point (n = 3)	0.2 ± 0.1
Ruffle Bar (n = 3)	0.4 ± 0.08
Little Egg (n = 2)	0.4 ± 0.1
East High (n = 5)	2.5 ± 1.2
JoCo (n = 5)	1.7 ± 1.0
May-2005	
Big Egg (n = 3)	0.2 ± 0.07
Elders Point West (n = 3)	0 ± 0
Yellow Bar (n = 5)	0.6 ± 0.3
Little Egg (n = 2)	0.2 ± 0.2
East High (n = 5)	0 ± 0
JoCo (n = 3)	0.6 ± 0.5

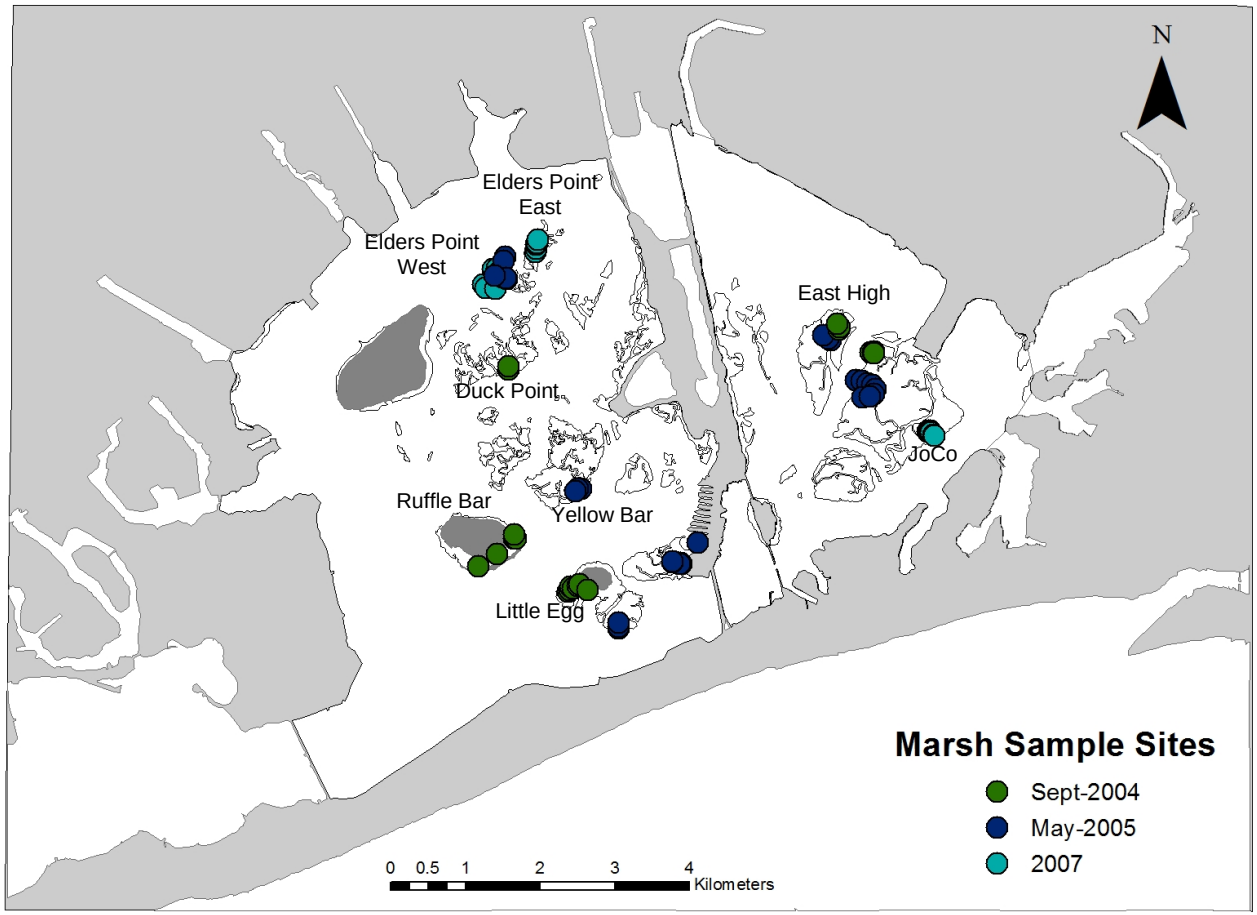

Figure 5-1. Marsh sampling sites in September-2004 and May-2005.

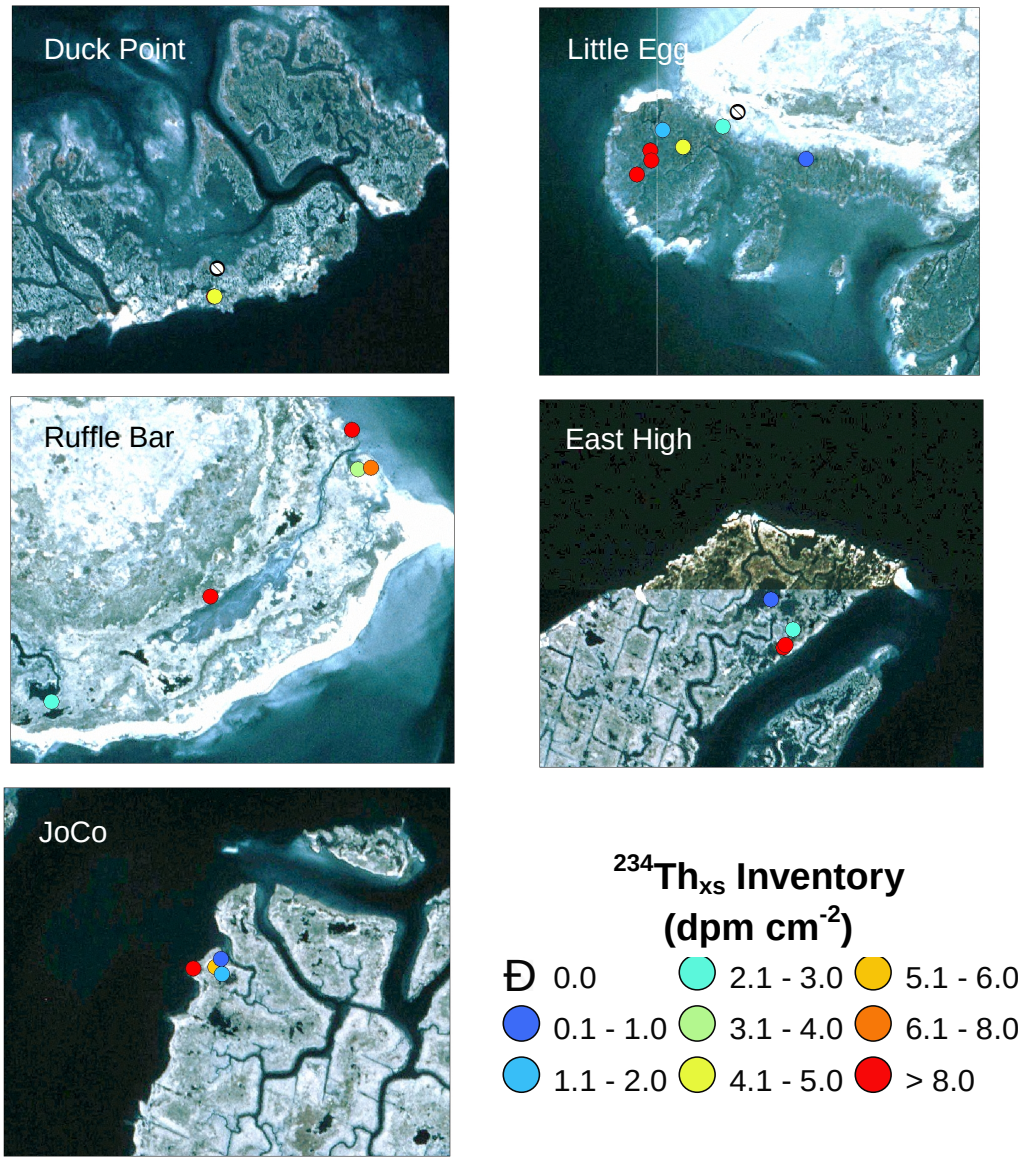

Figure 5-2. $^{234}Th_{xs}$ inventories (dpm cm^{-2}) in the surface sediments of select Jamaica Bay marsh islands sampled in September-2004.

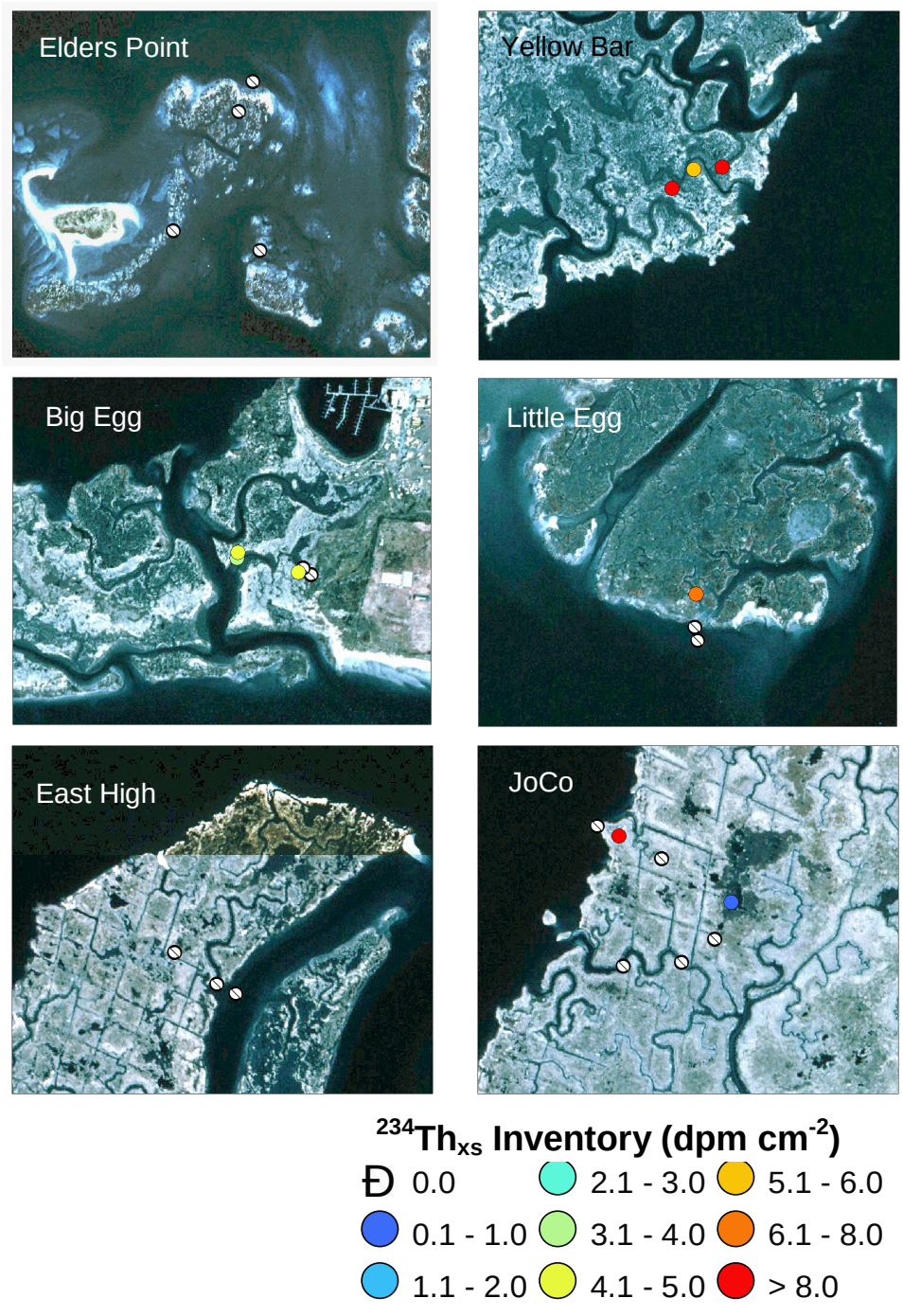

Figure 5-3. $^{234}Th_{xs}$ inventories (dpm cm^{-2}) in the surface sediments of select Jamaica Bay marsh islands sampled in May-2005.

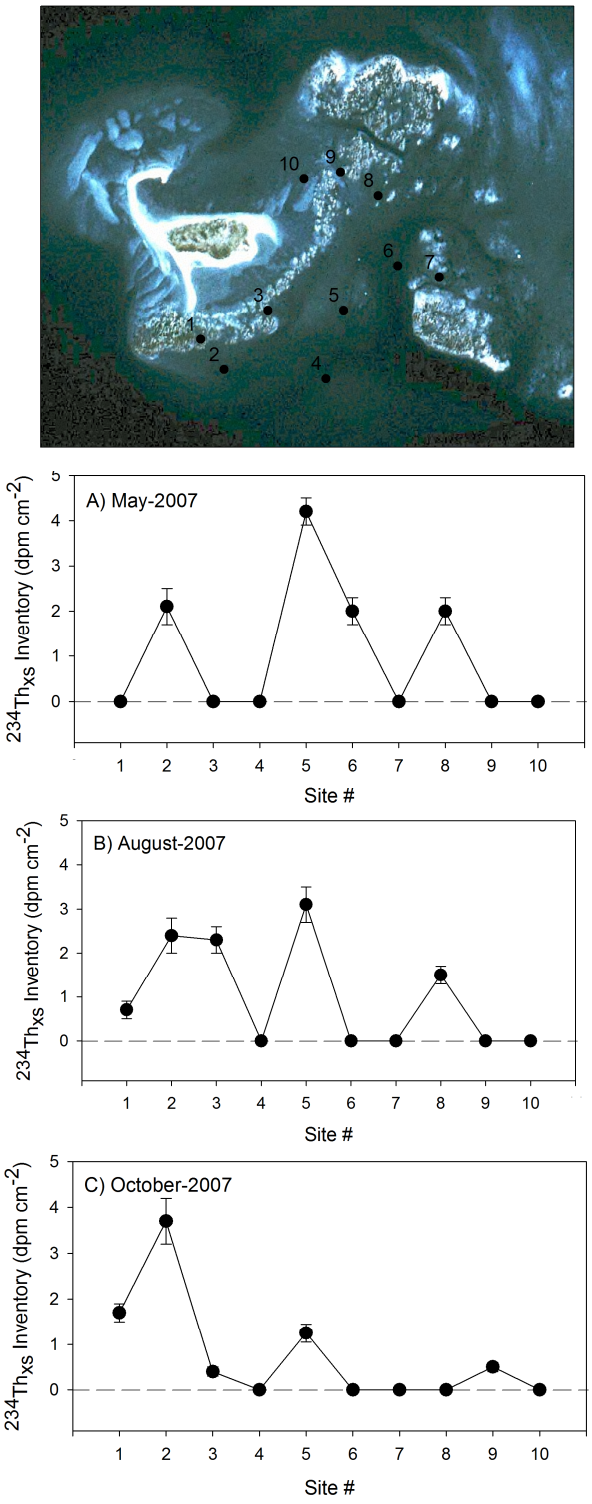

Figure 5-4. $^{234}Th_{xs}$ inventories (dpm cm^{-2}) in the surface sediments of Elders Point West sampled in A) May-2007, B) August-2007 and C) October-2007.

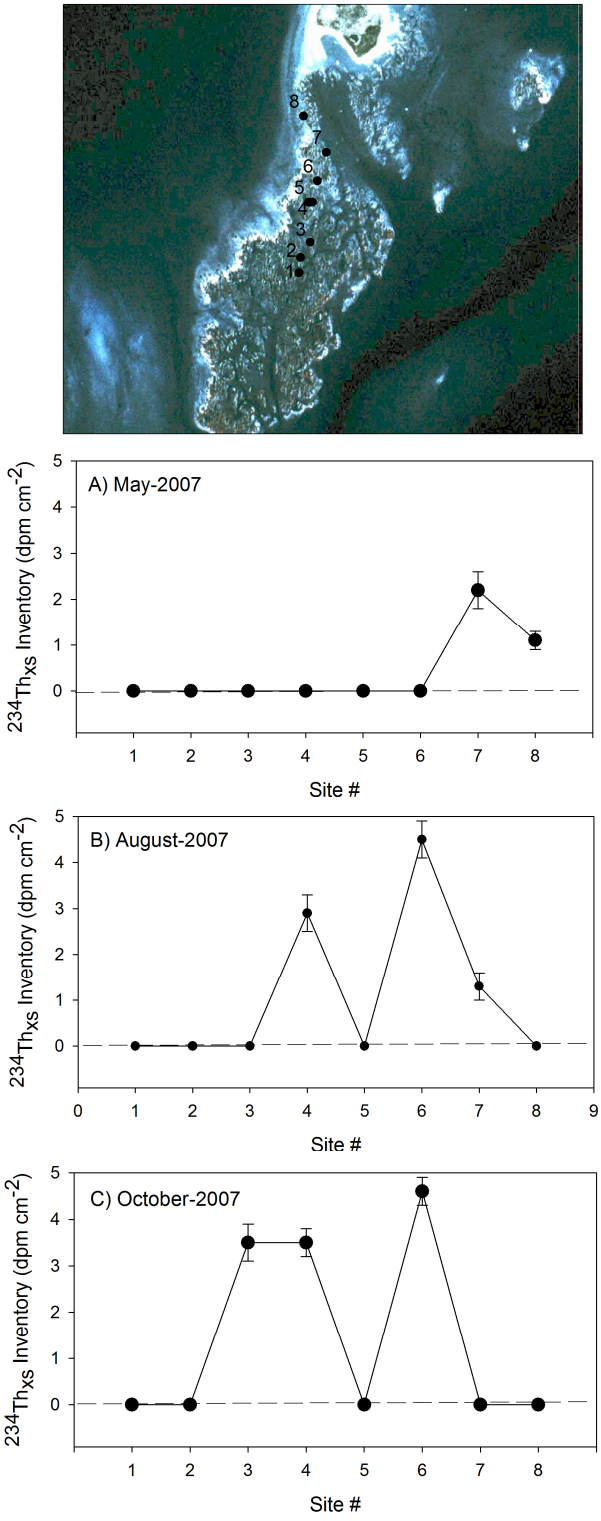

Figure 5-5. $^{234}Th_{xs}$ inventories (dpm cm^{-2}) in the surface sediments of Elders Point East sampled in A) May-2007, B) August-2007 and C) October-2007.

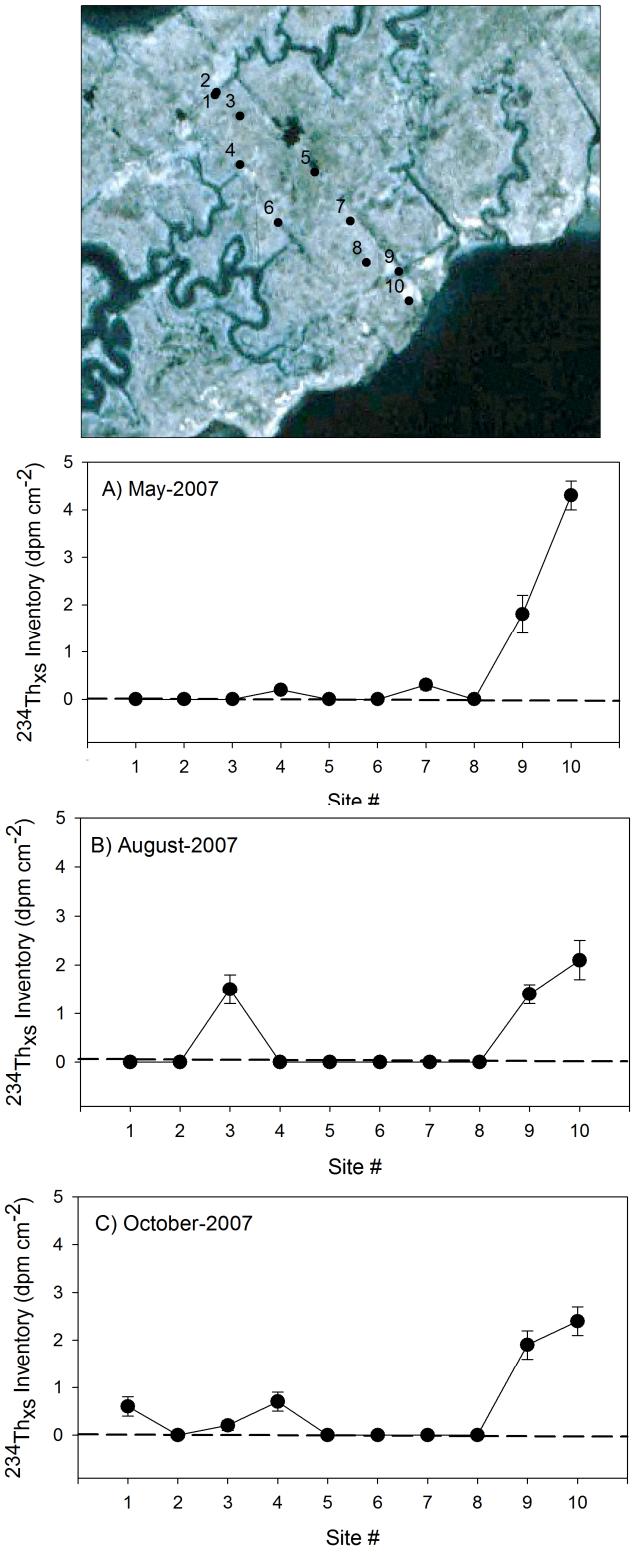

Figure 5-6. $^{234}Th_{xs}$ inventories (dpm cm^{-2}) in the surface sediments of JoCo sampled in A) May-2007, B) August-2007 and C) October-2007.

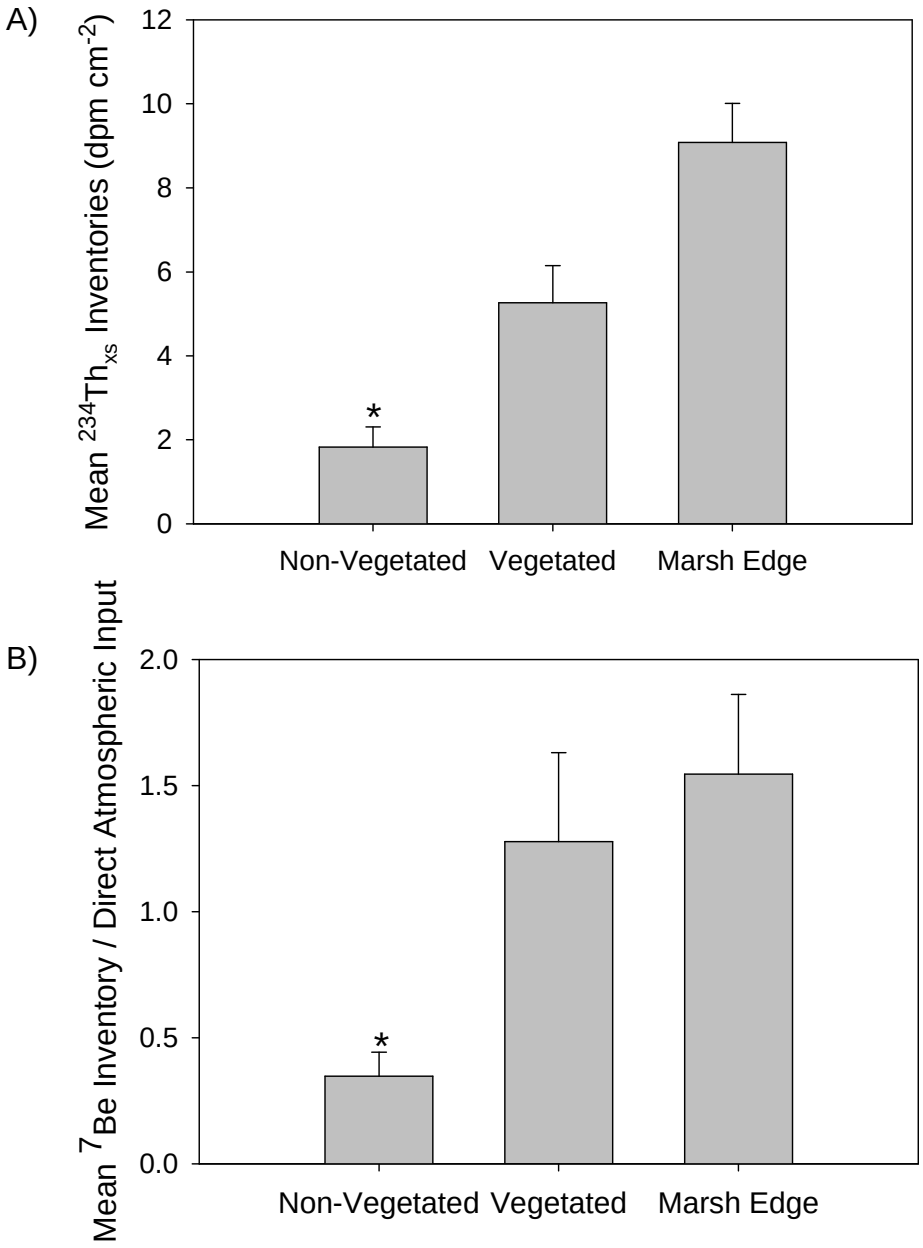

Figure 5-7 Mean inventories of A) $^{234}Th_{xs}$ and B) ^{7}Be on the marsh sites sampled that were characterized as non-vegetated, vegetated (not at the marsh edge) and the marsh edge. * denotes the non-vegetated sites are significantly lower ($p < 0.05$) than the vegetated and marsh edge sites.

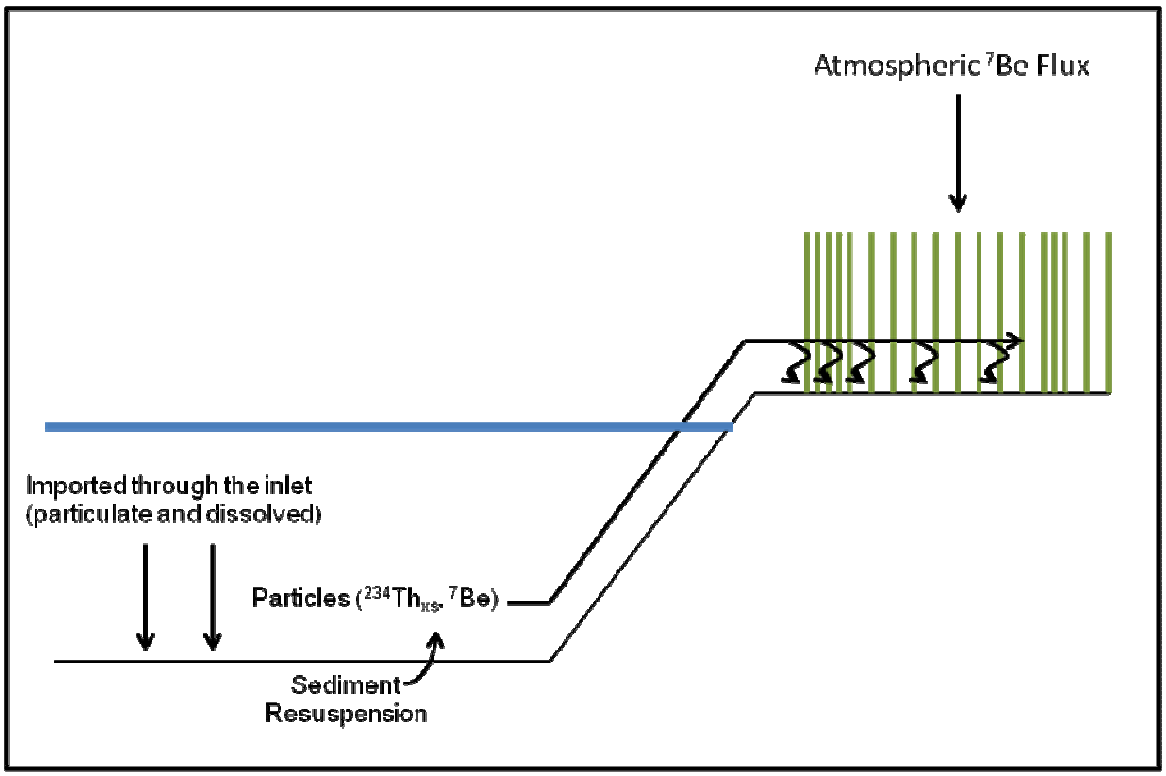

Figure 5-8 Schematic of the pathways of delivery of $^{234}Th_{xs}$ and ^{7}Be to the salt marshes

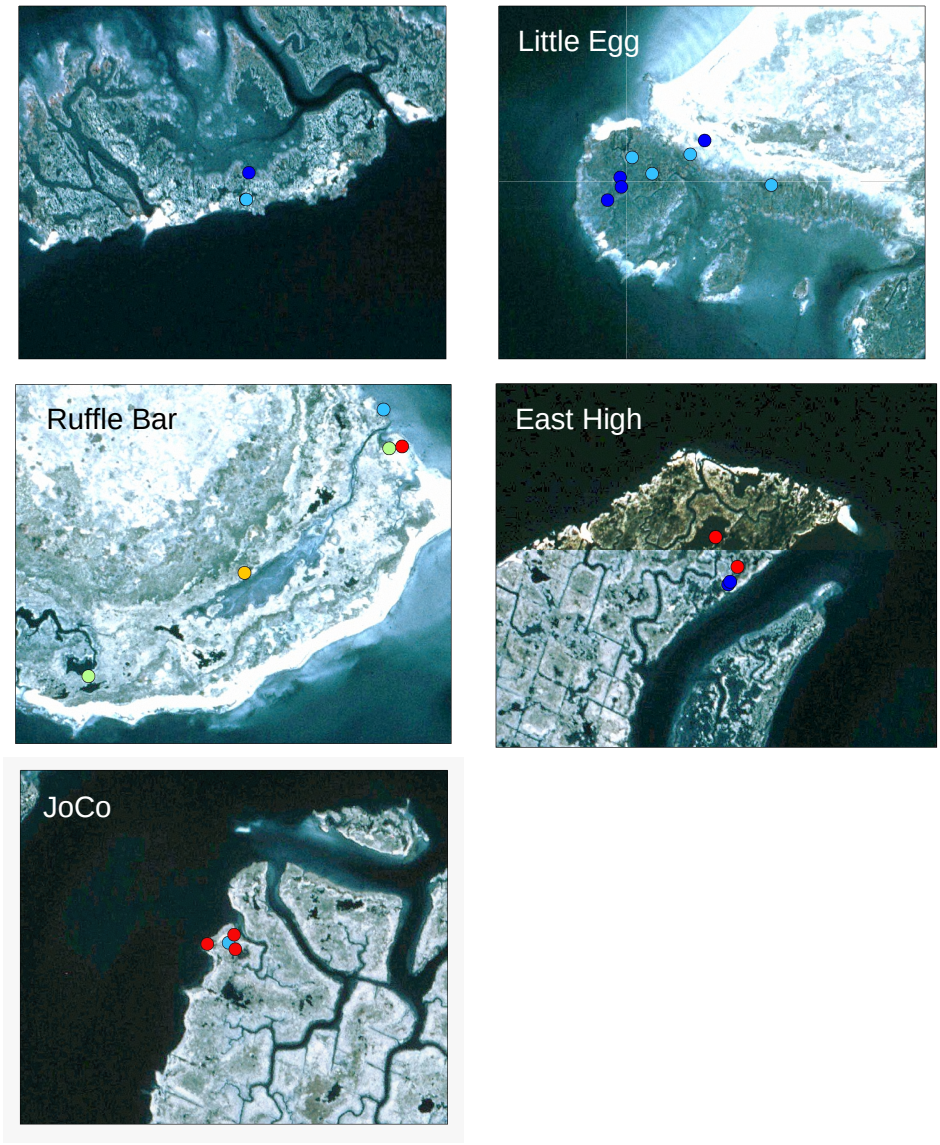

Figure 5-9 ^{7}Be inventories in the surface sediments of select marsh islands from September-2004

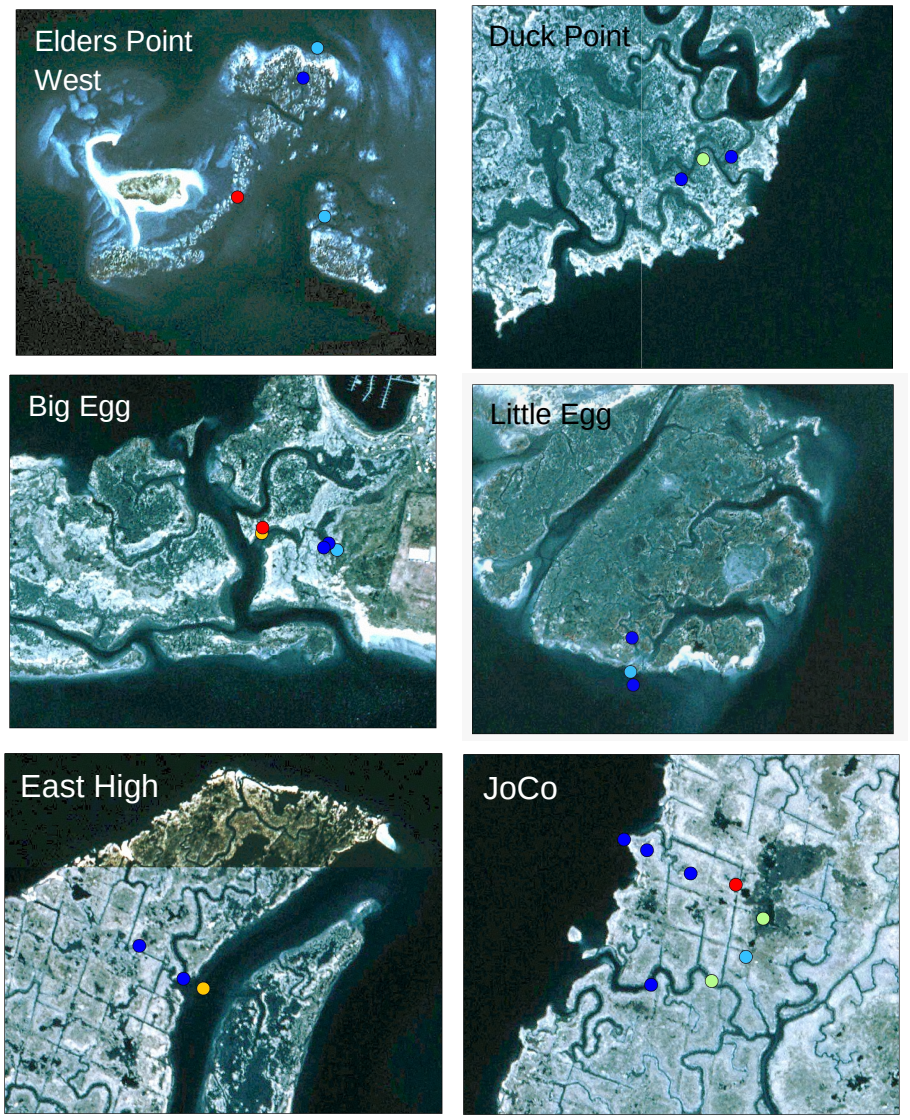

Figure 5-10 ^{7}Be inventories in the surface sediments of select marsh islands from May-2005

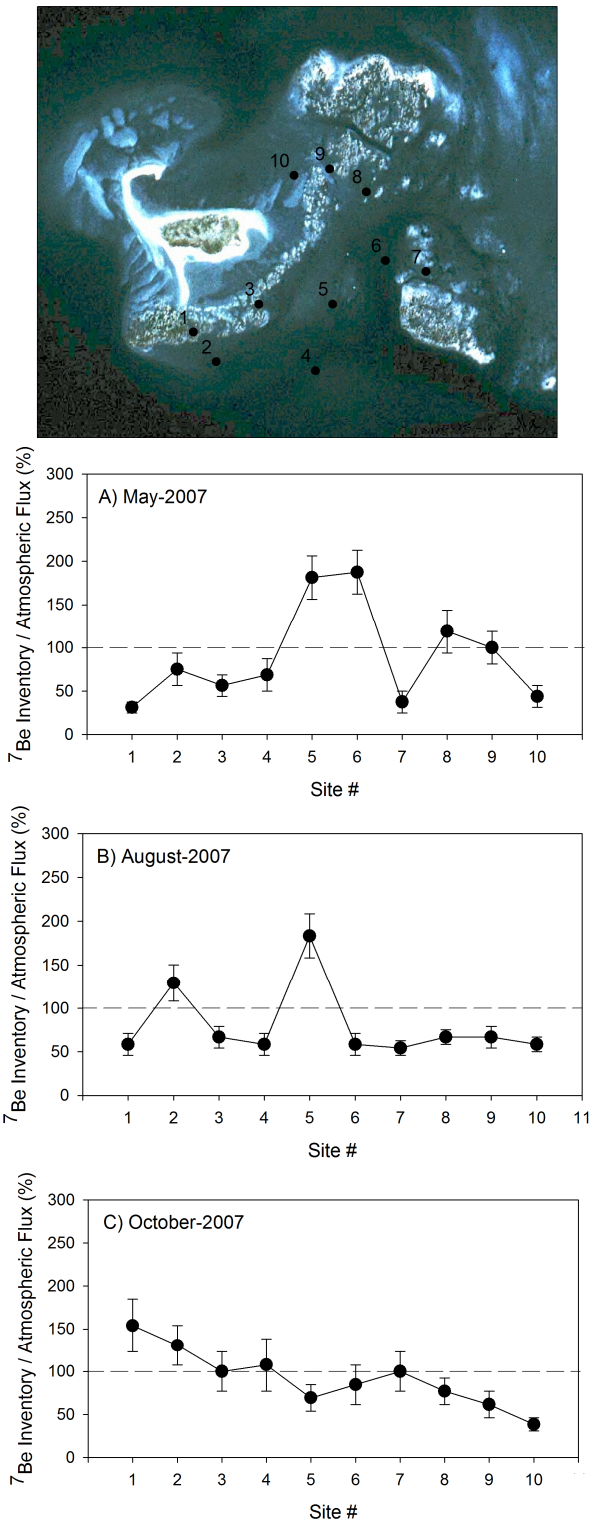

Figure 5-11. ^{7}Be inventories (dpm cm^{-2}) in the surface sediments of Elders Point West sampled in A) May-2007, B) August-2007 and C) October-2007.

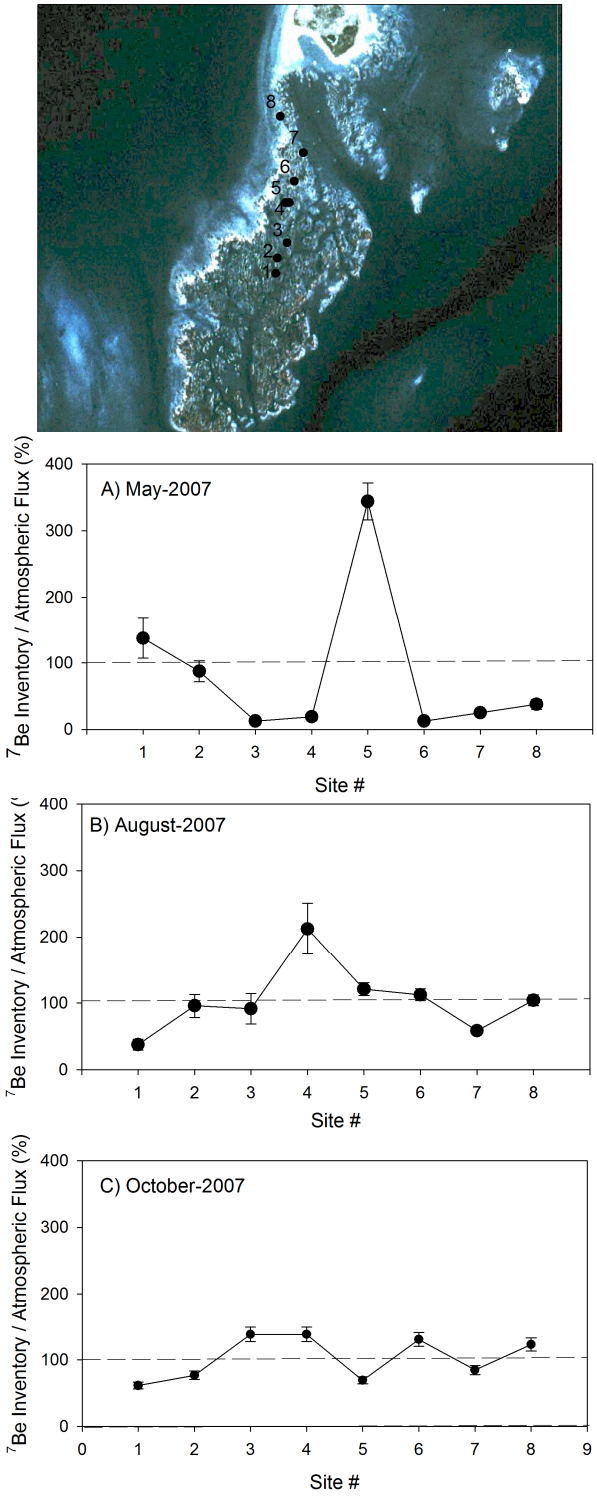

Figure 5-12. ^{7}Be inventories (dpm cm^{-2}) in the surface sediments of Elders Point East sampled in A) May-2007, B) August-2007 and C) October-2007.

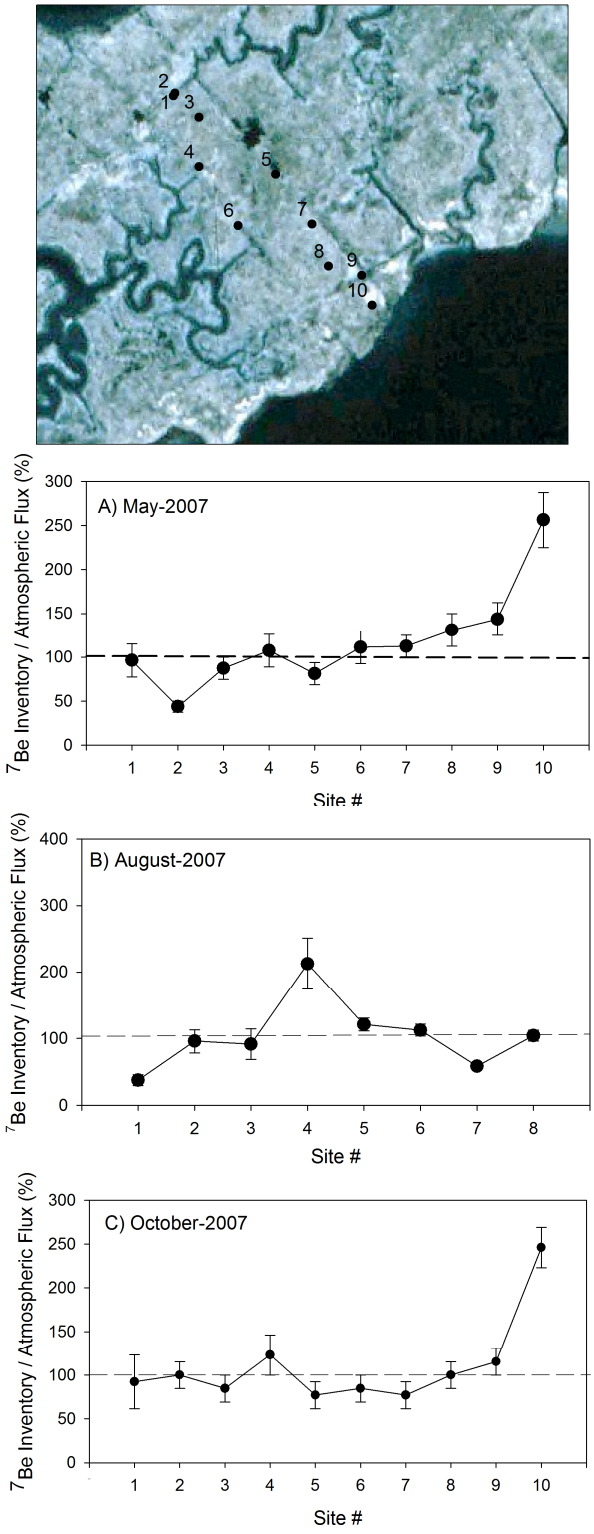

Figure 5-13. ^{7}Be inventories (dpm cm^{-2}) in the surface sediments of JoCo sampled in A) May-2007, B) August-2007 and C) October-2007.

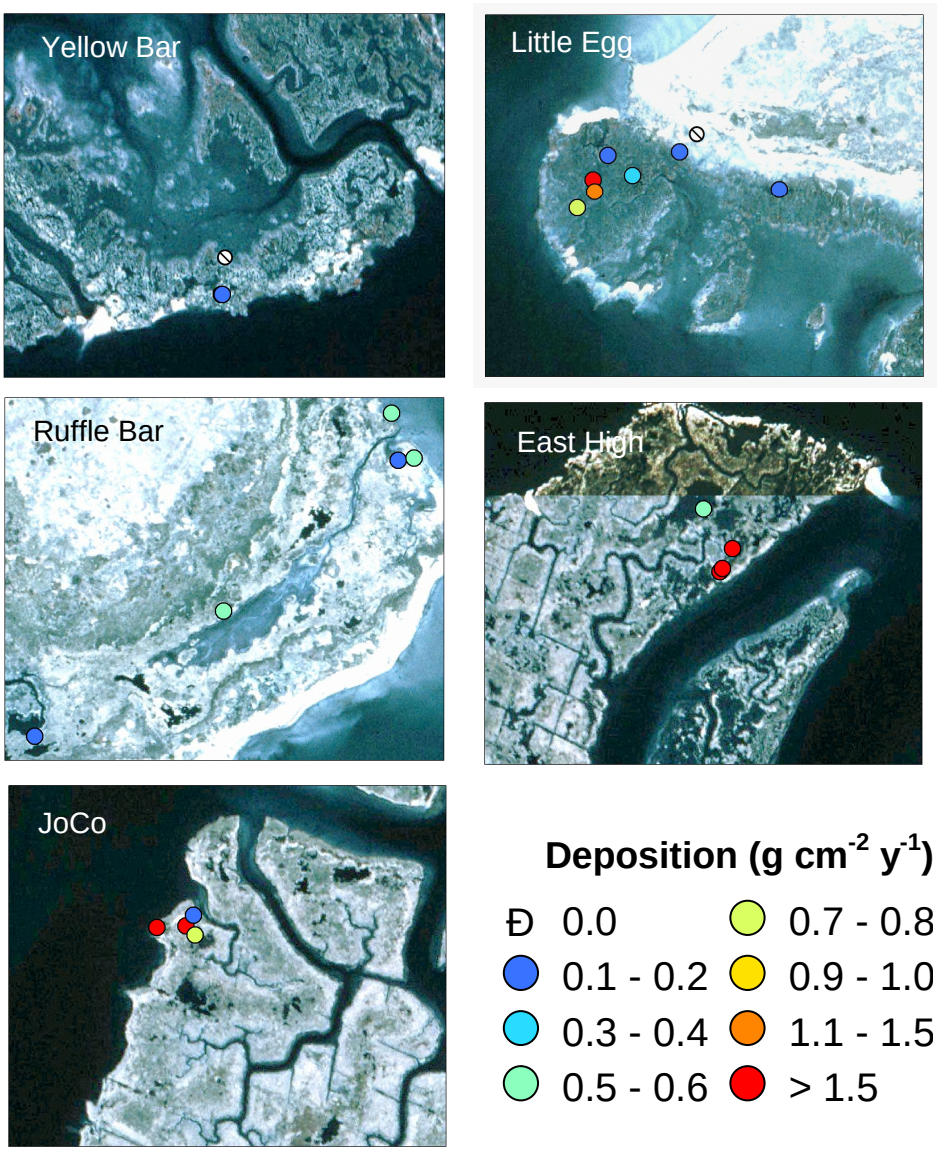

Figure 5-14. Rate of sediment deposition derived from $^{234}Th_{xs}$ inventories on select marsh sites in September-2004

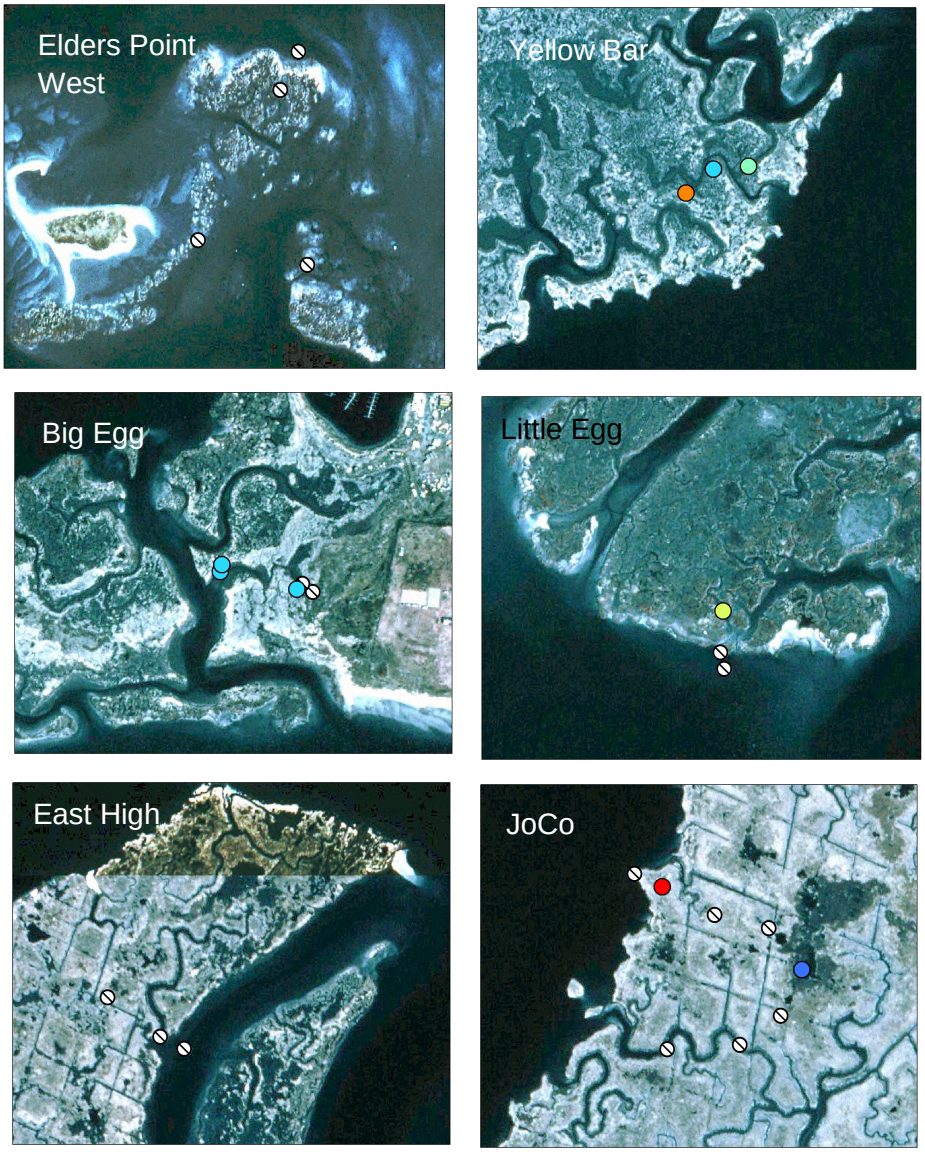

Figure 5-15. Rate of sediment deposition derived from $^{234}Th_{xs}$ inventories on select marsh sites in May-2005

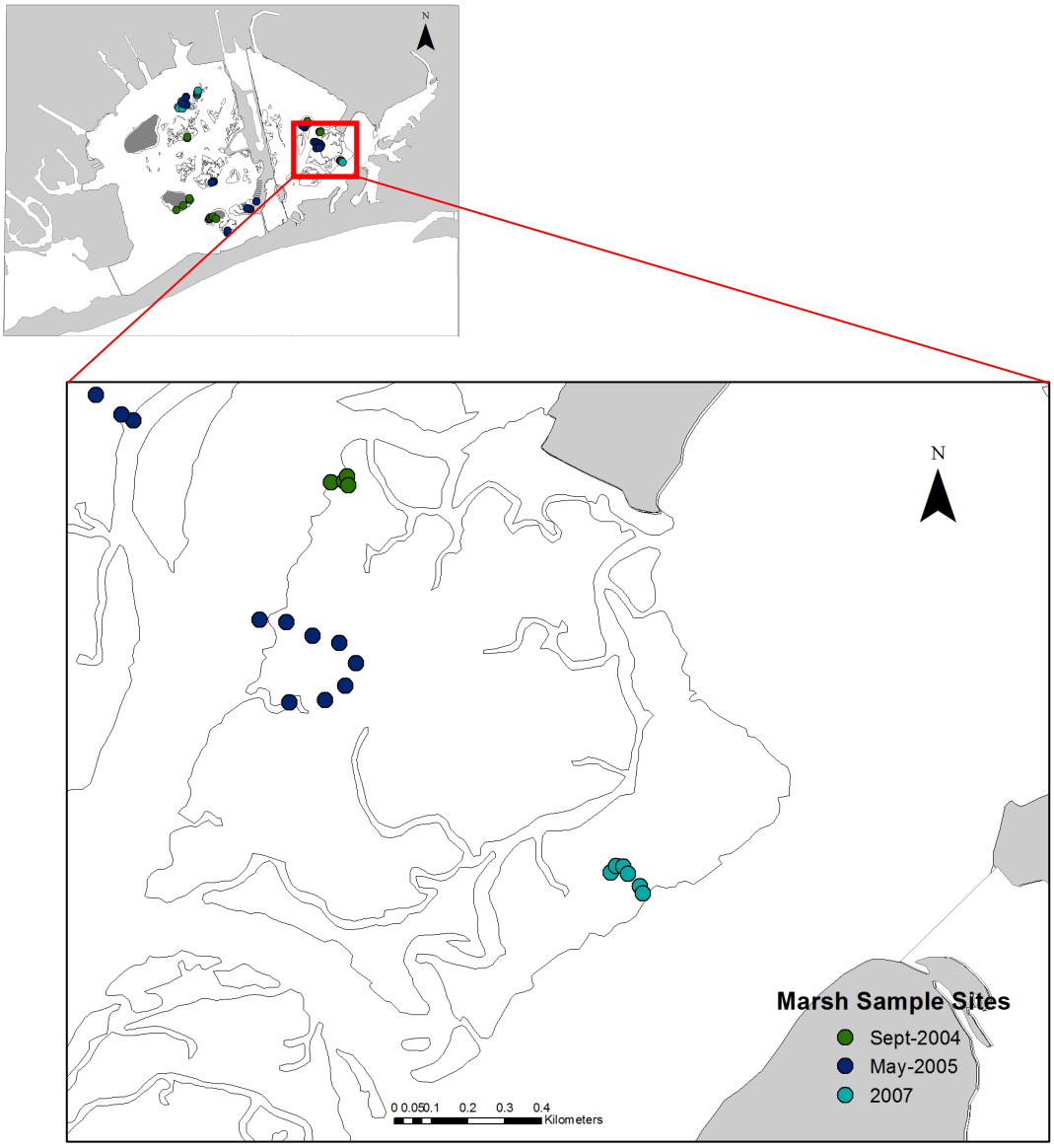

Figure 5-16. Sites sampled on JoCo marsh in September-2004, May-2005 and 2007 samping.

CHAPTER 6: Summary - Perspectives on the Sediment and Radionuclide Budgets of Jamaica Bay

Radionuclide Budgets

The purpose of this study was to use the spatial distribution and mass balances of the naturally-occurring radionuclides ^{234}Th, ^{7}Be and ^{210}Pb in Jamaica Bay sediments as indicators of sediment transport and deposition within the bay. These are useful tracers for sediment transport due to their strong affinity for fine particles and well-constrained sources.

Jamaica Bay is an urban coastal lagoon, with little riverine input and surrounded by impervious surface dominated uplands, limiting the direct input of sediment into the bay. Since 1959 analysis of aerial photographs indicated there has been 12% reduction in the size of the marsh islands measured within the bay (Hartig et al., 2002). One potential cause of marsh loss may be insufficient sediment accumulation on the marsh surface to keep pace with sea-level rise, leading to increased inundation and erosion (Hartig et al., 2002; Kolker, 2005; Swanson and Wilson, 2008). The mass balances of particle-reactive radionuclides ^{234}Th, ^{7}Be and ^{210}Pb elucidates the pathways of sediment (and radionuclides) into Jamaica Bay and the contributions from each source.

Mass balances of ^{234}Th and ^{210}Pb indicate that the importation of sediment into Jamaica Bay via Rockaway Inlet is significant to the budgets of these two radionuclides. Estimates of sediment import from the mass balance of $^{234}Th_{xs}$ and $^{210}Pb_{xs}$ were 4.3 to 38.5 × 10^{10} g y^{-1} for the $^{234}Th_{xs}$ budget and 4.2 to 15.8 × 10^{10} g y^{-1} for the $^{210}Pb_{xs}$ budget (Table 6-1). A sediment budget was constructed using ^{210}Pb-dervied mass accumulation

rates from in the bay subtidal and on the marsh islands. To balance the sediment sinks with the sediment inputs to Jamaica Bay a sediment import of $5.8 – 8.8 \times 10^{10}$ g y^{-1} was calculated. A previous attempt at a sediment budget using ^{210}Pb-dervied mass accumulation in the subtidal and on the marshes yielded a sediment import of $1.5 - 2.9 \times 10^{10}$ g y^{-1} (Bokuniewicz and Ellsworth, 1986). The estimates of sediment import through the various methods were similar (Table 6-1). However, the sediment import estimated from the mass balance of $^{234}Th_{xs}$ is likely an upper limit and reflect seasonal importation and episodic events that are not sustained over an annual basis. As well, import of sediment into Jamaica Bay may be more significant today than in the past. Previous studies have indicated that modifications to Jamaica Bay, such as dredging and armoring of the shoreline periphery have altered the hydrodynamics of Jamaica Bay changing it from a slight ebb dominated estuary to a flood dominated estuary (Swanson and Wilson, 2008).

The results of this study suggest that sediment importation is significant to Jamaica Bay. The implication is that some of the imported sediment may be available for deposition onto the surface of the salt marsh islands of the bay. Indeed, work conducted by Kolker (2005) and Cahoon and Lynch (unpublished data) suggest that sediment accumulation on the salt marsh islands measured appears to be sufficient to allow the accretion of the marsh surface to keep pace with current sea-level rise estimates.

Radionuclide Distributions in the Context of a Hydrodynamic Model of Jamaica Bay

It is interesting to compare the implication of the radionuclide mass balances found in this study with the sediment transport predicted from a hydrodynamic model of

the bay. The hydrodynamics of Jamaica Bay have been modified over time by dredging and deepening of channels within the bay and shore-line armoring of the bay periphery. Recent work conducted by Swanson and Wilson (2008) found an increase in tidal range across the Bay since the first half of the 20th century. In addition there has been an increase in the tidal asymmetry (M_4/M_2 tidal components) indicating that Jamaica Bay was weakly ebb dominated, but is now flood-dominated (R.E.Wilson, pers comm.).

Today Jamaica Bay is a weakly stratified and tidal active environment with estuarine circulation (Gordon et al., 2005; R.E. Wilson, pers. comm.). The tidal range (M_2) of Jamaica Bay is amplified from the western end to the far northeastern side of the basin (Grassy Bay) by a factor 1.2. The resulting barotropic tidal flow is flood dominant throughout the bay and contributes to maintain significant tidal flow through the bay's main channels (North Channel, Beach Channel and Broad Channel; Fig. 1-1). The barotropic tidal flow coupled with baroclinic estuarine circulation likely results in an increase of the flood dominant shear stress along the bottom of most channels (R.E. Wilson, pers. comm.).

A recent hydrodynamic model constructed for Jamaica Bay by R.E. Wilson (Stony Brook University) uses the bathymetry of the bay, salinity and tidal simulation to assess changes in near bottom tidal residual velocity, stratification in the water column and maximum bottom stress over a 90 hour period. The model results suggest that baroclinic induced estuarine circulation contributes to maintain a residual tidal upstream movement of near bottom currents within the major channels of the bay (Island Channel, North Channel, Beach Channel and Cross Channel; Fig. 6-1). The longitudinal salinity gradient (higher in the west than the east) in the bay contributes to variations in

stratification over a tidal period, with enhanced stratification in the North Channel and Island Channel during ebb tide.

The hydrodynamic model also considers the distribution of 5 size –classes of sediment in the subtidal bay (clay, silt, fine sand, medium sand and coarse sand, interpolated over the model grid) and uses tidal simulations to elucidate sediment transport patterns associated with tidal and estuarine circulation in Jamaica Bay over a 90 hour period (Fig. 6-2). The model does not include importation of sediment via the inlet, only the mobilization of the sediment already present in the subtidal bay. The results of the model show that the estuarine circulation of the bay, induced by the longitudinal salinity difference due to the input of wastewater and groundwater in the bay, produces a near-bottom current moving upstream within most channels. The model predicts tidal variations in clay and silt transport that show evidence of sediment transport due to variations in the near bottom currents during the flood and ebb tide. The results of the model show near-bottom concentrations of clay that are highest in the western bay (amidst the marsh islands) at high tide, (Fig. 6-3A) and at low tide, high concentrations of clay are again found in the western bay and in the eastern bay near JoCo marsh (Fig. 6-3B). The model also predicts that silt concentrations in the bottom water are high in the southern channel, extending into the eastern bay at both high and low water (Fig. 6-4; R.E. Wilson, Pers. Comm.).

Spatial variations in the predicted near-bottom concentrations of clay and silt during both high and low water were compared with inventories of $^{234}Th_{xs}$ and ^{7}Be measured in the subtidal sediments in September-2004, May-2005, November-2005 and July-2006, but no significant relationship was found. This is unsurprising as the input of

$^{234}Th_{xs}$ and ^{7}Be in Jamaica is complicated by import from the ocean via Rockaway Inlet and CSO events, respectively (see Chapters 2 and 4 for details). To limit the influence of the additional inputs of these radionuclides, the bay was divided in western and eastern sections (separated by Broad Channel Island). The inlet is directly connected to the western half of the bay and 3 of the 4 wastewater treatment plants found around the bay, as well as many of the CSO outfalls, are located in the western bay.

A significant correlation was found between ^{7}Be inventories in the subtidal sediments in the eastern bay and bottom concentration of silt and clay at low water ($n = 17$; $p < 0.01$ and 0.02, respectively). However, there was no significant relationship during the other sampling cruises. Rainfall in the 53 days prior to the May-2005 sampling cruise was ~ 19 cm, the lowest precipitation of the 4 cruises, and as such, CSO events may have been less likely prior to the cruise and therefore, not reflected in the ^{7}Be distribution in subtidal sediments. Thus, the ^{7}Be input to Jamaica Bay prior to May-2005 was likely dominated by the direct atmospheric flux, and the ^{7}Be inventories in May-2005 are more reflective of the processes represented in the hydrodynamic model. Nevertheless, even under conditions similar to the model, additional inputs of ^{7}Be implied by the mass balances of this radionuclide complicate direct comparison of the distribution of inventories with those of fine sediments predicted by the model.

The hydrodynamic model was also used to predict patterns of sediment deposition and erosion that resulted from tidal and estuarine circulation (Fig. 6-5A). The model results indicate that Grassy Bay, in the northeastern bay of the bay, is the major sink of sediment in the bay with erosion (or no net deposition) occurring through much of the rest of the bay (R.E. Wilson, Pers. Comm). Sediment accumulation rates derived from

$^{210}Pb_{xs}$ geochronologies indicate that fine sediment deposition is significant in the channels (Island Channel, 1.1 cm y^{-1}; North Channel, 1.0 cm $y^{-1;}$ Broad Channel 0.9 cm y^{-1}; and in Grassy Bay, 0.8 - 1.0 cm y^{-1}).

$^{234}Th_{xs}$ inventories were also used to derive rates of sediment deposition of material imported through the inlet (see Chapter 2; section 5-3). Patterns of $^{234}Th_{xs}$-derived deposition varied between sampling cruises, likely due to changes in the dominant wind patterns and storm events (see Chapter 2; Fig. 2-8). To mitigate some of the effects of changing winds and tides a compilation of the $^{234}Th_{xs}$-derived sediment deposition rates for the 4 sampling cruises was used to create a contour map of erosion and deposition (Fig. 6-5B). This contour map indicates that while sediment deposition does indeed occur in Grassy Bay and erosion is occurring in Broad Channel in the eastern bay, deposition of sediment is more widespread in the western bay than the hydrodynamic model predicts. Deposition in the North Channel and Island Channel derived from $^{234}Th_{xs}$ inventories is consistent with the long-term sediment deposition derived from $^{210}Pb_{xs}$-geochronologies, as previously discussed. The $^{234}Th_{xs}$-derived pattern indicates that Pumpkin Patch Channel is also a site of deposition. However, Pumpkin Patch Channel may only be a site of temporary storage as the surficial sediment in this area is dominated by sand-size particles (Fig. 3-1) and the $^{234}Th_{xs}$ measured in this area is likely confined to a thin, highly-active layer (see Chapter 2; section 5-1). Overtime, this thin layer may be transported and deposited in Grassy Bay, North Channel or Island Channel.

The mass balances of $^{234}Th_{xs}$ and $^{210}Pb_{xs}$, as well as a sediment budget constructed for the bay, indicate that importation of particles (and radionuclides) via Rockaway Inlet

is an important source of sediment into the bay. In contrast, the hydrodynamic model of Jamaica Bay assumes that sediment in the bay is at steady-state and the differences in the patterns of sediment deposition predicted by model and that are inferred from the radionuclide distributions may reflect this. In order to meaningfully compare and combine the hydrodynamic model with the radionuclides in the bay, the import of sediment needs be accounted for in the model, as well as additional sources of radionuclides to the bay (e.g. CSO events).

CSO Sources of ^{7}Be and ^{210}Pb to Jamaica Bay

A major source of ^{7}Be and ^{210}Pb into Jamaica Bay is direct atmospheric input. Mass balances of ^{7}Be and ^{210}Pb that were derived for Chesapeake Bay (Helz et al., 1985; Olsen et al., 1986; Dibb and River, 1989) and Long Island Sound (Benninger, 1978) found that direct atmospheric input was the dominant source of these radionuclides to these systems. However, in the Chesapeake Bay riverine input was thought to account for ~ 10% of the measured ^{210}Pb inventory in the subtidal sediments in the upper bay. Jamaica Bay has little riverine input and the dominant source of freshwater into the bay is from the wastewater treatment plants (Botton et al., 2006; O'Shea and Brosnan, 2000). During heavy or frequent rainfall events these waste-water treatment plants can become overloaded, bypassed, allowing untreated wastewater, as well as, sediment, ^{7}Be and ^{210}Pb to enter the bay directly.

The direct atmospheric source of ^{210}Pb and ^{7}Be to Jamaica Bay can account for 23 - 48% and 49 - 100% of the inventories in the bay sediments, respectively. Mass balances of ^{210}Pb and ^{7}Be indicate that combined sewer overflow events also may be a

significant source of these radionuclides into Jamaica Bay: input from CSO events accounts for 15 – 31% and 0 - 51% of $^{210}Pb_{xs}$ and ^{7}Be inventory, respectively. The input of these radionuclides from CSO events (particularly for ^{7}Be) complicates their use as tracers of sediment transport in Jamaica Bay. However, high inventories of ^{7}Be and ^{210}Pb in the deep channel near the CSO outfalls, following periods of heavy rainfall suggest deposition of material introduced during CSO events into these areas.

Sediment Inputs to Salt Marshes

The salt marsh islands of Jamaica Bay have decreased in extent and health over the last 30 years. Analysis of aerial photographs by Hartig et al. (2002) on select marsh islands showed an averaged decrease of ~ 38% since 1974. In addition to loss-of-area, there have been increased ponding within the marshes, widening of tidal creeks and sediment slumping along the marsh perimeter (Hartig et al., 2002). The causes proposed for the wetland loss in Jamaica Bay are sea-level rise (Hartig et al., 2002), decreased sediment input (Hartig et al., 2002), increased input of nutrients and organic material (Kolker, 2005) and modification to the bay leading to alteration to the bay's hydrodynamics.

Previous work shows that salt marshes within the bay are accumulating sediment at recent rates of ~0.25 – 0.41 cm y^{-1} (~0.05 – 0.08 g cm^{-2} y^{-1}; Kolker, 2005). The recent accretion rates derived from ^{210}Pb are in agreement with the limited sediment elevation table (SET) data from Jamaica Bay, which show accretion rates of ~0.44 cm y^{-1} in JoCo marsh, a relatively stable marsh island and 0.48 cm y^{-1} in Black Bank marsh, a deteriorating marsh island (2003 – 2009, Cahoon and Lynch, unpublished data reported

by P. Rafferty, National Parks Service). The presence of significant $^{234}Th_{xs}$ on the marsh islands in September-2004, May-2005, May-2007, August-2007 and October-2007 indicates sediment can be transferred to the salt marshes from the subtidal bay. The mean mass accumulation rate derived from the $^{234}Th_{xs}$ inventories on the measured marsh islands in September-2004 and May-2005 ranged from 0.0 to 2.5 g cm^{-2} y^{-1}.

However, these deposition rates are skewed to the high end due to the preferential sampling of the marsh edge during the September-2004 and May-2005 marsh sampling. These mass accumulation rates are higher than the annual rates measured by Kolker (2005) for this site (~ 0.08 g cm^{-2} y^{-1}) and likely reflect episodic events or short-term deposition that is not fully retained on the marsh over longer period of time. The averaged $^{234}Th_{xs}$ inventory on the marshes sampled, combined with previous work measuring long-term sediment accumulation and marsh accretion suggests that despite alterations to the sediment budget and hydrodynamics of the bay, sediment can be deposited on to the marsh islands. Indeed, the long-term sediment accumulation and accretion rates are sufficient for the salt marshes to keep pace with the current sea-level rise (0.3 cm y^{-1}). This suggests that other factors, such as edge erosion and the build-up of phytotoxins in marsh peat pore water as a result of enhanced organic loading and decomposition, may be responsible for marsh loss.

Table 6-1. Summary of sediment import estimates into Jamaica Bay.

Estimated Sediment Import ($g\ y^{-1}$)	**Method of Estimate**	**Reference**
$1.5 – 2.9 \times 10^{10}$	Sediment Budget Balance	Bokuniewicz and Ellsworth, 1986
$4.3 – 35.8 \times 10^{10}$	$^{234}Th_{xs}$ Mass Balance	This Study (see Chapter 2)
$5.8 – 8.8 \times 10^{10}\ g\ y^{-1}$	Based on mass accumulation rates (^{210}Pb Geochronology)	This Study (see Chapter 3)
$4.2 – 15.8 \times 10^{10}$	^{210}Pb Mass Balance	This Study (see Chapter 3)

* import estimate calculated from unaccounted for ^{210}Pb inventory in the gravity cores

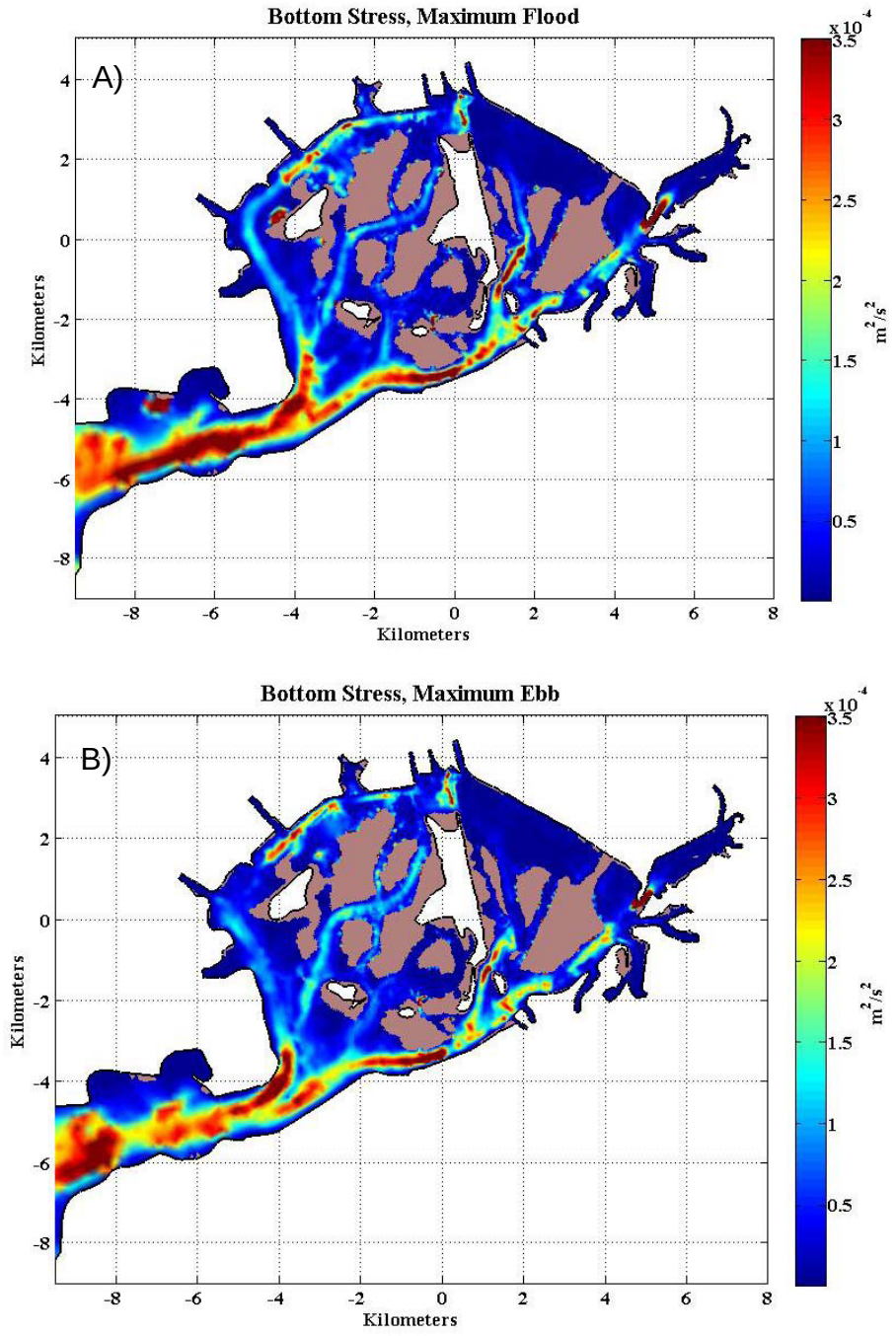

Figure 6-1 Maximum bottom stress during A) flood and B) ebb from the hydrodynamic model (provided by R.E. Wilson).

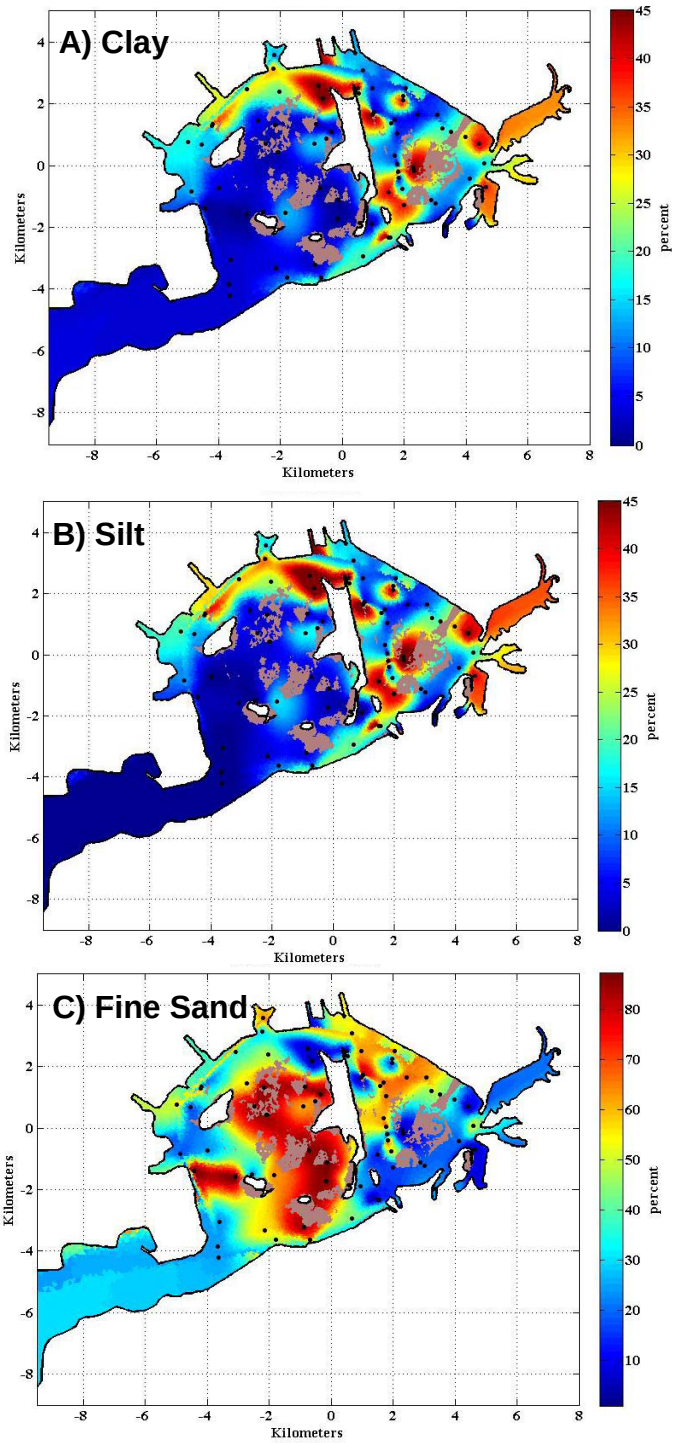

Figure 6-2 Initial distribution of A) clay, B) silt and C) fine sand interpolated from station data (provided by R.E. Wilson).

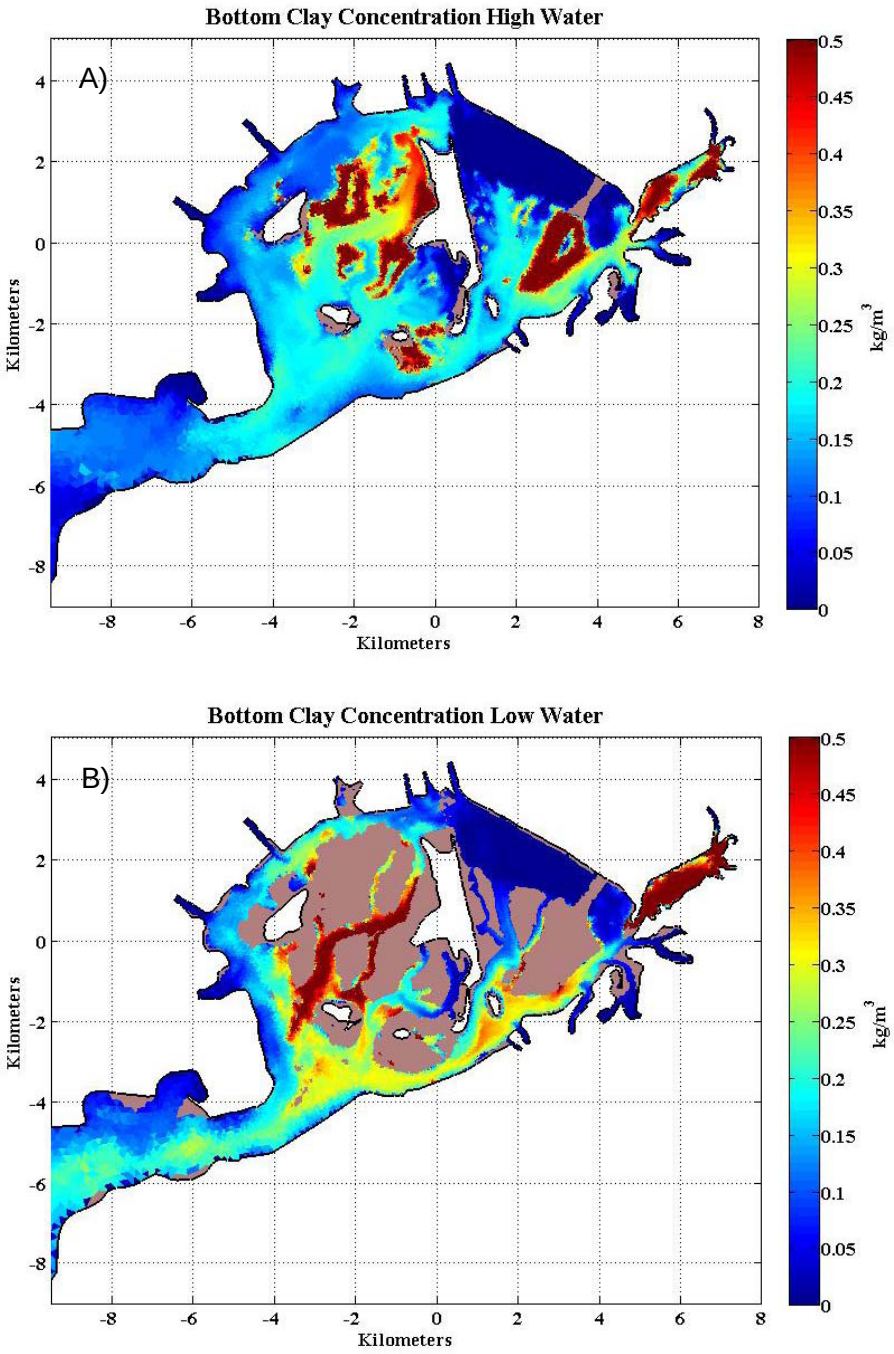

Figure 6-3. Bottom water concentrations of clay at A) High and B) Low Water predicted by the Jamaica Bay hydrodynamic model (provided by R.E. Wilson).

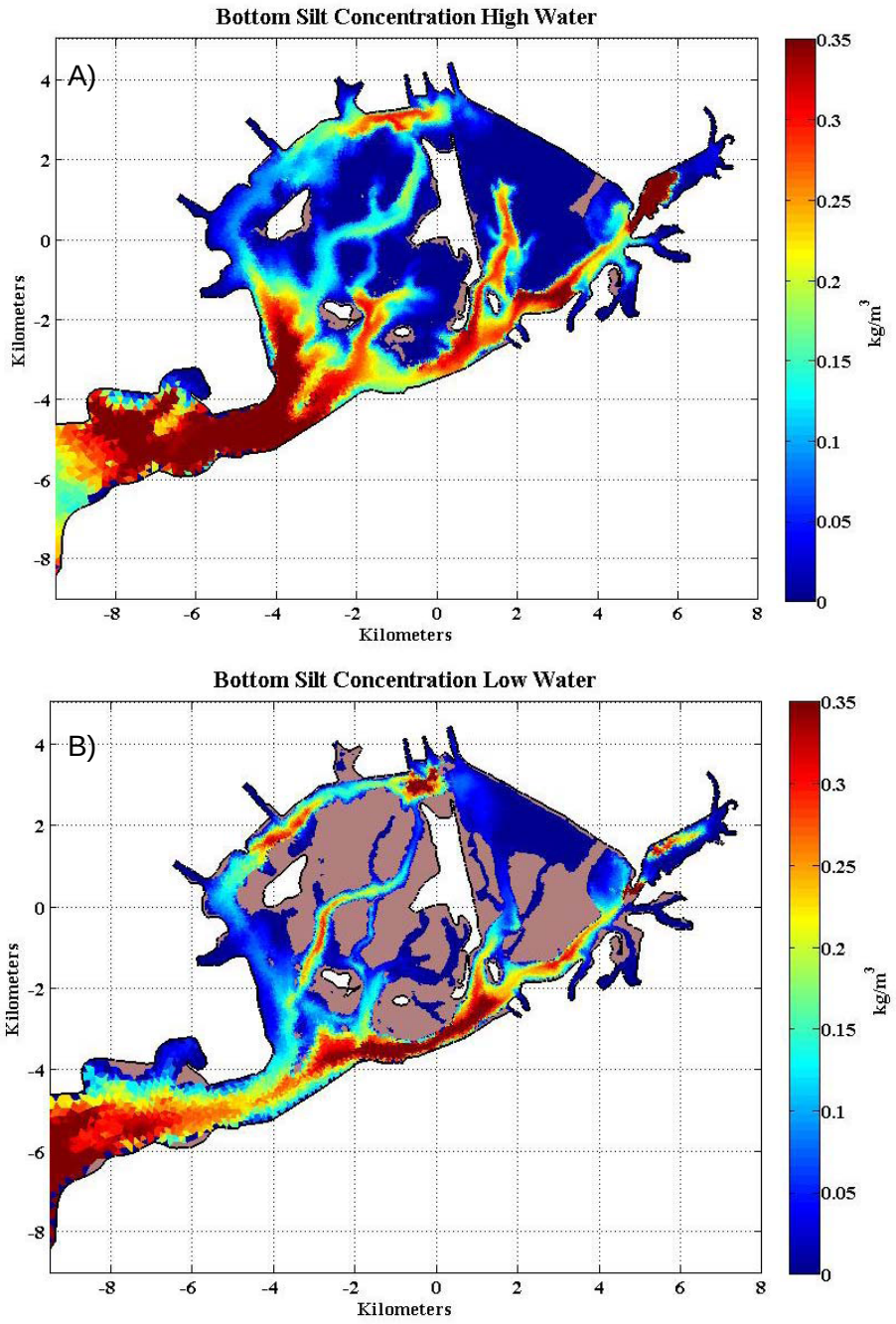

Figure 6-4. Bottom water concentrations of silt at A) High and B) Low Water predicted by the Jamaica Bay hydrodynamic model (provided by R.E. Wilson).

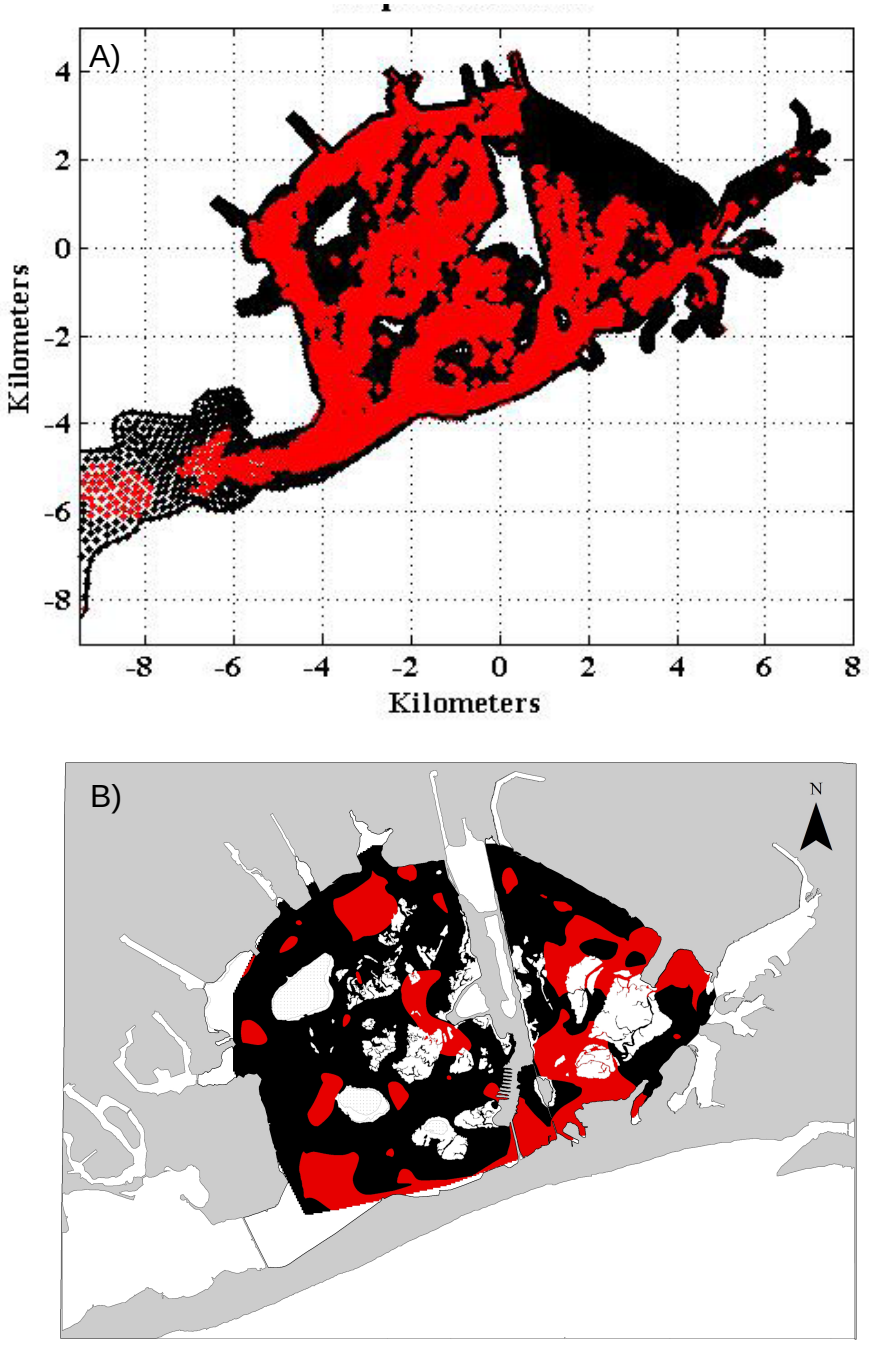

Figure 6-5. Spatial patterns of A) hydrodynamic model produced accumulation rates (provided by R.E. Wilson).and B) compilation of $^{234}Th_{xs}$-derived accumulation rates for the 4 sampling cruises. Black represents areas of deposition, red are areas of erosion.

References

Adams, D.A., J.S. O'Connor, and S.B. Weisberg (1998) *Sediment Quality of the NY/NJ Harbor System*. U. S. Environmental Protection Agency, Report No. 902-R-98-001.

Aller, R.C., L.K. Benninger and J.K. Cochran (1980) Tracking particle-associated processes in the nearshore environments by use of Th-234 and U-238 disequilibrium. *Earth Planet. Sci. Lett.* 47: 161-175.

Aller, R.C. and J.K. Cochran (1976) $^{234}Th/^{238}U$ disequilibrium in near-shore sediment: Particle reworking and diagenetic time scales. *Earth Planet. Sci. Lett., 29: 37-50.*

Appleby, P.G. and F. Oldfield (1992) Applications of Lead-210 to sedimentation studies. M. Ivanovich and R.S. Harmon (eds), Uranium-Series Disequilibrium: Applications to Environmental Problems, Clarendon Press, Oxford, pp. 731-778

Baskaran, M. (1995) A search for the seasonal variability on the depositional fluxes of ^{7}Be and ^{210}Pb. *Journal of Geophysical Research* 100: 2833-2840.

Baskaran, M. and P.H. Santchi (1993) The role of particles and colloids in the transport of radionuclides in the coastal environments of Texas. *Marine Chemistry* 43: 95-114.

Baskaran, M. and P.W. Swarzenski (2006) Seasonal variations on the residence times and partitioning of short-lived radionuclides (^{234}Th, ^{7}Be and ^{210}Pb) and depositional fluxes of ^{7}Be and ^{210}Pb in Tampa Bay, Florida. *Marine Chemistry* 104: 27-42.

Beck, A.J., J.P. Rapaglia, J.K. Cochran and H.J. Bokuniewicz (2007) Radium mass-balance in Jamaica Bay, NY: Evidence for a substantial flux of submarine groundwater. *Marine Chemistry* 106: 419-441.

Beer, J., A. Blinov, G. Bonani, R.C. Finkel, H.J. Hofmann, B. Lehmann, H. Oeschger, A. Sigg, J. Schwander, T. Saffelbach, M. Suter and W. Wolfi (1990) Use of 10Be in polar ice to trace the 11-year cycle of solar activity. *Nature* 347: 164-166.

Benninger, L.K. (1978) ^{210}Pb balance in Long Island Sound. *Gechimica et Cosmochimica Acta*, 42: 1165-1174.

Benninger, L.K., R.C. Aller, J.K. Cochran and K.K. Turekian (1979) Effects of biological mixing on the ^{210}Pb chronology and trace metal distribution in a Long Island sound sediment core. *Earth Planetary Science Letters*, 43: 241-259.

Benitez-Nelson, C.R., K.O. Buesseler, M.M. Rutgers van der Loeff, J.A. Andrews, L. Ball, G. Crossin and M.A.Charette (2001) Testing a new small-volume technique

for determining thorium-234 in seawater, *Journal of Radioanalytical and Nuclear Chemistry* 248: 795-799.

Benotti, M.J. and B.J. Brownawell (2007) Distriubtion of pharmaceuticals in an urban estuary during both dry- and wet-weather conditions. *Environmental Science and Technology* 41: 5795-5802.

Benotti, M. J., M. Abbene and S. A Terracciano (2007) Nitrogen Loading in Jamaica Bay, Long Island, New York: Predevelopment to 2005. USGS Open File Report SIR 2007-5051, 17 pp.

Bhandari, N., D. Lal, Rama (1970) Vertical structure of the troposphere as revealed by radioactive tracer studies. *Journal of Geophysical Research* 75: 2974-2980.

Bird, E.C. (1994) Physical Setting and Geomorphology of Coastal Lagoons. In *Coastal Lagoon Processes*, Björn Kjerfve (ed). Coastal Lagoon Processes, Elsevier, Amsterdam: 9-39.

Black, F.R. (1981) *Jamaica Bay: A History*. Gateway National Recreation Area New York, New Jersey.

Bokuniewicz, H., and J. Ellsworth (1986) Sediment budget for the Hudson system, *Journal of Northeastern Geology* 8: 158-164.

Bokuniewicz, H. J., J. A. Gebert and R. B. Gordon (1976) Sediment mass balance in a large estuary: Long Island Sound. *Estuarine and Coastal Marine Science* 4: 523-536.

Botton, M.L., R.E. Loveland, J.T. Tanacredi, and T. Itow (2006) Horseshoe Crabs (*Limulus polyphemus*) in an urban estuary (Jamaica Bay, New York) and the potential for ecological restoration. *Estuaries and Coasts* 29: 820-830.

Boyle, E.A.R., A.T. Collier, J.M. Dengler, A.C. Ng and R.F. Stallard (1974) On the chemical mass balance in estuaries. *Geochimica et Cosmochimica Acta*, 38: 1719-1728

Buesseler, K.O., C. Benitez-Nelson, M.M. Rutgers van der Loeff, J. Andrews, L. Ball, G. Crossin and M.A. Charette (2001) An intercomparison of small-and large-volume techniques for thorium-234 in seawater. *Marine Chemistry* 74: 15-28.

Canuel,, E.A., C.S. Martens, and L.K. Benninger (1990) Seasonal variations in ^{7}Be activity in the sediments of Cape Lookout Bight, North Carolina. *Geochimica et Cosmochimica Acta* 54: 237-245.

Carroll, J. and I. Lerche (2003) Sedimentary processes: Quantification using radionuclides (M.S. Baxter ed.), Radioactivity in the Environment, vol. 5.

Chabaux, F., B. Bourdon and J. Riotte (2008) U-Series geochemistry in weathering profiles, river waters and lakes. S. Krishnaswami and J.K. Cochran (eds). U-Th Series Nuclides in Aquatic Systems, pp. 49-91.

Charette, M.A. K.O. Buesseler, J.E. Andrews (2001) Utility of radium isotopes for evaluating the input and transport of groundwater-derived nitrogen to a Cape Cod estuary. *Limnology and Oceanography* 46: 465-470.

Christiansen, T., P.L. Wiberg and T.G. Milligan (2000) Flow and sediment transport on a tidal salt marsh surface. *Estuarine, Coastal and Shelf Science* 50: 315-331.

Church, T.M., C.K. Sommerfield, D.J. Velinsky, D. Point, C. Benoit, D. Amouroux, D. Plaa and O.F.X. Donard (2006) Marsh sediments as a records of sedimentation, eutrophication and metal pollution in the urban Delaware Estuary. *Marine Chemistry* 102: 72-95.

Cochran, J.K., D.J. Hirschberg and D. Amiel (2000) Particle mixing and sediment accumulation rates of Peconic Estuary sediments: A sediment accretion study in support of the Peconic Estuary Program. Report #: 0014400498181563

Cochran, J.K., D.J. Hirschberg, J. Wang and C. Dere (1998) Atmospheric deposition of metals to coastal waters (Long Island Sound, New York U.S.A.): Evidence from saltmarsh deposits. *Estuarine, Coastal and Shelf Science* 46; 503-522.

Cochran, J.K., M. Frignani, M. Salamanca, L.G. Bellucci and S. Guerzoni (1998) Lead-210 as a tracer of atmospheric input of heavy metals in the northern Venice Lagoon. *Marine Chemistry* 62: 15-29.

Corbett, D.R., B. McKee and M. Allison (2006) Nature of decadal-scale sediment accumulation on the western shelf of the Mississippi River delta. *Continental Shelf Research* 26, 2125-2140.

Corbett, D.R., D. Vance, E. Letrick, D. Mallinson and S. Culver (2007) Decadal-scale sediment dynamics and environmental change in the Albemarle Estuarine System, North Carolina. *Estuarine, Coastal and Shelf Science* 71: 717-729.

DeMaster, D.J., B.A. McKee, C.A. Nittrouer, Q. Jiangchu and C. Guodong (1985) Rates of sediment accumulation and particle reworking based on radiochemical measurements from continental shelf deposits in the East China Sea. *Continental Shelf Research* 4: 143-158.

DeMaster, D.J., S.A. Kuehl and C.A. Nittrouer (1986) Effects of suspended sediments on geochemical processes near the mouth of the Amazon River: Examination of biological silica uptake and the fate of particle-reactive elements. *Continental Shelf Research* 6: 107-125.

Diaz, R.J., D.C. Rhoads, J.A. Blake, R.K. Kropp and K.E. Keay (2008) Long-term trends of benthic habitats related to a reduction in wastewater discharge to Boston Harbor. *Estuaries and Coasts,* 31: 1184-1197.

Dibb, J. E. (1989) Atmospheric deposition of beryllium-7 in the Chesapeake Bay region. *Journal of Geophysical Research* 94: 2261-2265.

Dibb, J.E. and D.L. Rice (1989) Temporal and spatial distribution of beryllium-7 in the sediments of Chesapeake Bay. *Estuarine, Coastal and Shelf Science* 28: 395-406.

Doering, C. and R. Akber (2008) Beryllium-7 in near-surface air and deposition at Brisbane, Australia. *Journal of Environmental Radioactivity* 99: 461-467.

Ellsworth, J. (1986) Shore erosion as a source of fine-grained sediment to the lower Hudson River. M.S. Thesis, Stony Brook University, Stony Brook, NY, 96pp.

Feely, H.W., R.J. Lasen, C.G. Sanderson (1989) Factors that causes seasonal variations in beryllium-7 in surface air. *Journal of Environmental Radioactivity* 9: 223-249.

Feng, H., J.K. Cochran and D.J. Hirschberg (1999a) ^{234}Th and ^{7}Be as tracers for the transport and dynamics of suspended particles in partially mixed estuary. *Geochimica et Cosmochimica Acta*, 63: 2487-2505.

Feng, H., J.K. Cochran and D.J. Hirschberg (1999b) ^{234}Th and ^{7}Be as tracers for transport and sources of particle-associated contaminants in the Hudson River Estuary. *The Science of the Total Environment* 237/238: 401-418.

Ferguson, P.L., R.F. Bopp, S.N. Chillrud, R.C. Aller and B.J. Brownawell (2003) Biogeocehmistry of nonylphenol ethoxylatesin urban estuarine sediments. *Environment Science and Technology* 37: 3499-306.

Fisenne, I.M. (1968) Distribution of lead-210 and radium-226 in soil. Rep. UCRL-18140, pp. 145-158. Washington, D.C.: US At. Energy Comm.

French, J.R. and T. Spencer (1993) Dynamics of sedimentation in a tide-dominated back barrier salt marsh, Norfolk, UK. *Marine Geology* 110: 315-331.

Friedrichs, C. T., and J. E. Perry (2001) Tidal marsh morphodynamics, *Journal of Coastal Research* SP 27: 7-37.

Giffin, D. and D. R. Corbett (2003) Evaluation of sediment dynamics in coastal systems via short-lived radioisotopes. *Journal of Marine Systems* 42: 83-96.

González-Gómez, M. Azahra, J.J. López-Peñalver, A. Camacho-García, T.El. Bardouni and H. Boukhal (2006) Seasonal variability in ^{7}Be depositional fluxes at Granada, Spain. *Applied Radiations and Isotopes* 64: 228-234.

Gordon, A.L. and R.W. Houghton (2004) The water of Jamaica Bay: impact on sediment budget. In: *Proceeding, Jamaica Bay's Disappearing Salt Marshes.* New York: Jamaica Bay Institute, Gateway National Recreational Area, National Park Service.

Graustein, W.C. and K.K. Turekian (1996) Be-7 and Pb-210 indicate an upper troposphere source for elevated ozone in the summertime subtropical free troposphere of the eastern North Atlantic. *Geophysical Research Letters* 23: 539-542.

Hartig, E.K., V. Gornitz, A. Kolker, F. Mushacke, and D. Fallon (2002) Anthropogenic and climate-change impacts on salt marshes of Jamaica Bay, New York City. *Wetlands* 22: 71-89.

Heikkilä, U., J. Beer and V. Alfimov (2008) Beryllium-10 and beryllium-7 in precipitation in Düberdorf (440 m) and Jungfraujoch (3580 m), Switzerland (1998-2005). *Journal of Geophysical Research – Atmosphere* doi: 10.1029/2007JD009160.

Helz, G.R., G.H. Setlock, A.Y. Cantillo and W.S. Moor (1985/86) Processes controlling the regional distribution of ^{210}Pb, ^{226}Ra and anthropogenic zinc in estuarine sediments. *Earth and Planetary Science Letters* 76: 23-34.

Houghton, R., A. Gordon and B. Huber (2005) Dye Tracer Experiments in Jamaica Bay. Integrated Reconnaissance of the Physical and Biogeochemical Characteristics of Jamaica Bay: Initial Activity Phase. A Coordinated Program of the Gateway National Recreation Area and the Columbia Earth Institute, pp. 51-53.

Ioannidou, A. and C. Papastefanou (2006) Precipitation scavenging of ^{7}Be and ^{137}Cs radionuclides in air. *Journal of Environmental Radioactivity* 85: 121-136.

Iocco, L.E., P. Wilber, R.J. Diaz, D.G. Clarke and R.J. Will (2000) *Benthic Habitats of New York/New Jersey Harbor: 1995 Survey of Jamaica, Upper, Newark, Bowery and Flushing Bays Final Report.*

Interstate Environmental Commission, 2008 Annual Report, New York, New Jersey Connecticut, 99 pp.

Jamaica Plan: Final Environmental Impact Statement (2007) Appnedix I: WPCP and CSO impact analysis. 27 pp.

Kaste, J.M., S.A. Norton, C.T. Hess (2002) Enviromental chemistry of beryllium-7. P.H. Ribbe and J.J. Rosso (eds). Beryllium: Mineralogy, petrology, and geochemistry, Reviews in Mineralogy and Geochemistry, vol. 50, pp. 291-312.

Kjerfve, B. (1994) Coastal lagoons. In *Coastal Lagoon Processes*, Björn Kjerfve (ed). Coastal Lagoon Processes, Elsevier, Amsterdam: 1-7.

Kolker, A. (2005) The Impacts of Climate Variability and Anthropogenic Activities on Salt Marsh Accretion and Loss on Long Island. Stony Brook, New York: Stony Brook University Ph.D. thesis, 278p.

Ku, T.-L., K.G. Knauss and G.G. Mathieu (1977) Uranium in the open ocean: concentration and isotopic composition. *Deep Sea Research*: 24: 1005-1017.

Lal, D., P.K. Malhotra and B. Peters (1958) On the production of radioisotopes in the atmosphere by cosmic radiation and their application to meteorology. *Journal of Atmospheric and Solar-Terrestrial Physics* 12: 306-328.

Lal, D. and B. Peters (1967) Cosmic ray produced radioactivity on earth. In: Handbuch der Physik 46: 551-612.

LeCloarec, M-F., P. Bonté, I. Lefèvre, J-M Mouchel, S. Colbert (2007) Distribution of ^{7}Be, ^{210}Pb, and ^{137}Cs in watersheds of different scales in the Seine River basin: Inventories and residence times. *Science of the Total Environment* 375: 125-139.

Leonard, L.A. (1997) Controls of sediment transport and deposition in an incised mainland marsh basin, southeaster North Carolina. *Wetlands* 17: 263-274.

Leonard, L.A., A.C. Hine and M.E. Luther (1995) Surficial sediment transport and deposition processes in a *Juncus roemerianus* marsh, west-central Florida. *Journal of Coastal Research* 11: 322-336.

Lewis, D.M. (1976) The geochemistry of manganese, iron, uranium, lead-210 and major ions in the Susquehanna River. PhD Thesis. New Haven, CT. 272 pp.

Li, Y-H, P.H. Santschi, A. Kaufman, L.K. Benninger and H.W. Feely (1981) Natural radionuclides in waters of the New York Bight. *Earth and Planetary Science Letters* 55: 217-228.

Maeda, M. and H.L. Windom (1982) Behavior of uranium in two estuaries of the southeastern United States. *Marine Chemistry* 11: 427-436.

Matisoff, G., C.W. Wilson, and P.J. Whiting (2005) The $^{7}Be/^{210}Pb$ ratio as an indicator of suspended sediment age or fraction new sediment in suspension. *Earth Surface Processes and Landforms* 30: 1191-1201.

McCaffrey, R.J. (1977) A record of the accumulation of sediment and trace metals in a Connecticut, USA, salt marsh. PhD Thesis, New Haven, CT, 156 pp.

McKee, B.A. (2008) U- and Th-series nuclides in estuarine environments. Krishnaswami and J.K. Cochran (eds). U-Th Series Nuclides in Aquatic Systems, pp. 193-218.

McKee, B.A., D.J. DeMaster and C.A. Nittrouer (1984) The use of Th-234/U-238 disequilibrium to examine the fate of particle-reactive species on the Yangtze River. *Geology* 11: 631-633.

McKee, B.A., D.J. DeMaster and C.A. Nittrouer (1986) Temporal variability in the partitioning of thorium between dissolved and particulate phases on the Amazon shelf: Implication for the scavenging of particle-reactive species. *Continental Shelf Research* 6: 87-106.

McKee, B.A., D.J. DeMaster and C.A. Nittrouer (1987) Uranium geochemistry on the Amazon shelf: evidence for uranium release from bottom sediments. *Geochimica et Cosmochimica Acta* 51: 2779-2786.

McKee, B.A., C.A. Nittrouer and D.J. DeMaster (1983) Concepts of sediment deposition and accumulation applied to the continental shelf near the mouth of the Yangtze River. *Geology* 11: 631-633.

Mitsch, W.J. and G. Gosselink (2000) *Wetlands.* John Wiley & Sons, Inc.: New York, 920pp.

Moore, W.S. (1996) Large groundwater inputs to coastal waters revealed by Ra-226 enrichments. *Nature* 380: 612-614.

Neubauer, S.C, I.C. Anderson, J.A. Constantine and S.A.Kuehl (2002) Sediment deposition and accretion in a mid-Atlantic (U.S.A) tidal freshwater marsh. *Estuarine, Coastal and Shelf Science* 54: 713-727.

Noyce, J.R., T.S. Chen, D.T. Moore, J.N. Beck and P.K. Kuroda (1971) Temporal distributions of radioactivity and Sr-87/Sr-86 ratios during rainstorms. *Journal of Geophysical Research* 76: 646-656.

Olsen, C.R., I.L. Larsen, P.D. Lowry, and N.H. Cutshall, J.F. Todd, G.T.F. Wong and W.H. Casey (1985) Atmospheric fluxes and marsh-soil inventories of ^{7}Be and ^{210}Pb. *Journal of Geophysical Research* 90: 10487-10495.

Olsen, C.R., I.L. Larsen, P.D. Lowry, and N.H. Cutshall (1986) Geochemistry and deposition of ^{7}Be in river-estuarine and coastal waters. *Journal of Geophysical Research* 91: 896-908.

Olsen, C.R., M. Thein, I.L. Larsen, P.D. Lowry, P.J. Mulholland, N.H. Cutshall, J.T. Byrd and H.L. Windom (1989) Plutonium, lead-210, and carbon isotopes in the Savannah Estuary: Riverborne versus marine sources. *Environmental Science and Technology* 23: 1475-1481.

O'Shea, M.L. and T.M. Brosnan (2000) Trends in indicators of eutrophication in western Long Island Sound and the Hudson-Raritan Estuary. *Estuaries* 23: 877-901.

Ray, S.B., M. Mohanti and B.L.K. Somayajulu (1995) Uranium isotopes in the Mahanadi River-Estuarine system, India. *Estuarine, Coastal and Shelf Science* 40: 635-645.

Redfield, A. C. (1972) Development of a New England salt marsh. *Ecological Monographs* 42:201–237.

Renwick, W. H. and G. M. Ashley (1984) Sources, storages and sinks of fine-grained sediment in a fluvial-estuarine system. *Geological Society of America Bulletin* 94: 1343-1348.

Ritchie, J.C. and J.R. McHenry (1990) Application of radioactive fallout cesium-137 for measuring soil erosion and sediment accumulation rates and patterns: A review. *Journal of Environmental Quality* 19: 215-233.

Roman, C.T., J.A. Peck, J.R. Allen, J.W. King and P.G. Appleby (1997) Accretion of a New England (USA) salt marsh in response to inlet migration, storms and sea-level rise. *Estuarine, Coastal and Shelf Science* 45: 717-727.

Rubbenstone, J. (2005) Stable isotope evidence for water mass mixing in Jamaica Bay. Integrated Reconnaissance of the Physical and Biogeochemical Characteristics of Jamaica Bay: Initial Activity Phase. A Coordinated Program of the Gateway National Recreation Area and the Columbia Earth Institude, pp. 54-59.

Russell, I.J., C.E. Choquette, S.L. Fang, W.P. Dundulis, A.A. Pao and A.A. Pszenny (1981) Forest vegetation as a sink for atmospheric particulates: Quantitative studies in rain and dry deposition. *Journal of Geophysical Research* 86: 5247-5363.

Rutgers van der Loeff, M.M. and W.S. Moore (1999) The analysis of natural radionuclides in seawater. In: Methods of Seawater Analysis. Grasshoff, K.,M.Ehrhardt, K. Kremling (Eds.),. VerlagChemie, Weinhim, pp. 365-397.

Rutgers van der Loeff, M. R., M. M. Sarin, M. Baskaran, C. Benitez-Nelson, K. O. Buesseler, M. Charette, M. Dai, O. Gustafsson, P. Masqué, P. J. Morris, K. Orlandini, A. Rodriguez y Baena, N. Savoye, S. Schmidt, R. Turnewitsch, I. Vögel and J. T. Waples (2006) A review of present techniques and methodological advances in analyzing ^{234}Th in aquatic systems. *Marine Chemistry* 100: 190-212.

Santschi, P.H., Y.-H. Li and J. Bell (1979) Natural radionuclides in the water of Narragansett Bay. *Earth Planetary Science Letters* 45: 201-213.

Sharma, P., L.R. Gardner, W.S. Moore, and M.S. Bollinger. (1987) Sedimentation and bioturbation in a slat marsh as revealed by ^{210}Pb, ^{137}Cs, and ^{7}Be studies. *Liminology and Oceanography* 32: 313-326.

Sommerfield, C.K., C.A. Nittrouer and C.R. Alexander (1999) ^{7}Be as a tracer of flood sedimentation on the northern California continental margin. *Continental Shelf Research* 19: 335-361.

Strickney, A.P. and L.D. Stringer (1957) A study of the invertebrate bottom fauna Greenwich Bay, Rhode Island. *Ecology* 38: 111-122.

Stumpf, R.P. (1983) The process of sedimentation on the surface of a salt-marsh. *Estuarine, Coastal and Shelf Science.* 17: 495-508.

Suszkowski, D. J. (1978) Sedimentology of Newark Bay, New Jersey: an urban estuary, Ph.D. Thesis, University of Delaware, 222 pp.

Swanson, L.R. and R. E. Wilson (2008) Increased tidal ranges coinciding with Jamaica Bay development contribute to marsh flooding. *Jounral of Coastal Research* 24: 1565-1569.

Teal, J. and M. Teal. (1969) Life and Death of the Salt Marsh. Ballantine Books, New York, NY, USA.

Toole, J., M.S. Baxter and J. Thomson (1987) The behavior of uranium isotopes with salinity changes in three UK estuaries. *Estuarine, Coastal and Shelf Science* 25: 283-297.

Todd, J.F., G.T.F. Wong, C. Olsen and I.L. Larsen (1989) Atmospheric depositional characteristics of Beryllium 7 and Lead 210 along the southeastern Virginia coast. *Journal of Geophysical Research* 94: 11106-11116.

Turekian, K.K., Y. Nozaki, and L. Benninger (1977) Geochemistry of atmospheric radon and radon products. *Annual Review of Earth and Planetary Science* 5: 227-255.

Turekian, K. K., L. K. Benninger and E. P. Dion (1983) ^{7}Be and ^{210}Pb total depositional fluxes at New Haven, Connecticut, and Bermuda. *Journal of Geophysical Research* 88: 5411-5415.

An update on the disappearing salt marshes of Jamaica Bay, NY (2007) http://nbii-nin.ciesin.columbia.edu/jamaicabay/jbwppac/JBAC_NPS_SaltMarshReport_080207.pdf.

Vogler, S., M. Jung, and a. Mangini (1996) Scavenging of ^{234}Th and ^{7}Be in Lake Constance. *Limnology and Oceanography* 41: 1384-1393.

Walbrink, P.J. and A.S. Murray (1996) Distribution and variability of ^{7}Be soils under different surface cover conditions and its potential for describing soil redistribution processes. *Water Resources Research* 32: 467-476.

Wang, F.C., T. Lu and W.B. Sikora (1993) Intertidal marsh suspended sediment transport processes, Terrebonne Bay, Louisiana, U.S.A. *Journal of Coastal Research* 9: 209-220.

Wolfe, D.A., E.R. Long and G.B. Thursby (1996) Sediment toxicity in the Hudson-Raritan estuary: Distribution and correlations with chemical contaminations. *Estuaries* 19: 901-912.

Zeppie, C.R. (1977) Vertical profiles and sedimentation rates of Cd, Cr,Cu, Ni and Pb in Jamaica Bay, New York. M.S. Thesis. Stony Brook, NY. 85pp.

Zhu, J. and C.R. Olsen (2009) Beryllium-7 atmospheric deposition and sediment inventories in the Neponset River estuary, Massachusetts, USA. *Journal of Environmental Radioactivity* 100: 192-197.

Appendix 1: Gamma Spectrometry Analysis of Jamaica Bay Sediments

^{210}Pb, ^{234}Th, ^{214}Pb and ^{7}Be activities were measured using non-destructive gamma spectrometry by counting the wet samples on a Canberra 3800 mm^2 germanium detector for at least 24 hours. Three gamma detectors were used in this study and will be referred to as 3KA, 3KB and 3KC. The ^{210}Pb, ^{234}Th, ^{214}Pb and ^{7}Be are determined from gamma emissions at 46.5, 63.3, 352.0 and 477.6-keV, respectively (Fig. A1-1). The efficiency of each detector was used to convert counts per minute (cpm) for each radionuclide to disintegrations per minute (A; dpm) from:

$$A = (cpm - bkg) \div D_{Eff} \qquad (A1\text{-}1)$$

where bkg is the background count rate (cpm) at 46.5, 63.3, 352.0 and 477.6-keV for each detector and D_{Eff} is the efficiency of each detector at that energy (including the branching ratio).

The efficiency of each detector for ^{210}Pb, ^{234}Th, ^{214}Pb and ^{7}Be was measured using liquid standards and a well-analyzed sediment standard. At energy levels below 200-keV, some gamma emissions may be absorbed by the sediment (sample self-absorption), and this fraction is a function of sample density. To account for changes in self-absorption due to differences in sediment densities, the detectors were calibrated for ^{210}Pb and ^{234}Th using liquid standards with varying densities. Density differences between the standards were achieved by dissolving $PbNO_3$ into distilled water in 125 ml and 30 ml Nalgene wide-mouth jars (125 ml jar used for subtidal samples; see Chapters 2 and 4; 30 ml jar used for gravity cores subsamples; see Chapter 3) and then spiking each jar with ^{210}Pb (125 ml: 11125.7 dpm; 30 ml: 432.3 dpm) and ^{234}Th (125 ml: 2278.4 dpm;

30 ml: 795.5 dpm). Each standard was then each analyzed on the 3 Canberra gamma detectors and the cpm for ^{210}Pb and ^{234}Th was determined for each of these standards.

To calibrate for the self-absorption in each standard, an ^{241}Am (59.5-keV) source was placed on top of the standard and counted for 10 seconds to measure the transmission through each standard (T). The ^{241}Am source was then counted in the same manner through an empty jar (T_0) to determine the transmission of the source with no self-absorption. The ratio of T to T_0 was then plotted versus the ratio of cpm of ^{210}Pb and ^{234}Th in the standard and the known activity of ^{210}Pb and ^{234}Th of the standard. The linear relationship between T/T_0 and cpm/dpm demonstrates the self-absorption that occurs at the lower energies (< 200-keV) where increased density results in a lower T/T_0 and a lower cpm/dpm ratio (Figs. A1-2 to A1-5).

A similar measured of T/T_0 was made for each sediment sample and the activity of ^{210}Pb and ^{234}Th (in dpm) was then calculated for the sample by using the appropriate county efficiency at that T/T_0. Using detector 3KA as an example (Fig. A1-3A), the equation to convert from cpm to dpm for ^{234}Th (125 ml jar) is then:

$$A = (\text{cpm} - \text{background}) \div [0.001709 \times (T/T_0) + 0.001401] \qquad \text{(A1-2)}$$

where cpm is the counts per minute measured in each subtidal sample, T is the transmission of the ^{241}Am source through the sample, counted over 10 seconds and T_0 is the transmission of the ^{241}Am source through an empty jar. Using this method, the self-absorption of gammas at low energies and with varying densities can take into account for each sample. The plots of the standard data using the 125 ml jars (used in the subtidal

surficial sediment and marsh sampling; see Chapters 2, 4 and 5) and the 30 ml jars (used for counting the gravity cores; see Chapter 3) are shown in Figs. A1-2 to A1-5.

The detector efficiencies for the higher energy gamma emitters ^{214}Pb and ^{7}Be, were calculated using the well-analyzed sediment standard, IAEA-300. The IAEA-300 sediment was counted in the 30 ml Nalgene jar (used for the gravity cores; see Chapter 3) and the 125 ml Nalgene jar (used for subtidal samples; see Chapters 2 and 4) for ~ 24 hours on each detector. The detector efficiency at the ^{214}Pb (352-keV) peak was determined directly from the sediment standard by comparing the cpm from each detector to the know activity (D_{eff} = cpm/dpm; Table A1-1). The efficiency of each detector for ^{7}Be (477-keV) was determined using the equation of a power regression between the ^{226}Ra (186.0-keV), ^{214}Pb (352-keV) and ^{137}Cs (661.6-keV) and the cpm/(dpm × branching ratio) for each radionuclide (Table A1-1; Figs. A1-5, A1-6). The efficiency of the ^{214}Pb and ^{7}Be for the 30 ml and 125 ml wide-mouth Nalgene jars for each of the detectors is compiled in Table A1-2.

Excess ^{210}Pb and ^{234}Th as used in this study, were determined by subtracting out the parent activities (^{226}Ra and ^{238}U, respectively).

$$^{210}Pb_{xs} = {}^{210}Pb_{total} - {}^{210}Pb_{supported} \qquad \text{(A1-3)}$$

where $^{210}Pb_{xs}$ is the excess ^{210}Pb activity in dpm g^{-1}, $^{210}Pb_{total}$ is the total ^{210}Pb activity measured in the sample in dpm g^{-1} and $^{210}Pb_{supported}$ is the ^{210}Pb activity supported by the decay of its parent isotope ^{226}Ra, as determined from the ^{214}Pb activity in each sample in dpm g^{-1}. The supported ^{210}Pb (^{226}Ra) in the Jamaica Bay gravity cores ranged from 0.5 to 2.0 dpm g^{-1} (mean ~ 1.6 dpm g^{-1}). In the cores taken in Jamaica Bay excess ^{210}Pb activity

(dpm g^{-1}), generally, approaches 0 (± 0.5 dpm g^{-1}) at depths greater than 44 cm (see Tables A2-17 to A2-24).

Excess ^{234}Th was calculated from:

$$\text{Excess } ^{234}\text{Th}_{\text{sampling}} = [\text{Total } ^{234}\text{Th}_{\text{counting}} - ^{234}\text{Th}_{\text{supported}}] \times \exp(\lambda_{\text{Th}} \times \Delta t) \qquad \text{(A1-4)}$$

where Excess $^{234}Th_{sampling}$ is the excess ^{234}Th activity at the time of sampling (dpm g^{-1}), Total $^{234}Th_{counting}$ is the activity of ^{234}Th during the initial counting (dpm g^{-1}), $^{234}Th_{supported}$ is the activity of ^{234}Th (dpm g^{-1}) measured by recounting the sediment sampling 4-5 months after the sampling, λ_{Th} is the decay constant of ^{234}Th (0.02886 d^{-1}) and Δt is the time of decay (in days) between sample collection and counting. The supported ^{234}Th activity in the subtidal sediments ranged from 0.1 – 2.5 dpm g^{-1} (mean ~ 1.7 dpm g^{-1}; Tables A2-3, A2-7, A2-11 and A2-15). Excess ^{234}Th activity in the subtidal sediments during the four sampling cruises ranged from -0.3 to 14.7dpm g^{-1}. Excess ^{234}Th activities that were ± 0.3 dpm g^{-1} were assumed to be equivalent 0 when calculating the $^{234}Th_{xs}$ inventories (Tables A2-4, A2-8, A2-12 and A2-16).

Table A1-1 Activity of ^{226}Ra, ^{214}Pb and ^{137}Cs in the sediment standard IAEA-300.

	Reference Date for Standard: 1/1/1993				**Count Date: 9/1/2010**	
	Energy (keV)	**Activity of Standard (dpm)**	**Branching Ratio (BR) of the Radionuclide**	**dpm × BR**	**cpm****	**cpm/dpm**
^{226}Ra	186.0	46.7	0.033			
^{235}U		2.3	0.53			
^{238}U		53.5	0.02			
Total				3.8	0.4	0.1
^{214}Pb	352.0	46.7	0.37	17.3	0.7	0.04
^{137}Cs	661.6	623.3*	0.85	530.0	10.8	0.02

* ^{137}Cs activity was corrected for decay between reference date and count date.
**Counts from 3KA for the 30 ml Nalgene Jar, see Fig. A1-6A for plotted data

Table A1-2 Detector efficiency for ^{214}Pb and ^{7}Be determined using sediment standard IAEA-300 for the 3K Canberra Gamma detectors

Geometry	Detector	cpm/dpm ^{214}Pb × BR (352.0 keV)	cpm/dpm ^{7}Be × BR (477 keV)
30 ml	3KA	0.014178	0.002987
	3KB	0.013846	0.002973
	3KC	0.017056	0.003191
125 ml	3KA	0.010852	0.002297
	3KB	0.010295	0.002166
	3KC	0.010410	0.002238

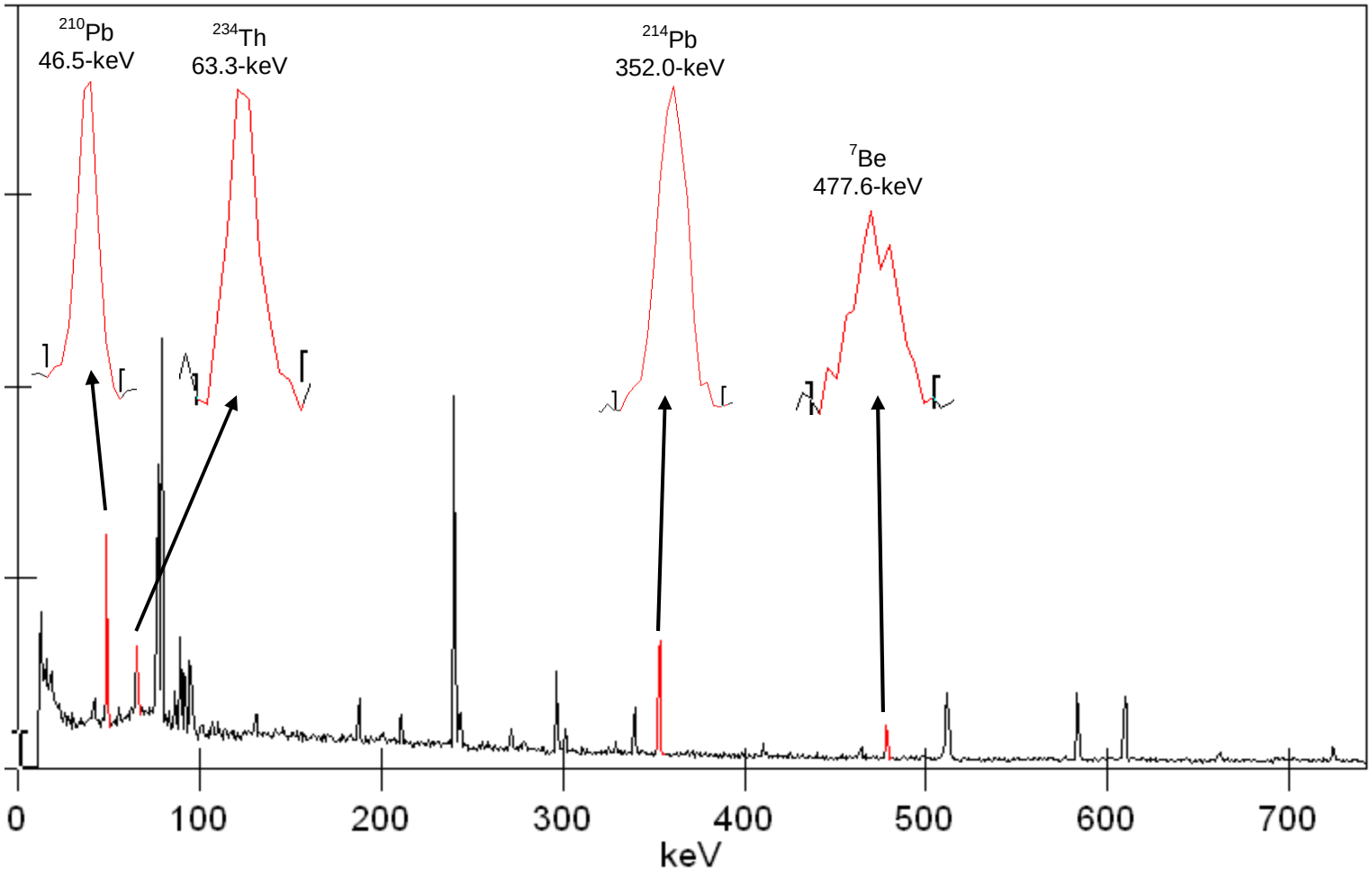
^{210}Pb
46.5-keV
^{234}Th
63.3-keV
^{214}Pb
352.0-keV
^{7}Be
477.6-keV
0
100
200
300
400
500
600
700
keV

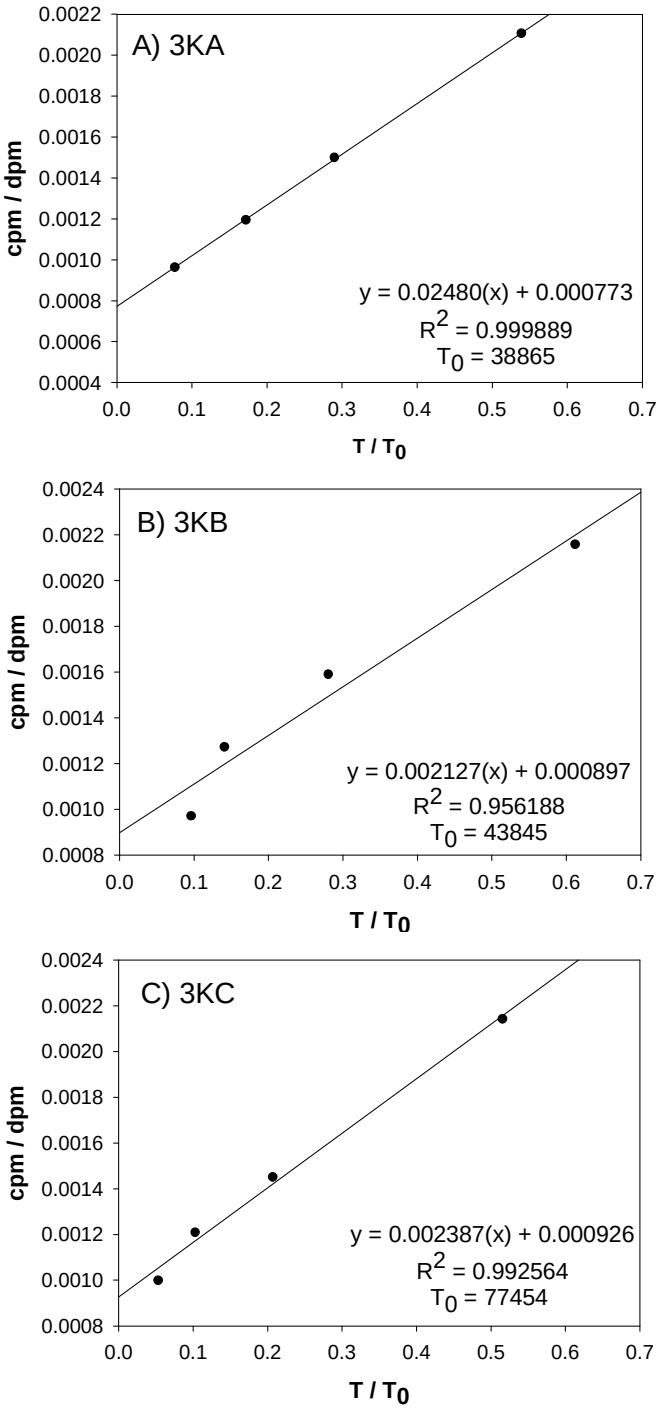

Figure A1-2 Linear relationship between cpm/dpm and T/T_0 using a 125 ml Nalgene jar. This relationship is used to calculate the detector efficiencies at the ^{210}Pb (46.5 keV) peak, where cpm is counts per minute, dpm is the known activity of the standards, T is the transmission of an ^{241}Am source through the sediment sample and T_0 is the transmission of the ^{241}Am source through an empty jar.

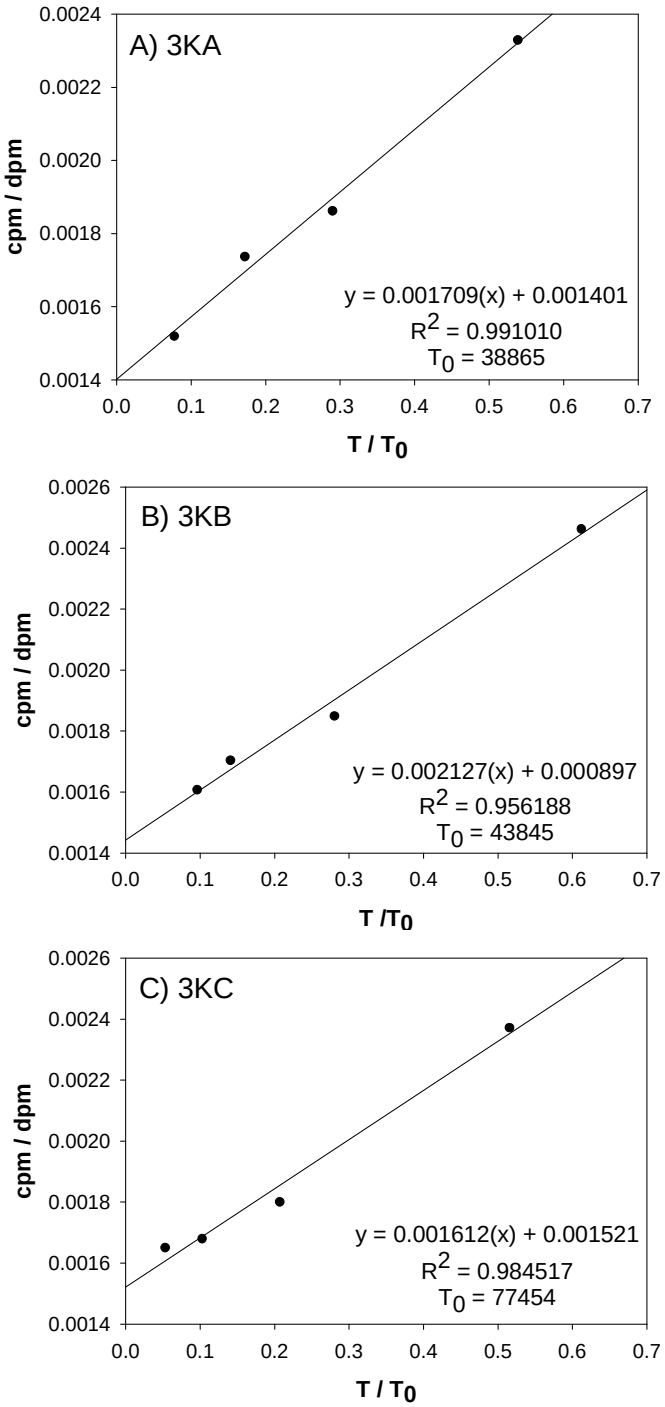

Figure A1-3 Linear relationship between cpm/dpm and T/T_0 using a 125 ml Nalgene jar. This relationship is used to calculate the detector efficiencies at the ^{234}Th (63.3 keV) peak, where cpm is counts per minute, dpm is the known activity of the standards, T is the transmission of an ^{241}Am source through the sediment sample and T0 is the transmission of the ^{241}Am source through an empty jar.

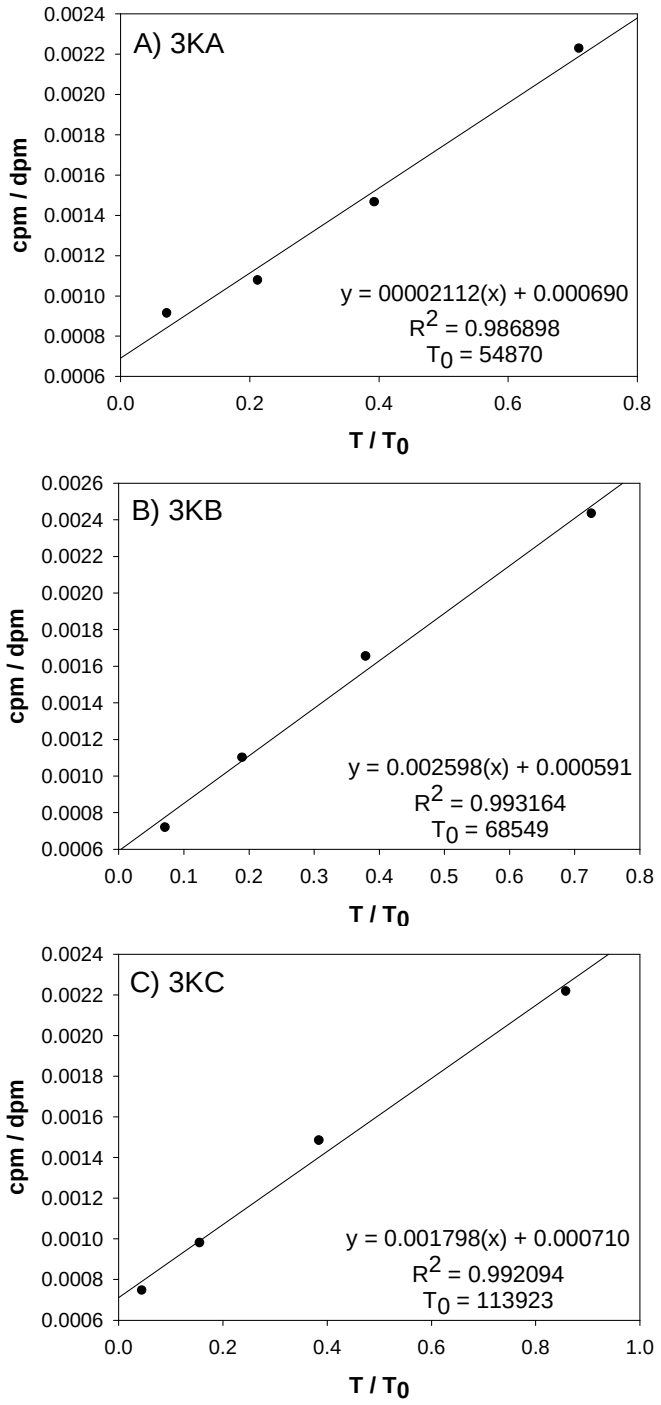

Figure A1-4 Linear relationship between cpm/dpm and T/T_0 using a 30 ml Nalgene jar. This relationship is used to calculate the detector efficiencies at the ^{210}Pb (46.5 keV) peak, where cpm is counts per minute, dpm is the known activity of the standards, T is the transmission of an ^{241}Am source through the sediment sample and T0 is the transmission of the ^{241}Am source through an empty jar.

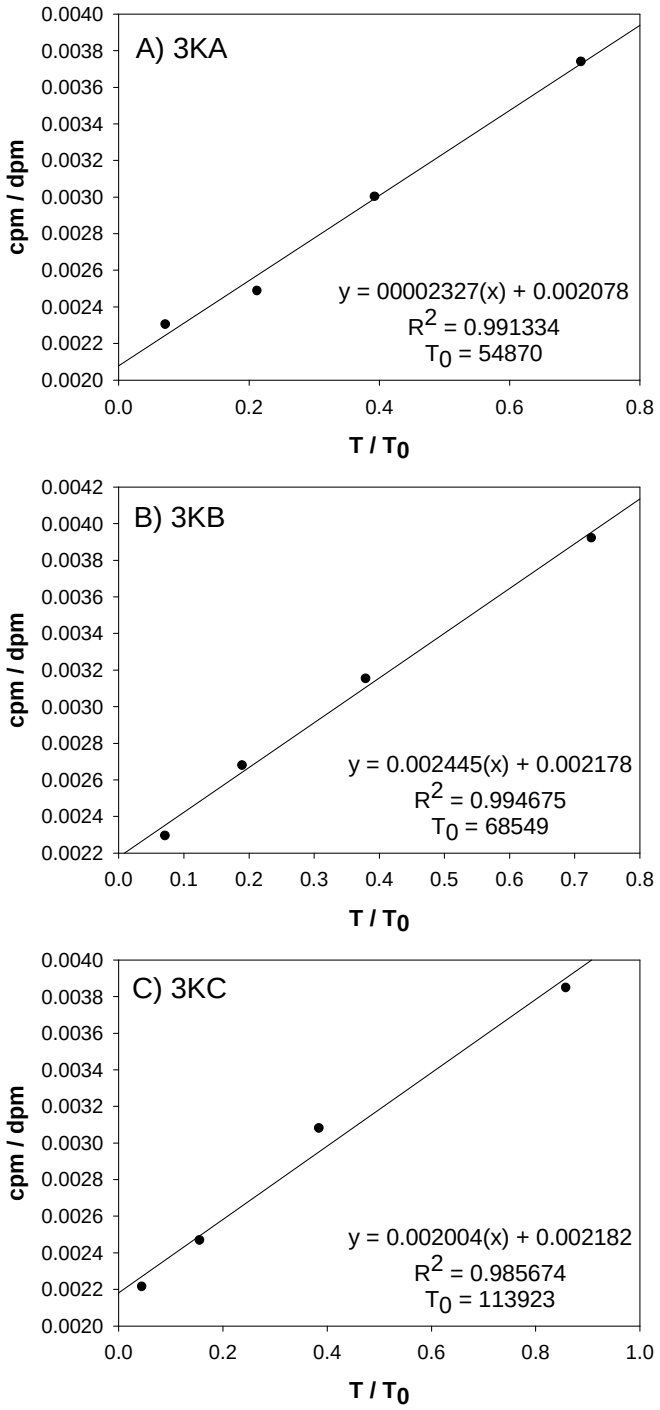

Figure A1-4 Linear relationship between cpm/dpm and T/T_0 using a 30 ml Nalgene jar. This relationship is used to calculate the detector efficiencies at the ^{234}Th (63.3 keV) peak, where cpm is counts per minute, dpm is the known activity of the standards, T is the transmission of an ^{241}Am source through the sediment sample and T0 is the transmission of the ^{241}Am source through an empty jar.

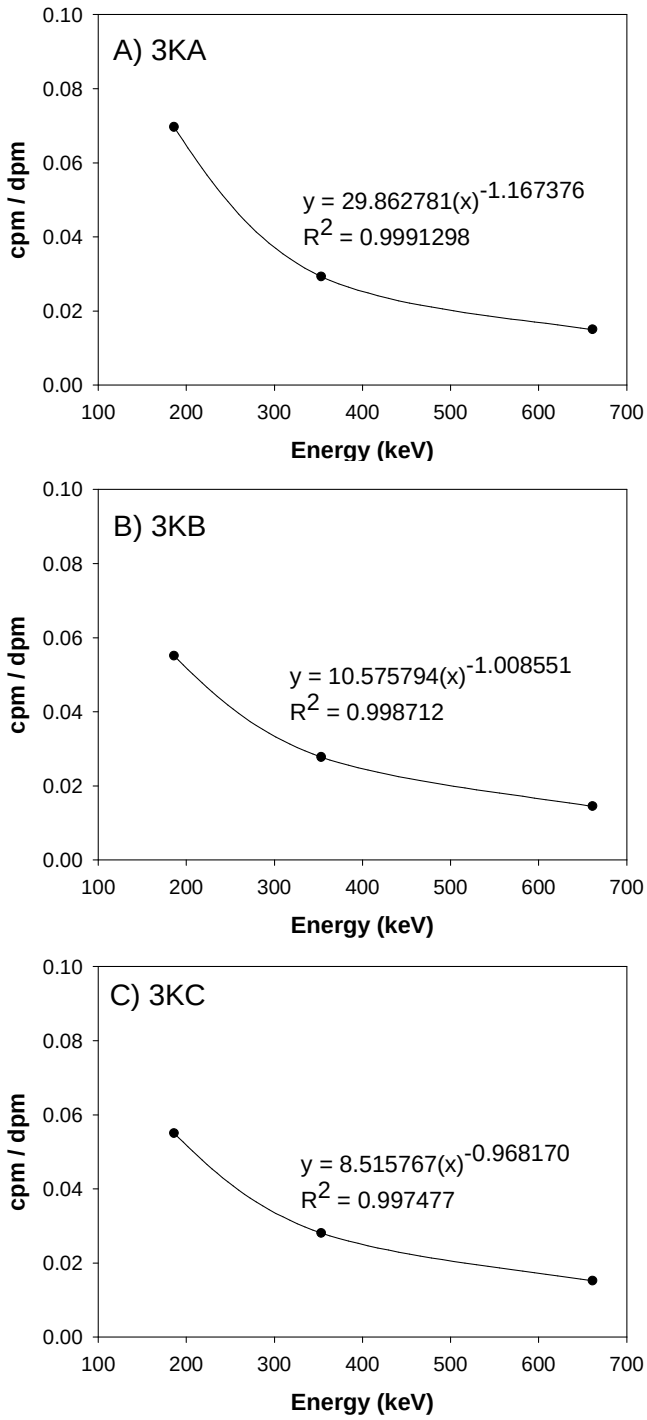

Figure A1-5 Relationship between detector efficiency (cpm/dpm) and the energy spectra using the sediment standard IAEA-300 on the Canberra gamma detectors (125 ml Nalgene jar).

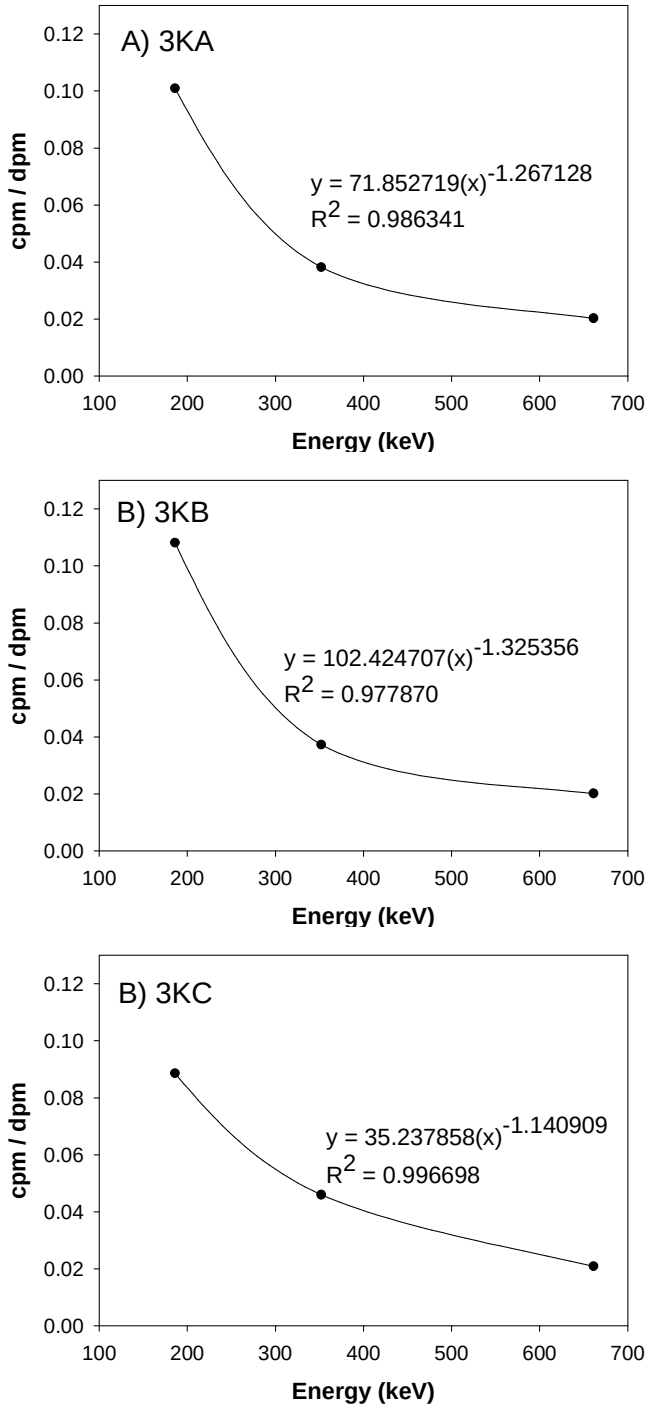

Figure A1-6 Relationship between detector efficiency (cpm/dpm) and the energy spectra using the sediment standard IAEA-300 on the Canberra gamma detectors (30 ml Nalgene jar).

APPENDIX 2

Table A2-1. September-2004 sample site coordinates, dry bulk density and sediment description.

Sample Date	Sample ID	Latitude	Longitude	Dry Bulk Density	Sediment Description
9/16/04	JB9-04-2	40 37.5498	73 49.9669	1.4	sandy
9/16/04	JB9-04-3	40 37.4332	73 50.0831	1.8	silty sand
9/16/04	JB9-04-4	40 36.5666	73 50.2336	1.8	sand
9/16/04	JB9-04-5	40 35.2334	73 50.3666	0.6	anoxic mud
9/16/04	JB9-04-6	40 36.1498	73 51.0337	1.7	sandy hermit crabs
9/16/04	JB9-04-7	40 36.3502	73 49.8331	1.9	fine sand, grey, hermit
9/16/04	JB9-04-8	40 36.0330	73 49.8500	1.4	black silty, mud
9/16/04	JB9-04-9	40 34.8999	73 50.2001	0.4	grey mud
9/16/04	JB9-04-10	40 34.8999	73 50.2001	1.0	grey mud
9/16/04	JB9-04-11	40 35.0167	73 51.0169	1.8	grey, silt, fine sand
9/16/04	JB9-04-12	40 35.1831	73 51.2835	1.9	fine sand, oxic layer
9/16/04	JB9-04-13	40 34.9001	73 52.3503	2.1	fine/medium sand
9/16/04	JB9-04-14	40 35.3333	73 52.3168	1.5	fine sand, black
9/16/04	JB9-04-15	40 36.0497	73 51.5665	2.2	fine sand, shell hash
9/16/04	JB9-04-16	40 36.3497	73 51.2997	1.2	fine sand, worm tube
9/16/04	JB9-04-17	40 37.3497	73 51.4664	1.7	fine sand
9/16/04	JB9-04-18B	40 37.1999	73 51.1831	1.8	fine sand
9/16/04	JB9-04-19	40 37.2000	73 51.2001	1.3	fine sand
9/16/04	JB9-04-20A	40 36.1668	73 53.1502	0.2	fine mud
9/16/04	JB9-04-20B	40 36.1668	73 53.1502	0.2	fine mud
9/16/04	JB9-04-21	40 37.3498	73 53.1334	0.5	fine organic gray mud
9/16/04	JB9-04-22	40 37.3500	73 52.9334	0.6	anoxic mud
9/16/04	JB9-04-22B	40 37.3500	73 52.9334	0.3	anoxic mud
9/16/04	JB-04-23	40 37.6834	73 52.7001	2.1	fine sand
9/16/04	JB9-04-25	40 37.9002	73 51.4336	1.6	fine sand

Table A2-1. Continued.

9/16/04	JB9-04-26	40 38.2665	73 51.1499	1.5	fine sand
9/16/04	JB-04-27A	40 38.1333	73 50.1497	1.9	anoxic mud
9/16/04	JB9-04-27C	40 38.1333	73 50.1497	0.5	anoxic mud
9/16/04	JB9-04-29C	40 38.1501	73 49.4165	0.5	anoxic mud
9/16/04	JB9-04-30	40 38.0830	73 48.3002	0.5	anoxic mud
9/16/04	JB9-04-31	40 37.6831	73 47.2169	0.2	anoxic mud
9/16/04	JB9-04-32	40 37.4833	73 46.9836	0.3	anoxic mud
9/16/04	JB9-04-33	40 37.4999	73 47.1663	0.3	anoxic mud
9/16/04	JB9-04-33B	40 37.4999	73 47.1663	1.0	anoxic mud
9/16/04	JB9-04-34	40 37.2997	73 46.5833	0.4	mud
9/16/04	JB9-04-35	40 36.9665	73 46.4667	1.9	sand
9/17/04	JB9-04-36	40 36.5500	73 46.4332	2.0	sand
9/17/04	JB9-04-38	40 25.7330	73 46.9837	2.1	medium sand
9/17/04	JB9-04-39	40 36.0163	73 47.1832	0.7	anoxic mud
9/17/04	JB9-04-40	40 35.8664	73 47.3668	1.3	sandy, oxidized layer
9/17/04	JB9-04-41	40 35.8664	73 47.3668	0.7	mud
9/17/04	JB9-04-44	40 35.3666	73 49.2667	1.8	sand
9/17/04	JB9-04-45	40 36.8834	73 52.3666	1.9	fine snad
9/17/04	JB9-04-46	40 37.7665	73 51.6331	1.5	very fine sand
9/17/04	JB9-04-47	40 37.6832	73 51.2500	1.4	fine sand
9/17/04	JB9-04-48	40 37.6911	73 50.3099	1.2	anoxic silty mud
9/17/04	JB9-04-50	40 37.8830	73 48.9834	1.7	fine sand
9/17/04	JB9-04-51	40 37.6833	73 48.5833	1.9	large live clam, mud
9/17/04	JB9-04-52	40 37.3831	73 48.5666	0.5	anoxic mud
9/17/04	JB9-04-53	40 37.1664	73 48.5166	0.2	mud
9/17/04	JB9-04-54	40 36.9664	73 48.4669	0.3	mud
9/17/04	JB9-04-55	40 36.8333	73 48.4501	0.2	muddy with some shells
9/17/04	JB9-04-56	40 36.8997	73 48.4501	0.6	silty mud
9/17/04	JB9-04-57	40 36.2498	73 48.3165	0.5	mud
9/17/04	JB9-04-58	40 36.4831	73 48.6670	1.0	mud
9/17/04	JB9-04-59	40 38.2167	73 49.3167	1.6	fine sand

Table A2-1. Continued.

9/17/04	JB9-04-61	40 36.5333	73 48.3498	0.5	mud
9/17/04	JB9-04-62	40 37.6333	73 45.7834	0.4	mud

Table A2-2. September-2004 $^{210}Pb_{xs}$ activity in subtidal surficial (0-5 cm) samples.

SAMPLE ID	Total Pb-210 (dpm g^{-1})	Error (±)	Supported Pb-210 (dpm g^{-1})	Error (±)	Excess Pb-210 (dpm g^{-1})	Error (±)
JB9-04-2	3.1	0.1	0.2	0.0	2.8	0.1
JB9-04-3	3.2	0.1	2.1	0.0	1.1	0.1
JB9-04-4	2.5	0.1	1.6	0.0	0.9	0.1
JB9-04-5	8.4	0.3	2.3	0.1	6.1	0.3
JB9-04-6	2.1	0.1	1.3	0.0	0.9	0.1
JB9-04-7	2.4	0.1	1.5	0.0	0.9	0.1
JB9-04-8	4.1	0.1	1.9	0.0	2.2	0.1
JB9-04-9	7.9	0.4	1.9	0.1	6.1	0.4
JB9-04-10	6.5	0.2	2.3	0.0	4.2	0.2
JB9-04-11	1.8	0.1	0.7	0.0	1.0	0.1
JB9-04-12	3.1	0.1	2.2	0.0	0.9	0.1
JB9-04-13	0.5	0.1	0.4	0.0	0.1	0.1
JB9-04-14	4.0	0.1	1.5	0.0	2.5	0.1
JB9-04-15B	2.0	0.1	0.9	0.0	1.1	0.1
JB9-04-16	4.9	0.1	3.4	0.1	1.5	0.2
JB9-04-17	2.7	0.1	1.9	0.0	0.8	0.1
JB9-04-18B	3.3	0.1	2.2	0.0	1.2	0.1
JB9-04-19	2.0	0.1	1.0	0.0	0.9	0.1
JB9-04-20A	15.9	0.6	1.6	0.1	14.3	0.6
JB9-04-20B	10.0	0.3	1.8	0.1	8.2	0.4
JB9-04-21	12.0	0.3	1.8	0.1	10.2	0.3
JB9-04-22	8.8	0.2	1.9	0.1	6.9	0.2
JB9-04-22B	16.2	0.6	2.5	0.1	13.8	0.6
JB-04-23	1.5	0.1	1.0	0.0	0.4	0.1
JB9-04-25	4.1	0.1	2.6	0.0	1.5	0.2
JB9-04-26	4.2	0.2	2.2	0.0	2.1	0.2
JB-04-27A	2.9	0.1	1.9	0.0	1.0	0.1
JB9-04-27C	8.0	0.2	2.0	0.1	6.0	0.2
JB9-04-29C	7.8	0.2	1.8	0.1	6.0	0.3

Table A2-2. Continued.

JB9-04-30	9.5	0.3	1.3	0.1	8.1	0.3
JB9-04-31	13.2	0.5	1.6	0.1	11.6	0.5
JB9-04-32	9.9	0.4	1.7	0.1	8.2	0.4
JB9-04-33	12.5	0.4	4.7	0.1	7.8	0.4
JB9-04-33B	2.2	0.1	0.7	0.0	1.5	0.1
JB9-04-34	12.3	0.4	0.2	0.0	12.1	0.4
JB9-04-35	3.4	0.1	2.1	0.0	1.2	0.1
JB9-04-36	0.7	0.1	0.4	0.0	0.2	0.1
JB9-04-38	3.1	0.1	2.1	0.0	1.0	0.1
JB9-04-39	7.4	0.2	1.7	0.1	5.7	0.2
JB9-04-40	2.4	0.1	1.4	0.0	1.0	0.1
JB9-04-41	7.3	0.2	1.6	0.1	5.7	0.3
JB9-04-44	4.2	0.1	1.0	0.0	3.3	0.1
JB9-04-45	2.7	0.1	1.6	0.0	1.2	0.1
JB9-04-46	4.4	0.1	2.8	0.0	1.6	0.1
JB9-04-47	3.9	0.1	2.8	0.0	1.1	0.1
JB9-04-48	4.0	0.1	1.8	0.0	2.2	0.1
JB9-04-50	3.0	0.1	2.1	0.0	0.9	0.1
JB9-04-51	2.7	0.1	2.3	0.0	0.4	0.1
JB9-04-52	3.2	0.3	1.4	0.1	1.8	0.3
JB9-04-53	3.4	0.5	1.6	0.1	1.8	0.5
JB9-04-54	2.7	0.3	1.8	0.1	0.9	0.4
JB9-04-55	3.4	0.4	1.8	0.1	1.5	0.4
JB9-04-56	3.9	0.2	2.6	0.1	1.2	0.2
JB9-04-57	4.1	0.3	2.0	0.1	2.0	0.3
JB9-04-58	4.0	0.2	1.9	0.0	2.0	0.2
JB9-04-59	2.1	0.1	1.2	0.0	0.9	0.1
JB9-04-61	7.5	0.3	1.8	0.1	5.7	0.3
JB9-04-62	11.6	0.3	1.7	0.1	9.9	0.3

Table A2-3. September-2004 ^{234}Th activities in subtidal samples.

SAMPLE ID	Total Th-234 Activity (dpm g^{-1})	Error (±)	Supported Th-234 Activity (dpm g^{-1})	Error (±)	Excess Th-234 Activity (dpm g^{-1})	Error (±)
JB9-04-2	3.4	0.2	2.1	0.2	1.2	0.3
JB9-04-3	2.5	0.2	1.8	0.1	0.6	0.2
JB9-04-4	1.5	0.1	1.5	0.1	0.0	0.1
JB9-04-5	4.5	0.7	1.6	0.4	2.9	0.8
JB9-04-6	1.3	0.1	1.3	0.1	0.0	0.2
JB9-04-7	2.2	0.1	1.5	0.1	0.7	0.1
JB9-04-8	2.5	0.2	1.8	0.2	0.7	0.3
JB9-04-9	2.5	0.4	2.0	0.3	0.5	0.5
JB9-04-10	3.7	0.4	2.1	0.2	1.6	0.5
JB9-04-11	1.8	0.1	1.3	0.1	0.5	0.1
JB9-04-12	3.3	0.3	2.4	0.2	0.9	0.3
JB9-04-13	0.3	0.1	0.3	0.1	0.0	0.1
JB9-04-14	1.9	0.1	1.6	0.1	0.4	0.2
JB9-04-15B	2.2	0.2	1.0	0.1	1.1	0.2
JB9-04-16	3.1	0.3	2.0	0.2	1.1	0.4
JB9-04-17	1.8	0.1	1.7	0.1	0.2	0.1
JB9-04-18B	3.1	0.3	1.3	0.1	1.8	0.3
JB9-04-19	2.9	0.3	1.0	0.1	1.9	0.3
JB9-04-20A	2.7	1.0	1.2	0.4	1.5	1.1
JB9-04-20B	4.0	0.0	2.4	0.0	1.6	0.0
JB9-04-21	3.1	0.4	1.4	0.3	1.7	0.5
JB9-04-22	3.4	0.3	1.9	0.1	1.5	0.4
JB9-04-22B	9.0	0.5	1.9	0.1	7.1	0.5
JB-04-23	1.5	0.1	1.0	0.1	0.5	0.2
JB9-04-25	2.5	0.2	2.2	0.2	0.3	0.2
JB9-04-26	1.3	0.1	1.6	0.2	-0.3	0.2
JB-04-27A	3.3	0.8	1.3	0.2	2.0	0.8
JB9-04-27C	4.9	0.6	1.9	0.2	3.0	0.6
JB9-04-29C	2.3	0.3	1.3	0.2	1.0	0.4
JB9-04-30	2.5	0.3	1.2	0.2	1.3	0.4
JB9-04-31	2.5	0.8	1.2	0.6	1.3	1.0
JB9-04-32	3.5	0.7	1.7	0.3	1.8	0.7

Table A2-3. Continued.

JB9-04-33	2.8	0.8	1.5	0.3	1.3	0.9
JB9-04-33B	1.2	0.1	1.2	0.1	0.0	0.1
JB9-04-34	2.3	0.2	1.8	0.2	0.5	0.2
JB9-04-35	3.6	0.4	1.8	0.2	1.8	0.4
JB9-04-36	0.8	0.1	0.6	0.1	0.2	0.1
JB9-04-38	3.5	0.2	2.3	0.1	1.2	0.2
JB9-04-39	3.0	0.3	1.7	0.2	1.3	0.4
JB9-04-40	2.1	0.3	1.2	0.2	0.9	0.4
JB9-04-41	3.0	0.6	2.0	0.3	1.0	0.6
JB9-04-44	0.8	0.1	0.6	0.1	0.1	0.1
JB9-04-45	2.3	0.2	1.5	0.1	0.8	0.2
JB9-04-46	2.0	0.2	1.7	0.2	0.3	0.3
JB9-04-47	2.4	0.2	2.2	0.2	0.1	0.3
JB9-04-48	3.0	0.2	1.9	0.2	1.1	0.3
JB9-04-50	2.4	0.2	1.9	0.2	0.4	0.3
JB9-04-51	1.8	0.1	1.9	0.1	-0.1	0.1
JB9-04-52	1.4	0.3	1.2	0.2	0.2	0.3
JB9-04-53	3.3	0.7	1.6	0.4	1.7	0.8
JB9-04-54	1.9	0.5	1.2	0.4	0.7	0.6
JB9-04-55	3.5	0.6	1.6	0.3	1.9	0.7
JB9-04-56	2.0	0.2	1.8	0.2	0.2	0.3
JB9-04-57	1.3	0.3	1.1	0.3	0.2	0.4
JB9-04-58	1.8	0.2	1.5	0.1	0.3	0.2
JB9-04-59	3.7	0.2	1.4	0.1	2.3	0.2
JB9-04-61	1.4	0.3	1.0	0.2	0.4	0.4
JB9-04-62	2.8	0.2	1.8	0.1	1.0	0.2

Table A2-4. September-2004 $^{234}Th_{xs}$ and ^{7}Be inventories in subtidal samples (0-5 cm).

SAMPLE ID	Excess Th-234 Inventory (dpm cm^{-2})	Error (±)	Be-7 Inventory (dpm cm^{-2})	Error (±)
JB9-04-2	8.4	0.8	2.5	0.5
JB9-04-3	5.8	0.5	1.8	0.6
JB9-04-4	0.1	0.0	5.1	0.5
JB9-04-5	8.0	1.4	7.1	0.8
JB9-04-6	0.2	0.0	3.2	0.5
JB9-04-7	6.7	0.5	4.3	0.6
JB9-04-8	5.0	0.6	3.1	0.5
JB9-04-9	1.0	0.2	4.5	0.3
JB9-04-10	8.0	1.3	15.7	0.8
JB9-04-11	4.5	0.4	1.0	0.5
JB9-04-12	8.4	0.6	2.1	0.7
JB9-04-13	0.3	0.0	0.4	0.3
JB9-04-14	2.8	0.0	0.0	0.0
JB9-04-15B	12.8	1.5	0.4	0.5
JB9-04-16	6.4	0.5	7.1	0.8
JB9-04-17	1.4	0.1	2.0	0.7
JB9-04-18B	16.0	1.7	3.4	0.6
JB9-04-19	12.3	2.9	0.0	0.0
JB9-04-20A	1.3	0.6	9.9	0.5
JB9-04-20B	1.8	0.2	7.1	0.6
JB9-04-21	4.2	0.5	25.8	0.9
JB9-04-22	4.3	0.9	5.8	0.6
JB9-04-22B	11.5	0.8	19.2	1.5
JB-04-23	5.2	0.5	1.8	0.8
JB9-04-25	2.6	0.3	2.0	0.5
JB9-04-26	-2.4	0.0	4.7	0.5
JB-04-27A	19.4	2.6	0.6	1.0
JB9-04-27C	7.8	1.1	8.7	0.6
JB9-04-29C	2.2	0.2	0.9	0.3
JB9-04-30	3.1	0.3	0.3	0.3
JB9-04-31	1.2	0.3	0.0	0.0
JB9-04-32	2.4	0.7	0.0	0.0

Table A2-4. Continued.

JB9-04-33	2.1	0.8	0.1	0.3
JB9-04-33B	0	0.1	0.5	0.3
JB9-04-34	0.9	0.1	3.9	0.4
JB9-04-35	16.7	2.1	2.7	1.2
JB9-04-36	2.5	0.0	0.1	0.4
JB9-04-38	12.0	0.7	0.5	0.6
JB9-04-39	4.1	0.4	0.7	0.6
JB9-04-40	6.3	1.3	1.0	0.4
JB9-04-41	3.3	1.2	6.3	0.6
JB9-04-44	1.3	0.2	0.0	0.0
JB9-04-45	7.5	0.8	5.6	0.7
JB9-04-46	2.6	0.2	2.7	0.6
JB9-04-47	0.9	0.1	2.8	0.5
JB9-04-48	6.5	0.7	0.3	0.5
JB9-04-50	3.6	0.4	0.5	0.5
JB9-04-51	0.0	0.0	6.0	0.6
JB9-04-52	0.4	0.0	0.4	0.0
JB9-04-53	2.0	0.5	6.4	0.6
JB9-04-54	1.1	0.2	7.4	0.5
JB9-04-55	2.3	1.2	6.8	0.5
JB9-04-56	0.5	0.1	4.2	0.4
JB9-04-57	0.5	0.1	5.4	0.4
JB9-04-58	1.5	0.1	0.1	0.3
JB9-04-59	17.9	1.8	0.9	0.4
JB9-04-61	1.0	0.1	7.9	0.5
JB9-04-62	2.2	0.2	0.2	0.3

Table A2-5. May-2005 sample site coordinates, dry bulk density and sediment description

Sample Date	Sample ID	Latitude	Longitude	Dry Bulk Density	Sediment Description
5/19/2005	JB5-05-1	40 37.3483	73 50.3513	0.2	organic mud
5/19/2005	JB5-05-2	40 38.3644	73 50.2365	1.5	muddy sand
5/19/2005	JB5-05-3	40 38.9117	73 51.2404	0.6	very fluffy mud
5/19/2005	JB5-05-4	40 38.6673	73 51.2814	1.1	silty mud
5/19/2005	JB5-05-5	40 38.4809	73 51.2967	0.3	mud
5/19/2005	JB5-05-6	40 38.3083	73 51.8786	0.8	fluffy mud
5/19/2005	JB5-05-7	40 37.7140	73 52.6740	1.1	muddy sand
5/19/2005	JB5-05-8	40 37.4104	73 53.2537	1.1	mud
5/19/2005	JB5-05-9	40 38.6097	73 49.2168	0.3	anoxic mud
5/19/2005	JB5-05-10	40 38.3003	73 49.3485	1.5	fine silty sand
5/19/2005	JB5-05-11	40 38.3071	73 49.0086	0.2	fluffy mud
5/19/2005	JB5-05-12	40 38.2900	73 48.2454	0.2	mud
5/19/2005	JB5-05-13	40 37.8299	73 47.9720	0.2	anoxic mud
5/19/2005	JB5-05-14	40 37.8165	73 47.5217	0.4	mud
5/19/2005	JB5-05-16	40 37.7419	73 48.5077	0.6	mud
5/19/2005	JB5-05-17	40 37.8363	73 49.0126	1.5	Sand
5/19/2005	JB5-05-18	40 37.4987	73 48.4511	0.4	fluffy mud
5/19/2005	JB5-05-19	40 37.1128	73 48.5104	0.3	fluffy mud
5/19/2005	JB5-05-20	40 36.7342	73 48.4349	0.3	mud
5/19/2005	JB5-05-21	40 36.3352	73 47.6966	1.5	mud
5/19/2005	JB5-05-22	40 36.8498	73 48.0661	0.5	mud
5/19/2005	JB5-05-23	40 35.6860	73 48.6790	1.6	mud
5/19/2005	JB5-05-24	40 36.2800	73 47.5912	0.6	mud
5/19/2005	JB5-05-25	40 36.6912	73 46.8058	0.7	fluffy mud
5/19/2005	JB5-05-26	40 37.2802	73 46.5837	0.5	fluffy mud
5/19/2005	JB5-05-27	40 36.8982	73 46.4488	0.7	fluffy mud
5/19/2005	JB5-05-28	40 37.4745	73 45.8991	1.0	sandy mud
5/19/2005	JB5-05-29	40 37.8571	73 45.2855	0.5	mud

Table A2-5. Continued.

5/20/2005	JB5-05-30	40 36.8182	73 53.2146	0.6	mud
5/20/2005	JB5-05-31	40 36.3891	73 53.3983	0.3	organic mud
5/20/2005	JB5-05-32	40 36.4461	73 52.6889	0.6	mud
5/20/2005	JB5-05-33	40 36.5973	73 52.5700	1.5	silty sand
5/20/2005	JB5-05-34	40 36.0185	73 52.6329	0.8	anoxic mud
5/20/2005	JB5-05-35	40 35.5523	73 52.3237	0.7	silty mud
5/20/2005	JB5-05-36	40 36.2166	73 52.0502	1.6	mud
5/20/2005	JB5-05-37	40 36.8265	73 51.7441	1.4	sand
5/20/2005	JB5-05-38	40 37.0221	73 51.3564	1.5	sand
5/20/2005	JB5-05-39	40 35.2055	73 52.2963	1.6	sand
5/20/2005	JB5-05-40	40 34.7055	73 52.3422	1.8	sand
5/20/2005	JB5-05-41	40 34.7716	73 51.8080	0.7	organic mud
5/20/2005	JB5-05-43	40 35.4141	73 51.6277	0.4	sand
5/23/2005	JB5-05-47	40 35.7995	73 50.9730	0.4	mud
5/23/2005	JB5-05-48	40 36.1986	73 51.1612	1.6	silty sand
5/23/2005	JB5-05-50	40 36.6144	73 50.8484	1.6	silty sand
5/23/2005	JB5-05-51	40 36.4685	73 50.2637	0.7	sandy mud
5/23/2005	JB5-05-52	40 36.2653	73 50.2076	0.8	silty sand
5/23/2005	JB5-05-53	40 36.1027	73 49.8445	1.4	silty sand
5/23/2005	JB5-05-54	40 36.0090	73 49.4483	0.3	mud
5/23/2005	JB5-05-55	40 36.6105	73 49.4931	0.4	mud
5/23/2005	JB5-05-56	40 36.1221	73 50.5370	1.6	sand
5/23/2005	JB5-05-57	40 36.0091	73 47.2649	0.2	mud
5/23/2005	JB5-05-58	40 35.7718	73 47.4210	0.3	mud

Table A2-6. May-2005 ^{210}Pb activities in subtidal samples.

Sample ID	Total Pb-210 (dpm g^{-1})	Error (±)	Supported Pb-210 (dpm g^{-1})	Error (±)	Excess Pb-210 (dpm g^{-1})	Error (±)
JB5-05-1	6.6	0.4	3.0	0.1	3.6	0.3
JB5-05-2	1.4	0.1	1.4	0.0	0.0	0.1
JB5-05-3	4.9	0.2	2.1	0.0	2.8	0.1
JB5-05-4	4.8	0.3	0.0	0.0	4.8	0.3
JB5-05-5	10.0	0.4	2.1	0.1	7.9	0.5
JB5-05-6	3.0	0.1	0.8	0.0	2.1	0.1
JB5-05-7	2.3	0.1	1.3	0.0	0.9	0.1
JB5-05-8	6.8	0.2	1.8	0.0	5.0	0.2
JB5-05-9	8.2	0.3	1.9	0.1	6.3	0.4
JB5-05-10	1.2	0.1	0.8	0.0	0.4	0.1
JB5-05-11	8.4	0.4	1.5	0.1	6.9	0.6
JB5-05-12	9.1	0.3	1.5	0.1	7.6	0.6
JB5-05-13	8.8	0.3	1.6	0.1	7.2	0.5
JB5-05-14	5.0	0.2	1.1	0.1	3.9	0.3
JB5-05-16	7.3	0.4	1.5	0.1	5.8	0.5
JB5-05-17	3.2	0.1	3.5	0.0	-0.3	0.1
JB5-05-18	6.6	0.3	1.5	0.1	5.1	0.3
JB5-05-19	6.7	0.3	2.3	0.1	4.3	0.2
JB5-05-20	0.0	0.0	0.0	0.0	0.0	0.0
JB5-05-21	8.0	0.3	2.1	0.1	5.9	0.4
JB5-05-22	3.7	0.2	3.9	0.1	-0.2	0.0
JB5-05-23	0.4	0.1	0.4	0.0	0.0	0.1
JB5-05-24	8.1	0.4	1.9	0.1	6.2	0.4
JB5-05-25	9.1	0.3	2.2	0.1	6.9	0.3
JB5-05-26	10.1	0.3	1.4	0.1	8.7	0.5
JB5-05-27	4.4	0.2	1.6	0.0	2.8	0.1
JB5-05-28	3.6	0.2	0.7	0.0	2.9	0.2
JB5-05-29	5.7	0.2	1.1	0.0	4.6	0.3
JB5-05-30	7.1	0.2	1.7	0.0	5.4	0.2
JB5-05-31	10.5	0.4	1.9	0.1	8.6	0.6
JB5-05-32	5.5	0.2	1.9	0.1	3.6	0.2
JB5-05-33	1.7	0.1	1.7	0.0	0.0	0.1
JB5-05-34	8.7	0.3	2.1	0.1	6.6	0.3
JB5-05-35	4.5	0.2	1.9	0.0	2.6	0.1

Table A2-6. Continued.

JB5-05-36	2.2	0.1	2.7	0.0	-0.4	0.1
JB5-05-37	2.3	0.1	2.9	0.1	-0.6	0.1
JB5-05-38	1.3	0.1	1.5	0.0	-0.2	0.1
JB5-05-39	0.6	0.1	0.8	0.0	-0.2	0.1
JB5-05-40	3.4	0.1	1.0	0.0	2.4	0.1
JB5-05-41	12.2	0.5	10.6	0.1	1.6	0.1
JB5-05-43	1.9	0.2	2.2	0.1	-0.3	0.1
JB5-05-47	5.5	0.2	2.2	0.1	3.4	0.2
JB5-05-48	3.4	0.1	0.7	0.0	2.7	0.1
JB5-05-50	1.4	0.1	1.3	0.0	0.1	0.1
JB5-05-51	3.7	0.2	2.2	0.0	1.5	0.1
JB5-05-52	1.2	0.1	1.2	0.0	0.0	0.1
JB5-05-53	3.4	0.2	3.3	0.0	0.1	0.1
JB5-05-54	7.5	0.3	2.0	0.1	5.5	0.3
JB5-05-55	7.8	0.3	2.1	0.1	5.7	0.3
JB5-05-56	3.1	0.2	2.4	0.0	0.7	0.1
JB5-05-57	10.8	0.4	1.8	0.1	9.0	0.6
JB5-05-58	8.7	0.4	1.5	0.1	7.2	0.6

Table A2-7. May-2005 ^{234}Th activities in subtidal sediments.

SAMPLE ID	Total Th-234 (dpm g^{-1})	Error (±)	Supported Th-234 (dpm g^{-1})	Error (±)	Excess Th-234 (dpm g^{-1})	Error (±)
JB5-05-1	2.5	0.3	2.4	0.4	0.1	0.5
JB5-05-2	1.2	0.1	1.1	0.1	0.1	0.1
JB5-05-3	4.0	0.2	2.2	0.2	1.8	0.2
JB5-05-4	4.0	0.4	2.4	0.2	1.6	0.4
JB5-05-5	3.6	0.4	2.1	0.2	1.6	0.4
JB5-05-6	2.0	0.2	1.7	0.2	0.3	0.3
JB5-05-7	1.8	0.2	0.7	0.1	1.2	0.2
JB5-05-8	3.5	0.3	2.3	0.2	1.2	0.4
JB5-05-9	2.5	0.3	2.0	0.1	0.5	0.3
JB5-05-10	0.9	0.1	0.8	0.1	0.1	0.1
JB5-05-11	1.8	0.7	2.1	0.1	-0.3	0.7
JB5-05-12	2.5	0.4	2.5	0.4	-0.1	0.5
JB5-05-13	2.3	0.2	2.3	0.2	0.0	0.3
JB5-05-14	3.4	0.7	2.8	0.2	0.6	0.7
JB5-05-16	3.6	0.3	2.2	0.2	1.4	0.4
JB5-05-17	3.6	0.4	2.2	0.1	1.4	0.4
JB5-05-18	3.9	0.6	3.0	0.3	0.9	0.7
JB5-05-19	5.0	0.4	2.4	0.2	2.6	0.5
JB5-05-20	3.5	0.2	2.4	0.1	1.1	0.2
JB5-05-21	1.9	0.3	1.8	0.2	0.1	0.3
JB5-05-22	2.4	0.0	1.8	0.2	0.6	0.2
JB5-05-23	0.3	0.3	0.3	0.1	0.0	0.3
JB5-05-24	3.9	0.2	2.4	0.2	1.5	0.3
JB5-05-25	2.0	0.3	2.3	0.2	-0.3	0.4
JB5-05-26	3.0	0.3	2.2	0.1	0.8	0.4
JB5-05-27	3.5	0.3	2.0	0.1	1.4	0.3
JB5-05-28	3.7	0.3	2.3	0.1	1.4	0.3
JB5-05-29	2.9	0.2	2.5	0.2	0.4	0.2
JB5-05-30	3.0	0.6	2.4	0.2	0.6	0.6
JB5-05-31	4.4	0.6	2.5	0.3	2.0	0.6
JB5-05-32	3.6	0.2	2.0	0.1	1.6	0.3
JB5-05-33	2.6	0.6	2.1	0.1	0.5	0.6
JB5-05-34	5.9	0.4	2.3	0.2	3.6	0.4
JB5-05-35	3.8	0.2	1.6	0.1	2.2	0.2

Table A2-7. Continued.

JB5-05-36	2.3	0.5	1.9	0.1	0.5	0.5
JB5-05-37	5.4	0.2	2.8	0.3	2.6	0.3
JB5-05-38	2.0	0.1	1.0	0.1	1.0	0.1
JB5-05-39	1.1	0.4	0.5	0.1	0.6	0.4
JB5-05-40	2.0	0.4	0.4	0.1	1.6	0.4
JB5-05-41	3.3	0.6	2.3	0.1	0.9	0.6
JB5-05-43	2.4	0.4	2.5	0.2	-0.1	0.4
JB5-05-47	5.0	0.2	2.4	0.1	2.6	0.2
JB5-05-48	2.0	0.3	0.6	0.0	1.3	0.3
JB5-05-50	2.2	0.4	1.1	0.1	1.1	0.4
JB5-05-51	4.7	0.3	2.5	0.2	2.2	0.3
JB5-05-52	3.4	0.4	1.7	0.2	1.7	0.4
JB5-05-53	3.8	0.3	2.5	0.1	1.3	0.3
JB5-05-54	4.5	0.7	2.6	0.2	1.9	0.8
JB5-05-55	5.9	0.4	3.4	0.2	2.5	0.5
JB5-05-56	1.5	0.7	0.6	0.1	0.9	0.7
JB5-05-57	13.1	3.4	2.8	0.3	10.3	3.4
JB5-05-58	17.1	2.4	2.4	0.3	14.7	2.4

Table A2-8. May-2005 $^{234}Th_{xs}$ and ^{7}Be inventories in subtidal samples.

SAMPLE ID	Excess Th-234 Inventory (dpm cm-2)	Error (±)	Be-7 Inventory (dpm cm^{-2})	Error (±)
JB5-05-1	0.1	0.0	3.7	0.3
JB5-05-2	1.0	0.1	4.0	0.9
JB5-05-3	4.2	0.4	2.2	0.2
JB5-05-4	5.2	0.5	1.5	0.4
JB5-05-5	2.1	0.3	9.5	0.5
JB5-05-6	1.3	0.2	2.4	0.3
JB5-05-7	4.2	0.0	2.8	0.4
JB5-05-8	4.6	0.3	4.8	0.6
JB5-05-9	0.7	0.1	2.5	0.3
JB5-05-10	0.6	0.1	1.4	0.3
JB5-05-11	0.0	0.1	0.9	0.2
JB5-05-12	0.0	0.0	0.2	0.4
JB5-05-13	0.0	0.0	0.2	0.2
JB5-05-14	1.0	0.2	0.6	0.4
JB5-05-16	3.9	0.5	2.6	0.8
JB5-05-17	7.6	0.4	1.5	0.9
JB5-05-18	1.6	0.3	1.5	0.3
JB5-05-19	4.0	0.6	4.6	0.5
JB5-05-20	1.7	0.2	0.0	0.0
JB5-05-21	1.0	0.1	12.0	2.0
JB5-05-22	1.4	0.2	1.9	0.4
JB5-05-23	0.0	0.0	4.9	0.7
JB5-05-24	4.4	0.6	9.7	1.0
JB5-05-25	0.0	0.1	1.7	0.2
JB5-05-26	2.1	0.3	1.2	0.5
JB5-05-27	5.2	0.5	4.9	0.4
JB5-05-28	5.9	0.3	5.2	0.6
JB5-05-29	1.1	0.1	0.9	0.3
JB5-05-30	1.8	0.3	2.9	0.4
JB5-05-31	2.8	0.2	3.2	0.4
JB5-05-32	5.0	0.3	2.4	0.3
JB5-05-33	4.0	0.2	1.2	0.3

Table A2-8. Continued.

JB5-05-34	6.8	0.8	4.8	0.9
JB5-05-35	5.8	0.7	1.8	0.3
JB5-05-36	3.8	0.4	3.0	0.7
JB5-05-37	6.9	1.5	3.1	0.9
JB5-05-38	5.3	0.7	0.5	0.2
JB5-05-39	5.2	0.6	0.3	0.3
JB5-05-40	5.0	0.6	1.1	0.6
JB5-05-41	3.2	0.3	1.0	0.3
JB5-05-43	0.0	0.0	1.5	0.3
JB5-05-47	5.2	0.6	4.0	0.5
JB5-05-48	5.5	0.6	5.2	0.5
JB5-05-50	5.9	0.5	1.0	0.3
JB5-05-51	4.6	0.8	1.7	0.4
JB5-05-52	4.2	0.6	1.8	0.3
JB5-05-53	5.9	0.4	1.4	0.3
JB5-05-54	3.2	0.5	3.2	0.3
JB5-05-55	4.9	0.3	0.9	0.4
JB5-05-56	7.0	0.6	0.8	0.4
JB5-05-57	9.0	1.2	0.6	0.5
JB5-05-58	7.0	1.9	0.3	0.7

Table A2-9. November-2005 sample site coordinates, dry bulk density and sediment description.

Sample Date	Sample ID	Latitude	Longitude	Dry Bulk Density	Sediment Description
11/8/2005	JB11-05-1	40 36.8712	73 53.1669	0.77	organic mud
11/8/2005	JB11-05-5	40 37.2278	73 53.3766	0.72	organic mud
11/8/2005	JB11-05-6	40 37.4276	73 53.3766	0.59	organic mud
11/8/2005	JB11-05-7	40 37.7139	73 52.6726	0.99	fluffy mud
11/8/2005	JB11-05-8	40 38.0093	73 52.3661	0.70	fluffy mud
11/8/2005	JB11-05-9	40 38.0263	73 52.0523	1.20	sandy mud
11/8/2005	JB11-05-10	40 38.2885	73 51.8399	0.74	fluffy mud
11/8/2005	JB11-05-11	40 38.6218	73 51.2794	0.58	fluffy mud
11/8/2005	JB11-05-12	40 38.4659	73 51.0358	0.73	organic mud
11/8/2005	JB11-05-14	40 38.4130	73 50.7181	0.61	fluffy mud
11/8/2005	JB11-05-15	40 38.4847	73 50.6949	0.49	fluffy mud
11/8/2005	JB11-05-16	40 38.5169	73 50.7305	1.71	sand
11/8/2005	JB11-05-17	40 38.3601	73 50.2387	1.24	fluffy mud
11/8/2005	JB11-05-18	40 38.0747	73 50.0201	0.59	fluffy mud
11/8/2005	JB11-05-19	40 37.3485	73 50.3130	1.76	silty sand
11/8/2005	JB11-05-20	40 37.3594	73 50.3241	1.77	sand
11/8/2005	JB11-05-21	40 37.0655	73 51.4805	1.75	sand
11/8/2005	JB11-05-22	40 36.8345	73 51.7291	1.71	sand
11/8/2005	JB11-05-23	40 35.7213	73 52.1472	0.54	organic mud
11/8/2005	JB11-05-24	40 35.4259	73 51.6211	0.82	organic mud
11/8/2005	JB11-05-25	40 35.4299	73 51.0418	1.96	sand
11/8/2005	JB11-05-26	40 35.8875	73 50.9112	1.66	sand
11/8/2005	JB11-05-27	40 36.1787	73 50.5772	0.73	fluffy mud
11/8/2005	JB11-05-28	40 36.4350	73 50.2082	1.67	sand
11/8/2005	JB11-05-29	40 35.9988	73 49.9931	0.75	fluffy mud
11/8/2005	JB11-05-30	40 36.0695	73 49.5537	0.64	organic mud
11/8/2005	JB11-05-31	40 36.3313	73 49.4157	0.52	organic mud
11/8/2005	JB11-05-32	40 35.1396	73 50.9319	1.30	muddy silt
11/8/2005	JB11-05-33	40 35.1212	73 49.8524	1.63	sand with shell hash

Table A2-9. Continued.

11/8/2005	JB11-05-34	40 35.29’	73 49.5368	1.78	sand with shell hash
11/8/2005	JB11-05-35A	40 38.9199	73 49.7989	0.63	organic mud
11/8/2005	JB11-05-35B	40 38.9199	73 49.7989	0.65	organic mud
11/8/2005	JB11-05-35C	40 38.9199	73 49.7989	0.64	organic mud
11/8/2005	JB11-05-38	40 38.6572	73 49.2131	0.54	organic mud
11/8/2005	JB11-05-39	40 38.3276	73 49.2700	0.45	fluffy mud
11/8/2005	JB11-05-40	40 38.0134	73 40.0421	0.49	fluffy mud
11/8/2005	JB11-05-41	40 38.3213	73 48.8139	0.56	fluffy mud
11/19/2005	JB11-05-42	40 38.3162	73 48.7416	0.64	fluffy mud
11/19/2005	JB11-05-43	40 38.3175	73 48.6557	0.53	fluffy mud
11/19/2005	JB11-05-44	40 38.2309	73 48.6473	0.53	fluffy mud
11/19/2005	JB11-05-45	40 38.2117	73 48.4064	0.52	fluffy mud
11/19/2005	JB11-05-46	40 38.0389	73 48.5259	0.52	fluffy mud
11/19/2005	JB11-05-47	40 37.8123	73 47.5310	0.18	fluffy mud
11/19/2005	JB11-05-48	40 37.3163	73 47.5995	0.20	fluffy mud
11/19/2005	JB11-05-49	40 37.8077	73 47.9660	0.20	fluffy mud
11/19/2005	JB11-05-50	40 37.7847	73 48.6702	0.57	silty mud
11/8/2005	JB11-05-51	40 37.4872	73 48.5953	0.25	fluffy mud
11/8/2005	JB11-05-52	40 37.1289	73 48.5009	0.20	fluffy mud
11/8/2005	JB11-05-53	40 36.8644	73 48.1141	0.40	fluffy mud
11/8/2005	JB11-05-54A	40 36.7865	73 48.4226	0.25	fluffy mud
11/8/2005	JB11-05-54B	40 36.7865	73 48.4226	0.26	fluffy mud
11/8/2005	JB11-05-54C	40 36.7865	73 48.4226	0.25	fluffy mud
11/19/2005	JB11-05-55	40 36.0077	73 49.0073	0.70	fine sand
11/8/2005	JB11-05-56	40 35.6663	73 48.7098	0.66	organic mud
11/8/2005	JB11-05-57	40 36.0971	73 48.2916	0.36	organic mud
11/19/2005	JB11-05-58	40 36.2908	73 47.5875	0.28	organic mud
11/19/2005	JB11-05-59	40 36.0209	73 47.2605	0.21	organic mud
11/19/2005	JB11-05-60	40 36.6973	73 46.8184	0.25	organic mud
11/19/2005	JB11-05-61	40 37.1732	73 46.8403	0.20	organic mud
11/19/2005	JB11-05-62	40 37.2764	73 46.5788	0.25	organic mud

Table A2-9. Continued.

11/19/2005	JB11-05-63	40 36.9074	73 46.4500	0.81	organic mud
11/19/2005	JB11-05-64	40 37.4729	73 45.9020	0.80	sand with shell hash
11/19/2005	JB11-05-65	40 37.8447	73 45.2914	0.25	organic mud

Table A2-10. November-2005 ^{210}Pb activity in subtidal samples.

SAMPLE ID	Total Pb-210 (dpm g^{-1})	Error (±)	Supported Pb-210 (dpm g^{-1})	Error (±)	Excess Pb-210 (dpm g^{-1})	Error (±)
JB11-05-1	6.5	0.2	2.1	0.1	4.3	0.2
JB11-05-5	5.6	0.4	1.8	0.1	3.8	0.4
JB11-05-6	5.7	0.3	2.0	0.1	3.7	0.3
JB11-05-7	3.9	0.2	1.4	0.0	2.5	0.2
JB11-05-8	5.2	0.3	1.7	0.1	3.5	0.3
JB11-05-9	3.0	0.2	2.0	0.0	1.0	0.2
JB11-05-10	6.1	0.3	1.9	0.1	4.2	0.3
JB11-05-11	6.7	0.2	2.0	0.0	4.7	0.2
JB11-05-12	6.2	0.1	2.2	0.0	4.0	0.1
JB11-05-14	5.2	0.3	1.2	0.1	4.0	0.3
JB11-05-15	6.6	0.4	2.1	0.1	4.5	0.5
JB11-05-16	0.8	0.1	0.7	0.0	0.1	0.1
JB11-05-17	2.3	0.2	2.5	0.1	-0.3	0.2
JB11-05-18	6.3	0.3	2.1	0.1	4.2	0.3
JB11-05-19	1.6	0.1	1.5	0.0	0.1	0.1
JB11-05-20	1.6	0.1	1.2	0.0	0.4	0.1
JB11-05-21	1.1	0.1	1.4	0.0	-0.3	0.1
JB11-05-22	1.9	0.1	1.8	0.0	0.2	0.1
JB11-05-23	6.8	0.5	2.1	0.1	4.7	0.5
JB11-05-24	5.9	0.3	2.3	0.1	3.6	0.3
JB11-05-25	1.8	0.1	1.7	0.0	0.1	0.1
JB11-05-26	0.9	0.1	0.6	0.0	0.3	0.1
JB11-05-27	7.2	0.3	2.0	0.1	5.2	0.3
JB11-05-28	1.8	0.1	1.7	0.0	0.1	0.1
JB11-05-29	7.0	0.2	1.9	0.0	5.1	0.2
JB11-05-30	7.4	0.2	2.0	0.0	5.3	0.2
JB11-05-31	7.2	0.4	1.7	0.1	5.5	0.4
JB11-05-32	3.1	0.2	1.4	0.0	1.6	0.2
JB11-05-33	6.6	0.3	1.9	0.1	4.7	0.3
JB11-05-34	0.8	0.1	1.1	0.0	-0.3	0.1
JB11-05-35A	6.8	0.4	2.5	0.1	4.3	0.4
JB11-05-35B	5.6	0.3	1.9	0.1	3.7	0.3
JB11-05-35C	6.5	0.3	1.9	0.1	4.6	0.3
JB11-05-38	6.7	0.4	1.6	0.1	5.1	0.4

Table A2-10. Continued.

JB11-05-39	6.3	0.4	1.4	0.1	4.9	0.4
JB11-05-40	6.6	0.4	1.0	0.1	5.6	0.4
JB11-05-41	6.1	0.3	2.0	0.1	4.1	0.4
JB11-05-42	6.1	0.3	1.8	0.1	4.3	0.3
JB11-05-43	6.3	0.5	1.9	0.1	4.4	0.5
JB11-05-44	5.0	0.4	1.4	0.1	3.6	0.4
JB11-05-45	5.5	0.4	1.6	0.1	3.9	0.4
JB11-05-46	6.1	0.3	1.6	0.1	4.5	0.3
JB11-05-47	6.0	0.4	1.4	0.1	4.6	0.5
JB11-05-48	5.3	0.3	1.6	0.1	3.7	0.3
JB11-05-49	5.7	0.4	1.6	0.1	4.1	0.4
JB11-05-50	4.0	0.2	2.2	0.1	1.8	0.2
JB11-05-51	6.1	0.4	1.4	0.1	4.7	0.4
JB11-05-52	6.0	0.5	1.8	0.1	4.2	0.5
JB11-05-53	2.4	0.2	2.2	0.1	0.2	0.2
JB11-05-54A	6.4	0.2	1.8	0.1	4.6	0.2
JB11-05-54B	5.6	0.2	1.6	0.0	4.0	0.2
JB11-05-54C	5.8	0.2	1.8	0.1	4.0	0.2
JB11-05-55	5.6	0.2	2.2	0.0	3.4	0.2
JB11-05-56	0.3	0.1	0.6	0.1	-0.3	0.1
JB11-05-57	5.4	0.3	1.8	0.1	3.6	0.3
JB11-05-58	5.8	0.4	1.8	0.1	4.0	0.4
JB11-05-59	7.3	0.4	1.8	0.1	5.5	0.4
JB11-05-60	6.7	0.3	2.0	0.1	4.7	0.3
JB11-05-61	6.2	0.5	1.6	0.1	4.6	0.5
JB11-05-62	6.5	0.4	1.5	0.1	5.0	0.4
JB11-05-63	1.6	0.2	1.1	0.0	0.5	0.2
JB11-05-64	3.2	0.2	1.8	0.0	1.4	0.2
JB11-05-65	6.5	0.3	1.5	0.0	5.0	0.3

Table A2-11. November-2005 ^{234}Th activities in subtidal samples.

Sample ID	Total Th-234 (dpm g^{-1})	Error (±)	Supported Th-234 (dpm g^{-1})	Error (±)	Excess Th-234 (dpm g^{-1})	Error (±)
JB11-05-1	2.6	0.2	1.8	0.1	0.7	0.2
JB11-05-5	2.7	0.3	2.2	0.1	0.5	0.4
JB11-05-6	2.3	0.2	2.0	0.1	0.3	0.3
JB11-05-7	2.1	0.2	2.1	0.2	0.0	0.2
JB11-05-8	2.2	0.3	2.0	0.2	0.2	0.3
JB11-05-9	2.4	0.1	1.6	0.1	0.7	0.2
JB11-05-10	4.2	0.4	2.1	0.2	2.1	0.4
JB11-05-11	2.9	0.2	2.0	0.2	0.9	0.3
JB11-05-12	2.7	0.1	2.1	0.2	0.6	0.2
JB11-05-14	2.9	0.3	2.1	0.2	0.8	0.4
JB11-05-15	2.5	0.6	1.8	0.4	0.7	0.7
JB11-05-16	1.2	0.1	0.6	0.1	0.6	0.1
JB11-05-17	2.4	0.2	2.1	0.2	0.3	0.3
JB11-05-18	3.4	0.3	1.7	0.3	1.7	0.4
JB11-05-19	1.7	0.1	1.2	0.0	0.5	0.1
JB11-05-20	2.6	0.2	1.3	0.1	1.3	0.2
JB11-05-21	1.5	0.2	1.2	0.1	0.3	0.2
JB11-05-22	2.3	0.2	1.5	0.1	0.8	0.2
JB11-05-23	5.0	0.6	2.1	0.3	2.9	0.7
JB11-05-24	2.0	0.3	1.5	0.2	0.5	0.4
JB11-05-25	1.3	0.2	1.3	0.2	0.0	0.3
JB11-05-26	0.6	0.1	0.4	0.1	0.1	0.1
JB11-05-27	3.0	0.4	1.2	0.2	1.8	0.5
JB11-05-28	2.3	0.2	1.2	0.1	1.0	0.3
JB11-05-29	4.3	0.3	1.8	0.2	2.5	0.3
JB11-05-30	3.9	0.3	1.6	0.2	2.3	0.4
JB11-05-31	2.0	0.4	1.3	0.3	0.7	0.5
JB11-05-32	3.3	0.2	1.5	0.1	1.8	0.2
JB11-05-33	0.4	0.1	0.4	0.1	0.0	0.1
JB11-05-34	0.9	0.1	0.6	0.1	0.3	0.2
JB11-05-35A	2.6	0.5	2.0	0.2	0.6	0.5
JB11-05-35B	2.9	0.4	1.8	0.2	1.1	0.4
JB11-05-35C	3.1	0.3	1.5	0.3	1.6	0.4
JB11-05-38	4.0	0.4	2.1	0.3	1.9	0.5

Table A2-11. Continued.

JB11-05-39	1.5	0.5	1.3	0.4	0.2	0.7
JB11-05-40	3.3	0.4	2.0	0.3	1.3	0.5
JB11-05-41	4.5	0.5	1.5	0.2	3.0	0.5
JB11-05-42	4.7	0.5	2.0	0.3	2.7	0.6
JB11-05-43	2.3	0.3	2.2	0.2	0.1	0.4
JB11-05-44	3.4	0.6	1.5	0.3	1.9	0.7
JB11-05-45	4.2	0.5	2.3	0.3	1.9	0.6
JB11-05-46	3.0	0.3	1.9	0.2	1.2	0.3
JB11-05-47	5.1	0.7	1.6	0.3	3.5	0.7
JB11-05-48	4.4	0.4	1.6	0.3	2.8	0.6
JB11-05-49	4.1	0.5	1.8	0.2	2.3	0.5
JB11-05-50	4.3	0.8	2.2	0.6	2.1	1.0
JB11-05-51	2.5	0.2	0.1	0.1	2.4	0.2
JB11-05-52	4.8	0.7	1.3	0.3	3.5	0.7
JB11-05-53	4.2	0.5	1.6	0.2	2.6	0.5
JB11-05-54A	6.7	0.3	1.7	0.2	5.1	0.4
JB11-05-54B	6.4	0.3	1.8	0.3	4.6	0.4
JB11-05-54C	7.3	0.4	2.2	0.2	5.1	0.5
JB11-05-55	4.1	0.3	2.5	0.2	1.6	0.3
JB11-05-56	0.9	0.3	0.7	0.1	0.1	0.3
JB11-05-57	6.8	0.6	2.2	0.2	4.6	0.6
JB11-05-58	4.8	0.5	1.4	0.2	3.4	0.6
JB11-05-59	7.6	0.7	2.0	0.3	5.7	0.7
JB11-05-60	5.4	0.5	2.1	0.2	3.3	0.5
JB11-05-61	3.1	0.5	2.1	0.4	1.0	0.6
JB11-05-62	5.8	0.5	1.7	0.3	4.1	0.6
JB11-05-63	3.8	0.4	0.9	0.1	3.0	0.4
JB11-05-64	4.2	0.4	2.0	0.1	2.2	0.4
JB11-05-65	7.2	0.4	2.4	0.2	4.8	0.4

Table A2-12. November-2005 $^{234}Th_{xs}$ and ^{7}Be Inventories in Subtidal Samples.

SAMPLE ID	Excess Th-234 Inventory (dpm cm^{-2})	Error (±)	Be-7 Inventory (dpm cm^{-2})	Error (±)
JB11-05-1	2.8	0.2	22.9	0.7
JB11-05-5	2.0	0.2	28.8	1.1
JB11-05-6	0.9	0.1	9.1	0.5
JB11-05-7	0.0	0.0	20.5	0.7
JB11-05-8	0.7	0.1	4.1	0.5
JB11-05-9	4.5	0.4	2.6	0.4
JB11-05-10	7.7	1.0	5.8	0.6
JB11-05-11	2.7	0.3	27.6	0.5
JB11-05-12	2.3	0.2	5.0	0.2
JB11-05-14	2.5	0.3	4.6	0.5
JB11-05-15	1.7	0.2	14.6	1.0
JB11-05-16	5.2	0.8	1.5	0.2
JB11-05-17	2.1	0.3	2.8	0.7
JB11-05-18	4.9	0.6	5.8	0.5
JB11-05-19	4.3	0.3	2.4	0.2
JB11-05-20	11.3	1.2	2.2	0.5
JB11-05-21	2.5	0.4	0.0	0.0
JB11-05-22	6.5	0.7	3.2	0.5
JB11-05-23	7.9	1.4	11.6	0.9
JB11-05-24	2.2	0.3	0.2	0.0
JB11-05-25	0.0	0.0	0.0	0.0
JB11-05-26	1.0	0.2	0.0	0.0
JB11-05-27	6.7	0.7	9.7	0.7
JB11-05-28	8.6	1.1	2.0	0.5
JB11-05-29	9.2	0.8	7.1	0.5
JB11-05-30	7.3	0.7	2.8	0.3
JB11-05-31	1.9	0.2	4.3	0.6
JB11-05-32	11.7	1.3	5.6	0.5
JB11-05-33	0.0	0.0	0.1	0.0
JB11-05-34	3.0	0.6	0.0	0.0
JB11-05-35A	2.1	0.2	0.5	0.1

Table A2-12. Continued.

JB11-05-35B	3.5	0.3	2.9	0.5
JB11-05-35C	5.0	0.5	1.8	0.4
JB11-05-38	5.0	0.6	2.6	0.7
JB11-05-39	0.6	0.1	4.4	0.6
JB11-05-40	3.3	0.5	1.0	0.4
JB11-05-41	8.4	0.8	2.9	0.5
JB11-05-42	8.6	0.9	0.0	0.0
JB11-05-43	0.3	0.0	3.8	0.7
JB11-05-44	4.9	0.7	0.2	0.7
JB11-05-45	4.9	0.5	1.9	0.5
JB11-05-46	3.1	0.4	0.9	0.4
JB11-05-47	3.2	0.4	0.0	0.0
JB11-05-48	2.9	0.3	0.0	0.0
JB11-05-49	2.3	0.3	0.0	0.2
JB11-05-50	6.1	0.7	1.8	0.2
JB11-05-51	3.1	2.3	1.7	0.2
JB11-05-52	3.6	0.5	3.1	0.3
JB11-05-53	5.3	0.6	2.7	0.3
JB11-05-54A	6.3	0.9	3.5	0.2
JB11-05-54B	6.0	0.7	2.8	0.2
JB11-05-54C	6.4	0.8	2.0	0.2
JB11-05-55	5.4	0.5	1.7	0.3
JB11-05-56	0.4	0.2	0.5	0.6
JB11-05-57	8.3	0.9	5.5	0.4
JB11-05-58	4.8	0.5	3.0	0.3
JB11-05-59	5.8	0.9	0.7	0.3
JB11-05-60	4.0	0.4	2.3	0.2
JB11-05-61	1.0	0.2	1.0	0.3
JB11-05-62	5.1	0.5	1.3	0.2
JB11-05-63	12.1	2.2	3.1	0.6
JB11-05-64	8.8	0.9	0.0	0.0
JB11-05-65	6.1	0.4	0.9	0.2

Table A2-13. July-2006 sample site coordinates dry bulk density and sediment description.

Sample Date	Sample ID	Latitude	Longitude	Dry Bulk Density	Sediment Description
7/12/2006	JB7-06-1	40 35.49604	73 51.0066	1.42	sand
7/12/2006	JB7-06-2	40 35.9043	73 50.9159	1.60	silty sand
7/12/2006	JB7-06-3	40 36.1808	73 50.5616	0.51	organic mud
7/12/2006	JB7-06-4	40 36.2603	73 50.1935	1.25	silt mud with algae
7/12/2006	JB7-05-5	40 35.9982	73 49.9825	0.44	organic mud and ulva
7/12/2006	JB7-06-6	40 36.0781	73 49.5478	0.23	organic mud
7/12/2006	JB7-06-7	40 36.3394	73 49.4128	0.35	organic mud
7/12/2006	JB7-06-8	40 36.2235	73 51.9263	1.55	sand with shell hash
7/12/2006	JB7-06-9	40 36.8437	73 51.7318	1.55	sandy silt
7/12/2006	JB7-06-10	40 37.0719	73 51.4704	1.32	sand with shell hash
7/12/2006	JB7-06-11	40 37.2186	73 50.7884	1.50	silty sand
7/12/2006	JB7-06-12	40 37.3664	73 50.3247	1.33	sandy silt
7/12/2006	JB7-06-13	40 38.0725	73 50.0173	0.45	organic mud
7/12/2006	JB7-06-14	40 38.3585	73 50.2401	1.29	sand
7/12/2006	JB7-06-15	40 38.4142	73 50.7259	0.37	organic mud
7/12/2006	JB7-06-16	40 38.4907	73 50.7019	0.40	organic mud
7/12/2006	JB7-06-17	40 38.5153	73 50.7348	1.61	coarse sand
7/12/2006	JB7-06-18	40 38.4714	73 51.0485	0.51	organic mud
7/12/2006	JB7-06-19	40 38.6246	73 51.2843	0.65	organic mud
7/12/2006	JB7-06-20	40 38.2928	73 51.8406	0.47	organic mud with clams
7/12/2006	JB7-06-21	40 38.0252	73 52.0579	1.23	silty mud
7/12/2006	JB7-06-22	40 38.0131	73 52.3654	1.24	coarse sand
7/12/2006	JB7-06-23	40 38.2626	73 52.6783	0.62	mud
7/12/2006	JB7-06-24	40 37.5771	73 52.9948	0.64	clam shells
7/12/2006	JB7-06-25	40 37.4189	73 53.2394	0.62	organic mud
7/12/2006	JB7-06-26	40 37.2256	73 53.3767	0.64	mud with clams and worms
7/12/2006	JB7-06-27	40 36.8679	73 53.1648	0.58	organic mud
7/12/2006	JB7-06-28	40 36.5434	73 52.9759	0.77	organic mud

Table A2-13. Continued.

7/12/2006	JB7-06-29	40 36.5428	73 52.4114	1.44	sand
7/12/2006	JB7-06-30	40 36.2706	73 52.7152	0.89	sandy mud
7/12/2006	JB7-06-31	40 35.9303	73 52.5663	0.67	organic mud
7/12/2006	JB7-06-32	40 35.7111	73 52.1488	0.52	fluffy mud
7/12/2006	JB7-06-33	40 35.4280	73 51.6161	0.69	fluffy mud
7/12/2006	JB7-06-35	40 35.2840	73 49.5454	1.63	sand
7/12/2006	JB7-06-36	40 35.9980	73 49.0060	0.55	organic mud
7/12/2006	JB7-06-37	40 35.6626	73 48.7205	1.59	sand
7/12/2006	JB7-06-38	40 36.0967	73 48.3029	0.65	organic mud
7/12/2006	JB7-06-39	40 36.8590	73 48.1128	0.73	organic mud
7/12/2006	JB7-06-40	40 36.7817	73 48.4255	0.36	fluffy mud
7/12/2006	JB7-06-41	40 37.1289	73 48.5023	0.34	fluffy mud
7/12/2006	JB7-06-42	40 37.4930	73 48.5888	0.30	fluffy mud
7/12/2006	JB7-06-43	40 37.7885	73 48.6687	0.57	fluffy mud
7/12/2006	JB7-06-44	40 38.0259	73 49.0483	0.32	fluffy mud
7/12/2006	JB7-06-45	40 38.3281	73 49.2693	0.25	fluffy mud
7/12/2006	JB7-06-46	40 38.6595	73 49.2230	0.41	fluffy mud
7/12/2006	JB7-06-47	40 38.3223	73 48.8068	0.41	fluffy mud
7/12/2006	JB7-06-48	40 38.3221	73 48.7380	0.35	fluffy mud
7/12/2006	JB7-06-49	40 38.3126	73 48.6530	0.32	fluffy mud
7/12/2006	JB7-06-50	40 38.2298	73 48.6459	0.27	fluffy mud
7/12/2006	JB7-06-51	40 38.2084	73 48.4008	0.31	fluffy mud
7/12/2006	JB7-06-52	40 38.0384	73 48.5316	0.26	fluffy mud
7/12/2006	JB7-06-53	40 37.8088	73 47.9702	0.35	fluffy mud
7/12/2006	JB7-06-54	40 37.5570	73 47.6193	0.22	fluffy mud
7/12/2006	JB7-06-55	40 37.7134	73 47.3795	0.23	fluffy mud
7/12/2006	JB7-06-57	40 36.2936	73 47.5938	0.32	fluffy mud
7/12/2006	JB7-06-58	40 36.0247	73 47.2568	0.22	fluffy mud
7/12/2006	JB7-06-59	40 36.2670	73 47.1241	0.33	fluffy mud
7/12/2006	JB7-06-60	40 36.4731	73 47.1360	0.37	fluffy mud
7/12/2006	JB7-06-61	40 36.7007	73 46.8325	0.35	fluffy mud
7/12/2006	JB7-06-62	40 37.1743	73 46.8466	0.23	fluffy mud

Table A2-13. Continued.

7/12/2006	JB7-06-63	40 37.2752	73 46.5717	0.34	fluffy mud
7/12/2006	JB7-06-64	40 36.9070	73 46.4543	0.99	mud with clams
7/12/2006	JB7-06-65	40 37.4773	73 45.9054	0.64	mud with clams

Table A2-14. July-2006 ^{210}Pb activities in subtidal samples.

SAMPLE ID	Total Pb-210 (dpm g^{-1})	Error (±)	Supported Pb-210 (dpm g^{-1})	Error (±)	Excess Pb-210 (dpm g^{-1})	Error (±)
JB7-06-1	1.76	0.14	1.61	0.04	0.15	0.15
JB7-06-2	1.12	0.12	0.76	0.02	0.36	0.12
JB7-06-3	6.23	0.28	2.22	0.07	4.01	0.29
JB7-06-4	2.64	0.13	2.10	0.04	0.54	0.13
JB7-05-5	6.13	0.23	1.83	0.05	4.29	0.24
JB7-06-6	6.62	0.63	1.64	0.18	4.98	0.66
JB7-06-7	8.58	0.30	1.41	0.06	7.17	0.30
JB7-06-8	1.63	0.18	1.44	0.05	0.19	0.19
JB7-06-9	1.45	0.12	1.66	0.04	-0.21	0.12
JB7-06-10	2.47	0.16	1.49	0.04	0.98	0.17
JB7-06-11	2.02	0.14	2.02	0.05	0.00	0.15
JB7-06-12	1.80	0.21	1.48	0.07	0.32	0.22
JB7-06-13	6.53	0.25	2.20	0.07	4.34	0.26
JB7-06-13B	6.59	0.26	1.66	0.05	4.93	0.27
JB7-06-14	1.69	0.12	1.30	0.03	0.39	0.13
JB7-06-15	6.39	0.27	2.31	0.07	4.08	0.28
JB7-06-16	8.21	0.30	1.77	0.06	6.43	0.30
JB7-06-17	0.46	0.08	0.47	0.02	-0.01	0.08
JB7-06-18	6.93	0.18	1.58	0.04	5.35	0.19
JB7-06-19	5.30	0.15	2.00	0.03	3.30	0.15
JB7-06-20	12.77	0.43	1.84	0.05	10.93	0.43
JB7-06-21	3.60	0.20	1.39	0.03	2.21	0.20
JB7-06-22	1.34	0.11	0.80	0.02	0.54	0.11
JB7-06-23	5.83	0.25	1.48	0.05	4.35	0.25
JB7-06-24	6.46	0.23	1.93	0.05	4.53	0.24
JB7-06-25	6.78	0.23	1.66	0.05	5.12	0.24
JB7-06-26	5.86	0.24	1.68	0.05	4.18	0.25
JB7-06-27	8.10	0.25	1.69	0.04	6.41	0.25
JB7-06-28	5.56	0.19	1.66	0.04	3.90	0.19
JB7-06-29	2.65	0.13	2.94	0.04	-0.29	0.13
JB7-06-30	2.89	0.18	1.58	0.05	1.30	0.18
JB7-06-31	6.00	0.22	2.04	0.05	3.96	0.23
JB7-06-32	8.81	0.30	1.86	0.07	6.95	0.31

Table A2-14. Continued.

JB7-06-33	6.54	0.22	2.06	0.05	4.48	0.23
JB7-06-34A	2.79	0.12	1.73	0.03	1.06	0.12
JB7-06-35	0.78	0.08	0.85	0.02	-0.06	0.08
JB7-06-36	6.77	0.25	2.52	0.06	4.24	0.26
JB7-06-37	0.42	0.07	0.37	0.01	0.04	0.07
JB7-06-38	4.68	0.19	1.64	0.04	3.04	0.19
JB7-06-39	3.11	0.16	1.89	0.04	1.21	0.17
JB7-06-40	7.95	0.33	1.60	0.06	6.35	0.33
JB7-06-41	8.50	0.33	1.59	0.07	6.91	0.33
JB7-06-42	9.39	0.41	1.60	0.07	7.80	0.41
JB7-06-43	5.92	0.26	1.86	0.06	4.06	0.27
JB7-06-44	8.00	0.35	1.76	0.09	6.24	0.36
JB7-06-45	8.87	0.39	1.34	0.07	7.53	0.40
JB7-06-46	8.32	0.29	1.86	0.06	6.47	0.30
JB7-06-47	10.10	0.32	1.96	0.07	8.14	0.33
JB7-06-48	10.50	0.35	1.55	0.06	8.95	0.35
JB7-06-49	11.20	0.39	1.76	0.08	9.44	0.40
JB7-06-50	9.27	0.41	1.56	0.09	7.71	0.42
JB7-06-51	12.56	0.44	1.74	0.07	10.82	0.45
JB7-06-52	9.80	0.35	1.38	0.07	8.42	0.36
JB7-06-53	7.99	0.29	1.59	0.06	6.40	0.30
JB7-06-54	8.03	0.47	1.84	0.12	6.19	0.49
JB7-06-55	8.05	0.43	1.65	0.09	6.40	0.44
JB7-06-57	8.45	0.33	1.60	0.06	6.85	0.34
JB7-06-58	11.51	0.58	1.69	0.15	9.83	0.60
JB7-06-59	10.44	0.37	1.83	0.07	8.61	0.37
JB7-06-60	9.25	0.27	1.72	0.06	7.53	0.28
JB7-06-61	9.74	0.31	1.67	0.06	8.08	0.31
JB7-06-62	9.59	0.48	1.57	0.11	8.02	0.49
JB7-06-63	10.57	0.31	1.80	0.07	8.77	0.32
JB7-06-64	2.76	0.14	1.51	0.04	1.25	0.14
JB7-06-65	4.07	0.37	2.22	0.09	1.84	0.38
JB7-06-66	11.43	0.35	1.64	0.08	9.80	0.36

Table A2-15. July-2006 ^{234}Th activities in subtidal samples.

Sample ID	Total Th-234 (dpm g^{-1})	Error (±)	Supported Th-234 (dpm g^{-1})	Error (±)	Excess Th-234 (dpm g^{-1})	Error (±)
JB7-06-1	1.3	0.1	1.2	0.1	0.1	0.2
JB7-06-2	0.8	0.1	0.6	0.1	0.2	0.1
JB7-06-3	3.7	0.3	1.7	0.3	2.0	0.5
JB7-06-4	2.4	0.1	2.0	0.2	0.4	0.2
JB7-05-5	2.8	0.2	1.3	0.1	1.5	0.2
JB7-06-6	1.6	0.4	1.8	0.3	-0.2	0.5
JB7-06-7	1.7	0.3	1.6	0.2	0.1	0.4
JB7-06-8	1.3	0.1	1.4	0.1	-0.2	0.1
JB7-06-9	1.3	0.1	1.5	0.1	-0.2	0.1
JB7-06-10	1.8	0.2	1.6	0.1	0.1	0.2
JB7-06-11	1.9	0.2	1.8	0.1	0.0	0.2
JB7-06-12	1.4	0.2	1.3	0.1	0.1	0.2
JB7-06-13	2.3	0.3	1.7	0.1	0.6	0.3
JB7-06-14	1.4	0.1	1.2	0.1	0.3	0.2
JB7-06-15	2.8	0.3	2.0	0.2	0.8	0.3
JB7-06-16	2.4	0.3	2.0	0.2	0.5	0.4
JB7-06-17	0.4	0.1	0.3	0.1	0.1	0.1
JB7-06-18	2.0	0.2	1.2	0.2	0.9	0.3
JB7-06-19	1.8	0.2	1.5	0.2	0.2	0.2
JB7-06-20	1.9	0.2	1.2	0.2	0.7	0.3
JB7-06-21	2.2	0.2	1.2	0.1	1.0	0.2
JB7-06-22	1.2	0.1	0.9	0.1	0.3	0.1
JB7-06-23	2.9	0.2	1.4	0.2	1.4	0.3
JB7-06-24	4.8	0.3	2.3	0.2	2.5	0.4
JB7-06-25	2.8	0.2	2.3	0.1	0.6	0.3
JB7-06-26	3.2	0.3	1.8	0.1	1.4	0.3
JB7-06-27	2.1	0.2	2.0	0.2	0.2	0.3
JB7-06-28	2.5	0.2	1.8	0.2	0.7	0.2
JB7-06-29	22.7	0.2	2.1	0.2	0.6	0.3
JB7-06-30	1.2	0.1	1.3	0.2	-0.1	0.2
JB7-06-31	3.5	0.3	2.0	0.2	1.5	0.3
JB7-06-32	3.9	0.4	2.1	0.3	1.7	0.5
JB7-06-33	3.3	0.3	2.3	0.2	1.1	0.3
JB7-06-34	2.9	0.2	1.0	0.1	2.0	0.2

Table A2-15. Continued

JB7-06-35	0.7	0.1	0.8	0.1	-0.1	0.1
JB7-06-36	3.6	0.4	1.1	0.2	2.5	0.4
JB7-06-37	0.5	0.1	0.2	0.0	0.3	0.1
JB7-06-38	3.5	0.2	1.9	0.1	1.6	0.3
JB7-06-39	5.2	0.4	2.0	0.2	3.2	0.4
JB7-06-40	2.0	0.4	1.2	0.3	0.7	0.5
JB7-06-41	3.4	0.4	1.4	0.2	2.0	0.5
JB7-06-42	4.5	0.3	2.1	0.3	2.4	0.4
JB7-06-43	4.9	0.4	2.2	0.2	2.7	0.4
JB7-06-44	4.3	0.3	2.1	0.3	2.2	0.4
JB7-06-45	4.2	0.2	1.2	0.3	3.1	0.4
JB7-06-46	5.3	0.3	2.1	0.2	3.2	0.4
JB7-06-47	3.9	0.2	1.9	0.2	2.0	0.3
JB7-06-48	5.4	0.4	1.3	0.2	4.1	0.4
JB7-06-49	4.8	0.3	1.6	0.2	3.2	0.4
JB7-06-50	4.1	0.3	1.7	0.2	2.4	0.4
JB7-06-51	5.7	0.3	1.9	0.3	3.8	0.5
JB7-06-52	4.0	0.3	1.6	0.2	2.4	0.4
JB7-06-53	4.1	0.3	1.3	0.2	2.8	0.4
JB7-06-54	3.8	0.4	1.0	0.2	2.8	0.4
JB7-06-55	4.4	0.4	2.0	0.2	2.4	0.5
JB7-06-57	4.0	0.3	1.4	0.3	2.6	0.4
JB7-06-58	6.2	0.5	1.8	0.4	4.3	0.7
JB7-06-59	4.3	0.3	1.2	0.2	3.1	0.4
JB7-06-60	5.1	0.4	1.8	0.2	3.4	0.5
JB7-06-61	4.3	0.3	1.1	0.1	3.2	0.3
JB7-06-62	5.4	0.4	1.5	0.4	3.9	0.6
JB7-06-63	6.8	0.3	2.0	0.3	4.8	0.4
JB7-06-64	4.4	0.3	1.8	0.1	2.6	0.3
JB7-06-65	3.9	0.3	2.0	0.2	1.9	0.4
JB7-06-66	9.0	0.3	1.8	0.3	7.2	0.4

Table A2-16. July-2006 $^{234}Th_{xs}$ and ^{7}Be inventories in subtidal samples.

SAMPLE ID	Excess Th-234 Inventory (dpm cm^{-2})	Error (±)	Be-7 Inventory (dpm cm^{-2})	Error (±)
JB7-06-1	0.8	0.1	3.6	0.4
JB7-06-2	1.5	0.3	0.9	0.3
JB7-06-3	0.0	0.0	2.7	0.4
JB7-06-4	2.4	0.2	6.6	0.5
JB7-05-5	3.4	0.4	1.6	0.2
JB7-06-6	0.0	0.0	0.0	0.0
JB7-06-7	0.0	0.0	6.6	0.4
JB7-06-8	0.0	0.0	0.0	0.0
JB7-06-9	0.0	0.0	1.6	0.4
JB7-06-10	0.9	0.1	6.1	0.6
JB7-06-11	0.3	0.0	2.2	0.5
JB7-06-12	0.5	0.1	0.0	0.0
JB7-06-13	1.3	0.1	3.6	0.3
JB7-06-14	1.8	0.2	2.0	0.4
JB7-06-15	1.4	0.1	5.9	0.3
JB7-06-16	1.0	0.1	2.6	0.3
JB7-06-17	0.8	0.2	0.1	0.3
JB7-06-18	2.2	0.2	2.4	0.2
JB7-06-19	0.8	0.1	2.3	0.2
JB7-06-20	1.7	0.2	5.5	0.3
JB7-06-21	6.2	0.9	5.7	0.4
JB7-06-22	2.1	0.3	5.1	0.4
JB7-06-23	4.5	0.7	2.3	0.4
JB7-06-24	8.0	0.9	4.0	0.4
JB7-06-25	1.7	0.2	4.3	0.4
JB7-06-26	4.4	0.5	4.6	0.4
JB7-06-27	0.5	0.1	2.1	0.3
JB7-06-28	2.8	0.3	1.5	0.3
JB7-06-29	4.6	0.4	2.4	0.4
JB7-06-30	0.0	0.0	14.9	0.7
JB7-06-31	5.0	0.5	3.0	0.3
JB7-06-32	4.6	0.7	3.0	0.5

Table A2-16. Continued.

JB7-06-33	3.7	0.4	1.2	0.3
JB7-06-34	14.0	1.8	3.7	0.5
JB7-06-35	0.0	0.0	2.0	0.3
JB7-06-36	6.9	0.6	4.5	0.4
JB7-06-37	2.1	0.5	2.1	0.3
JB7-06-38	5.2	0.5	2.9	0.4
JB7-06-39	11.5	1.3	5.5	0.4
JB7-06-40	1.3	0.2	0.9	0.3
JB7-06-41	3.3	0.4	2.2	0.3
JB7-06-42	3.7	0.5	1.1	0.3
JB7-06-43	7.6	1.0	0.9	0.4
JB7-06-44	3.5	0.5	0.7	0.3
JB7-06-45	3.8	0.5	0.0	0.0
JB7-06-46	6.7	0.6	2.4	0.4
JB7-06-47	4.2	0.4	0.6	0.2
JB7-06-48	7.2	0.7	1.1	0.3
JB7-06-49	5.1	0.5	0.5	0.3
JB7-06-50	3.1	0.4	0.1	0.2
JB7-06-51	6.0	0.7	0.0	0.0
JB7-06-52	3.2	0.4	0.0	0.0
JB7-06-53	5.0	0.5	1.0	0.3
JB7-06-54	3.0	0.4	0.0	0.0
JB7-06-55	2.8	0.5	0.0	0.0
JB7-06-57	4.2	0.5	3.7	0.4
JB7-06-58	4.8	1.0	0.0	0.0
JB7-06-59	5.3	0.6	3.6	0.4
JB7-06-60	6.2	0.6	3.6	0.3
JB7-06-61	5.7	0.5	2.8	0.3
JB7-06-62	4.5	0.9	0.4	0.4
JB7-06-63	8.2	0.8	0.3	0.2
JB7-06-64	12.9	1.2	10.3	0.6
JB7-06-65	6.1	0.9	7.0	0.6
JB7-06-66	12.0	1.2	0.0	0.0

Table A2-17 ^{210}Pb activity, ^{137}Cs activity, dry bulk density and loss-on-ignition of gravity core 1.

Core 1	Latitude: 40°36.7218			Longitude: 73°48.6471		
Depth	Total ^{210}Pb Activity (dpm g^{-1})	Supported ^{210}Pb Activity (dpm g^{-1})	Excess ^{210}Pb Activity (dpm g^{-1})	^{137}Cs Activity (dpm g^{-1})	Dry Bulk Density (dpm cm^{-3})	Loss-On-Ignition (%)
0 – 2	13.4 ± 0.9	1.9 ±0.1	11.5 ± 1.0	0.02 ± 0.01	0.4	34
2 – 4	16.6 ± 1.1	1.5 ± 0.1	15.1 ± 1.1	0.03 ± 0.02	0.4	21
4 – 6	9.3 ± 0.7	1.5 ± 0.08	7.8 ± 0.7	0.04 ± 0.02	0.5	31
6 – 8	9.7 ± 0.8	1.4 ± 0.1	8.3 ± 0.8	0.03 ± 0.02	0.6	29
8 – 10	9.3 ± 0.8	1.2 ± 0.1	8.1 ± 0.8	0.05 ± 0.02	0.5	7
10 – 12	9.8 ± 1.0	1.4 ± 0.1	8.4 ± 1.0	0.06 ± 0.02	0.6	3
12 – 14	8.8 ± 1.0	1.3 ± 0.1	7.5 ± 1.0	0.06 ± 0.03	0.6	6
14 – 16	7.0 ± 0.6	1.0 ± 0.1	6.0 ± 0.6	0.06 ± 0.03	0.6	5
16 – 18	7.4 ± 0.9	1.6 ± 0.1	5.7 ± 0.9	0.07 ± 0.01	0.7	9
18 – 20	6.8 ± 0.8	1.1 ± 0.1	5.7 ± 0.8	0.06 ± 0.02	0.7	11
20 – 24	5.0 ± 0.4	1.5 ± 0.1	3.5 ± 0.4	0.08 ± 0.02	0.8	9
24 – 28	5.9 ± 0.6	1.8 ± 0.1	4.1 ± 0.6	0.2 ± 0.04	0.9	9
28 – 32	4.9 ± 1.0	1.5 ± 0.1	3.4 ± 1.0	0.08 ± 0.02	1.0	8
32 – 36	2.2 ± 0.1	1.4 ± 0.1	0.8 ± 0.1	0.3 ± 0.04	1.1	17
36 – 40	2.4 ± 0.4	1.6 ± 0.1	0.8 ± 0.4	0.5 ± 0.04	1.1	8
40 – 44	2.6 ± 0.9	1.2± 0.1	1.4 ± 0.9	0.3 ± 0.03	1.2	8
44 – 48	1.4 ± 0.1	1.4 ± 0.1	0 ± 0.1	0.2 ± 0.04	1.3	6

Table A2-18 ^{210}Pb activity, ^{137}Cs activity, dry bulk density and loss-on-ignition of gravity core 2

Core 2	Latitude: 40°36.1260			Longitude: 73°47.6989		
Depth	Total ^{210}Pb Activity (dpm g^{-1})	Supported ^{210}Pb Activity (dpm g^{-1})	Excess ^{210}Pb Activity (dpm g^{-1})	^{137}Cs Activity (dpm g^{-1})	Dry Bulk Density (dpm cm^{-3})	Loss-On-Ignition (%)
0 – 2	10.7 ± 1.1	1.7 ± 0.1	9.0 ± 1.1	0.02 ± 0.01	0.5	7
2 – 4	17.8 ± 1.3	1.3 ± 0.1	16.6 ± 1.3	0.03 ± 0.02	0.5	6
4 – 6	12.5 ± 0.9	1.4 ± 0.1	11.1 ± 1.0	0.05 ± 0.02	0.6	4
6 – 8	9.3 ± 0.7	1.4 ± 0.1	7.9 ± 0.7	0.03 ± 0.01	0.8	14
8 – 10	7.4 ± 0.7	1.6 ± 0.1	5.9 ± 0.7	0.04 ± 0.01	1.0	6
10 – 12	6.6 ± 0.7	1.2 ± 0.1	5.4 ± 0.7	0.03 ± 0.01	1.0	5
12 – 14	7.8 ± 0.6	1.4 ± 0.1	6.4 ± 0.6	0.04 ± 0.01	1.0	5
14 – 16	7.3 ± 0.7	1.1 ± 0.1	6.2 ± 0.7	0.06 ± 0.01	1.0	4
16 – 18	6.7 ± 0.7	1.0 ± 0.1	5.7 ± 0.7	0.08 ± 0.03	0.9	5
18 – 20	6.3 ± 0.5	1.0 ± 0.1	5.3 ± 0.5	0.1 ± 0.03	1.1	6
20 – 24	6.0 ± 0.6	1.3 ± 0.1	4.7 ± 0.6	0.1 ± 0.04	1.0	5
24 – 28	3.6 ± 0.6	0.7 ± 0.06	2.9 ± 0.6	0.2 ± 0.07	1.2	5
28 – 32	3.3 ± 0.5	1.2 ± 0.1	2.1 ± 0.6	0.1± 0.03	1.2	6

Table A2-19 ^{210}Pb activity, ^{137}Cs activity, dry bulk density and loss-on-ignition of gravity core 3.

Core 3	Latitude: 40°35.3230			Longitude: 73°45.6211		
Depth	Total ^{210}Pb Activity (dpm g^{-1})	Supported ^{210}Pb Activity (dpm g^{-1})	Excess ^{210}Pb Activity (dpm g^{-1})	^{137}Cs Activity (dpm g^{-1})	Dry Bulk Density (dpm cm^{-3})	Loss-On-Ignition (%)
0 – 2	19.3 ± 1.1	1.4 ± 0.1	17,.9 ± 1.1	0.1 ± 0.04	0.9	48
2 – 4	16.8 ± 1.2	1.7 ± 0.1	15.1 ± 1.2	0.3 ± 0.09	0.9	31
4 – 6	10.4 ± 0.8	1.4 ± 0.1	9.0 ± 0.8	0.1 ± 0.04	1.2	21
6 – 8	6.0 ± 0.5	1.3 ± 0.1	4.7 ± 0.5	0.1 ± 0.02	1.9	45
8 – 10	6.3 ± 0.6	1.8 ± 0.1	4.5 ± 0.06	0.2 ± 0.03	1.5	7
10 – 12	5.7 ± 0.6	1.7 ± 0.1	4.0 ±0.6	0.1 ± 0.03	1.6	6
12 – 14	3.1 ± 0.7	1.9 ± 0.1	1.2 ± 0.7	0.1 ± 0.03	1.4	8
14 – 16	4.7 ± 0.6	1.5 ± 0.1	3.2 ± 0.6	0.2 ± 0.03	1.3	7
16 – 18	4.8 ± 0.7	1.4 ± 0.1	3.2 ±0.6	0.2 ± 0.03	1.4	5
18 – 20	4.2 ± 0.7	1.6 ± 0.1	2.6 ± 0.7	0.1 ± 0.03	1.0	8
20 – 24	4.0 ± 0.7	1.7 ± 0.1	2.4 ± 0.8	0.06 ± 0.03	1.2	8
24 – 28	2.5 ± 0.7	1.6 ± 0.1	0.9 ± 0.7	0.08 ± 0.03	1.1	6
28 – 32	2.8 ± 0.7	1.5 ± 0.1	1.3 ± 0.7	0.1 ± 0.05	1.1	8
32 – 36	3.0 ± 1.1	1.7 ± 0.1	1.3 ± 1.1	0.09 ± 0.04	1.0	6
36 – 40	3.1 ± 0.6	1.5 ± 0.1	1.6 ± 0.6	0.04 ± 0.02	1.1	5
40 – 44	2.4 ± 1.0	1.6 ± 0.1	0.8 ± 1.0	0.05 ± 0.03	1.1	6
44 – 48	2.8 ± 0.7	1.7 ± 0.1	1.1 ± 0.7	0.07 ± 0.05	1.1	5
48 - 56	1.6 ± 0.3	1.4 ± 0.1	0.2 ± 0.3	0.0 ± 0.03	1.3	4
56 – 64	1.3 ± 0.2	1.2 ± 0.1	0.1 ±0.2	0.0 ± 0.02	1.3	5
64 – 72	1.3 ± 0.1	1.1 ± 0.1	0.2 ± 0.1	0.0 ± 0.04	1.2	7
72 - 80	2.5 ± 0.7	2.1 ± 0.2	0.4 ± 0.7	0.0 ± 0.02	1.4	3

Table A2-20 ^{210}Pb activity, ^{137}Cs activity, dry bulk density and loss-on-ignition of gravity core 4.

Core 4	Latitude: 40°37.9199		Longitude: 73°48.2059			
Depth	Total ^{210}Pb Activity (dpm g^{-1})	Supported ^{210}Pb Activity (dpm g^{-1})	Excess ^{210}Pb Activity (dpm g^{-1})	^{137}Cs Activity (dpm g^{-1})	Dry Bulk Density (dpm cm^{-3})	Loss-On-Ignition (%)
0 – 2	19.2 ± 1.8	2.4 ± 0.3	16.8 ± 1.8	0.02 ± 0.01	0.2	39
2 – 4	17.4 ± 1.7	2.0 ± 0.3	15.4 ± 1.7	0.03± 0.02	0.2	47
4 – 6	18.5 ± 1.4	1.5 ±0.2	16.9 ±1.5	0.03 ± 0.01	0.2	49
6 – 8	12.9 ± 1.2	1.8 ± 0.2	11.1 ± 1.2	0.05 ± 0.02	0.2	43
8 – 10	12.7 ± 1.4	1.5 ± 0.2	11.2 ± 1.4	0.06 ± 0.01	0.2	12
10 – 12	13.3 ± 1.3	1.8 ± 0.2	11.5 ± 1.4	0.06 ± 0.01	0.2	11
12 – 14	10.3 ± 1.6	0.7 ± 0.2	9.6 ± 1.6	0.1 ± 0.06	0.2	14
14 – 16	8.0 ± 1.4	2.0 ± 0.3	6.0 ± 1.4	0.1 ± 0.04	0.2	12
16 – 18	8.6 ± 1.2	1.5 ± 0.2	7.1 ± 1.2	0.1 ± 0.07	0.2	21
18 – 20	8.9 ±1.5	0.5 ± 0.2	8.4 ± 1.5	0.2 ± 0.06	0.2	20
20 – 24	8.3 ± 1.3	2.4 ± 0.2	5.9 ± 1.3	0.2 ± 0.06	0.3	14
24 – 28	4.6 ± 1.0	1.5 ± 0.2	3.1 ± 1.0	0.2 ±0.1	0.2	20
28 – 32	4.2 ± 0.8	1.7 ±0.2	2.5 ± 0.8	0.2 ± 0.09	0.2	11
32 – 36	3.4 ± 0.8	1.4 ±0.2	2.0 ± 0.8	0.5 ± 0.1	0.2	15
36 – 40	3.0 ± 0.4	1.9 ±0.2	1.1 ± 0.4	0.3 ± 0.1	0.2	14
40 – 44	2.9 ± 0.5	1.2 ± 0.2	1.7 ± 0.5	0.2 ± 0.2	0.2	13
44 – 48	1.8 ± 0.5	1.7 ± 0.2	0.1 ± 0.5	0.9 ± 0.1	0.3	9
48 - 56	1.7 ± 0.3	1.5 ± 0.1	0.2 ± 0.4	0.2 ± 0.06	0.5	9
56 – 64	2.0 ± 0.3	1.8 ± 0.1	0.2 ±0.4	0.1 ± 0.04	0.5	10
64 – 72	2.5 ± 0.3	2.2 ± 0.1	0.2 ± 0.3	0.03 ± 0.02	1.3	1

Table A2-21 ^{210}Pb activity, ^{137}Cs activity, dry bulk density and loss-on-ignition of gravity core 5.

Core 5	Latitude: 40°38.4668			Longitude: 73°48.9809		
Depth	Total ^{210}Pb Activity (dpm g^{-1})	Supported ^{210}Pb Activity (dpm g^{-1})	Excess ^{210}Pb Activity (dpm g^{-1})	^{137}Cs Activity (dpm g^{-1})	Dry Bulk Density (dpm cm^{-3})	Loss-On-Ignition (%)
0 – 2	20.0 ± 1.5	2.0 ± 0.2	18.0 ± 1.6	0.1 ± 0.05	0.4	31
2 – 4	13.1 ± 1.0	0.8 ± 0.1	12.3 ±1.0	0.1 ± 0.03	0.5	25
4 – 6	10.5 ± 1.0	1.2 ± 0.1	9.3 ±1.0	0.1 ± 0.03	0.5	21
6 – 8	13.2 ± 1.0	0.9 ± 0.1	12.3 ± 1.0	0.1 ± 0.07	0.4	24
8 – 10	12.2 ± 1.0	1.1 ± 0.1	11.1 ± 1.0	0.1 ± 0.04	0.4	11
10 – 12	10.6 ± 0.8	0.9 ± 0.1	9.7 ± 0.8	0.1 ± 0.03	0.4	12
12 – 14	10.4 ± 0.9	1.6 ± 0.1	8.9 ± 0.9	0.1 ± 0.04	0.5	10
14 – 16	7.0 ± 1.0	1.3 ±0.1	5.7 ± 1.0	0.1 ± 0.03	0.5	8
16 – 18	6.7 ± 0.6	1.4 ± 0.1	5.4 ± 0.6	0.2 ± 0.06	0.5	14
18 – 20	7.3 ± 0.9	1.7 ± 0.1	5.7 ± 0.9	0.1 ± 0.04	0.5	10
20 – 24	6.1 ± 0.8	1.5 ± 0.1	4.6 ± 0.8	0.2 ± 0.08	0.5	8
24 – 28	4.1 ± 0.5	1.5 ± 0.1	2.7 ± 0.5	0.2 ± 0.09	0.5	7
28 – 32	3.7 ± 0.5	1.3 ± 0.1	2.4 ± 0.5	0.5 ± 0.09	0.5	8
32 – 36	3.7 ± 0.5	1.3 ± 0.1	2.5 ± 0.5	0.4 ± 0.06	0.5	10
36 – 40	2.2 ± 0.4	1.6 ± 0.1	0.6 ± 0.4	0.2 ± 0.05	0.6	11
40 – 44	2.4 ± 0.2	1.6 ± 0.1	0.8 ± 0.3	0.2 ± 0.03	0.7	5
44 – 48	1.7 ± 0.2	1.6 ± 0.1	0.1 ± 0.2	0.09 ± 0.03	0.7	5
48 - 56	1.9 ± 0.2	1.3 ± 0.1	0.6 ± 0.2	0.04 ± 0.02	0.7	9

Table A2-22 ^{210}Pb activity, ^{137}Cs activity, dry bulk density and loss-on-ignition of gravity core 1.

Core 6	Latitude: 40°35.9408			Longitude: 73°52.6980		
Depth	Total ^{210}Pb Activity (dpm g^{-1})	Supported ^{210}Pb Activity (dpm g^{-1})	Excess ^{210}Pb Activity (dpm g^{-1})	^{137}Cs Activity (dpm g^{-1})	Dry Bulk Density (dpm cm^{-3})	Loss-On-Ignition (%)
0 – 2	23.5 ± 1.7	1.9 ± 0.2	21.6 ± 1.7	0.1 ± 0.05	0.3	0
2 – 4	18.9 ± 1.4	1.9 ± 0.1	16.9 ± 1.4	0.1 ± 0.05	0.6	0
4 – 6	17.5 ±1.2	1.6 ±0.1	15.9 ±1.2	0.08 ± 0.03	0.6	5
6 – 8	9.1 ± 0.5	1.0 ± 0.05	8.0 ± 0.5	0.04 ± 0.02	0.9	15
8 – 10	7.1 ± 0.4	0.9 ± 0.04	6.1 ± 0.4	0.05 ± 0.02	1.1	1
10 – 12	7.0 ± 0.5	1.3 ± 0.1	5.7 ± 0.5	0.03 ± 0.02	0.8	3
12 – 14	6.5 ± 0.9	1.8 ± 0.1	4.7 ± 0.9	0.1 ± 0.03	0.7	10
14 – 16	6.4 ± 0.7	1.6 ± 0.1	4.8 ± 0.7	0.05 ± 0.03	0.9	5
16 – 18	5.6 ± 0.7	1.5 ± 0.1	4.1 ± 0.7	0.09 ± 0.03	0.8	8
18 – 20	4.7 ± 0.8	2.0 ± 0.1	2.7 ± 0.8	0.09 ±0.04	0.8	10
20 – 24	3.7 ± 0.5	1.5 ±0.1	2.2 ± 0.5	0.09 ± 0.03	0.8	6
24 – 28	2.7 ± 0.4	1.6 ± 0.1	1.1 ± 0.4	0.1 ±0.04	0.9	4
28 – 32	2.0 ± 0.5	1.4 ± 0.1	0.6 ± 0.5	0.07 ± 0.03	0.8	8
32 – 36	2.3 ± 0.3	1.8 ± 0.1	0.5 ± 0.3	0.1 ± 0.03	1.1	11

Table A2-23 ^{210}Pb activity, ^{137}Cs activity, dry bulk density and loss-on-ignition of gravity core 7.

Core 7	Latitude: 40°37.2068			Longitude: 73°53.4947		
Depth	Total ^{210}Pb Activity (dpm g^{-1})	Supported ^{210}Pb Activity (dpm g^{-1})	Excess ^{210}Pb Activity (dpm g^{-1})	^{137}Cs Activity (dpm g^{-1})	Dry Bulk Density (dpm cm^{-3})	Loss-On-Ignition (%)
0 – 2	22.9 ± 1.6	2.1 ± 0.2	20.8 ± 1.6	0.02 ± 0.01	0.4	34
2 – 4	24.6 ± 1.5	1.6 ± 0.1	22.9 ±1.5	0.03 ± 0.01	0.5	48
4 – 6	18.9 ± 1.1	1.4 ± 0.1	17.5 ± 1.1	0.03 ± 0.01	0.5	23
6 – 8	16.9 ± 1.4	1.4 ± 0.1	15.5 ± 1.4	0.05± 0.02	0.5	7
8 – 10	19.2 ± 1.2	1.2 ± 0.1	17.9 ±1.2	0.03 ± 0.01	0.5	17
10 – 12	11.5 ± 0.9	1.8 ± 0.1	9.7 ± 0.9	0.1 ±0.05	0.5	26
12 – 14	17.2 ± 1.1	2.0 ± 0.1	15.2 ± 1.1	0.09 ± 0.03	0.5	13
14 – 16	14.4 ± 0.9	1.5 ± 0.1	12.9 ± 0.8	0.07 ± 0.04	0.5	6
16 – 18	16.2 ± 1.2	1.9 ± 0.1	14.3 ± 1.2	0.08 ± 0.05	0.5	9
18 – 20	12.7 ± 1.1	1.7 ± 0.1	11.0 ± 1.1	0.08 ± 0.04	0.5	13
20 – 24	11.8 ± 1.2	1.6 ± 0.1	10.3 ±1.2	0.06 ± 0.03	0.5	21
24 – 28	10.2 ± 0.9	2.3 ± 0.1	7.9 ± 0.9	0.2 ± 0.04	0.6	6
28 – 32	10.1 ± 1.1	1.9 ± 0.1	8.2 ± 1.1	0.2 ± 0.05	0.6	12
32 – 36	9.3 ± 0.7	1.6 ± 0.1	7.7 ± 0.7	0.3 ± 0.04	0.6	13
36 – 40	6.3 ± 0.6	2.4 ± 0.1	3.9 ± 0.6	0.1 ± 0.04	1.1	4
40 – 44	5.5 ± 0.6	1.9 ± 0.1	3.6 ± 0.6	0.1± 0.04	1.0	3
44 – 48	4.7 ± 0.6	1.9 ± 0.1	2.8 ± 0.6	0.3 ± 0.05	0.7	8
48 - 56	3.5 ± 0.6	2.1 ± 0.1	1.4 ± 0.6	0.4 ±0.04	0.9	26
56 – 64	2.9 ± 0.4	1.9 ± 0.1	1.0 ± 0.4	0.2 ± 0.04	0.8	18

Table A2-24 ^{210}Pb activity, ^{137}Cs activity, dry bulk density and loss-on-ignition of gravity core 8.

Core 8	Latitude: 40°38.5649			Longitude: 73°50.8787		
Depth	Total ^{210}Pb Activity (dpm g^{-1})	Supported ^{210}Pb Activity (dpm g^{-1})	Excess ^{210}Pb Activity (dpm g^{-1})	^{137}Cs Activity (dpm g^{-1})	Dry Bulk Density (dpm cm^{-3})	Loss-On-Ignition (%)
0 – 2	12.1 ± 1.1	1.8 ± 0.2	10.2 ±1.1	0.05 ± 0.03	0.4	32
2 – 4	18.7 ± 1.4	1.5 ± 0.1	17.2 ± 1.5	0.08 ± 0.02	0.5	21
4 – 6	12.3 ± 0.8	1.0 ± 0.1	16.2 ± 1.4	0.08 ± 0.03	0.5	20
6 – 8	12.2 ± 1.4	1.0 ± 0.1	11.2 ± 1.4	0.06 ± 0.03	0.5	8
8 – 10	8.4 ± 0.6	0.9 ± 0.1	7.5 ± 0.6	0.07 ± 0.02	0.5	8
10 – 12	10.2 ± 1.2	1.8 ± 0.1	8.4 ± 1.2	0.05 ± 0.02	0.5	7
12 – 14	13.4 ± 0.9	1.2 ± 0.1	12.2 ± 0.9	0.06 ±0.05	0.6	13
14 – 16	11.1 ± 0.7	1.3 ± 0.1	9.8 ± 0.7	0.2 ± 0.04	0.6	10
16 – 18	10.7 ± 1.0	1.6 ± 0.1	9.1 ± 1.0	0.3 ± 0.07	0.6	16
18 – 20	5.8 ± 0.7	1.2 ± 0.1	4.6 ± 0.7	0.2 ± 0.06	0.6	9
20 – 24	5.7 ± 0.7	1.3 ± 0.1	4.4 ± 0.7	0.2 ±0.04	0.7	16
24 – 28	4.7 ± 0.5	1.1 ± 0.1	3.6 ± 0.5	0.08 ±0.02	1.0	11
28 – 32	2.0 ± 0.2	1.0 ± 0.1	1.0 ± 0.2	0.07 ± 0.02	1.4	5
32 – 34	1.7 ± 0.3	1.4 ± 0.1	0.3 ± 0.3	0.09 ± 0.02	1.5	6

A2-25. September-2004 marsh sample site coordinates, dry bulk density and location description.

Sample Date	Sample ID	Latitude	Longitude	Dry Bulk Density ($g\ cm^{-3}$)	Marsh Island	Location Description
9/22/2004	JB9-04-64	40 35.7877	73 51.4717	0.6	Ruffle Bar	Dead Area
9/22/2004	JB9-04-65	40 35.8767	73 51.2908	1.5	Ruffle Bar	Tidal Creek Bed
9/22/2004	JB9-04-66	40 35.9842	73 51.1230	0.4	Ruffle Bar	High marsh, sparse vegetation, mussels
9/22/2004	JB9-04-67	40 35.9857	73 51.1081	1.2	Ruffle Bar	High marsh thick vegetation mat
9/22/2004	JB9-04-68	40 36.0183	73 51.1288	0.6	Ruffle Bar	Slumping margin, dense vegetation, mussels
9/22/2004	JB9-04-69	40 35.5960	73 50.6227	1.7	Little Egg	Marsh edge
9/22/2004	JB9-04-70	40 35.6164	73 50.6074	1.6	Little Egg	Area between marsh edge and tidal creek
9/22/2004	JB9-04-71	40 35.6077	73 50.6062	1.7	Little Egg	High marsh, In Alterniflora
9/22/2004	JB9-04-72	40 35.6341	73 50.5930	0.8	Little Egg	High marsh, In Alterniflora
9/22/2004	JB9-04-74	40 35.6192	73 50.5698	1.0	Little Egg	Dead area admist vegetative islands
9/22/2004	JB9-04-75	40 35.6361	73 50.5249	1.7	Little Egg	High standing, sandy marsh
9/22/2004	JB9-04-76	40 35.6426	73 49.9404	2.6	Little Egg	Edge of dredge spoil
9/22/2004	JB9-04-77	40 35.6076	73 50.4303	1.7	Little Egg	High, inner marsh
9/22/2004	JB9-04-78	40 37.2088	73 51.1595	0.4	Duck Point	Marsh edge
9/22/2004	JB9-04-79	40 37.2088	73 51.1588	0.6	Duck Point	Dead area
9/22/2004	JB9-04-82	40 37.2326	73 51.1556	0.4	Duck Point	Marsh edge
9/22/2004	JB9-04-83	40 37.4687	73 48.0153	0.3	East High	Marsh edge
9/22/2004	JB9-04-84	40 37.4709	73 48.0131	0.2	East High	Dead area, lots of Ulva,
9/22/2004	JB9-04-85	40 37.4838	73 48.0044	0.3	East High	Dead area, lots of Ulva,
9/22/2004	JB9-04-86	40 37.5100	73 48.0288	0.2	East High	Dead area
9/22/2004	JB9-04-87	40 37.2985	73 47.7112	0.3	JoCo	Edge of marsh
9/22/2004	JB9-04-88	40 37.2994	73 47.6864	0.2	JoCo	Just interior from edge

A2-25 Continued

9/22/2004	JB9-04-89	40 37.3063	73 47.6799	0.9	JoCo	Edge of creek
9/22/2004	JB9-04-90	40 37.2933	73 47.6787	0.1	JoCo	Mid-marsh

A2-26. September-2004 ^{210}Pb activities in surficial (0-5 cm) marsh samples.

Sample ID	Total Pb-210 (dpm g^{-1})	Error (±)	Supported Pb-210 (dpm g^{-1})	Error (±)	Excess Pb-210 (dpm g^{-1})	Error (±)
JB9-04-64	7.5	0.3	0.5	0.02	7.0	0.3
JB9-04-65	2.0	0.1	0.5	0.01	1.5	0.1
JB9-04-66	9.7	0.4	0.5	0.03	9.2	0.4
JB9-04-67	1.7	0.1	0.7	0.02	1.1	0.1
JB9-04-68	4.9	0.3	0.6	0.03	4.3	0.3
JB9-04-69	1.6	0.1	0.6	0.01	1.1	0.1
JB9-04-70	1.4	0.1	0.7	0.01	0.7	0.1
JB9-04-71	1.9	0.1	0.5	0.01	1.3	0.1
JB9-04-72	3.3	0.2	1.0	0.02	2.3	0.2
JB9-04-74	2.8	0.1	0.7	0.02	2.2	0.1
JB9-04-75	1.0	0.1	0.2	0.01	0.7	0.1
JB9-04-76	1.0	0.1	0.3	0.01	0.7	0.1
JB9-04-77	1.1	0.1	0.3	0.01	0.8	0.1
JB9-04-78	3.2	0.2	0.5	0.02	2.7	0.2
JB9-04-79	2.8	0.1	0.6	0.02	2.2	0.1
JB9-04-82	3.3	0.2	0.6	0.01	2.7	0.2
JB9-04-83	2.3	0.3	0.5	0.03	1.8	0.3
JB9-04-84	4.5	0.4	0.4	0.03	4.1	0.4
JB9-04-85	2.9	0.3	0.3	0.02	2.6	0.3
JB9-04-86	7.3	0.4	0.3	0.03	7.0	0.4
JB9-04-87	6.9	0.5	1.1	0.06	5.9	0.5
JB9-04-88	18.8	0.8	0.5	0.06	13.3	0.8
JB9-04-89	4.2	0.2	0.1	0.01	4.1	0.2
JB9-04-90	21.3	1.0	0.3	0.06	13.2	1.0

A2-27. September-2004 ^{234}Th activities in surficial (0-5 cm) marsh samples.

SAMPLE ID	Total Th-234 Activity (dpm g^{-1})	Error (±)	Supported Th-234 Activity (dpm g^{-1})	Error (±)	Excess Th-234 Activity (dpm g^{-1})	Error (±)
JB9-04-64	2.5	0.3	1.6	0.2	0.9	0.4
JB9-04-65	2.9	0.2	1.8	0.1	1.2	0.3
JB9-04-66	3.7	0.6	2.2	0.4	1.5	0.7
JB9-04-67	2.6	0.2	1.5	0.1	1.1	0.2
JB9-04-68	4.7	0.3	1.8	0.2	2.9	0.4
JB9-04-69	2.4	0.2	1.3	0.1	1.1	0.2
JB9-04-70	5.4	0.2	1.8	0.1	3.6	0.2
JB9-04-71	3.5	0.2	1.6	0.1	2.0	0.3
JB9-04-72	2.3	0.3	1.8	0.3	0.5	0.4
JB9-04-74	2.6	0.3	1.7	0.2	0.9	0.4
JB9-04-75	1.1	0.1	0.8	0.1	0.3	0.2
JB9-04-76	0.7	0.1	0.9	0.1	-0.1	0.1
JB9-04-77	1.0	0.0	0.9	0.0	0.1	0.1
JB9-04-78	9.3	0.7	1.6	0.3	7.7	0.7
JB9-04-79	2.9	0.4	1.4	0.3	1.5	0.5
JB9-04-82	1.3	0.3	1.4	0.3	-0.1	0.4
JB9-04-83	7.3	0.8	1.1	0.4	6.1	0.9
JB9-04-84	3.7	0.5	0.1	0.0	3.6	0.5
JB9-04-85	3.6	0.5	1.0	0.3	2.5	0.6
JB9-04-86	2.5	0.6	1.5	0.5	1.0	0.8
JB9-04-87	8.3	2.2	1.9	0.9	6.3	2.4
JB9-04-88	9.5	0.7	1.8	0.3	7.7	0.7
JB9-04-89	1.8	0.1	1.7	0.1	0.2	0.2
JB9-04-90	4.0	0.7	2.0	0.5	2.0	0.9

A2-28. September-2004 $^{234}Th_{xs}$ and ^{7}Be inventories in marsh samples (0-5 cm).

SAMPLE ID	Excess Th-234 Inventory (dpm cm-2)	Error (±)	Be-7 Inventory (dpm cm^{-2})	Error (±)
JB9-04-64	2.8	0.4	2.1	0.2
JB9-04-65	9.1	1.0	2.0	0.1
JB9-04-66	3.0	0.3	3.1	0.3
JB9-04-67	7.0	0.4	2.0	0.1
JB9-04-68	8.4	0.6	4.1	0.3
JB9-04-69	9.4	1.0	1.1	0.1
JB9-04-70	12.8	1.9	0.4	0.1
JB9-04-71	12.5	1.7	0.6	0.1
JB9-04-72	1.8	0.2	0.6	0.1
JB9-04-74	4.9	0.3	1.6	0.1
JB9-04-75	2.5	0.3	1.7	0.1
JB9-04-76	0.0	0.0	1.8	0.0
JB9-04-77	0.8	0.1	0.3	0.0
JB9-04-78	16.1	0.9	2.0	0.3
JB9-04-79	4.7	0.3	3.9	0.1
JB9-04-82	0.0	0.0	0.0	0.1
JB9-04-83	9.8	1.0	1.3	0.4
JB9-04-84	3.6	1.1	1.2	0.3
JB9-04-85	3.8	0.3	1.4	0.1
JB9-04-86	1.0	0.2	4.1	0.4
JB9-04-87	6.3	0.9	4.1	0.6
JB9-04-88	6.1	0.5	4.2	0.8
JB9-04-89	0.8	0.0	1.2	0.1
JB9-04-90	1.4	0.1	4.3	0.9

A2-29 May-2005 marsh sample site coordinates, dry bulk density and location

Sample Date	Sample ID	Latitude	Longitude	Dry Bulk Density (g cm^{-3})	Marsh Island	Location Description
5/24/2005	JB5-05-59	40 35.7845	73 49.5387	0.2	Big Egg	Next to dead area
5/24/2005	JB5-05-60	40 35.7905	73 49.5486	0.3	Big Egg	Dead area
5/24/2005	JB5-05-61	40 35.7868	73 49.5543	0.3	Big Egg	Vegetated area near restoration site
5/24/2005	JB5-05-62	40.35.8005	73 49.6271	0.8	Big Egg	Creek bank
5/24/2005	JB5-05-63	40 35.8054	73 49.6256	0.4	Big Egg	High, dead area
5/24/2005	JB5-05-64	40 38.0241	73 51.1782	1.0	Elders Point	Intertidal area, lots of ulva
5/24/2005	JB5-05-65	40 37.9967	73 51.1957	1.1	Elders Point	Intertidal area, lots of ulva
5/24/2005	JB5-05-66	40 37.8700	73 51.1723	1.4	Elders Point	Vegetated, low area
5/24/2005	JB5-05-68	40 37.8880	73 51.2755	1.7	Elders Point	Sandy area
5/24/2005	JB5-05-69	40 37.1031	73 47.8268	1.6	JoCo	Intertidal area
5/24/2005	JB5-05-70	40 37.0935	73 47.8001	0.3	JoCo	Intertidal area adjacent to vegetation
5/24/2005	JB5-05-71	40 37.0724	73 47.7501	0.3	JoCo	Dense vegetation
5/24/2005	JB5-05-72	40 37.0622	73 47.6991	0.3	JoCo	Dense vegetation
5/24/2005	JB5-05-73	40 37.0322	73 47.6685	0.2	JoCo	salt flat with Salicornia
5/24/2005	JB5-05-74	40 36.9988	73 47.6889	0.2	JoCo	Vegetation next to ditch
5/24/2005	JB5-05-75	40 36.9757	73 47.7979	0.2	JoCo	Tidal Creek Bed
5/24/2005	JB5-05-76	40 36.9782	73 47.7283	0.3	JoCo	Vegetated area
5/24/2005	JB5-05-77	40 37.3933	73 48.0904	0.4	East High	Spartina area
5/24/2005	JB5-05-78	40 37.4022	73 48.1130	0.2	East High	Near tidal channel
5/24/2005	JB5-05-79	40 37.4314	73 48.1628	0.4	East High	Intertidal
5/24/2005	JB5-05-81	40 36.3421	73 50.4810	0.2	Yellow Bar	Intertidal area
5/24/2005	JB5-05-82	40 36.3402	73 50.5141	0.3	Yellow Bar	Edge of ponding area
5/24/2005	JB5-05-83	40 36.3232	73 50.5410	0.5	Yellow Bar	In ponded area
5/24/2005	JB5-05-85	40 35.3252	73 50.1438	1.7	Little Egg	Vegetated area
5/24/2005	JB5-05-86	40 35.3371	73 50.1471	1.7	Little Egg	Between vegetated area and dredge spoil
5/24/2005	JB5-05-87	40 35.3674	73 50.1444	1.6	Little Egg	Vegetated area

Table A2-30. May-2005 ^{210}Pb activities in surficial (0-5 cm) marsh samples.

Sample ID	Total Pb-210 (dpm g^{-1})	Error (±)	Supported Pb-210 (dpm g^{-1})	Error (±)	Excess Pb-210 (dpm g^{-1})	Error (±)
JB5-05-59	9.4	0.4	1.1	0.1	8.4	0.4
JB5-05-60	8.8	0.4	1.0	0.1	7.7	0.4
JB5-05-61	19.4	0.6	2.7	0.1	16.7	0.6
JB5-05-62	4.0	0.2	1.5	0.0	2.5	0.2
JB5-05-63	6.8	0.3	1.1	0.1	5.6	0.3
JB5-05-64	1.8	0.1	2.0	0.0	-0.2	0.1
JB5-05-65	2.7	0.1	2.2	0.0	0.6	0.2
JB5-05-66	1.1	0.1	1.4	0.0	-0.2	0.1
JB5-05-68	0.6	0.1	0.6	0.0	0.0	0.1
JB5-05-69	17.3	1.2	15.3	0.3	2.0	1.2
JB5-05-70	1.8	0.1	1.9	0.0	-0.1	0.1
JB5-05-71	2.8	0.3	1.1	0.1	1.7	0.3
JB5-05-72	8.8	0.5	0.6	0.1	8.2	0.5
JB5-05-73	3.3	0.3	0.8	0.1	2.5	0.3
JB5-05-74	8.0	0.4	1.0	0.1	7.1	0.4
JB5-05-75	4.2	0.3	1.3	0.1	2.9	0.3
JB5-05-76	7.6	0.3	1.0	0.1	6.6	0.3
JB5-05-77	10.2	0.5	2.6	0.1	7.7	0.5
JB5-05-78	0.0	0.1	0.0	0.1	0.0	0.1
JB5-05-79	2.4	0.3	1.5	0.0	0.9	0.3
JB5-05-81	0.0	0.1	0.0	0.1	0.0	0.1
JB5-05-82	5.1	0.3	2.0	0.1	3.1	0.3
JB5-05-83	1.8	0.2	1.4	0.1	0.4	0.3
JB5-05-85	0.0	0.0	0.1	0.1	-0.1	0.1
JB5-05-86	0.0	0.0	0.1	0.1	-0.1	0.1
JB5-05-87	0.7	0.0	0.7	0.0	0.0	0.0

Table A2-31. May-2005 ^{234}Th activities in surficial (0-5 cm) marsh samples.

SAMPLE ID	Total Th-234 Activity (dpm g^{-1})	Error (±)	Supported Th-234 Activity (dpm g^{-1})	Error (±)	Excess Th-234 Activity (dpm g^{-1})	Error (±)
JB5-05-59	4.4	0.6	4.2	0.4	0.2	0.7
JB5-05-60	3.7	0.5	4.0	0.4	-0.3	0.7
JB5-05-61	12.7	0.8	9.3	0.3	3.4	0.9
JB5-05-62	2.4	0.2	1.5	0.1	0.9	0.3
JB5-05-63	5.0	0.4	2.7	0.2	2.3	0.5
JB5-05-64	2.6	0.3	2.6	0.1	0.0	0.3
JB5-05-65	2.1	0.2	2.3	0.1	-0.2	0.2
JB5-05-66	0.3	0.1	0.4	0.2	-0.2	0.2
JB5-05-68	0.2	1.3	0.5	0.1	-0.2	1.3
JB5-05-69	1.6	0.1	1.5	0.1	0.1	0.2
JB5-05-70	14.3	0.7	1.2	0.1	13.1	0.7
JB5-05-71	8.0	0.4	8.3	0.3	-0.3	0.5
JB5-05-72	2.5	0.2	2.3	0.1	0.1	0.2
JB5-05-73	6.0	1.0	5.4	0.5	0.6	1.1
JB5-05-74	8.4	0.5	8.7	0.5	-0.3	0.7
JB5-05-75	5.6	0.4	5.8	0.5	-0.2	0.6
JB5-05-76	4.9	0.5	5.2	0.3	-0.2	0.6
JB5-05-77	5.6	0.3	5.9	0.3	-0.3	0.4
JB5-05-78	4.7	0.2	4.7	0.2	-0.1	0.3
JB5-05-79	4.3	0.2	4.4	0.3	-0.1	0.4
JB5-05-81	24.9	1.3	14.6	0.6	10.2	1.4
JB5-05-82	11.9	0.8	8.2	0.6	3.8	1.0
JB5-05-83	11.0	0.7	4.1	0.1	6.9	0.7
JB5-05-85	0.8	0.2	0.9	0.2	-0.1	0.3
JB5-05-86	0.8	0.1	1.1	0.3	-0.2	0.3
JB5-05-87	1.4	0.1	0.6	0.1	0.8	0.1

Table A2-32. May-2005 $^{234}Th_{xs}$ and ^{7}Be inventories in marsh samples (0-5 cm).

SAMPLE ID	Excess Th-234 Inventory (dpm cm-2)	Error (±)	Be-7 Inventory (dpm cm^{-2})	Error (±)
JB5-05-59	0.0	0.2	1.1	0.3
JB5-05-60	0.0	0.5	0.4	0.4
JB5-05-61	4.2	0.3	0.5	0.3
JB5-05-62	3.8	0.5	2.1	0.3
JB5-05-63	4.8	0.6	5.6	0.4
JB5-05-64	0.0	0.5	1.1	0.3
JB5-05-65	0.0	0.2	0.1	0.4
JB5-05-66	0.0	0.3	1.1	0.5
JB5-05-68	0.0	0.4	4.9	2.5
JB5-05-69	0.0	0.1	0.0	0.1
JB5-05-70	19.7	1.4	0.5	0.2
JB5-05-71	0.0	0.1	0.6	0.2
JB5-05-72	0.0	0.2	13.0	2.4
JB5-05-73	0.6	0.1	1.5	0.3
JB5-05-74	0.0	0.1	1.2	0.2
JB5-05-75	0.0	0.3	0.6	0.2
JB5-05-76	0.0	0.2	2.4	0.4
JB5-05-77	0.0	0.1	2.2	0.3
JB5-05-78	0.0	0.1	1.3	0.1
JB5-05-79	0.0	0.1	0.4	0.1
JB5-05-81	10.2	0.7	0.0	0.0
JB5-05-82	5.6	0.5	1.9	0.4
JB5-05-83	15.9	1.6	0.5	0.6
JB5-05-85	0.0	0.2	0.5	0.1
JB5-05-86	0.0	0.3	1.0	0.2
JB5-05-87	6.3	0.9	0.6	0.2

Table A2-33 2007 marsh sample site coordinates and dry bulk density

Sample ID	Latitude	Longitude	Dry Bulk Density	Marsh Island
JoCo-2007-1	40 36.7647	73 47.2129	0.2	JoCo
JoCo-2007-2	40 36.7636	73 47.2137	0.3	JoCo
JoCo-2007-3	40 36.7559	73 47.2018	0.1	JoCo
JoCo-2007-4	40 36.7381	73 47.2021	0.2	JoCo
JoCo-2007-5	40 36.7350	73 47.1660	0.2	JoCo
JoCo-2007-6	40 36.7168	73 47.1840	0.2	JoCo
JoCo-2007-7	40 36.7170	73 47.1493	0.2	JoCo
JoCo2-2007-8	40 36.7018	73 47.1418	0.2	JoCo
JoCo-2007-9	40 36.6984	73 47.1262	0.3	JoCo
JoCo-2007-10	40 36.6875	73 47.1214	0.2	JoCo
EElders-2007-1	40 38.0585	73 50.8917	2.1	Elders East
EElders-2007-2	40 38.0699	73 50.8901	0.8	Elders East
EElders-2007-3	40 38.0811	73 50.8807	0.9	Elders East
EElders-2007-4	40 38.1103	73 50.8780	2	Elders East
EElders-2007-5	40 38.1153	73 50.8816	2	Elders East
EElders-2007-6	40 38.1259	73 50.8728	2.1	Elders East
EElders-2007-7	40 38.1469	73 50.8639	2	Elders East
EElders-2007-8	40 38.1736	73 50.8855	1.9	Elders East
WElders-2007-1	40 37.8257	73 51.3895	2	Elders West
WElders-2007-2	40 37.8038	73 51.3678	1.8	Elders West
WElders-2007-3	40 37.8456	73 51.3260	1.8	Elders West
WElders-2007-4	40 37.7964	73 51.2722	2.1	Elders West
WElders-2007-5	40 37.8449	73 51.2550	2	Elders West
WElders-2007-6	40 37.8763	73 51.2034	0.9	Elders West
WElders-2007-7	40 37.8678	73 51.1646	1.9	Elders West
WElders-2007-8	40 37.9267	73 51.2210	1.7	Elders West
WElders-2007-9	40 37.9438	73 51.2562	1.5	Elders West
WElders-2007-10	40 37.9393	73 51.2903	1.6	Elders West

Table A2-34 2007 $^{234}Th_{xs}$ and ^{7}Be inventories in marsh samples (0 - 5 cm)

Sample ID	May-2007 Excess ^{234}Th Inventory (dpm cm^{-2})	May-2007 ^{7}Be Inventory (dpm cm^{-2})	August-2007 Excess ^{234}Th Inventory (dpm cm^{-2})	August-2007 ^{7}Be Inventory (dpm cm^{-2})	October-2007 Excess ^{234}Th Inventory (dpm cm^{-2})	October-2007 ^{7}Be Inventory (dpm cm^{-2})
JoCo-2007-1	0 ± 0.2	2.5 ± 0.3	0 ± 0.1	1.1 ± 0.3	0.6 ± 0.2	3.2 ± 0.4
JoCo-2007-2	0 ± 0.1	0.7 ± 0.2	0 ± 0.2	1.7 ± 0.2	0 ± 0.1	1.3 ± 0.3
JoCo-2007-3	0 ± 0.2	0.8 ± 0.3	1.5 ± 0.3	3.1 ± 0.4	0 .2 ± 0.1	1.1 ± 0.2
JoCo-2007-4	0.2 ± 0.1	3 ± 0.4	0 ± 0.1	0.4 ± 0.1	0.7 ± 0.1	1.6 ± 0.3
JoCo-2007-5	0 ± 0.1	1.3 ± 0.2	0 ± 0.1	0.4 ± 0.1	0 ± 0.1	1.0 ± 0.2
JoCo-2007-6	0 ± 0.1	2.1 ± 0.4	0 ± 0.1	1.8 ± 0.3	0 ± 0.1	1.1 ± 0.2
JoCo-2007-7	0.3 ± 0.2	1.8 ± 0.3	0 ± 0.1	2.9 ± 0.3	0 ± 0.1	1.5 ± 0.3
JoCo2-2007-8	0 ± 0.1	2.1 ± 0.4	0 ± 0.1	0.9 ± 0.2	0 ± 0.1	1.3 ± 0.3
JoCo-2007-9	1.8 ± 0.3	2.3 ± 0.3	1.4 ± 0.3	2.9 ± 0.3	1.9 ± 0.4	1.0 ± 0.2
JoCo-2007-10	4.3 ± 0.3	4.1 ± 0.3	2.1 ± 0.3	3.8 ± 0. 4	2.4 ± 0.4	1.2 ± 0.2
EElders-2007-1	0 ± 0.1	2.2 ± 0.4	0 ± 0.1	0.9 ± 0.2	0 ± 0.1	0.8 ± 0.2
EElders-2007-2	0 ± 0.1	1.4 ± 0.3	0 ± 0.1	2.3 ± 0.4	0 ± 0.1	1.0 ± 0.2
EElders-2007-3	0 ± 0.1	0.2 ± 0.1	0 ± 0.1	2.2 ± 0.3	3.5 ±0.4	1.8 ± 0.3
EElders-2007-4	0 ± 0.1	0.3 ± 0.1	2.9 ± 0.4	5.1 ± 0. 4	3.5 ± 0.4	1.8 ± 0.4
EElders-2007-5	0 ± 0.1	5.5 ± 0.4	0 ± 0.1	2.9 ± 0.3	0 ± 0.2	0.9 ± 0.2
EElders-2007-6	0 ± 0.1	0.2 ± 0.1	4.5 ± 0.5	2.7 ± 0. 3	4.8 ± 0.5	1.7 ± 0.3
EElders-2007-7	2.2 ± 0.3	0.4 ± 0.2	1.3 ± 0.3	1.4 ± 0.2	0 ± 0.2	1.1 ± 0.2
EElders-2007-8	1.1 ± 0.2	0.6 ± 0.2	0 ± 0.1	2.5 ± 0. 3	0 ± 0.2	1.6 ± 0.3
WElders-2007-1	0 ± 0.2	0.5 ± 0.2	0.7 ± 0.2	1.4 ± 0. 2	1.7 ± 0.3	2.0 ± 0.3
WElders-2007-2	2.1 ± 0.4	1.2 ± 0.3	2.4 ± 0.3	3.1 ± 0.3	3.7 ± 0.4	1.7 ± 0.3
WElders-2007-3	0 ± 0.2	0.9 ± 0.2	2.3 ± 0.4	1.6 ± 0. 3	0.4 ± 0.1	1.3 ± 0.2
WElders-2007-4	0 ± 0.1	1.1 ± 0.3	0 ± 0.1	1.4 ± 0.3	0 ± 0.1	1.4 ± 0.3
WElders-2007-5	4.2 ± 0.4	2.9 ± 0.3	3.1 ± 0.5	4.4 ± 0.4	1.3 ± 0.3	0.9 ± 0.2
WElders-2007-6	2 ± 0.3	3 ± 0.4	0 ± 0.1	1.4 ± 0.2	0 ± 0.1	1.1 ± 0.2
WElders-2007-7	0 ± 0.1	0.6 ± 0.2	0 ± 0.1	1.3 ± 0.2	0 ± 0.1	1.3 ± 0.3
WElders-2007-8	2 ± 0.3	1.9 ± 0.2	1.5 ± 0.3	1.6 ± 0. 3	0 ± 0.1	1.0 ± 0.2
WElders-2007-9	0 ± 0.2	1.6 ± 0.3	0 ± 0.1	1.6 ± 0.2	0.5 ± 0.2	0.8 ± 0.2
WElders-2007-10	0 ± 0.1	0.7 ± 0.2	0 ± 0.1	1.4 ± 0.3	0 ± 0.1	0.5 ± 0.2